



Investigation into the Impact of Biosurfactant in Heavy Oil Reservoirs

Sunday Victor Ukwungwu

(B. Eng., M.Sc.)

School of Computing, Science and Engineering
Petroleum Technology and Spray Research Group
University of Salford, Manchester, UK

Supervisors

Dr. A. J. Abbas
Professor G. G. Nasr

Submitted in Partial Fulfilment of the Requirement of the Degree of Doctor of Philosophy, October 2017

Table of Contents

Table of Contents	ii
List of Tables	ix
List of Figures.....	x
Acknowledgement	xiv
Declaration.....	xv
Nomenclature	xvi
Conversion Table	xix
Publications and Conference	xx
Abstract.....	xxi
Chapter 1	1
1 Introduction	1
1.1 Problem Statement.....	3
1.2 Contribution to research	4
1.3 Aim	4
1.4 Objectives	4
1.5 Thesis Outline.....	5
Chapter 2	6
2 Literature Review	6
2.1 Significance of Enhanced Oil Recovery.....	6
2.2 Factors Influencing remaining oil Saturation	6
2.3 Understanding formation Wettability	7
2.4 Wettability alteration	10
2.5 A pore level view.....	11
2.6 Wetting in porous media.....	12
2.7 The use of biosurfactant in microbial enhanced oil recovery.....	12
2.8 Surfactant and Biosurfactant	13
2.8.1 Chemistry, Structure and Classification of Surfaces active compounds	14
2.8.2 Biosurfactant Producing Microorganisms	16
2.8.3 Biosurfactant in the Petroleum Industry	17
2.9 Classification and mechanisms of MEOR.....	18
2.9.1 Classification of MEOR.....	18
2.9.2 MEOR mechanism.....	19
2.10 Influence of culture medium composition on biosurfactant production.....	20

2.10.1	Carbon Source.....	21
2.10.2	Nitrogen Source	22
2.11	Economical and promising alternatives for Biosurfactant Production	23
2.12	Biosurfactants as potential candidate for wetting agents.....	23
2.13	Waterflooding	25
2.14	Biosurfactant flooding	25
2.15	Theoretical Background of Pendant Drop Interfacial Tension.....	26
2.16	Measurement of Contact Angle	29
2.17	Chapter summary.....	29
Chapter 3	31
3	Experimental Apparatus, Materials and Procedure	31
3.1	Overview	31
3.2	Phase-I: Microbial Culture.....	34
3.2.1	Experimental Apparatus and Materials.....	34
3.2.1.1	Fume cupboard	34
3.2.1.2	Eppendorf mastercycler® pro S	34
3.2.1.3	Measurement of the Cell Concentration by Optical Density (OD)	35
3.2.1.4	Growth Media.....	36
3.2.1.5	Microorganism.....	36
3.2.1.6	Reference Strains	37
3.2.2	Procedure of data collection.....	37
3.2.2.1	Nutrient Agar-Luria Broth.....	37
3.2.2.2	Bacterial strain revival.....	38
3.2.2.3	Growth at Different Temperatures	38
3.2.2.4	Stock Solution (Preservation of the Strains).....	38
3.2.2.5	Determination of Phenotypic Characteristics	40
3.2.2.5.1	Colony Morphology of Microorganisms	40
3.2.2.5.2	Gram-Staining	40
3.2.2.5.3	PCR Amplification	41
3.2.2.6	Serial Dilution for bacterial strain	43
3.2.2.7	Biosurfactant Extraction Process.....	44
3.2.3	Error and Accuracy	44
3.3	Phase-II: Interfacial Tension and Contact Angle	44
3.3.1	Experimental Apparatus and Materials.....	45

3.3.1.1	The TEMCO Pendant Drop	45
3.3.1.2	The Quizix pump	50
3.3.1.3	Fluid Samples	51
3.3.1.4	Produced Biosurfactants	52
3.3.2	Procedure of data collection.....	52
3.3.2.1	Dilutions of produced biosurfactants with brine.	52
3.3.2.2	Procedure for Interfacial Tension and Contact Angle Measurements.....	54
3.3.2.3	Filling the system with liquid	54
3.3.2.4	Pressurizing the IFT cell using the hand pump	55
3.3.2.5	Experimental run/IFT measurement	56
3.3.2.6	Cleaning of the IFT Cell	57
3.3.2.7	Precautions.....	57
3.3.3	Error and Accuracy	58
3.4	Phase-III: Qualitative Wettability Test.....	59
3.4.1	Experimental Apparatus and Materials.....	59
3.4.1.1	The Soxhlet Extraction	59
3.4.1.2	Principle of the Soxhlet extraction method	60
3.4.1.3	Rock Samples	61
3.4.2	Procedure of data collection.....	62
3.4.2.1	The Soxhlet extraction/Core Cleaning	62
3.4.2.2	Core Sample preparation for crude oil treatment	63
3.4.2.3	Core Sample Preparation for bio-surfactant treatments	64
3.4.2.4	Floating test	65
3.4.2.5	Two phase separation test.....	65
3.4.3	Error and Accuracy	66
3.5	Phase-IV: Core Flooding	66
3.5.1	Experimental Apparatus and Materials.....	66
3.5.1.1	Description of CoreLab UFS-200.....	67
3.5.1.2	Core Holder	70
3.5.1.3	The Injection System	71
3.5.1.3.1	Floating-Piston Accumulators	71
3.5.1.3.2	Metering Pump and Overburden Pressure Pump	73
3.5.1.4	The Collection System.....	74
3.5.1.5	The Data Acquisition and Control System.	75

3.5.1.6	Back-Pressure Regulator, Pressure Gauges, Air Actuated Valves, and Pressure Transducers	75
5.5.1		75
5.5.1.7	Materials	75
3.5.2	Procedure of data collection.....	76
5.5.2		76
5.5.2.1	Initial Setup.....	76
3.5.2.2	Filling the Floating-Piston Accumulators with Lexan CC Cells.....	76
3.5.2.3	Inserting Sample in the Core Holder	77
3.5.2.4	Applying Overburden Pressure and Back Pressure	77
3.5.2.5	Fluid Injection System.....	78
3.5.2.5.1	Saturating the sample with formation water.....	79
3.5.2.5.2	Displacing the formation water with crude oil	79
3.5.2.5.3	Displacing the crude oil with distilled water (waterflooding).....	80
3.5.2.5.4	Displacing the crude oil with bio-surfactant (bioflooding)	80
3.5.2.6	End Test.....	80
3.5.3	Errors and Accuracy	81
3.6	Chapter Summary	81
Chapter 4		83
4	Result and Discussions	83
4.1	Overview	83
4.2	Phase I - Microbial Culture	84
4.2.1	Culture and Growth.....	84
4.2.2	Phenotypic Characteristics.....	84
4.2.2.1	Colony Morphology of Microorganisms	84
4.2.2.2	Gram Staining.....	88
4.2.3	PCR Amplification.....	88
4.2.4	Serial Dilutions	88
4.2.5	Measurement of the Cell Concentration by Optical Density (OD).....	93
4.3	Phase II - Interfacial Tension and Contact Angle.....	94
4.3.1	Interfacial Tension Measurements.....	94
4.3.1.1	<i>Bacillus subtilis</i> (BS-1) cells.....	95
4.3.1.2	<i>Bacillus subtilis</i> (BS-1) cell-free.....	99
4.3.1.3	<i>Bacillus licheniformis</i> (BS-2) with cells	100

4.3.1.4	<i>Bacillus licheniformis</i> (BS-2) cell-free	103
4.3.1.5	<i>Paenibacillus polymyxa</i> (BS-3) Cells	107
4.3.1.6	<i>Paenibacillus polymyxa</i> (BS-3) cell-free	108
4.3.1.7	Comparison of IFT with temperature and time for <i>BS-1</i> , <i>BS-2</i> and <i>BS-3</i> Biosurfactants with Cells.....	110
4.3.1.8	Comparison of the effect of IFT with temperature for supernatant <i>BS-1</i> , <i>BS-2</i> and <i>BS-3</i> Biosurfactants	112
4.3.2	Contact Angle Measurements	114
4.3.2.1	Film (oil-drop) formation	116
4.4	Phase III - Qualitative Wettability Tests	119
4.4.1	Floating Test	119
4.4.2	Two-phase separation test.....	122
4.5	Phase - IV: Core flooding.....	126
4.5.1	Oil Recovery	128
4.6	Summary.....	132
Chapter 5		134
5	Risk Assessment in Utilising Biosurfactant produced from the <i>Bacillus</i> Genus	134
5.1	Introduction	134
5.2	Oil and gas production wastewater.....	135
5.3	Produced water	135
5.4	Risk Matrices	136
5.5	Microbial Pesticide Name: <i>Bacillus licheniformis</i> strain DSM 1918.....	137
5.5.1	Identification and Overview	137
5.5.2	Physical/Chemical Properties Assessment	138
5.5.3	Ecological Risk Assessment	138
5.5.4	Human Health Risk Assessment.....	138
5.6	Microbial Pesticide Name: <i>Bacillus subtilis</i> strain DSM 3256	142
5.6.1	Identification and Overview	142
5.6.2	Human Health Risk Assessment.....	143
5.6.3	Ecological Risk Assessment	143
5.7	Microbial Pesticide Name: <i>Paenibacillus polymyxa</i> strain DSM 3256	147
5.7.1	Biological and ecological properties.....	147
5.7.2	Effects on the environment	147
5.7.3	Effects on human health.....	148

5.7.4	Hazard severity	148
5.7.5	Sources of exposure	148
5.7.6	Risk Characterization.....	149
5.8	Summary.....	153
Chapter 6	154
6	Economic Analysis Using <i>BS-2</i> Biosurfactant to Enhance Residual Oil in Nembe field, Niger delta.	154
6.1	Introduction	154
6.2	Consideration of Economic Parameters and Assumptions.....	155
6.2.1	Total Capital Cost for Drilling the Injection Well	155
6.2.2	Estimation of operating expenditure (OPEX).....	156
6.2.2.1	Preparation of Biosurfactant	156
6.2.3	Revenue generated from the sales of Oil produced	157
6.2.4	Estimation of Depreciation Cost/Tax.....	158
6.3	Cash Flow Model.....	159
6.4	Net Present Value (NPV) Analysis	161
6.5	Net Cash Flow of Oil Recovery	162
6.6	Payback (Payout) Period	164
6.7	Break-even point for the Injection Well	164
6.8	Chapter summary.....	166
Chapter 7	167
Conclusions and Future Works	167
7.1	Conclusions	167
7.2	Future Works	169
References	170
APPENDICES	182
Appendix A	Journal Publications and Conferences	182
Appendix B	16S ribosomal RNA gene	183
Appendix C:	The DROPimage program	187
Appendix D:	Experimental IFT data for <i>BS-1</i> cells (<i>B. subtilis</i> cells)	195
Appendix E:	IFT data with time and pressure for <i>BS-1</i> (<i>B. subtilis</i> cells)	195
Appendix F:	Experimental IFT data for <i>BS-1</i> cell-free	198
Appendix G:	Variation of IFT data with time and pressure for <i>BS-1</i> (<i>B. subtilis</i> cell-free) supernatant	198

Appendix H: IFT with temperature at constant pressure for <i>BS-2</i> with cells.....	201
Appendix I: IFT with time for <i>BS-2</i> biosurfactant with cells.....	201
Appendix J: IFT with pressure at constant temperatures for <i>BS-2</i> cell-free.....	202
Appendix K: IFT with time for <i>BS-2</i> cell-free supernatant.....	203
Appendix L: IFT with pressure at constant temperatures for <i>BS-3</i> cells.....	204
Appendix M: Experimental IFT data for <i>BS-3</i> cell-free.....	205
Appendix N: IFT data with time and pressure for <i>BS-3</i> cell-free supernatant	206
Appendix O: Comparison of IFT with temperature for <i>BS-1</i> , <i>BS-2</i> & <i>BS-3</i> with cells.	208
Appendix P: Comparison of IFT with time for <i>BS-1</i> & <i>BS-2</i> biosurfactants with cells	
211	
Appendix Q: Comparison of IFT with temperature for cell-free <i>BS-1</i> , <i>BS-2</i> & <i>BS-3</i> ..	216
Appendix R: Comparison of IFT with time for cell-free biosurfactants	219

List of Tables

Table 2.1: Use of cheap raw materials to produce biosurfactants by various microbial strains	24
Table 3.1: Strains used in this study.	37
Table 3.2: Nucleotide sequence of the 16s rRNA gene	42
Table 3.3: Crude-oil Characteristics	51
Table 3.4: Composition of formation water.....	52
Table 3.5: Density measurements for cultured biosurfactants	53
Table 3.6: Core Characterisation	61
Table 4.1: Greatest contact angle reduction of all produced biosurfactant.....	115
Table 4.2: Wettability effect on sandstone grains after treatment with biosurfactants	122
Table 4.3: Data analysis for recovery factor	130
Table 5.1: Probability of occurrence.....	140
Table 5.2: Risk rating matrix	141
Table 5.3: Planned response (mitigation)	142
Table 5.4: Probability of occurrence.....	145
Table 5.5: Risk rating matrix	146
Table 5.6: Planned response (mitigation)	147
Table 5.7: Probability of occurrence.....	151
Table 5.8: Risk rating matrix	152
Table 5.9: Planned response (mitigation)	153
Table 6.1: Typical cost estimate for drilling an injection well	156
Table 6.2: Annual operating costs.....	157
Table 6.3: Annual sales of oil produced	158
Table 6.4: Cash flow at 10% discount rate of drilling an injection well.....	163
Table 6.5: Cost Summary of Drilling Injection Well.....	165

List of Figures

Figure 1.1: Process of microbial recovery of crude oil using biosurfactant	2
Figure 2.1: Forming a transition zone.....	9
Figure 2.2: Wetting in pores	11
Figure 2.3: Surfactant structure of surfactin (C ₅₃ H ₉₃ N ₇ O ₁₃).....	14
Figure 2.4: Structure of a (bio/surfactant) molecule.....	15
Figure 2.5: Surfactant adsorption process at interface.....	16
Figure 2.6: The basic process of microbial enhanced oil recovery	18
Figure 2.7: Cyclic microbial oil recovery	19
Figure 2.8: Microbial flooding recovery.....	20
Figure 2.9: Pendant drop method.....	28
Figure 3.1: Structure and sequence of experimental methodology	33
Figure 3.2: Retrieving of the selected bacteria strains.....	34
Figure 3.3: Eppendorf mastercycler® pro S	35
Figure 3.4: UV spectrophotometer	35
Figure 3.5: Liquid nutrient broths.....	36
Figure 3.6: Pouring a plate of nutrient agar	38
Figure 3.7: Stock solutions of the revived freezed dreid strains.....	39
Figure 3.8: Serial dilution for bacteria strain	43
Figure 3.9: Schematic illustration of the pendant drop set-up	46
Figure 3.10: The complete set-up of the IFT-cell.....	47
Figure 3.11: Low temperature/high pressure interfacial tension/contact angle cell apparatus	48
Figure 3.12: Pressure transducer/acquisition section.....	49
Figure 3.13: The Quizix pump.....	50
Figure 3.14: Crude oil and synthetic formation water	51
Figure 3.15: MSM and dilutions of produced biosurfactants for cells and cell-free cultures	54
Figure 3.16: Soxhlet kit	59
Figure 3.17: Heating mantle	60
Figure 3.18: Heating Mantle (Temperature) controller	60
Figure 3.19: The soxhlet extraction process	61
Figure 3.20: Sandstone core plugs	62
Figure 3.21: Crushed grains of sizes 300 µm and 225 µm.	63

Figure 3.22: Aging of the sandstone cores in crude oil	63
Figure 3.23: Saturation of bandera gray sandstone in <i>BS-1</i> <i>BS-2</i> and <i>BS-3</i>	64
Figure 3.24: Saturation of scioto sandstone in <i>BS-1</i> <i>BS-2</i> and <i>BS-3</i>	64
Figure 3.25: Floating test (a) oil-wet rock (b) water-wet rock	65
Figure 3.26: Two phase separation test (a) oil-wet rock (b) water-wet rock.....	66
Figure 3.27: Cross-section of the UFS-200 core flooding equipment.....	68
Figure 3.28: Schematic diagram of the flow path used in the core flooding experiment.....	69
Figure 3.29: Core holder	70
Figure 3.30: A cross-section of the hassle core holder	71
Figure 3.31: Floating-piston accumulators	72
Figure 3.32: CC cells	72
Figure 3.33: Metering Isco pumps	73
Figure 3.34: Overburden pump and relevant reservoirs	74
Figure 3.35: Hameg electronic balance	74
Figure 3.36: Adjustable and fixed end plug.....	77
Figure 3.37: The fluid Injection process.....	79
Figure 4.1: Isolation of pure cultures and growth of bacteria.....	85
Figure 4.2: Bacteria growth after 48 hours, stores at 30°C.....	86
Figure 4.3: Bacteria growth after 48 hours, stores at 37°C.....	87
Figure 4.4: Appearance of gram-positive cells of the selected strains	90
Figure 4.5: Sequence alignment for the selected strains.....	91
Figure 4.6: View of bacteria colonies from <i>Bacillus subtilis</i> at different dilutions.....	92
Figure 4.7: Effect of temperature on IFT for crude oil/distilled water system.....	95
Figure 4.8: Experimental of IFT data with temperature for <i>Bacillus subtilis</i> cells	97
Figure 4.9: Pressure effect on IFT for <i>BS-1</i> cells	98
Figure 4.10: Temperature effect on IFT for <i>BS-1</i> cell-free biosurfactant.....	99
Figure 4.11: Effect of pressure on IFT for cell-free <i>BS-1</i> -biosurfactant	100
Figure 4.12: Pressure effect on IFT for <i>BS-2</i> biosurfactant cells.....	101
Figure 4.13: IFT with temperature at varying pressures for <i>BS-2</i> with cells.....	102
Figure 4.14: IFT with time for <i>BS-2</i> biosurfactant at 42°C	103
Figure 4.15: Variation of IFT with time for <i>BS-2</i> biosurfactant at 75°C	103
Figure 4.16: IFT with temperature at varying pressures for <i>BS-2</i> biosurfactant cell-free	104
Figure 4.17: IFT with time for <i>BS-2</i> biosurfactant cell-free at 32°C	106
Figure 4.18: IFT with time for <i>BS-2</i> biosurfactant cell-free at 42°C	106

Figure 4.19: IFT with time for <i>BS-2</i> biosurfactant cell-free at 75°C	106
Figure 4.20: IFT with temperature at varying pressures for <i>BS-3</i> with cells.....	107
Figure 4.21: Pressure effect on IFT for <i>BS-3</i> cell-free at varying temperatures.....	108
Figure 4.22: Temperature effect on IFT for <i>BS-3</i> cell-free at varying pressures.....	109
Figure 4.23: Comparison of IFT with temperature for biosurfactants with cells	111
Figure 4.24: Comparison of IFT with temperature for supernatant biosurfactants	113
Figure 4.25: Effect of drop size on contact angle values for different pressures at 75°C.....	116
Figure 4.26: Film formation of oil with <i>Bacillus subtilis cells</i> biosurfactant at; (a) 26°C, 0.15 MPa (b) 42°C, 0.15 MPa (c) 60°C, 13.89 MPa.....	116
Figure 4.27: Film formation of oil with <i>Bacillus licheniformis</i> biosurfactant cells at 0.15 MPa; (a) 26°C, (b) 42°C, (c) 75°C	117
Figure 4.28: Film formation of oil with <i>Bacillus subtilis cell-free</i> biosurfactant at; (a) 26°C, 0.15 MPa (b) 42°C, 12.51 MPa (c) 75°C, 10.44 MPa.....	117
Figure 4.29: Film formation of oil with <i>Bacillus licheniformis cell-free</i> biosurfactant at 3.10 MPa; (a) 26°C, (b) 42°C, (c) 75°C	117
Figure 4.30: Film formation of oil with <i>paenibacillus polymyxa cell-free</i> biosurfactant at 10.44 MPa (a) 32°C, (b) 42°C, (c) 75°C	118
Figure 4.31: Control test for distilled water and untreated grain samples without biosurfactant (a) Scioto, (b) Bandera gray	119
Figure 4.32: Distilled water and treated scioto grain sample in biosurfactant with cells	120
Figure 4.33: Distilled water and treated bandera gray grain sample in biosurfactant with cells	121
Figure 4.34: Distilled water and treated scioto grain sample in cell-free biosurfactants.....	121
Figure 4.35: Distilled water and treated bandera gray grain sample in cell-free biosurfactants	122
Figure 4.36: Distilled water with kerosene plus treated grain samples in biosurfactants for both cells and cell-free	123
Figure 4.37: Distilled water with sunflower plus treated grain sample in biosurfactant with cells	124
Figure 4.38: Distilled water with sunflower plus treated grain sample in cell-free biosurfactants.	124
Figure 4.39: Distilled water flooding versus time	127
Figure 4.40: Biosurfactant flooding versus time.	127

Figure 4.41: Differential pressure across the sample versus time for the water flooding cycle	128
Figure 4.42: Differential pressure across the sample versus time for the biosurfactant flooding cycle.....	129
Figure 4.43: Oil recovery curves with injected pore volumes	131
Figure 4.44: Comparison between surfactant solutions in residual oil recovery	132
Figure 5.1: Stages of risk assessment	135
Figure 5.2: Adopted 3×3 impact matrix.....	137
Figure 5.3: Probability impact grid.....	141
Figure 5.4: Probability impact grid.....	146
Figure 5.5: Probability impact grid.....	152
Figure 6.1: Cooperate cash flow diagram.....	160
Figure 6.2: Payback period for drilling the injection well.....	164
Figure 6.3: Break-even graph of enhanced recovery using <i>BS-2</i> biosurfactant.....	166

Acknowledgement

With gratitude in my heart, I thank God for bringing me this far to successfully complete this dream despite all odds. And to my wonderful parents, who have always been the source of my inspiration, I cannot thank you enough for how much you invested in my education; you are truly the world's best anyone would wish for. May the good Lord continue to bless you and grant you long life. To my supervisors, Dr. A. J. Abbas and Prof. Nasr, I sincerely appreciate your support, encouragements and guidance during my research study. It was a good experience working with you.

To my lecturers and staff, Dr. Enyi, Dr. Burby, and Mr Alan Mappin, I appreciate all the help, advice and academic support especially during my laboratory experimental work. And to all my colleagues in the Petroleum and Spray Research Group, I want to say big thank you for being part of my success story, it was a lot of fun working with you and knowing you. And a special thanks to, Dr. Heather Allison and Sean Goodman, from the department of Functional and Comparative Genomics, Institute of Integrative Biology, University of Liverpool, for their support in carrying out the phase I of this study.

I appreciate my dearest siblings and especially my twin, for your prayers, love, and the trust you have in me. You guys are just the best siblings I could ever have wished for, even with miles apart, you all are always close to my heart. I will sure make you and our family proud for believing so much in me. Thank you for your prayers; it gave me so much grace to journey smoothly through my lowest moments.

To my darling wife, my jewel of inestimable value, my ever-smiling wife, I thank you for your patience, love and endurance throughout my research study; you have and will always be my pillar and source of strength. Thank you for bearing forth our little angel and daughter and for caring for her while I studied, you both are everything I work and live for. May God bless and keep you both. Now that I have completed my studies, I will surely make up for all the times I was unavoidably absent at home.

Finally, to all my friends and relatives who have always been there to support and encourage me when I needed it the most, may God bless you and reward you for your kindness. I give special thanks to Esosa, Chika, Oge, Ifeanyi, Isaac, Kevin, Emeka, Francis, Busayo, Ebimor, Lucky; you guys have always looked out for me.

Declaration

I **Ukwungwu Sunday Victor**, declare that this thesis report is my original work, and has not been submitted elsewhere for any award. Any section, part or phrasing that has been used or copied from other literature or documents copied has been clearly referenced at the point of use as well as in the reference section of this thesis.

.....

Signature

.....

Date

.....

Approved by

Dr A. J. Abbas
(Supervisor)

.....

Prof. G. G. Nasr
(Supervisor)

Nomenclature

<i>BS-1</i>	<i>Bacillus subtilis</i>
<i>BS-2</i>	<i>Bacillus licheniformis</i>
<i>BS-3</i>	<i>Paneabacillus Polymyxa</i>
$\text{CaCl}_2\text{H}_2\text{O}$	Calcium Dichloride Hydrate
$\text{C}_{53}\text{H}_{93}\text{N}_7\text{O}_{13}$	Surfactin
CFU	Colony Forming Unit
CEOR	Chemical Enhanced Oil Recovery
CMC	Critical Micelle Concentration
DDH ₂ O	Double Distilled water
DNA	Deoxyribonucleic Acid
dNTPs	Deoxynucleotide Triphosphates
DSMZ	<i>Deutsche Sammlung von Mikroorganismen und Zellkulturen.</i>
EOR	Enhanced Oil Recovery
HCl	Hydrochloric acid
ID	Identity
IFT	Interfacial Tension
$\text{K}_2\text{HPO}_4\cdot 2\text{H}_2\text{O}$	Potassium Phosphate dibasic
$\text{KH}_2\text{PO}_4\cdot 2\text{H}_2\text{O}$	Potassium dihydrogen Phosphate
KNO_3	Potassium Nitrate
LB	Luria Broth
MEOR	Microbial Enhanced Oil Recovery
$\text{MgSO}_4\cdot 7\text{H}_2\text{O}$	Magnesium Sulfate Heptahydrate
MIOR	Microbial Improved Oil Recovery

MSM	Minimum Salt Medium
NaCl	Sodium Chloride
Na ₂ S	Sodium Sulfide
(NH ₄) ₂ SO ₄	Ammonium Sulfate
NEB	New England Bioscience
OD	Optical Density
PCR	Polymerase Chain Reaction
PREL	Permeameter Relative Permeability Studies
PTFE	Polytetrafluoroethylene
rRNA	Ribosomal Ribonucleic Acid
REV	Reverse Primers
USEPA	United States Environmental Protection Agency
CEPA	Canadian Environmental Protection Agency
UV	Ultra Violet

List of Symbols

μ	Fluid viscosity (cp)
Δp	Pressure head loss across the media (pascals)
A	Area (m ²)
C _s	Concentration of substrate
K	Absolute permeability (md)
L	Length (cm ³)
MPa	Mega Pascal
P _{sc}	Pressure at standard conditions (kPa)
P _{wf}	Wellbore flowing pressure (psia or Pa)
P _d	Dewpoint pressure (psia or Pa)

Q	Volumetric flow rate (Mscfd)
T _{sc}	Temperature at standard conditions (K)
V	Volume (m ³ /s)

Conversion Table

Parameters	SI Units	Other Conversion Factors
Pressure	1 atm	101.325 KPa 0.101325 MPa 14.7 psi
Viscosity	1 Ns/m ²	1000 cP
Flowrate	1 litre/s	60,000 ml/min
Mass	1 Kg	1000 g
Length	1 m	1000 mm 3.2808333ft 39.37 in
Temperature	0°C	32°F 273.15 K
Volume	1 m ³	1000 litres 6.28983 bbl
	1 bbl/day	0.1589873 m ³ /day
Time	1 day	24 hr 86400s
Density	1 Kg/m ³	8.3304 lb/gal
Area	1 m ²	10.76387 ft ² 1550 in ²

Publications and Conference

1. **Ukwungwu, S.V.**, Abbas, A.J. and Nasr, G.G., 2016. Experimental investigation of the impact of biosurfactants on residual-oil recovery. 18th International Conference on Biological Ecosystems and Ecological Networks, Madrid, Spain, 24 - 25 March 2016.
2. **Ukwungwu, S.V.**, Abbas, A.J. and Nasr, G.G., 2016. Experimental investigation of the impact of biosurfactants on residual-oil recovery. *International Journal of Biological, Biomolecular, Agricultural, Food and Biotechnological Engineering*, 10(3), pp.130-133.
3. **Ukwungwu, S.V.**, Abbas, A.J. and Nasr, G.G., Allison, H., Goodman, S., 2017. Wettability Effects on Bandera Gray Sandstone using Biosurfactants. *Journal of Engineering Technology*. Volume 6, Issue 2, July, 2017, PP.605-617.

(See Appendix A)

Abstract

Exploitation of oil resources in mature reservoirs is essential for meeting future energy demands. Despite the primary and secondary oil recovery, significant amount of residual oil is still left behind in the reservoir, necessitating tertiary recovery methods. These typically includes surfactant flooding, polymer flooding, Microbial Enhanced Oil Recovery (MEOR) etc. To exemplify the potential of microorganisms to degrade heavy crude oil to reduce its viscosity, is part of a process known as MEOR. In recent times surfactants produced by microbes have gained wider acceptability in the petroleum industry due to their low toxicity and ease with which they are naturally broken down in the environment. Petrochemical-based synthetic surfactants are currently used in substantial amounts to increase recovery of hydrocarbons, and these surfactants are more recalcitrant in the environment.

The present study therefore, uses a technique to utilise microbes that will economically achieve a scale of Enhanced Oil Recovery (EOR) through biosurfactant production, lowering of interfacial tension (IFT) and contact angle, changes in rock wettability of sandstone grains and biosurfactant flooding. Three biosurfactants were produced under laboratory conditions, from three species of the genus *bacillus* using sucrose 3% (w/v) as their carbon source for growth and metabolism. These species produced biosurfactants of different specific activities that resulted in different impacts on IFT and contact angle. The biosurfactants produced are *BS-1*, *BS-2* & *BS-3*. After applying the cell-free extracellular biosurfactants to the system, the results show that there is reduction in interfacial tension from 56.95 mN/m to 4.49 mN/m, 6.69 mN/m, and 10.94 mN/m. Also, the contact angle of the oil film was significantly reduced from 147.04° to 111.84°, when the cell-free extracellular biosurfactant (*BS-2*) was applied to the system.

Qualitative wettability tests were also performed on the sandstone crushed rock samples, which shows that, the spent culture medium changes wettability of the grains to water-wet and intermediate-wet. It should be noted that the decomposition property of sucrose as a carbon source makes it eco-friendly for biosurfactant production. The biosurfactant flooding also found to have a recovery of 38% (an interval of nominally 8%) against 30% water flooding, due to the development of a water-wet state, which was achieved by flooding the core with 5PV of *BS-2* supernatant solution.

Economic analysis was also considered in determining the possible profitability of the corresponding MEOR method with addition of biosurfactant costs that were utilised during this study. The case study results of these analysis show that the cumulative cashflow, indicated a payback period of 2.54 years for a capital investment of \$45.32 million, given a typical oil production of 2,720 barrel per day. Moreover, with this type of biosurfactant (*BS-2) supernatant*, it has become evident that there can be an enhance recovery in the heavy oil reservoir by changing the wettability of rock grains. This thus, provides new tools for use in EOR schemes that leads to promising environmental sustainability.

Chapter 1

1 Introduction

Exploitation of oil resources in mature reservoirs is an essential task for meeting the current and future energy demands. Advances in petroleum biotechnology in recent years has been driven by the growing global demand for sustainable technologies, that improves the efficiency of petrochemical processes in the oil industry (De Almeida et al., 2016), as well as providing promising schemes for oil recovery. An important tertiary oil recovery technique is Microbial Enhanced Oil Recovery (MEOR) which is an eco-friendly technology and cost-effective alternative (Banat et al., 2010) to both thermal and chemical enhanced oil recovery methods, in which microbes or their metabolic products are used to drive the residual oil trapped in the reservoirs (de Lima & de Souzaa, 2014; Filho, Carioca, Gonzales, de Lucena, & Tavares, 2012; S. Johnson, Salehi, Eisert, & Fox, 2009). The potential of microorganisms to produce sufficient biosurfactants, starting with low-cost substrates raw materials is mainly to degrade heavy crude oil to reduce viscosity and improve hydrocarbon mobilization. This is considered to be very effective in enhancing crude oil recovery from reservoirs (Sarafzadeh et al., 2014; Silva et al., 2014). Since thermophilic spore-forming bacteria can thrive in very extreme conditions in oil reservoirs (up to 80°C), they are the most suitable organisms for this purpose (Nicholson, Munakata, Horneck, Melosh, & Setlow, 2000; Shibulal et al., 2014).

Surfactants of microbial origin in the last decade have become of great interest because of their advantages over their chemical counterparts, which include low toxicity, biodegradability, effectiveness in adverse environmental conditions, ability to produce from renewable resources and environmental compatibility (Filho et al., 2012). These benefits of metabolic products can be explored in solving many problems often encountered during oil production in respect to improving the recovery of crude oil from reservoir rocks (Lazar, Petrisor, & Yen, 2007). It is therefore very necessary to protect the environment by utilizing microbial flooding technique for EOR processes, and the products of microbial fermentation of carbohydrates. The fundamental cause for leaving oil behind is economics. In general, the process of recovering oil from any conventional reservoir requires firstly, a pathway which connects oil in the pore spaces of a reservoir to the surface, and secondly, sufficient energy in the reservoir to drive the oil to the surface. Lack of these inter-linked requirements in a reservoir results in oil getting left behind (Springham, 1984). The varying permeability of petroleum reservoirs is also a major concern in EOR processes. It is important to know that

the chemicals used for EOR must be compatible with the physical and chemical environments of oil reservoirs.

The use of biosurfactant follow four main strategies as shown in Figure 1.1, from production *ex situ* (batch and continuous culture), to subsequent injection into the reservoir along with the water flood. The production of biosurfactant is dependent on medium composition under controlled setting and thus excess of carbon/energy source promotes the production of surface active agents (Fallon 2011).

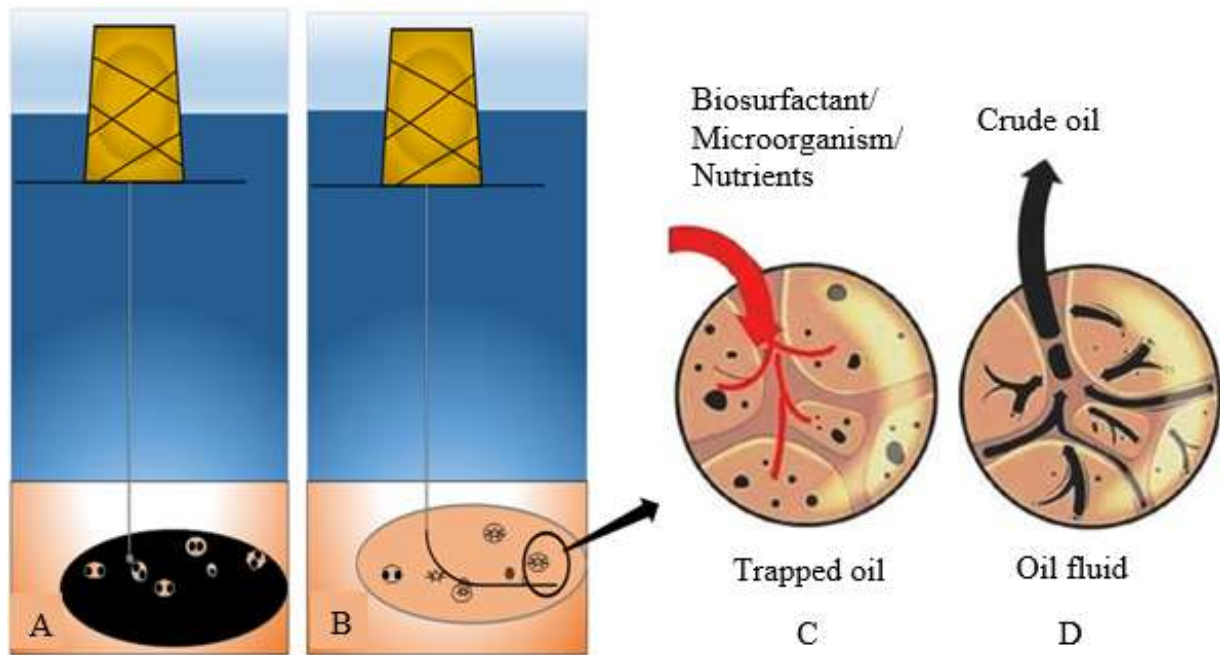


Figure 1.1: Process of microbial recovery of crude oil using biosurfactant

(A) Oil extraction using natural reservoir pressure. (B) Decreased pressure in oil well (C) Main strategies of biosurfactant used to release oil. (D) Oil well pressure restored facilitating oil extraction. **Source:** (De Almeida et al., 2016)

Also, in *in situ* MEOR method, biosurfactants producing microorganisms injected into the reservoir at the cell/oil interface within the reservoir formation will progress into high permeability zones at first. Then, at a later stage will grow and occlude those zones due to their size and the negative charges on their cell surface (Al-Hattali, 2012; Springham, 1984). These microbial cells would play an important part in the surface interactions at interphases between oil and water, where they preferentially position themselves. Lastly, augmenting nutrients is important as essential elements are injected into the reservoir to stimulate the growth of desired indigenous microorganisms producing biosurfactant. These eventually

helps to increase the sweep efficiency, and thus a more efficient oil transport can be achieved (Al-Bahry et al., 2013; Bachmann, Johnson, & Edyvean, 2014).

On a fundamental level, the process of MEOR results in beneficial effects such as formation of stable oil-water emulsions, reduced interfacial tension/capillary forces, clogging the high permeable zones and the breakdown of the oil film in the rocks which are important for maximizing and extending the reservoir life time (Al-Bahry et al., 2013; Bachmann et al., 2014).

Oil advancement through porous media is expedited by modifying the interfacial properties of the oil-water minerals. In such a system, microbial activity alters fluidity (viscosity reduction, miscible flooding); displacement efficiency (decrease of interfacial tension, increase of permeability); sweep efficiency (mobility control, selective plugging); and driving force (reservoir pressure). The second principle is known as upgrading. In this case, the degradation of heavy oils into lighter ones occurs by microbial activity. Instead, it can also aid in the removal of sulphur from heavy oils as well as the removal of heavy metals (H. Al-Sulaimani et al., 2011; Sen, 2008; Vazquez-Duhalt & Quintero-Ramirez, 2004). Microorganisms can synthesize useful products by fermenting low-cost substrates or raw materials. Therefore, MEOR can substitute Chemical Enhanced Oil Recovery (CEOR), which is a very pricey technology (Banat et al., 2010; Lazar et al., 2007). In MEOR, the chosen microbial strains are used to synthesize compounds analogous to those used in CEOR processes, to increase the recovery of oil from depleted and marginal reservoirs.

1.1 Problem Statement

Environmental impacts, surfactant cost and oil price are the three main parameters that have effect on the robustness of the surfactant flooding in oil reservoirs. Interfacial tension reduction and wettability alteration of the reservoir rocks are the two-main mechanism of oil recovery by utilizing surfactant flooding. There are a number of methods used to improve well productivity by earlier studies of MEOR (Davis & Updegraff, 1954; Kuznetsov, 1950; Updegraff & Wren, 1954) were based on three broad areas: injection, dispersion, and propagation of microorganisms in petroleum reservoirs; selective degradation of oil components to improve flow characteristics; and production of metabolites by microorganisms and their effects (Shibulal et al., 2014).

Great emphasis has been given to the ecological effects (Dusseault, 2001; Ivanković & Hrenović, 2010; Venhuis & Mehrvar, 2004; Ying, 2006) caused by chemical surfactants due to their toxicity and difficulty of degrading in the environment. Increasing ecological concerns, development in biotechnology, and the rise of more stringent environmental laws have prompted biosurfactants being a potential option to the synthetic surfactants available in the market. For as long as oil production will continue, the adoption of an environmentally friendly technique for enhancing effective oil recovery must be considered. Specifically, this study is focused on the following aspects:

- Environmental impact: addressing the adverse effects of CEOR on the eco-system, this study utilises thermophilic spore-forming bacteria to grow on a carbohydrate substrate which are easily degradable.
- Producing schemes: different producing schemes may affect the composition structure between the values of flowing and static properties and the amount of trapped oil in the reservoir, which may in turn influence the well productivity and hence the ultimate oil recovery from the reservoir. Changing the wettability of the rock and the manner in which the well is brought into flowing condition can affect the pore spaces and subsequently prolong the life of mature fields.

1.2 Contribution to research

Utilisation of biosurfactants through re-generation and characterisation of related species, leading to optimisation of the ultimate oil transport and enhancing oil recovery.

1.3 Aim

To develop a technique for MEOR in heavy oil reservoirs to effectively transport residual oil left behind and economically beneficial, when compared to other conventional techniques.

1.4 Objectives

1. To isolate pure culture and investigate the strain of bacteria that can be effectively used to produce the required biosurfactant through the addition of LB broth and culturing on LB agar plates.
2. To investigate surface reaction of these biosurfactants in reducing the interfacial tension and contact angle of heavy oil.

3. To investigate changes in wettability for different types of rocks and for a variety of biosurfactants using the qualitative wettability tests.
4. To investigate biosurfactants that can change formation wettability by measuring unsteady-state relative permeability before and after biosurfactant treatments through core flooding.
5. To develop an economic evaluation for the MEOR project.

1.5 Thesis Outline

This thesis is arranged in part structures, with each section providing the set of information and actions carried out as contained in the study as follows;

Chapter 2: This chapter presents a literature review on the role of biosurfactants in enhancing oil recovery as well as laboratory and field projects of MEOR. The chapter includes existing techniques on oil and gas recovery, and other associated issues on flow behaviour are discussed.

Chapter 3: In this chapter, the description of the experimental procedure for producing biosurfactant using the spread plate technique in culturing the bacteria species was outlined. Biosurfactant screening for reduction in interfacial tension, brief description of the IFT measurement equipment by TEMCO and a description of the IFT software/procedure were also presented. Two methods for qualitative wettability tests were also discussed and a description of the UFS-200 core flooding equipment.

Chapter 4: This chapter discusses the analysis and outcome of the laboratory investigations that proved a positive approach to enhancing oil recovery while comparing with relevant literatures.

Chapter 5: The environmental risk analysis was evaluated for all three produced biosurfactant, for any possible treats of the microbes to the environment.

Chapter 6: The economic viability of the experimental outcome was considered, if the project were to be escalated into actual field project.

Chapter 7: This chapter give the conclusion of the entire thesis and future works that could be further researched into.

Chapter 2

2 Literature Review

2.1 Significance of Enhanced Oil Recovery

To meet the global demand for energy consumption, it has become imperative to increase oil reserve through Enhanced Oil Recovery (EOR). A good understanding and definition of oil reserves must be determined to obtain what the life of a hydrocarbon reservoir is, since natural depletion (primary recovery) of a reservoir allows very limited recovery of the oil in place (Hammershaimb, Kuuskraa, & Stosur, 1983). Reserves refer to the amount of oil that can be produced from a reservoir under existing economics and with available technology, which is given by the following material balance equation in Eqn (2.1).

$$\begin{aligned} \text{Present reserve} = & \text{Past reserve} + \text{Additional reserve} \\ & - \text{Production reserve} \end{aligned} \quad (2.1)$$

With the current increase in demand for energy consumption (Miller & Sorrell, 2014; R. Santos, Loh, Bannwart, & Trevisan, 2014), it has become necessary to either maintain oil reserves by implementing new techniques to increase the percentage of recovery from existing reservoirs, drill new wells or discover new fields, to meet this demand. However, the likelihood of discovering large fields is declining (Michael J McInerney, Nagle, & Knapp, 2005; Muggeridge et al., 2014; Sun, Zhang, Chen, & Gai, 2017), and this has encouraged the need to increase the percentage of recovery from known reserves with the practical solution through the application of EOR methods.

2.2 Factors Influencing remaining oil Saturation

EOR implies a reduction of the remaining oil saturation. There are three major factors which influences the remaining oil saturation in a reservoir. The first factor is the capillary number (N_c), which affects the pore level oil displacement (Alvarado & Manrique, 2010), and it's defined as the ratio of the viscous forces to surface or interfacial tension forces, denoted as;

$$N_c = \frac{\mu \times v}{\sigma \cos\theta} \quad (2.2)$$

Where; v , is the Darcy velocity (m/s), μ the displacing fluid viscosity (Pa. s), σ , the interfacial tension (IFT) (mN/m) and θ , is the contact angle.

The second factor affecting recovery is described by a dimensionless number, mobility ratio (M), (Alvarado & Manrique, 2010), defined as;

$$M = \frac{\gamma D}{\gamma d} \quad (2.3)$$

Where; λD , is the mobility of the displacing fluid (BS-2 biosurfactant), and λd , the mobility of the displaced fluid (heavy crude oil).

$$\gamma = \frac{k}{\mu} \quad (2.4)$$

Where; k , is the effective permeability (md) and μ , is the viscosity (cp).

A value of $M > 1$ is considered unfavourable as it indicates that the mobility of the displacing fluid is higher than that of the displaced fluid, yielding poor sweep efficiency due to viscous fingering. Usually, this condition occurs at the interface of the two fluids in question. A typical case may have presented itself in this study while conducting the bio-flooding, if for instance the flow rate was set higher than 0.5 ml/min. The value of $M < 1$ is more favourable as the injected fluid displaces the oil in a more piston like manner (Aronofsky, 1952). The mobility ratio affects the macroscopic displacement efficiency. The third factor is reservoir heterogeneity that can influence the remaining oil saturation. Reservoirs can contain impermeable lithological divisions and heterogeneous porosity/permeability distributions that notably affect the fluid flow path and distribution.

2.3 Understanding formation Wettability

With multiple phases flowing in the reservoir, understanding wettability becomes important (WG Anderson, 1986; William Anderson, 1986; Anderson, 1987a, 1987b). However, even during primary recovery, wettability influences productivity and oil recovery (Morrow, 1990). The original wettability during and after hydrocarbon migration influence the profile of initial water saturation, Swi , and production characteristics in the formation.

Most reservoirs are water-wet prior to oil migration and exhibit a long transition zone, through which saturation changes gradually from mostly oil with irreducible water at the top

of the transition zone to water at the bottom. This distribution is determined by the bouyancy-based pressure, P_c as seen in Figure 2.1. Oil migrating into an oil-wet reservoir would display a different saturation profile: essentially maximum oil saturation down to the base of the reservoir. This difference reflects the ease of invasion by a wetting fluid. Wettability also affects the amount of oil that can be produced at the pore level, as measured after waterflood by the residual oil saturation (S_{or}). In a water-wet formation, oil remains in the larger pores, where it can snap off, or become disconnected from a continuous mass of oil, and become trapped. In an oil-wet or mixed-wet formation, oil adheres to surfaces, increasing the probability of a continuous path to a producing well and resulting in a lower S_{or} (Abdallah et al., 1986).

A homogenous formation exhibits a zone of transition from high oil saturation at the top to high water saturation at the bottom (blue curves). This saturation transition has its origin in the capillary pressure, P_c , which is the difference between the water and oil pressures at the interface (Figure 2.1).

$$P_c = P_{nw} - P_w \quad (2.5)$$

$$P_c = \rho g h \quad (2.6)$$

$$P_c = \frac{2\gamma \cos\theta}{r} \quad (2.7)$$

Where;

P_c = capillary pressure, P_{nw} = pressure in nonwetting phase, P_w = pressure in wetting phase, ρ = density difference between phases, g = gravitational acceleration, h = height of capillary rise, γ = interfacial tension, θ = contact angle, r = inner radius of capillary.

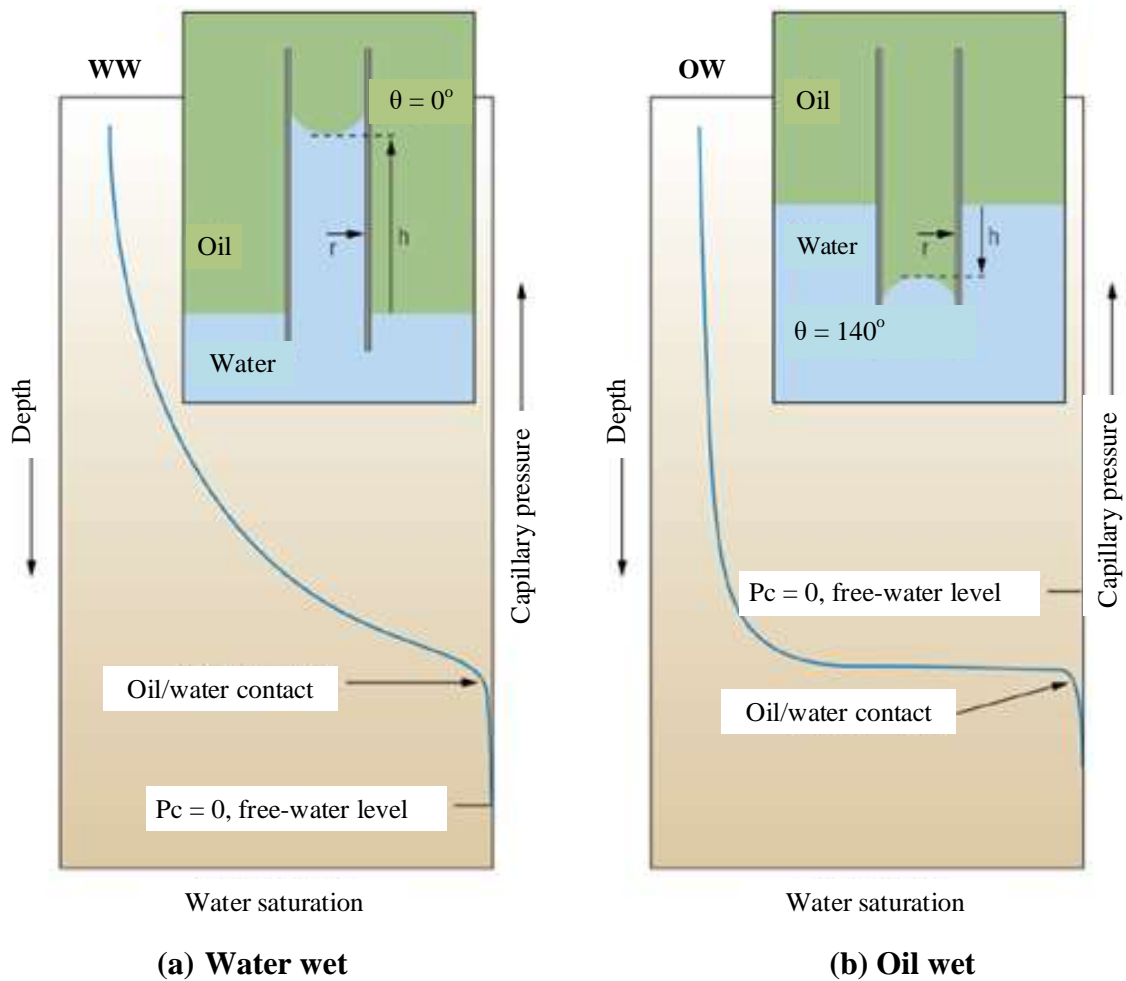


Figure 2.1: Forming a transition zone

Source: (Abdallah et al., 1986)

In a capillary tube, water-wetting (WW) surface forces cause water to rise (a), displacing oil, but if the tube inner surface is oil-wetting (OW), the oil will push water down (b). The wetting force, and therefore P_c , is inversely proportional to the capillary radius. The capillary rise, h , is determined by the balance of wetting forces and the weight of fluid displaced from the bulk-fluid interface. Translating this to a porous formation, there is a free-water level (FWL) defined where the capillary pressure between water and oil is zero. Since porous rocks have a distribution of pore and pore-throat sizes (similar to a distribution of capillary tubes) at any given height above the FWL, the portion of the size distribution that can sustain water at that height will be water-saturated. At greater height, the buoyancy of oil in water provides greater capillary pressure to force water out of similar voids. In a water-wet formation (left), the oil/water contact is above the FWL indicating that pressure must be applied to force oil into the largest pores. In an oil-wet formation (right), the contact is below the FWL,

signifying that pressure must be applied to force the water phase into the largest pores. The oil/water contact divides the zone containing mostly oil from the one containing mostly water.

Because the impact of wettability extends from pore scale to reservoir scale, wettability can affect project economics. Through the parameters S_{wi} and S_{or} , wettability influences oil recovery, one of the most important quantities in the exploration and production business. In addition, the relative permeabilities of oil and water vary with formation wettability. In projects with huge upfront capital expenditures for facilities, such as those in deepwater areas, failure to understand wettability and its ramifications can be costly.

Wettability affects waterflood performance, which also can involve significant upfront spending (Abdallah et al., 1986; Anderson, 1987b). Imbibition forces (the tendency of a formation to draw in the wetting phase) determine how easily water can be injected and how it moves through a water-wet formation. Water breakthrough occurs later in a waterflood, and more oil is produced before the water breaks through in a water-wet reservoir than in an oil-wet reservoir.

The sole purpose of culturing the biosurfactants for enhanced oil recovery in this study, is to be able to overcome the wetting forces that trap the oil, through reduction in interfacial tension and wettability alteration. The idea is to alter the wetting preference of the formation to be more water-wet, and to decrease the interfacial tension between the fluids, thereby decreasing the wetting forces.

2.4 Wettability alteration

Wetting forces lead to an equilibrium condition between at least three substances: a solid and two fluids (Abdallah et al., 1986), the constituents and conditions for all three substances influence the wetting preference. Thus, we must consider the oil components, the brine chemistry and the mineral surface, as well as the system temperature, pressure and saturation history (Buckley, Liu, & Monsterleet, 1998). The key to changing the wettability of a naturally water-wet surface is the oil composition, and this is because any wettability-altering components are in the oil phase. These are polar compounds in resins and asphaltenes, both of which combine hydrophilic and hydrophobic characteristics. Bulk oil composition determines the solubility of the polar components (Al-Maamari & Buckley, 2003). For

components of an oil to alter wetting, the oil phase must displace brine from the surface. The surface of a water-wet material is coated by a film of the water phase (Hirasaki, 1991).

2.5 A pore level view

The application of the wetting principles discussed above is complicated by pore geometry. Understanding a contact angle is easiest when the surface is a smooth plane. However, pore walls are not smooth, flat surfaces, and typically, more than one mineral species composes the matrix surrounding the pores. In reality, the complex geometry of a pore is defined by the grain surfaces surrounding it. The capillary entry pressure in this geometry relates to the inscribed radius of the largest adjacent pore throat. Although most of the pore body may fill with oil, the interstices where the grains meet is insufficient to force the non-wetting oil phase into those spaces (Abdallah et al., 1986).

Thus, depending on the pore and pore-throat geometry and the surface roughness, some parts of the pore space are oil-filled and the others are brine-filled (assuming no gas saturation). Some solid surfaces are in contact with oil, and for some or all of those surfaces, the water film may not be stable. The surface wetting preference can be changed where the fill is not stable, resulting to a situation of mixed wettability, where some parts of the pore surface are water-wetting and others are oil-wetting. The generally accepted theory is that because of the way this condition arose (Figure 2.2), the large pore spaces are more likely to be oil-wetting, and the small pore spaces and interstices within pores are more likely to be water-wetting (Radke, Kovscek, & Wong, 1992; Salathiel, 1973).

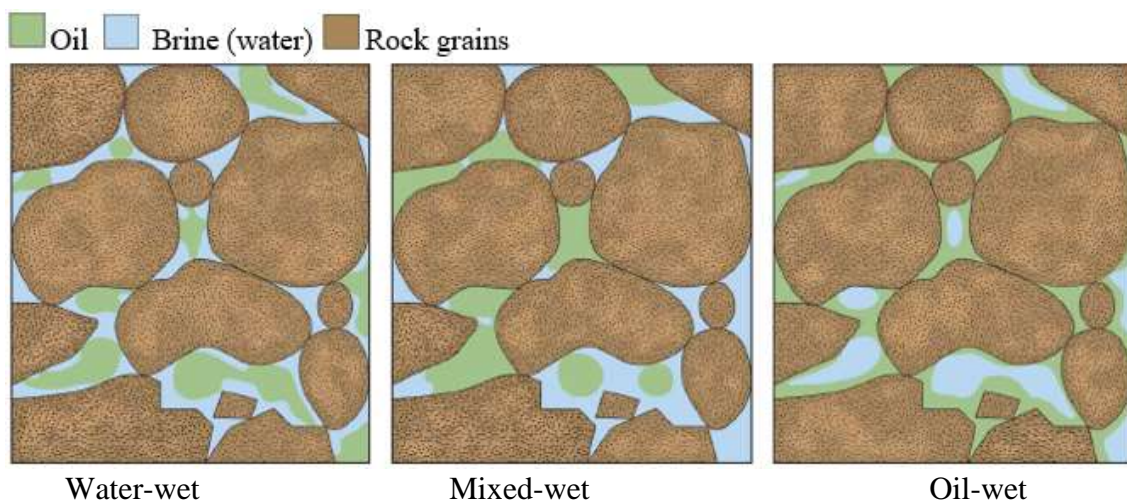


Figure 2.2: Wetting in pores

Source: (Abdallah et al., 1986)

2.6 Wetting in porous media

For any alteration of core wettability, the initially brine-saturated cores are flooded with crude oil to establish an initial water saturation and an initial measurement of the oil permeability is made. The value of initial water saturation, aging time, and aging temperature are the main variables associated with the extent of wetting alteration at this stage.

Darcy's Law describes the relationship between pressure head loss and flow rate in a homogenous porous media saturated with a monophasic fluid, which is moving through it (Dake, 2001). In the absence of gravity and for a linear geometry, fluid flow rates depend on:

- The geometry of the system; area (A) and Length (L)
- Fluid viscosity (μ)
- Pressure head loss across the media (Δp)

Experiments have shown that, other variables remaining constant, rate (Q) is proportional to A and Δp and inversely proportional to μ and L.

Thus;

$$Q = \frac{kA\Delta P}{\mu L} \quad (2.8)$$

2.7 The use of biosurfactant in microbial enhanced oil recovery

In numerous parts of the world for example the North Sea, Mexico, Angola, Brazil, etc., oil production has been experiencing decline because of oil field development. The increasing high price of crude oil with attendant increase in demand on world markets and the difficulty in discovering new oil fields as an alternative to the exploited oil fields in recent years has contributed to oil decline. Roughly, around 67% of the aggregate petroleum reservoirs in the world are made up of residual oil, which speaks of the relative inefficiency of the primary and secondary production methods. A large amount of residual crude oil in depleted reservoirs can be recovered using MEOR method since the current extraction technique leaves behind about two-third of the original oil in place. This low cost working technology can be used to extract about half the leftover residual oil by utilizing microorganisms to haul out the remaining oil from the reservoirs (Shibulal et al., 2014). In *in situ* MEOR technique, microorganisms inoculated with water are injected into the well and at first will advance into

high permeability zones, which takes close to a fortnight to do their job. The permeable medium of reservoir rock is a natural habitat for microorganisms. The organisms then grow and occlude those zones at a later stage because of their size and the negative charge on their cell surface (Al-Hattali, 2012). This is accomplished by these organisms producing carbon dioxide and methane, gases that enter the pores, actively working at the oil-water interface to possibly squeeze out every ounce of oil. These microorganisms likewise produce biosurfactants that decrease the tension between oil and the rock surface, which help to release the oil. The chemical reaction of these microorganisms in oil releases alcohol and volatile fatty acids. The alcohol reduces the viscosity of the heavy oil, making it sufficiently light enough to flow out. The fatty acids solubilize the rock surface and in this way push oil off them. These alterations of the physical and chemical properties of reservoir rocks and crude oil, extends an opportunity to reverse the declining pattern of oil production by increasing the sweep efficiency and possibly maintain a curve with a positive slope (Rebecca S. Bryant & Burchfield, 1989).

2.8 Surfactant and Biosurfactant

The use of organic substrates for biological oil recovery is considered as a more favourable method than other physical and chemical methods. The amphipathic nature (short chain fatty acids) of surfactant compounds enables it to have both the polar and non-polar sides, which enables them to interact with two phases of immiscible emulsions. On an industrial scale, surfactants are applied to oil reservoirs for the recovery of residual oil (heavy oil fractions) trapped in the rocks (Perfumo, Rancich, & Banat, 2010). This has prompted the need to enhance the recovery of oil from oil reservoirs utilizing biologically based EOR process, also known as MEOR (Sen, 2008).

Biosurfactants, like surfactants are surface active agents that can reduce surface and interfacial tension between oil and water because of their low molecular weight, whereas, their high molecular weight (emulsan) enhances the mobility of heavy oil (Banat et al., 2010; Rosenberg & Ron, 1999). Biological surfactants also reduce viscosity and increase the feasibility of oil recovery processes like micellar flooding, rock wetting and de-emulsification (Brown, 2010; Lazar et al., 2007). Biosurfactant have recently been the focus of extensive research and are preferred to their chemical counterparts because of their several advantages which includes; lower toxicity, non-hazardous, biodegradability, environmentally friendly

and production from renewable raw materials (Desai & Banat, 1997; Pacwa-Płociniczak, Płaza, Piotrowska-Seget, & Cameotra, 2011).

The use of biosurfactants can be considered beneficial as a relatively inexpensive method of oil recovery; however, the bulk availability compared to their synthetic counterparts, limits their application in field studies except for rhamnolipids. *Bacillus* group of bacteria are known for producing potent lipopeptide biosurfactant such as *Surfactin* (Figure 2.3) and *Lychenysin*, using different raw materials have been widely been studied for their high surface activities (Nitschke & Pastore, 2006). The ‘bipolar’ structure of surfactants, have the capacity to partition fluid mixtures that vary in polarity for example oil-water emulsions. Their structure additionally makes it feasible for them to reduce surface and interfacial tensions in both aqueous solutions and hydrocarbon mixtures, making them the ideal candidate for enhanced oil recovery (Desai & Banat, 1997; Shepherd, Rockey, Sutherland, & Roller, 1995).

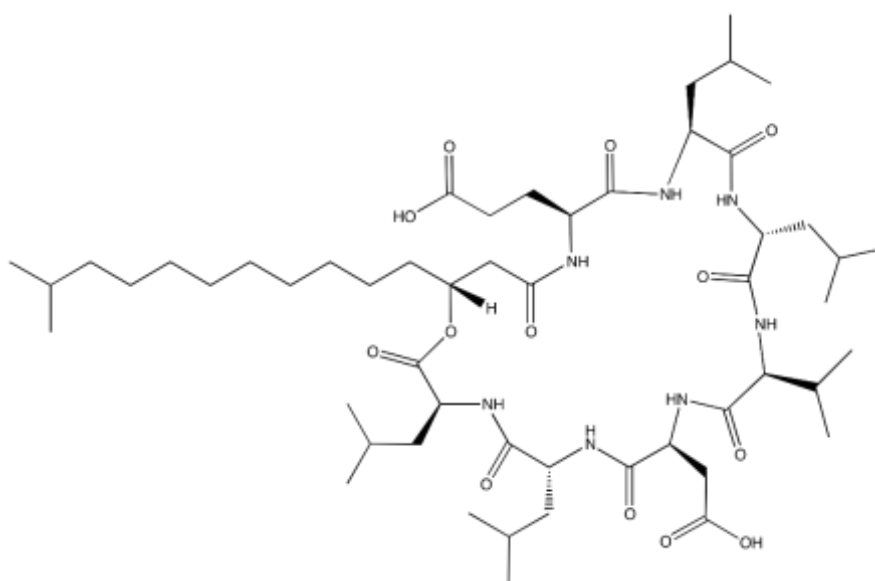


Figure 2.3: Surfactant structure of surfactin ($C_{53}H_{93}N_7O_{13}$)

Source: (Louisajb, 2011)

2.8.1 Chemistry, Structure and Classification of Surfaces active compounds

Surface active agents (bio/surfactants) are of synthetic or biological origin. They are amphiphilic surface active agents (short-chain fatty acids), with a characteristic structure consisting of one molecular component that will have little attraction (solubility) for the surrounding phase (solvent), and a chemical component that have a strong attraction

(solubility) for the surrounding phase. In these aqueous system, the hydrophobic (their tails) is the nonpolar chain hydrocarbon and hydrophilic (their heads) or polar end moieties that reduce the surface tension of a liquid, the interfacial tension between two liquids, or that between a liquid and a solid of the medium in which they are dissolved (Taylor, 2001). A schematic of a surfactant molecule structure is shown in Figure 2.4.

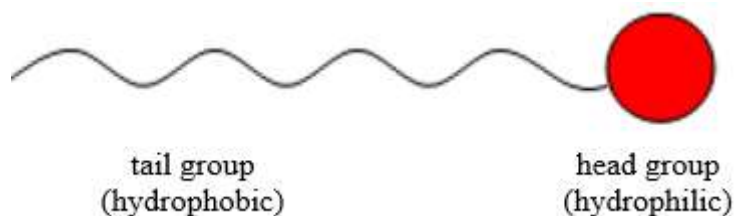


Figure 2.4: Structure of a (bio/surfactant) molecule

Source: (Salehi, 2009)

de Guertechin, (2001) classified surfactants into four general groups, and it is the nature of the polar head group which is important to apportion surfactants into various categories. These groups are; *anionic*, (negative charge), *cationic* (positive charge), *nonionic* (wetting agent), and *zwitterionic* (both a negative and a positive charge). These materials have the tendency to adsorb at the interfaces of a system, or to form aggregates in solution at very low molar concentrations.

This surfactant adsorption phenomenon can be explained thus that when a surfactant is dissolved in a solvent (water), the hydrophobic group causes an unfavourable distortion (ordering) of the liquid structure and the result would be an increase in the overall free energy of the system and a decrease in the overall entropy of the system as seen in Figure 2.5. This entropy of the system can be regained when surfactant molecules are transferred to an interface and the associated water molecules are released. Therefore, the surfactant will adsorb, or it may undergo some other process like micelle formation to lower the energy of the system. On the other hand, the presence of surfactant molecules at the interface decreases the amount of work required to increase the interfacial area, resulting in a decrease of surface or interfacial tensions.

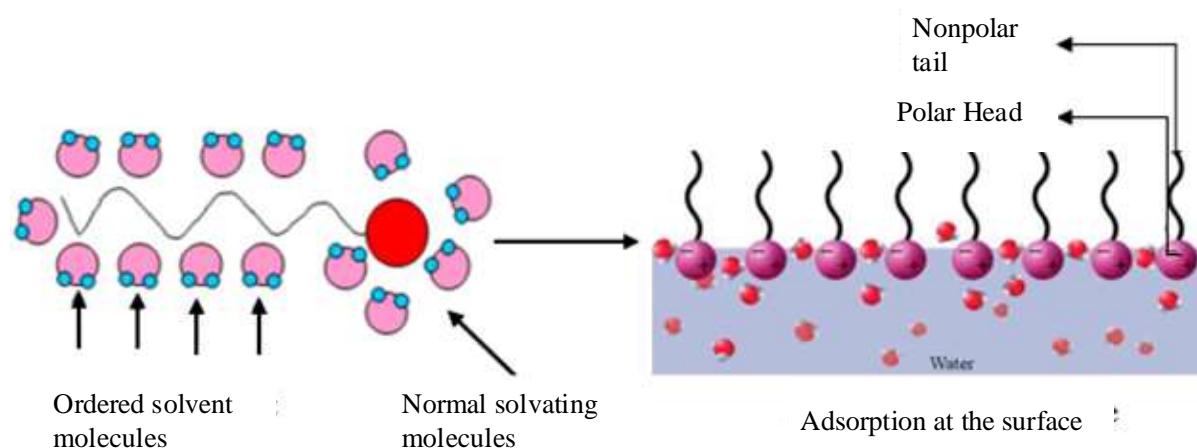


Figure 2.5: Surfactant adsorption process at interface

Source: (Myers, 1999)

2.8.2 Biosurfactant Producing Microorganisms

A number of microorganisms, such as bacteria, yeast and fungi are some of things that produce biosurfactants in an extracellular process synthesizing useful low-cost substrates or raw materials (P. K. Rahman & Gakpe, 2008). Oil contaminated soil with a large amount of hydrocarbons that are composed of complex chemical structure such as aliphatic and aromatic hydrocarbons, have biosurfactants producing microorganisms present in them. This makes the production of biosurfactant a required characteristic of hydrocarbon-degrading bacteria (Bento, de Oliveira Camargo, Okeke, & Frankenberger, 2005). Microorganisms can also produce biosurfactants and utilise the hydrocarbons as substrate either through mineralising them or converting them into harmless products. Biosurfactants producing bacteria along with nutrients have been introduced by most studies into the oil wells in order to permit their growth and activity. However, the suitability of this MEOR strategy, requires bacteria to thrive and be metabolically active at extreme conditions which are characteristic of petroleum reservoirs (Magot, 2005).

Among bacteria, the genus *Pseudomonas* is known for its capacity to produce extensive quantities of glycolipids. A lipopeptide biosurfactant named Surfactin, is produced from *Bacillus subtilis* which is an eight-member cyclic compound made up of seven amino acids and a B-hydroxydecanoic acid moiety. Nakano, Corbell, Besson, & Zuber, (1992), suggested that, based on the presence of a gene locus (*spf*) surfactin is produced. The *spf* gene indicates

production of biosurfactant in many *Bacillus species* creating the basis of the study conducted by (Hsieh, Li, Lin, & Kao, 2004). *Candida bombicola* and *Candida lipolytica* are among the most commonly studied yeast for the production of biosurfactants (Campos et al., 2013).

Most of the biosurfactants are known for their high molecular weight lipid complexes which are normally produced under highly aerobic conditions. Ex-situ production in aerated bioreactors makes this production achievable. The *in-situ* production (and action) becomes advantageous when their large-scale application and soil is encountered. Maintenance of anaerobic microorganisms and their anaerobic synthesis of biosurfactants are required when there is low oxygen availability under the conditions outlined above. Therefore, screening for anaerobic biosurfactants producers in these conditions is of immense importance (M. J. McInerney, Javaheri, & Nagle, 1990).

2.8.3 Biosurfactant in the Petroleum Industry

The hypothesis for use of microorganisms in the improvement of oil recovery was initially proposed for the first time by Beckman in 1926. Zobell was the first to carry out investigation of petroleum microbiology with application in microbial enhanced oil recovery and this provided a base for researchers to carry out further experiments in that area. The results of these investigations have constantly revealed that under reservoir conditions such as high temperature, pressure and salinity, certain microbes along with proper nutrients and bio-catalysts can grow and produce biosurfactants, alcohols, bio-polymers, gases and acids as metabolic by products (Zobell, 1946). By altering saturations and rock wettability these metabolic products can displace trapped oil thus, resulting in enhanced oil recovery from oil reservoirs.

According to Zobell the main mechanisms behind oil release from permeable media are processes such as bacterial metabolites that break up inorganic carbonates; bacterial gases which reduce the viscosity of oil, thus increasing its flow; surface-active substances or wetting agents produced by some microbes; and the high affinity of bacteria for solids to crowd off the oil films, processes by which bacterial products (gases, acids, solvents, surface-active agents, and cell biomass) releasing oil from the sand pack columns in wet labs were patented by Zobell (Shibulal et al., 2014).

2.9 Classification and mechanisms of MEOR

2.9.1 Classification of MEOR

Tertiary recovery has remained an attractive but unrealized prospect for the oil business. One type of tertiary oil recovery that does not need exceptional investments is microbial enhanced oil recovery. With abundant and easily producible oil supplies diminishing, MEOR could be the breakthrough to conventional water flooding. Figure 2.6, shows the basic process in MEOR, which can be actualized by two noteworthy methodologies: either as *in situ* procedure utilizing indigenous microorganisms or *ex situ* process where bioproducts are created outside of oil wells and directly injected to enhance oil recovery (Perfumo 2010). The single well stimulation as depicted in Figure 2.7 has also been termed a very effective MEOR method.

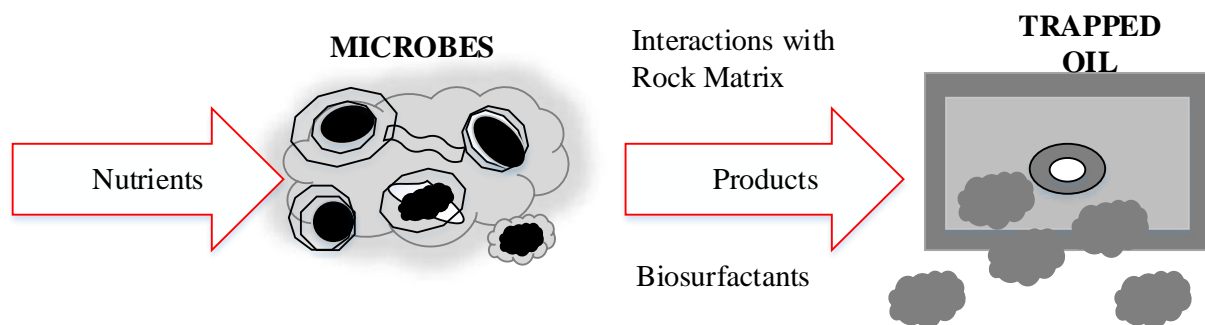


Figure 2.6: The basic process of microbial enhanced oil recovery

Source: (Perfumo 2010)

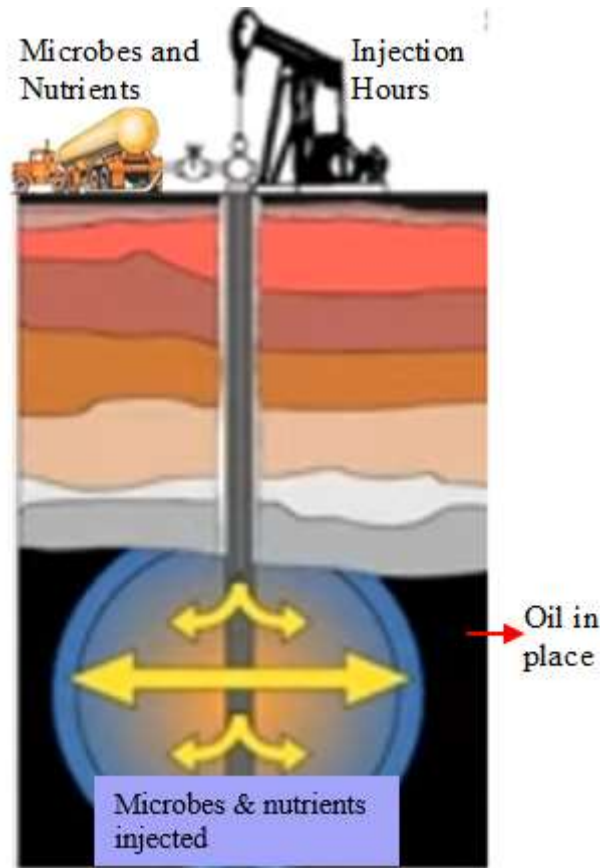


Figure 2.7: Cyclic microbial oil recovery

Source: (Hsieh et al., 2004)

2.9.2 MEOR mechanism

The main mechanism for MEOR process is identified based on the end products generated from bacteria metabolism. Rock dissolution, reduction in viscosity and permeability were classified as some of the main mechanisms for MEOR (Janshekar 1985). These mechanisms are similar to that of chemical EOR technique with a difference in the required products coming from bacteria metabolism, and it's expected to satisfy the basic law of thermodynamics. These mechanisms have been proposed to take place through solubilisation, mobilisation, or emulsification, increasing the contact area of hydrocarbons (Santos et al., 2016), as shown in Figure 2.8. More so, it is very necessary to know the characteristics of a reservoir before selection of the type of microbe to use since MEOR mechanism could differ from bacteria to bacteria.

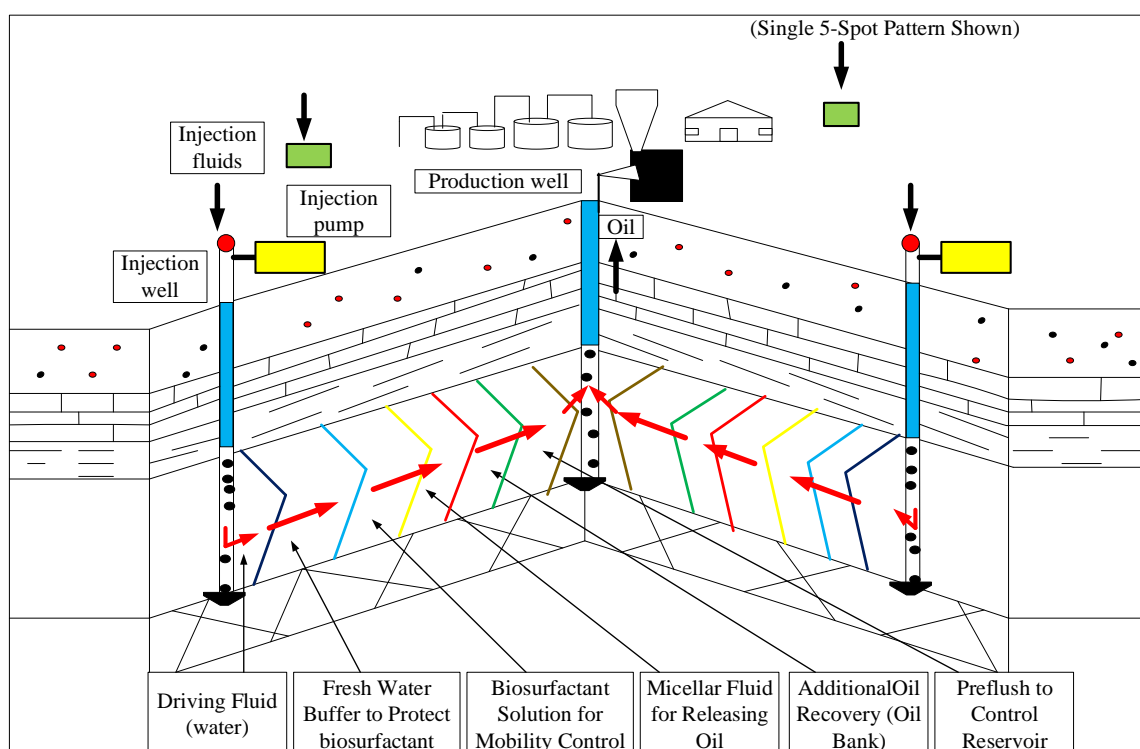


Figure 2.8: Microbial flooding recovery

Source: (Sheehy, 2008)

2.10 Influence of culture medium composition on biosurfactant production

The productions of biosurfactants are seen predominantly during their growth on water immiscible substrates. However, biosurfactants may be produced by some yeast in the presence of different forms of substrates, like carbohydrates. The usage of different carbon sources changes the structure of biosurfactant produced and its properties, and can be exploited to get products with preferred properties for specific applications.

Several investigations carried out relating to the optimization of the physicochemical properties in biosurfactant production, have shown some similarities in the culture conditions, in developing these microbes. In almost all cases, the inoculum used was prepared and incubated overnight, which is the ideal procedure for better results. However, in some experiments the inoculum was isolated from an oil contaminated soil. Based on literature biosurfactants have been cultured at different ranges of temperature and pH in a controlled fermenter. For example, Anita and Roberto, (2014) used vinasse as a substrate in the fermentation process for the production of biosurfactants well as inoculum fermentation media by *Bacillus subtilis* PC, in order to reduce environmental impacts generated by this effluent and cut down production costs. The operating conditions; temperature and stirring rate were kept constant at 30°C and 120 rpm, and pH value of 6.5. The successful isolation

of an anaerobic thermophilic bacterium named AR80 was evaluated by Purwasena, Sugai, & Sasaki, (2014) to know its probability as a candidate for MEOR. It was identified as a strain belonging to the *Petrotoga* sp. AR80 decreased the oil viscosity by 60% in the culture medium and grew well in a reservoir of brine supplemented with yeast extract (0.05 g/l). The most suitable conditions in which AR80 grows well are at temperatures between 50°C and 70°C and at salinity of <30 g/L. The core flooding experiment revealed that this bacterium can possibly enhance MEOR and reduce excessive costs.

The production experiments of *Bacillus subtilis* lipopeptide biosurfactant was carried out at 37°C and at pH 7.0 (Ghribi and Ellouze, 2011), using carbohydrate as the carbon source and ammonium chloride as inorganic nitrogen source. The inocula was incubated in a rotatory shaker at 200rpm and kept overnight. Special conditions were devised to produce biosurfactant from three *Candida* strains at culture conditions of temperature, 20°C and pH 7.0 (Mandy et al., 2012). Sucrose concentration of 1.0% and (NH₄)₂SO₄ concentration of 12% nitrogen source was best for biosurfactant production. Yields of biosurfactants grown on *Bacillus licheniformis* strain were considerably higher in cultures grown anaerobically at a C/N ratio of 1:24, pH 7.0, and temperature of 30°C. Concentrations of NaCl and Na₂S and on water characteristics in the medium broth favoured biosurfactant production (Gogotov and Miroshnikov, 2009).

2.10.1 Carbon Source

Carbon is a very essential component of media for microbial growth and different microorganisms that produce biosurfactant. It is therefore important to select a suitable carbon supplements which would affect the composition of the produced biosurfactant. A biosurfactant produced by *Y. lipolytica* IA 1055 was identified by Sarubbo et al., (2001), using glucose as a carbon source and concluded that the stimulation of biosurfactant production is independent on the presence of hydrocarbons. Kitamoto et al., (2001) studied the production of mannosylerythritol lipids (MEL), a biosurfactant produced by *Candida antarctica*, using different *n*-alkanes as carbon source. The productivity of MEL was significantly affected by the chain-length of the alkane substrates, with the highest productivity obtained from *n*-octadecane. Zinjarde & Pant, (2002), demonstrated the surfactant biosynthesis by *Y. lipolytica* NCIM 3589 using soluble carbon source such as glycerol, glucose and sodium acetate. Reduction in surface tension was better when glucose, sucrose, yeast extract, beef extract, sodium pyruvate and tri sodium citrate were used as

carbon sources. Mannan-proteins have been produced by *Kluyveromyces marxianus*, using lactose as the soluble substrate (Lukondeh, Ashbolt, & Rogers, 2003). The soy molasses, a by-product from the production of soyabean oil, plus oleic acid were tested as carbon sources for the production of sophorolipids by the yeast *C. bombicola* (Solaiman, Ashby, Nuñez, & Foglia, 2004). Recently, Karimi, Mahmoodi, Niazi, Al-Wahaibi, & Ayatollahi, (2012) investigated *Enterobacter cloacae* strain which produced different amounts of biosurfactants in the growth culture, using sucrose and n-dodecane as the carbon source. Results indicated that *E. cloacae* had the ability to adhere to the desired surface. The described carbon source, like glycerol, glucose, acetates and other organic acids, as well as pure n-alkanes are quite expensive and cannot reduce the cost of biosurfactant production. An approach to lessen the cost is partial or complete replacement of pure reagents with industrial/agricultural mixtures (Saharan, Sahu, & Sharma, 2012).

2.10.2 Nitrogen Source

Nitrogen is important in the biosurfactant production medium because it is an essential component of the proteins that are essential for the growth of microbes and for production of enzymes for the fermentation process. Several sources of nitrogen have been used for the production of biosurfactants, such as sodium nitrate, meat extract and malt extract (Mata-Sandoval, Karns, & Torrents, 2001), urea, peptone, ammonium sulphate, ammonium nitrate (Thanomsub et al., 2004). Yeast extract is the most widely used nitrogen source for biosurfactant production, but its required concentration depends on the nature of microorganism and the culture medium to be used. The production of biosurfactants often occurs when the nitrogen source is depleted in the culture medium, during the stationary phase of cell growth. Lukondeh et al., (2003) investigated the production of biosurfactant by *K. marxianus* FII 510700 using yeast extract (2 g L⁻¹) and ammonium (5 g L⁻¹) as nitrogen sources.

The composition and characteristics of biosurfactants are influenced by the external electron acceptor for respiration, nature of the nitrogen source, presence of sulphur, manganese, iron, magnesium and phosphorus in the media. Therefore, the fundamental factors for understanding, forecasting and designing MEOR projects successfully is to determine which mechanisms that allow bacteria to increase oil recovery (Shabani Afrapoli, Nikooee, Alipour, & Torsater, 2011).

2.11 Economical and promising alternatives for Biosurfactant Production

For the production of commercially viable biosurfactants, the development of efficient and successfully optimized bioprocesses, including optimization of the culture conditions and cost-effective recovery processes for maximum biosurfactant production and recovery needs to be improved. More so, the use of inexpensive and waste substrate for the formulation of fermentation media which lower the initial raw material costs involved in the process needs to be harnessed. The use of agro-based low-cost raw materials (Table 2.1), have been explored extensively and were found to be suitable for microbial growth and substrates for biosurfactant production (Al-Bahry et al., 2013; Joshi et al., 2008).

2.12 Biosurfactants as potential candidate for wetting agents

In investigating wettability alteration at pore scale, Karimi et al., (2012) used *Enterobacter Cloacae* strain which produced different amounts of biosurfactants in the growth culture, using sucrose and *n*-dodecane as the carbon source. This strain which was isolated from an oil contaminated soil sample is a facultative anaerobic gram-negative bacterium that changed the wettability towards water-wet state. High amounts of biosurfactants were produced from *E. cloacae* and when *n*-dodecane was used, it considerably reduced the surface tension. Also the contact angle measurement high-lighted the importance of inclusion of microbial cells for wettability alteration. (Afrapoli, Crescente, Alipour, & Torsaeter, 2009), revealed the effectiveness of *Rhodococcus sp.* 094 (an alkane oxidizing bacteria), to increase oil recoveries from Berea sandstone cores using the Amott index method. The bacteria was isolated from the sea water (fjord of Trondheim) that has the tendency of extremely forming a stable crude oil-in-water emulsion. Interfacial tension reduction and the effect of wettability on residual oil saturation resulted during metabolic activities. The experimental results by Kowalewski, Rueslåtten, Steen, Bødtker, & Torsæter, (2006), showed the importance of bacterial on IFT reduction and wettability change towards water wet. The oil degrading bacteria (Aerobic mesophilic) used, grew on the oil-water interface with saturated sandstone core and cultured at temperatures between 20°C-45°C for optimum growth. However, the core (sandstone) experiment carried out revealed a low total production of oil. It is interesting to note here that the growing of bacteria in this interface can result to a major increase in oil recovery upon water flooding. The application of bacterial/fungal biofilms on quartz resulted in wettability changes in the direction of more oil wet, characterized by high dome-spherical droplets of water, with contact angle of greater than 90°C (Polson et al., 2010).

Table 2.1: Use of cheap raw materials to produce biosurfactants by various microbial strains

Low cost or waste raw material	Biosurfactant type	Producer microbial strain	Maximum yield (g/l)	Reference
Rapeseed oil	Rhamnolipids	<i>Pseudomonas</i> sp. DSM 2874	45	(Trummmler, Effenberger, & Sylclatk, 2003)
Babassu oil	Sophorolipids	<i>Candida lipolytica</i> IA 1055	11.72	(Vance-Harrop, Gusmão, & Campos-Takaki, 2003)
Turkish corn oil	Sophorolipids	<i>Candida bombicola</i> ATCC 22214	400	(Pekin, Vardar-Sukan, & Kosaric, 2005)
Sunflower and soybean oil	Rhamnolipids	<i>Pseudomonas aeruginosa</i> DS10-129	4.31	(K. S. M. Rahman, Rahman, McClean, Marchant, & Banat, 2002)
Sunflower oil	Lipopeptide	<i>Serratia marcescens</i>	2.98	(K. S. M. Rahman et al., 2002)
Soybean oil	Mannosylerythritol lipid	<i>Candida</i> sp. SY16	95	(H.-S. Kim et al., 2006)
Oil refinery waste	Glycolipids	<i>Candida Antarctica</i> , <i>Candida apicola</i>	10.5	(Deshpande & Daniels, 1995)
Curd whey and distillery waste	Rhamnolipids	<i>Pseudomonas aeruginosa</i> strain BS2	0.92	(Dubey & Juwarkar, 2004)
Potato process effluents	Lipopeptide	<i>Bacillus subtilis</i>	2.7	(Noah, Bruhn, & Bala, 2005)
Cassava flour wastewater	Lipopeptide	<i>B. subtilis</i> ATCC21332, <i>B. subtilis</i> LB5a	2.2	(Nitschke & Pastore, 2006)

Source: (Muthusamy, Gopalakrishnan, Ravi, & Sivachidambaram, 2008)

2.13 Waterflooding

A predominant fraction of the world's oil reservoirs is produced by the solution gas drive mechanism (Gulick & McCain Jr, 1998). This drive mechanism has low energy and thus leaving behind large quantities of oil trapped in small pores of the rock formation, when the production reaches its economic limit. In addition, poor displacement efficiency, viscosity forces and reservoir heterogeneities contributes to the problem of leaving behind huge reserves of unproduced oil (Elraies & Tan, 2012; D. K. F. Santos, Rufino, Luna, Santos, & Sarubbo, 2016). One of the cheapest and most popular means of maintaining and restoring reservoir energy is waterflooding. Waterflooding is the most predominant improved recovery process in both onshore and offshore regions. This recovery method consists of injecting water through an injector well to push oil to the producing wellbore, which can lead to an increase of total recovery up to 40 – 50% of OOIP (Bachmann et al., 2014).

The history of waterflooding goes back to the 1860s. However, the use of waterflooding as a means of recovery was not widely accepted until the 1950's where there was discovery of several gigantic reservoirs (i.e. Wasson, Slaughter, Levelland, North and South Cowden, Means, and Seminole) in West Texas (Gulick & McCain Jr, 1998). These reservoirs were found in highly heterogeneous shallow shelf carbonates and had a solution gas drive mechanism. Thus, the reservoir energy depleted within a few years and producing rates rapidly dropped. Consequently, it was crucial to find a way to restore and maintain the reservoir energy, hence the wide use of water injection.

2.14 Biosurfactant flooding

MEOR is the tertiary recovery of oil in which microbes or their metabolic products are used to enhance and recover residual oil. Zobell, (1946), patented a process for secondary oil recovery, using anaerobic, hydrocarbon-utilising, and sulfate-reducing bacteria such as *Desulfovibrio* species *in situ*. Updegraff & Wren, (1954), the proposed that this bacterium use molasses as a nutrient to produce large amounts of organic acids and carbon dioxide to enhance oil recovery in wet labs. In studies conducted by Bond, (1961), he injected 5,000 gal of agar medium containing sand and *Desulfovibrio hydrocarbonoclasticus* into a sandstone reservoir initially producing 15 bbl/day, at a depth of 3,000 ft. The well was shut for 3 months after injecting the inoculum, for the bacterial growth and action. After production started again, the well produced 25 bbl/day.

The process of injecting bacterial spores along with nutrients into a reservoir was patented by (ZoBell, 1947). In his findings, a medium containing molasses and spores of *Clostridium roseum* was passed through a sand packed column saturated with oil. The spores would germinate in the reservoir and enhance oil recovery from the reservoir rock, bringing about a 30% increase in oil recovery. Similar results in the release of oil was studied by A. Johnson, (1979), inoculating a mixed culture of *Bacillus* and *Clostridium* spp. (1 to 10 gal) with crude molasses and mineral salts as nutrients, in 150 stripper wells in the USA. These wells have an average reservoir temperature of 38°C, depths 200 to 1000 ft, porosities were 10 to 30% and producing at an average of 2 bbl/day. The additional recovery averaged between 20 to 30% across all the wells. Yarbrough & Coty, (1983), reported increase in oil production from 0.6 bbl/day to 2.1 bbl/day in field test performed in Arkansas, after injecting *Clostridium acetobutylicum* with a 2% solution of beet molasses, during a 6-month period.

In the later works, Rebecca S Bryant & Douglas, (1988), utilised different bacterial strains in Berea sandstone cores which gave additional recovery of 32% compared to water flooding, and some spore forming bacteria even showed 50-60% additional oil recovery. A mixed culture of aerobic and anaerobic bacteria with acid-hydrolysed substances from peat and soils was introduced by (Kuznetsov, 1963), and shut in the well for 6 months. When production reopened, the rate of oil released rose to 300 bbl/day from 275 bbl/day. It is important to know the right amount of bacterial to inject into the reservoir to prevent plugging of the pores to allow for efficient mobilisation of microorganisms through the reservoir pore spaces. One of the main function of biosurfactants is to reduce interfacial tension and in Section 3.3, the IFT experiments were conducted and discussed in Section 4.3.

2.15 Theoretical Background of Pendant Drop Interfacial Tension

The drop shape analysis is a convenient way to measure interfacial tension with the following two principal assumption; firstly, the drop is symmetric about a central vertical axis (it is irrelevant from the direction the drop is viewed) and secondly, the drop is not in motion implying that viscosity and inertia are playing a role in determining its shape (Woodward, 2013). The shape of a liquid drop being acted upon solely by gravitational and surface energy forces is given by the Laplace equation,

$$\gamma = \frac{\Delta\rho g R_o^2}{\beta} \quad (2.10)$$

Where γ (mN/m) is interfacial (surface) tension,

$\Delta\rho$ is the mass density difference between the drop and the surrounding medium (drop density is the oil density while brine density is the external phase density),

g is the gravitational constant,

R_O (nm) is the radius of curvature at the drop apex and

β is the shape factor, as defined by this equation.

Surface tension is determined by a 2-step process. The size parameters R_O and β is first determined from the drop profile and secondly the surface tension is calculated from these parameters by the Laplace equation given above.

The equation describing the drop profile are derived from the Young-Laplace equation and represented in dimensionless form below;

$$\frac{d\theta}{ds} = 2 - \beta y - \frac{\sin \theta}{x} \quad (2.11)$$

$$\frac{dx}{ds} = \cos \theta \quad (2.12)$$

$$\frac{dy}{ds} = \sin \theta \quad (2.13)$$

The co-ordinates x , y , s and θ are illustrated in the pendant drop method profile below.

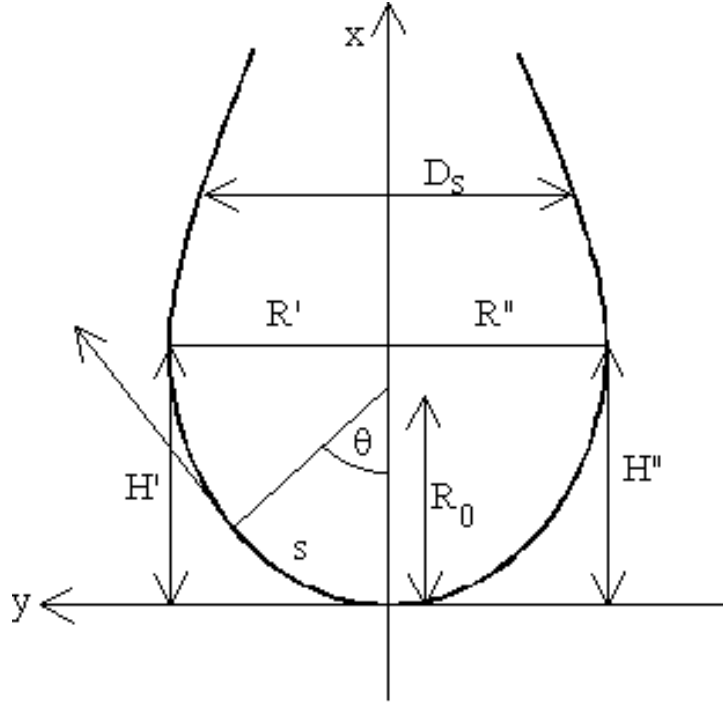


Figure 2.9: Pendant drop method

Source: (Hansen, 1990)

For normal pendant drops that are sufficiently long in order to measure D_s , the maximum diameter, D_E , and the ratio $\sigma = D_s/D_E$ is used (D_s is the drop diameter measured horizontally at the distance D_E from the drop apex).

For pendant drops that are too short to determine D_s , the drop “height”, H , is used and the “radius”, $R = D_E/2$. Therefore, substituting H for R_0 in Equation 2, we have,

$$\gamma = \frac{(\Delta\rho g H^2)}{\beta} \quad (2.14)$$

The values for R_0 and β are found from experimental profile data by several numerical smoothing techniques. For pendant drops, the central axis of the drop is determined by a first order regression line through all data points, using the y-values as the independent and x-values as the dependent variables. However, when using subpixel resolution, results may be improved by correcting for small deviations in the vertical direction, i.e. drop skewness. New x-coordinates are calculated by the equation,

$$x_i' = x_i - a y_i' \quad x_i'' = x_i' - a y_i'' \quad (2.15)$$

Where x' and x'' are the corrected coordinates for the left and right side of the drop, respectively (y' and y'' have opposite signs). More so, the y -values may be corrected in a similar way by using the factor $\sqrt{1 - a^2}$, but these corrections will be very small, because a is very small, and may be neglected. For the determination of R_0 and β , the values for the two sides are averaged; in addition, an asymmetry factor can be calculated from the equation,

$$Ass = (H' - H'') / (H' + H'') \quad (2.16)$$

Here, H is the drop “height”.

What needs to be considered when measuring surface and interfacial tension is the size of the droplet used, which will help to achieve reliable results. At the point when measuring interfacial tension, both density difference and interfacial tension have an impact on the required droplet size. As a rule of thumb, smaller the density difference, bigger the droplet has to be.

2.16 Measurement of Contact Angle

In measuring contact angle, this programme utilises a distinct technique which main strategy uses the full theoretical drop profile that is ascertained in the curve fitting part of an interfacial tension calculation. This implies that the entire drop must be visible, and that the surface must be undisturbed, for example articles like rods and pipette should not be present. Since every one of the conditions of interfacial tension must be satisfied, the contact angle calculation will always be performed when interfacial tensions are measured. Of the theoretical co-ordinates calculated by the numerical integration of the Young-Laplace equation, not very many would coincide with the drop’s endpoint (the horizontal crosshair cursor). The program will therefore interpolate between the two (2) points on each side of the end, utilizing 2 extra points away in a cubic introduction method. This interpolation has been shown to give exceptionally precise values compared to the exact theoretical calculation.

2.17 Chapter summary

- This chapter began by explaining the significance of enhanced oil recovery, influencing factors of remaining oil saturation, and an understanding of wettability. It then detailed the use of biosurfactants in microbial enhanced oil recovery, and identified the main mechanism for this process which includes; reduction in viscosity permeability, rock dissolution, interfacial tension and wettability.

- It further describes several culture medium for bacteria growth, which depend a lot on the carbon source, as it can also change the structure of the biosurfactant produced.
- This chapter also presented promising alternatives that are economical for biosurfactant production, *in-situ* and *ex situ* biosurfactant flooding and a theoretical understanding of the pendant drop equipment utilised later in this study.

The next chapter gives an illustration in a flow chart and discussion of the experimental research methods that will help achieve this research objectives.

Chapter 3

3 Experimental Apparatus, Materials and Procedure

3.1 Overview

This Chapter describes the experimental procedures in Figure 3.1, which were utilised for the successful progression of this study and details the steps involved to ensure that the results obtained were accurate. This chapter covers four phases which includes:

- **Phase I – Microbial Culture:** The isolation and reviving of selected microbes from freeze dried condition was carried out in a fume cupboard to produce bio-surfactants. A description of how the growth media is made is detailed in Section 3.2.1.4 As well as aseptically pouring of agar on petri dishes to prevent contamination and further characterisation of these microbes to determine if they are gram positive bacterial described in Section 3.2.2.1. Proper labelling of agar plates and broths to include name (initials), date and code was ensured to prevent any mix up and enable identification of the different species.
- **Phase II – Interfacial tension and Contact Angle:** The assay used here for the qualitative screening of the produced bio-surfactants was to check for possible reduction in IFT/contact angle. An extensive experiment was carried out across varying temperature, pressure and time to observe the different behaviours of the bio-surfactants. A positive result could give an indication that the produced bio-surfactants can possibly be utilised in enhancing oil recovery. The fluid sample characteristics are detailed in Section 3.3.1.3 as well as the description of the technique used is detailed in Section 3.3.1.1 using the DROPimage programme designed by ramé-hart laboratory.
- **Phase III – Qualitative Wettability Tests:** Two methods for qualitative wettability tests is presented in summary which applies the principle of floatation is described in Section 3.4. The rock grains will be treated with both the oil sample and bio-surfactants to change the grain chemistry thus altering the wettability. Two methods were implored which includes; the floating test and two-phase separation test.

- **Phase IV - Coreflooding:** A description of the core flooding experiment is presented in Section 3.5.1.1 and consists of the major parts of the apparatus which includes the injection system, core holder, the collection system and the data acquisition and control system. The flooding was conducted using the *BS-2* biosurfactant that gave the greatest reduction on interfacial tension of the crude oil, to evaluate its treatment in effectively altering the wettability of Bandera Gray sandstone to enhance oil recovery.

The flow chart (Figure 3.1) represents the steps of the experimental procedure in a summary.

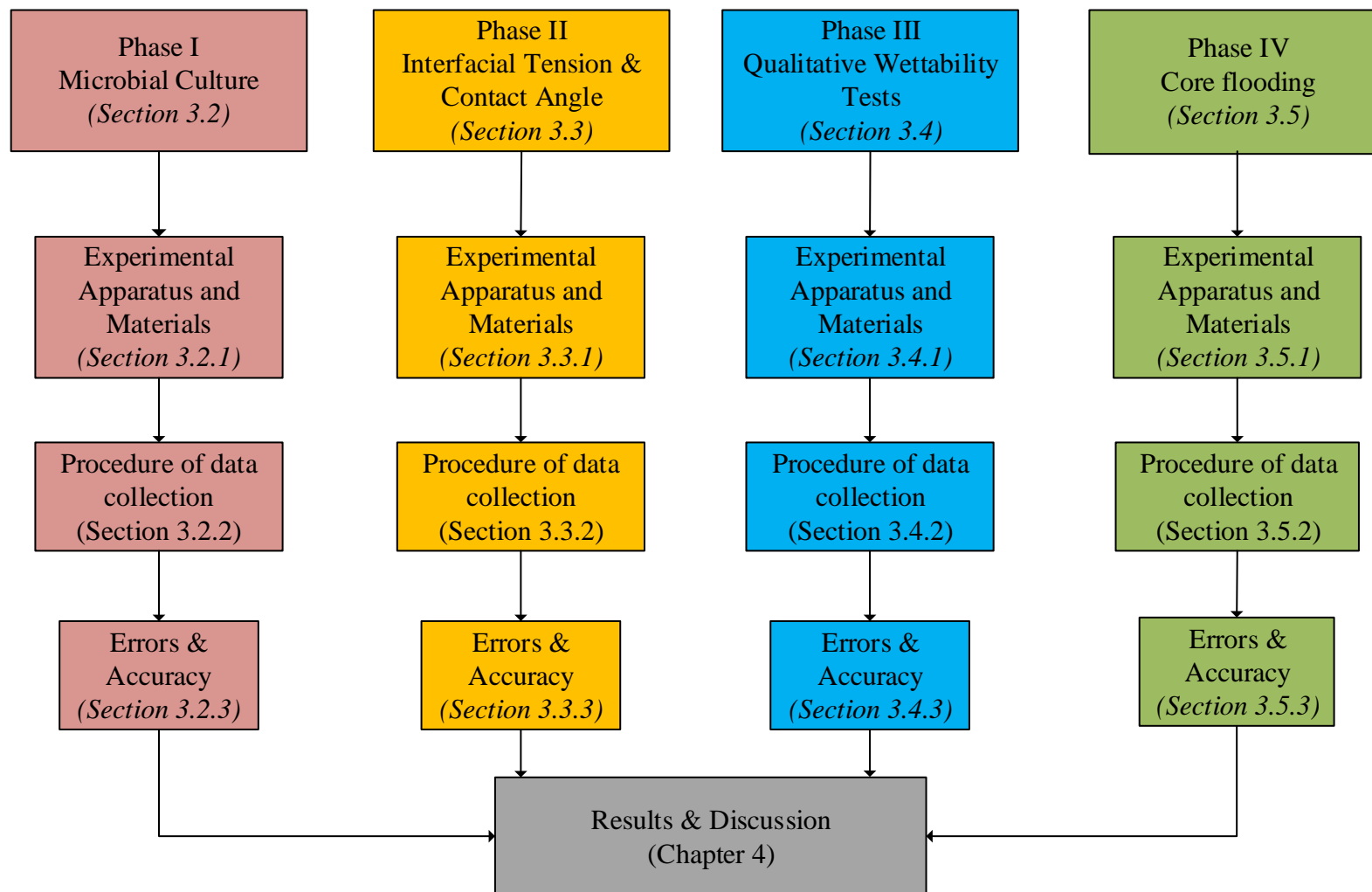


Figure 3.1: Structure and sequence of experimental methodology

3.2 Phase-1: Microbial Culture

3.2.1 Experimental Apparatus and Materials

3.2.1.1 Fume cupboard

The fume cupboard as seen in Figure 3.2, is a large piece of equipment, which was used in the retrieval of the bacteria strains for biosafety, and to prevent contaminating the strains from any external source. The principle of operation is simple: air is drawn in front (open) side of the cabinet, and either expelled outside the building or made safe through filtration and fed back into the room.



Figure 3.2: Retrieving of the selected bacteria strains

3.2.1.2 Eppendorf mastercycler® pro S

The PCR amplification was carried out with the Eppendorf Mastercycler pro S (Eppendorf AG, Hamburg, Germany) which is a fast PCR cycler. It is used to control the temperature of aqueous solutions, suspensions, and emulsions as seen in Figure 3.3. This equipment uses a technique to amplify specific DNA fragments. Only a single DNA fragment is needed to generate a million to a billion copies with a device like this. Tubes with the samples consisting of the right ingredients are placed in the device to start the reaction, and a program is set-up.

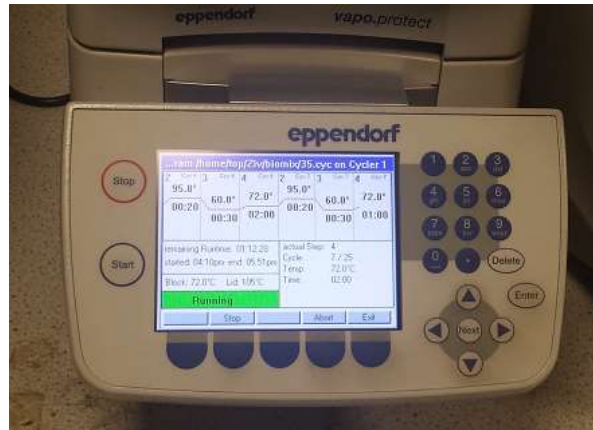


Figure 3.3: Eppendorf mastercycler® pro S

3.2.1.3 Measurement of the Cell Concentration by Optical Density (OD)

Certain covalent bonds in molecules are able to absorb energy at particular wavelengths stretching from infrared to ultraviolet. The absorbance is readily detected by using spectrometer which sends light of a specific wavelength through the sample. The light scattering technique was used to obtain the concentration of cell-free cultures after centrifugation since it cannot measure the cell number or the colony forming unit (CFU). The pure cultures were used to calibrate the system for all organisms and taking care that the cuvette used maintained the correct orientation for adequate passage of light. In Figure 3.4, the 6705-model series UV spectrophotometer has a minimum wavelength of 190 nm and a maximum wavelength of 1000 nm. In this study, the wavelength was set to 600 nm and it directly measures turbidity.



Figure 3.4: UV spectrophotometer

3.2.1.4 Growth Media

Minimal salt medium: Sucrose (30 g L⁻¹), KNO₃ (5 g L⁻¹), KH₂PO₄·2H₂O (1 g L⁻¹), K₂HPO₄·2H₂O (1 g L⁻¹), NaCl (3 g L⁻¹), MgSO₄·7H₂O (0.2 g L⁻¹), CaCl₂·H₂O (0.2 g L⁻¹), was stirred in a duran with 1L distilled water for 30 minutes to mix thoroughly and pH was adjusted to 6.8. The medium was then filter sterilized using a 0.22µm filters and delivered into ninety six (96) universal tubes to a volume of 10 mL each, using an electronic stripette as seen in Figure 3.5. MSM medium was also filter sterilised into durans, containing 200ml and 400ml of media. These were to be the formation media for bacterial cultures, which the interfacial measurements would be later carried out.



Figure 3.5: Liquid nutrient broths

3.2.1.5 Microorganism

As all oil reservoirs are essentially devoid of oxygen, anaerobic bacteria are generally preferred in field applications. The types of bacteria used in this study are listed below and are facultative anaerobes and are able to grow on nutrient agars (Table 3.1).

1. *B. subtilis* was obtained freeze dried from Leibniz Institute DSMZ-German Collection of Microorganisms and Cell Cultures. The organism was maintained and stored as recommended by DSMZ (Nakamura, Roberts, & Cohan, 1999).
2. *B. licheniformis*, type strain from Leibniz Institute DSMZ-German Collection of Microorganisms and Cell Cultures (Chester, 1901), was maintained on nutrient agar at 37°C.
3. *Paenibacillus polymyxa*, type strain formally known as *Bacillus polymyxa* was obtained from Leibniz Institute DSMZ-German Collection of Microorganisms and

Cell Cultures (Ash, Priest, & Collins, 1994). This strain was isolated from field soil in Germany

3.2.1.6 Reference Strains

Table 3.1: Strains used in this study.

Group	Strain	Origin and reference number
Bacteria	<i>Bacillus subtilis</i>	DSM 3256
	<i>Bacillus licheniformis</i>	DSM 1913
	<i>Paenibacillus polymyxa</i>	DSM 740

Strains were used as negative and positive controls for PCR amplifications and gram stain. Sufactants were cultured using specified media that matches with formation water of the proposed reservoir. DSMZ, Deutsche Sammlung von Mikroorganismen und Zellkulturen.

3.2.2 Procedure of data collection

3.2.2.1 Nutrient Agar-Luria Broth

Yeast extract (5 gL⁻¹), peptone (10 gL⁻¹), and sodium chloride (10 gL⁻¹) was prepared in a 1L duran and stirred for 30 minutes with the aid of a magnetic stirrer and flea. Agar (15 gL⁻¹) was added after stirring to produce LB agar. The broth nutrient agar was then autoclaved at 125 °C and 1.6 bar for 45 minutes. Broth was cooled to room temperature and stored at 5 °C until the time of use. Agar was allowed to cool down and then poured into petri dishes and allowed to set before storing upside down to prevent condensation (Figure 3.6). Also, the pouring of the plate (Figure 3.6), was carried out around a bunsen burner to keep the surrounding air from contamination.

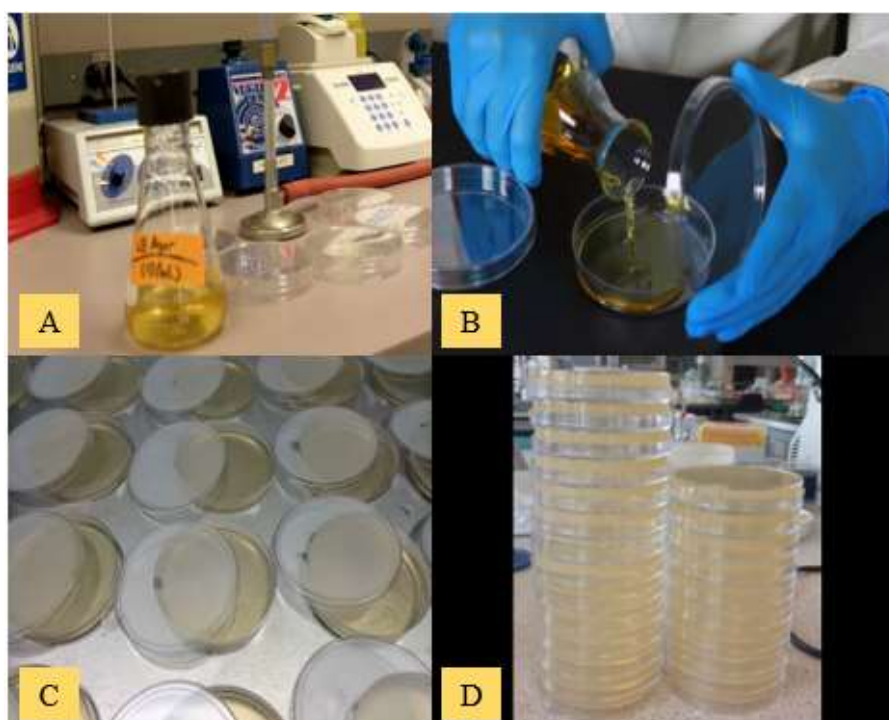


Figure 3.6: Pouring a plate of nutrient agar

3.2.2.2 Bacterial strain revival

This procedure was carried out in a fume cupboard, to prevent any external contamination. Freeze dried strains (DSM 3256, DSM 1913 and DSM 740) were carefully removed from glass tubes using a diamond cutter. 1000 μL of freshly prepared LB media was added to each sample with the aid of generic filters to dissolve the freeze dried strains. The strains were left for 20 minutes to dissolve properly and with the aid of a sterile inoculating loop it was stirred to further aid dissolution.

3.2.2.3 Growth at Different Temperatures

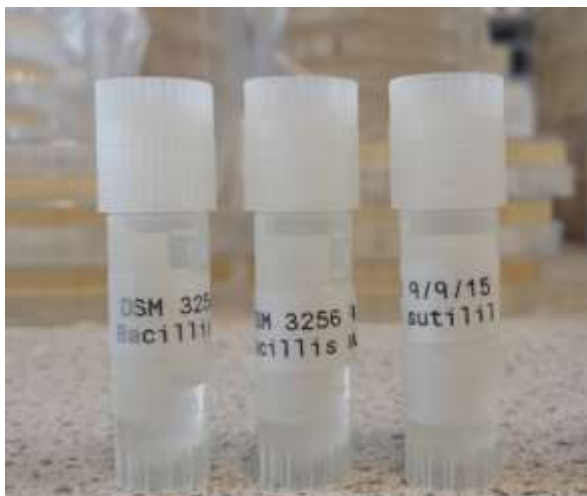
The strains were plated on three (3) agar plates separately and further inoculated into broths previously made, imploring sterile inoculating loop and generic filters respectively. The broth for the three samples where placed in a 30 °C shaking incubator to aid growing. Two samples of the different strains on agar plates were placed in a 37 °C incubator and one sample strain each in a 30 °C incubator to compare which temperature the bacteria grows faster. The growth was checked periodically.

3.2.2.4 Stock Solution (Preservation of the Strains)

A stock solution is a concentrated solution that will be diluted to a lower concentration for actual use. They help to conserve the strains and save preparation time. A stock solution was

prepared by measuring out 750 μ L of 50% diluted glycerol solution and poured into a vial (three each) for the different strains. A further addition of a colony of bacteria from each strain was added to each set of vials separately and vortexed at 1000 rev/min for proper mixing, shown in Figure 3.7. They were then stored at a temperature of -80 °C for preservation.

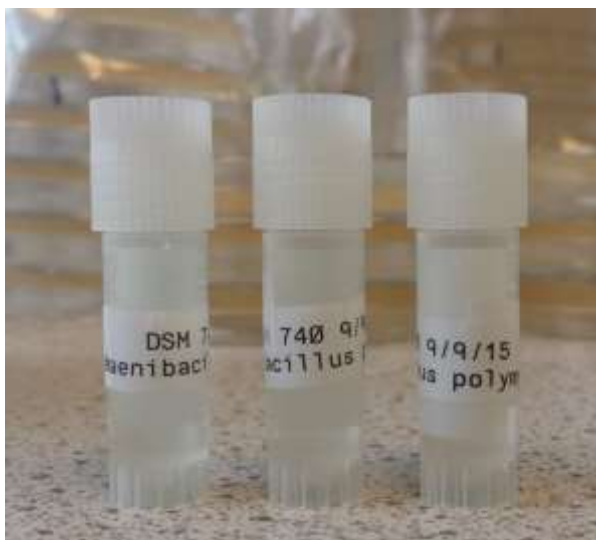
The essence of using glycerol to make the stock solution is such that the bacteria can be stored (kept alive) for as long as needed. The extreme low temperature prevents any further growth of the bacterium.



A. DSM 3256: *Bacillus subtilis*



B. DSM 1913: *Bacillus licheniformis*



a) DSM 740: *Paenibacillus polymyxa*

Figure 3.7: Stock solutions of the revived freeze-dried strains

3.2.2.5 Determination of Phenotypic Characteristics

3.2.2.5.1 Colony Morphology of Microorganisms

On solid agar media, there are various physical appearance that colonies of bacterial and fungal usually exhibit. Characteristics of colonies of a specific microbial species are markedly stable. The characteristic morphology of a microbial colony ordinarily indicates and likely proposes a particular type of microorganism upon examination of gross morphology. Along these lines, any identification scheme for a microbial isolate ought to begin with an intensive depiction of the appearances of colonies. Tentative identification of type of organism (bacterial or fungal) and suspected genera or species, based on colonial morphology, may help early avoidance of an extensive variety of other microbial types thus reducing the number of potential candidates in the subsequent identification steps.

Furthermore, colonial morphology is critical in perceiving mutational changes in the populace which occur upon repeated sub culturing of microbial strains. Mutant colonies generally indicate changes in colonial properties, for example, surface, texture, or colour, which can be easily separated from the wild sort. A description of colony characteristics more often than not, includes the shape (structure), margin, elevation, optical properties, texture, and pigmentation of the colonies.

3.2.2.5.2 Gram-Staining

The gram stain is the most important and universally used technique in the bacteriology laboratory in differentiating bacterial species into two large groups (gram-positive and gram-negative). This technique helps to understand how the gram stain reaction affects both varieties of bacteria based on the biochemical and structural differences of their cell walls. Gram-positives have a thick, moderately impermeable wall that resist decolorization and is made out of peptidoglycan and secondary polymers. Gram-negatives has a thin peptidoglycan layer in addition to an overlying lipid-protein bilayer known as the outer membrane, which can be disturbed by decolorization (Beveridge, 2001).

The procedure is based on the ability of the microorganism to retain color of the stains used during the stain reaction. Gram-positive bacteria are not decolorized by alcohol and will remain as purple (retaining the initial violet stain). The gram-negative bacteria are

decolorized by the alcohol, losing the color of the primary stain, purple (hence show the pink counter stain).

In the gram-stain method for each bacterium:

1. A loop full of the culture was spread on microscopic glass slides and first heat fixed by passing the slide through flame for about 3 seconds until a thin film is formed and allowed to dry.
2. The heat fixed smear was then stained with a basic dye, Crystal Violet, for 30 seconds, which is taken up in similar amounts by the bacteria.
3. After rinsing under tap water, the slides was treated with iodine (I₂) for 30 seconds, which is mordant to fix the stain.
4. The slides was then destained by washing briefly with acetone for 2 seconds.
5. Lastly, counterstained with a paler dye of different color (safranin) for 30 seconds. It was then allowed to dry and viewed under a light microscope.

3.2.2.5.3 PCR Amplification

Polymerase Chain Reaction is an in vitro technique utilised in amplifying DNA sequences with the aid of oligonucleotide primers that are complimentary to specific sequences in the target gene (Willey, 2008; Wilson & Walker, 2010). The region of the chromosome for DNA sequencing must be short comprising of variable sequence flanked by greatly conserved region. To be able to differentiate microorganisms, there must be sufficient variability within the selected sequence. Furthermore the chosen sequence should not be horizontally transmissible to other strains of species (Olive & Bean, 1999).

Subsamples of 3-10 ml of the media from the incubations were filtered through a 0.2 µm filter in order to collect microbial cells on the filter surface. DNA extraction was carried out using the method described by (Griffiths, Whiteley, O'Donnell, & Bailey, 2000) with exception that 1 µg / µl⁻¹ glycogen was added prior to the PEG precipitation stage to increase nucleic acid precipitation efficiency. DNA quantification was performed using Qubit 3.0 Fluorometer and specified reagents (Life Technologies). Samples were stored at -20°C.

Bacteria 16S rRNA genes were amplified with polymerase chain reaction (PCR), using

forward primer pA and reverse primer pH, in Table 3.2. Triplicate 20 µl PCR reactions were performed for each sample using Phusion high fidelity polymerase and corresponding buffer. A mix of 0.2 µl Phusion polymerase (NEB), 4 µl Phusion HF buffer (NEB), 0.4 µl dNTPs (Fisher, 2016), 1 µl of FW and 1 µl REV primer and distilled H₂O was added to 1-3 µl of template DNA up to 20 µl. PCR was performed under the following conditions:

Step 1: Initial denaturation; In this step, the samples are heated to 95°C for 10 minutes, with the main purpose to activate TAQ DNA polymerase.

Step 2: Denaturation; 95°C, 30 seconds. In this step, the double stranded DNA fragment melts open to single stranded fragments.

Step 3: Annealing; 55°C, 30 seconds. Here the hydrogen bonds formed between the primers and the DNA template.

Step 4: Extension; 72°C, 1 minute. A new DNA strand is synthesized behind the primers.

Step 5: Repeat step 2, 3 and 4 for 30 cycles. The number of target DNA will grow exponentially

Step 6: Final extension at 72°C for 5 minutes. This step is performed to ensure the remaining single strand are fully extended.

Step 7: Hold at 4°C for indefinite time, to limit TAQ polymerase activity.

Table 3.2: Nucleotide sequence of the 16s rRNA gene

Primer sequences (5-3 orientation)	Gene target	Annealing temperature, T (C)
AGAGTTTGATCCTGGCTCAG	16s rRNA	55°C
AAGGAGGTGATCCAGCCGCA		

Source: (Edwards, Rogall, Blöcker, Emde, & Böttger, 1989)

Amplicons were gel excised from a 1.5% agarose gel based on band specific excision and purified using Isolate II PCR kit (Bioline). Purified amplicons were then sent to Source Bioscience for sequencing and returned results analysed and using Geneious and BLAST.

The blast program (basic local alignment search tool) is a web search tool to show the identity and similarity (99% - 99.5%) between different species belonging to the same genus.

3.2.2.6 Serial Dilution for bacterial strain

A set of serial dilutions was made for all three strains. In Figure 3.8, a sample of culture in a broth was diluted to 10^{-7} . Streak plating was then carried out using diluted solutions at 10^{-1} , 10^{-4} , and 10^{-6} on agar plates. This was done because agar plate allows accurate counting of the microorganisms, resulting from the equal distribution across the plate. This cannot be done with a fluid solution (broth).

In this study, the dilution series was calculated in the format below;

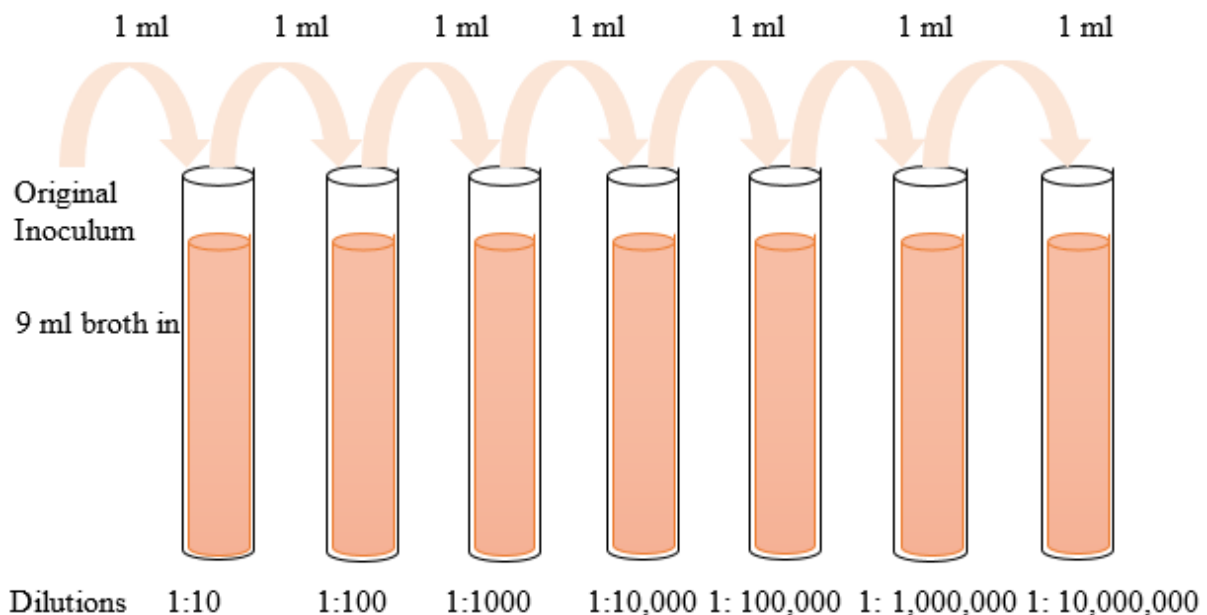


Figure 3.8: Serial dilution for bacteria strain

$$\text{Dilution factor for tube} = \frac{\text{amount of sample}}{\text{Volume of specimen transfered} + \text{volume of diluent tube}} \quad (3.1)$$

The total dilution factor = previous dilution factor of tube \times dilution of the next tube

For this serial dilution;

1 ml culture = 10^{-1} for the first tube

0.1 ml added to 0.9 ml = previous dilution 10^{-1} (first tube) \times 10^{-1} (second tube) = 10^{-2} total dilution.

After successfully culturing, growing and testing the produced bio-surfactants in this section, these bio-surfactants were then introduced into the formation water in a glass bottle at a ratio of 1:1, with a total volume of 400 ml.

3.2.2.7 Biosurfactant Extraction Process

The biosurfactant was finally extracted and produced using the following protocol. A 400 ml of prepared LB broth was inoculated at time point 0 to 0.1 Abs at 600 nm with the selected bacterial culture. After 24-hour growth, cell-free supernatant from the culture broth was obtained by centrifugation at $10,000 \times g$ (m/s^2) for 20 min at $4^\circ C$. The remaining cells were removed by filtration using a $0.2 \mu m$ filters. The cell-free supernatant underwent acid precipitation by adjusting the pH2 using 6 M HCl, and placed at $4^\circ C$ overnight. The precipitate was separated by centrifugation at a relative centrifugal force (RCF) of $10,000 \times g$ (m/s^2) for 25 min at $4^\circ C$ and extracted two times with methanol and solvent evaporated using a rotary evaporator at $50^\circ C$ (Pathak, Keharia, Gupta, Thakur, & Balaram, 2012). Finally, the crude biosurfactant was collected and weighed for total surfactant extraction concentration.

3.2.3 Error and Accuracy

- i. Sample specimen containers (petri dishes, test tubes) were correctly labelled to include, name of the strain, date of preparation and initials of the collector.
- ii. Safety precautions were put in place to avoid contamination of the samples, by wearing safety gloves, and maintaining a sterile environment by flame sterilisation, prior to processing the samples.
- iii. The incubation temperature for growing the cultures was maintained for effective growth rates.
- iv. In using the UV spectrophotometer for measuring the absorbent, the system was first calibrated at a wavelength of 600 nm, by firstly inserting the blank UV quartz cuvettes which is the prepared media (substrate), and then followed with the bacteria samples. This gave a tolerance of ± 0.099 .

3.3 Phase-II: Interfacial Tension and Contact Angle

As all oil reservoirs are essentially devoid of oxygen, anaerobic bacteria are generally preferred in field applications. The types of bacteria used in this study are aerobic microorganism. *Bacillus* are aerobic or facultative anaerobic (having the ability to be aerobic

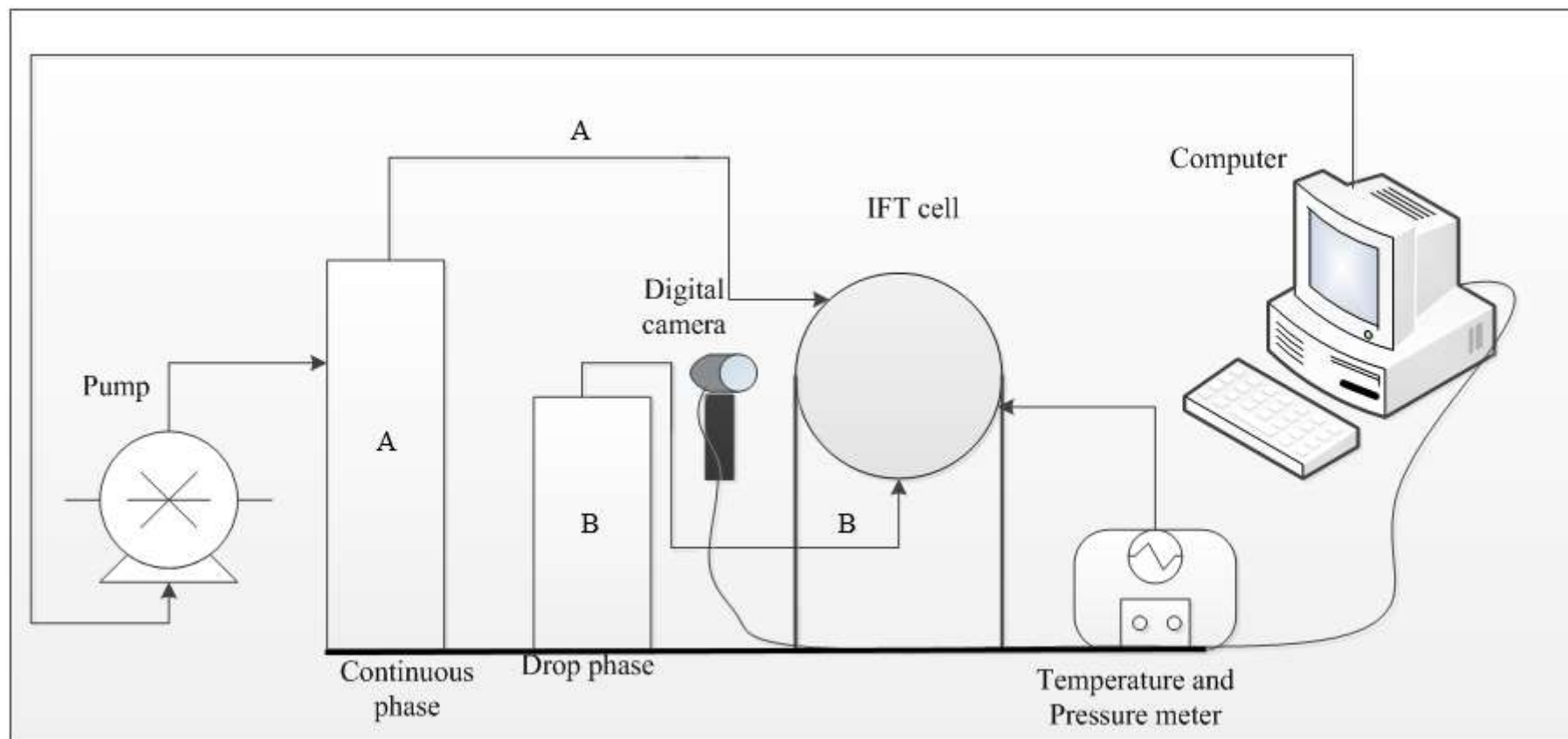
or anaerobic) depending on the species. They are also facultative fermentative and can grow on nutrient agar.

An extensive laboratory study was conducted for the measurement of the interfacial tension between oil-synthetic formation water-bio-surfactant, covering pressure ranges of 0.15 to 13.89 MPa and temperatures of 26 to 75°C. The laboratory experiments were conducted using the pendant drop method combined with the solution of the Laplace equation for capillarity for the profile of the oil drop in the oil-brine equilibrium environment. Measurements were made for each set of temperature and water salinity for pressures of (0.15, 3.10, 5.10, 10.44, 12.51 and 13.89) MPa for a total of 285 IFT (mN/m) measurements.

3.3.1 Experimental Apparatus and Materials

3.3.1.1 The TEMCO Pendant Drop

Investigations of surface and interfacial tension by a pendant drop apparatus consists typically of three parts: a viewing environmental chamber, temperature and pressure control, and observation system to visualise the drop and a data acquisition system to infer the interfacial tension from the pendant drop profile. This can be seen in the schematic sketch in Figure 3.9 and complete set-up as seen in Figure 3.10. The IFT-10 Cell operates to 68.95 MPa (10000 psi) at 176 °C (350°F). Within this range, most reservoir conditions can be safely simulated. The TEMCO Pendant Drop visual cell requires a light source to illuminate an oil drop in its glass windowed chamber approximately 41.5 cm³ by volume. This pendant drop method requires the fluid filling the cell to be transparent, to enable viewing of the drop of the other fluid inside. In this study, with the aid of the pump, the brine-bio-surfactant flowed from the continuous phase into the IFT cell (reservoir), while the oil sample flowed from the drop phase through the capillary needle into the cell. The pendant oil drop (a clinging bubble of oil in brine) was observed in silhouette by the low-power video microscope as seen in Figure 3.11. In Figure 3.12, the temperature and pressure meter were used to regulate the different variations of the reservoir conditions investigated and in turn, operating the DROPImage Advanced software through the computer. The oil drop is equilibrated with other fluids, and if desired, in contact with rock crystals, to simulate in-situ reservoir conditions. Measurement of the oil drop dimensions and fluid densities enables calculation of surface tension. Rigid film formation and aging effects may also be observed.



A. Brine-bio-surfactant, B. Crude oil

Figure 3.9: Schematic illustration of the pendant drop set-up

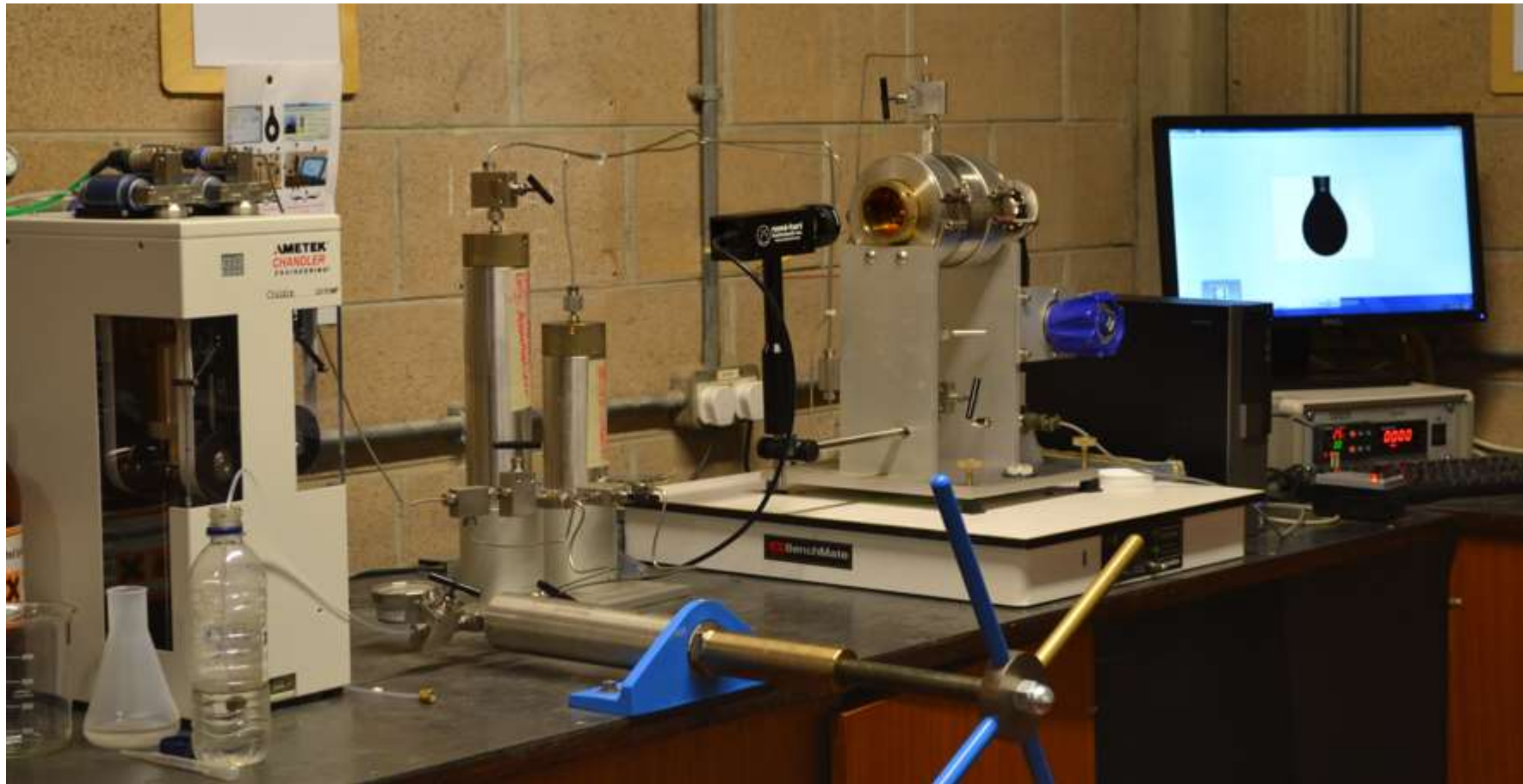


Figure 3.10: The complete set-up of the IFT-cell

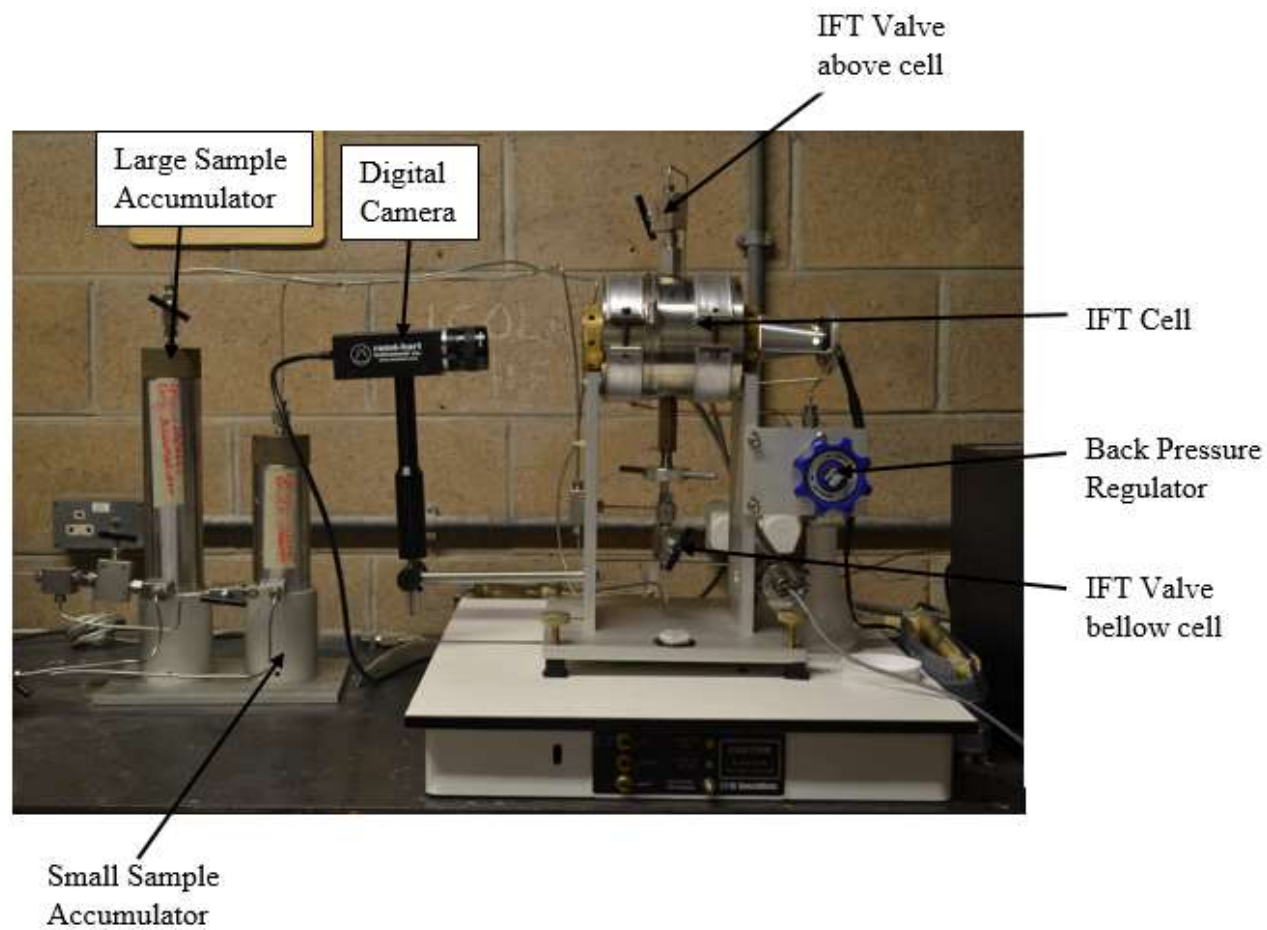


Figure 3.11: Low temperature/high pressure interfacial tension/contact angle cell apparatus

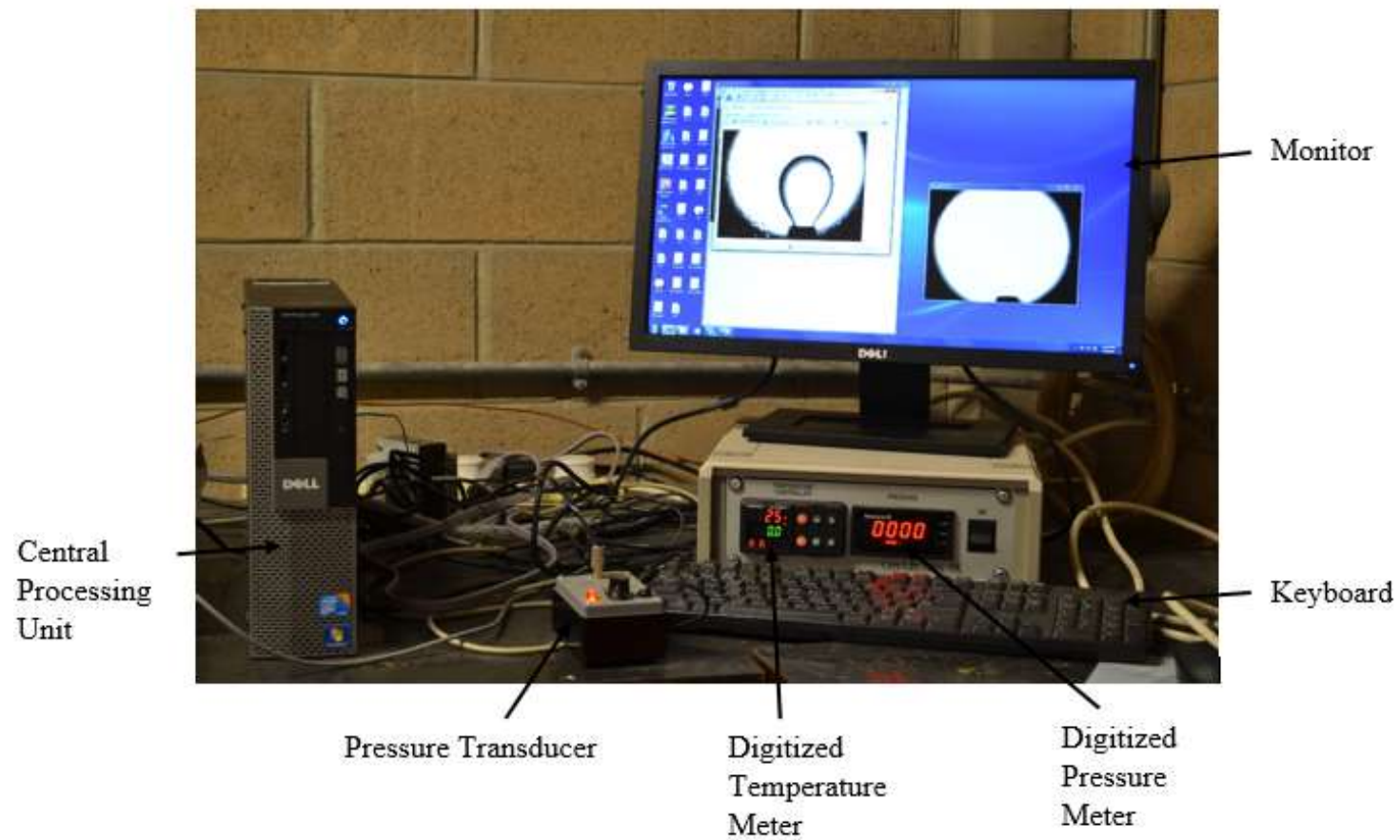


Figure 3.12: Pressure transducer/acquisition section

3.3.1.2 The Quizix pump

The QX series pump (QX-6000) is a completely integrated, self-contained pump Figure 3.13. It is a precision metering pump that can be controlled with a front panel attached directly to the pump, or connected to a computer and operated through Quizix Pump Works© software. The QX series can be used for liquid blending; liquid metering and oil industry applications for example, core analysis. It contains a pump controller which coordinates the activity of two totally independent, positive displacement piston pumps. These two piston pumps can each be used separately for single stroke volumes, or as a pair to give pulseless continuous fluid flow for a single fluid. It can exert a maximum pressure of 6,000 psi, with a maximum flow rate of 50 ml per minute, having stroke volume of 12.3 ml and piston diameter of 0.375 inches.



Figure 3.13: The Quizix pump

3.3.1.3 Fluid Samples

The characteristics of the crude oil from the Niger Delta oil field, and the composition of the synthetic formation water are listed in Table 3.3 and Table 3.4 respectively, and shown in Figure 3.14. The formation water used in this study was reconstructed in the laboratory on the basis of specific formation water analysis from the formation of interest.

Table 3.3: Crude-oil Characteristics

API gravity	Viscosity (cSt)	Density (g/cm ³)	Salt Content (ptb)	Classification
20.3	134.828	0.9322	13.9	Heavy oil



Figure 3.14: Crude oil and synthetic formation water

Table 3.4: Composition of formation water

Salt	Concentration (g/l)
pH @ 25.0 °C	8.17
Calcium Chloride CaCl ₂ ·6H ₂ O	0.8609
Magnesium Chloride MgCl ₂ ·6H ₂ O	0.5102
Sodium Chloride NaCl	21.3026
Sodium Tetraoxosulphate VI Na ₂ SO ₄	0.0887
Sodium bicarbonate NaHCO ₃	14.428
Sodium Carbonate Na ₂ CO ₃	0.8250

3.3.1.4 Produced Biosurfactants

The produced biosurfactants (supernatant and with cells), used in these investigations are represented below with the following abbreviations: **BS-1**: *Bacillus subtilis*, **BS-2**: *Bacillus licheniformis* and **BS-3**: *Paenibacillus Polymyxa*

3.3.2 Procedure of data collection

3.3.2.1 Dilutions of produced biosurfactants with brine.

It should be noted here that for every set of these experiments, the continuous phase comprised of a serial dilution of cells/cell-free biosurfactants with formation water and the drop phase was crude oil. The temperature ranges from $26^{\circ}\text{C} \leq T \leq 75^{\circ}\text{C}$ and pressure, $0.15 \text{ MPa} \leq P \leq 13.89 \text{ MPa}$. Experiments were conducted in real time and lasted between 5.5 hours – 6 hours.

The density calculation for the serial dilution of the synthetic formation water with both supernatant cell-free biosurfactants and biosurfactant with cells follow the same pattern as shown below for **BS-2** cells and presented in Table 3.5 for other biosurfactants used in this study.

Volume, V of solution = 100 ml

Weight of measuring cylinder (W_{tc}) = 47.12 g

W_{tc} + formation water (H_2O_f) = 146.45

$$\text{Mass, } M \text{ of } H_2O_f = W_{tc} - (W_{tc} + H_2O_f) \quad (3.2)$$

$$M = 146.45 - 47.12 = 99.33$$

$$\text{Density, } \rho = \frac{M}{V} \quad (3.3)$$

$$\rho = \frac{99.33}{100} = 0.9933 \text{ g/m}^3$$

Table 3.5: Density measurements for cultured biosurfactants

Biosurfactants	Densities
<i>BS-1</i> Cells	0.9863
<i>BS-1</i> Cell-free	0.9763
<i>BS-2</i> Cells	0.9933
<i>BS-2</i> Cell-free	0.9823
<i>BS-3</i> Cells	0.9939
<i>BS-3</i> cell-free	0.9870

The volume of the produced biosurfactants were kept constant at 200 ml, for both cultures of cells and cell-free. The biosurfactants were diluted serially with the synthetic brine to a ratio of 1:1, thus the addition of 200 ml of synthetic brine with the aid of sterilised filters to prevent contamination of the solution making the total solution 400 ml (Figure 3.15). For optimum measurements, the calibration of the capillary tube was necessary before beginning any experiment. The diameter of the needle was 3.03 mm and measured with the aid of a digital Vernier calliper.



Figure 3.15: MSM and dilutions of produced biosurfactants for cells and cell-free cultures

3.3.2.2 Procedure for Interfacial Tension and Contact Angle Measurements

Given below is a step wise procedure from start to finish of the experimental procedure of how the IFT cell was operated and maintained after use. These procedures help to simulate an actual reservoir condition. Temperature was controlled by an automatic Watlow temperature controller system and wrapping a heating jackets around the IFT cell. The detailed Dropimage program utilised in calculating the IFT and contact angle can be seen in Appendix C.

3.3.2.3 Filling the system with liquid

The brine/bio-surfactant solution was added to the reservoir (IFT cell) by filling each pump cylinder manually using PumpWorks and the following procedure.

- i. Compressed air (4-8 bar) was switched on which connects to the automatic quizik pump and then the entire IFT system was powered on.
- ii. The PumpWorks software was initiated and to fill the pump cylinder with fluid, the safety operating pressure was set to 100 psi (700 kPa) and flow rate set to 50 ml/min.
- iii. The deliver valve was opened, and the fill valve was closed. The direction was set to extend and pump cylinder 2A was started. The end of the fluid outlet tubing was placed into a container of liquid and watched for air bubbles as the piston extends and air is pushed out of the cylinder barrel.
- iv. When the pump cylinder reaches the Max Extend position, the deliver valve was closed and fill valve opened with the direction switched to Retract. The pump cylinder

was re-started and as the piston retracts, fluid was drawn into the cylinder barrel. Then on the next extend stroke mostly air was still delivered out of the fluid outlet fitting.

- v. The procedure was repeated until a piston stroke was reached where no air bubbles come out, only liquid. End with a retract stroke.
- vi. After completely purging of air, the filling of the cell commenced. The automatic pump valve 1B sample valve was connected to a 400 ml beaker already filled with brine solution.
- vii. The valve connecting the automatic pump to the outer phase (100cc accumulator) was fully opened (counter-clock wise). Valve above outer phase accumulator was open and valve below was closed. Valve above cell connected to contact angle was opened and valve under cell connected to needle was closed. The Back Pressure (BP) regulator was turned fully counter clockwise.
- viii. The fill valve was opened to retract fluid in the piston, and deliver valve opened to extend fluid into the continuous phase.
- ix. This procedure continued until the cell (reservoir) was completely filled with brine solution. And this was observed with fluid outing from the exit valve into a beaker.
- x. The pump was then isolated by closing the valve that connects the pump and the continuous phase accumulator and then switched off from the power source.

3.3.2.4 Pressurizing the IFT cell using the hand pump

- i. The 400 ml beaker was filled with brine solution and connected to the manual pump sample valve. The top and bottom valve connecting the 100cc and 50cc accumulator was closed and the sample valve opened. The vacuum barrel of the hand pump was filled with fluid on full counter-clock wise turning, close valve.
- ii. Close valve above cell, connected to contact angle.
- iii. To develop pressure, both valves connecting the outer phase and sample phase were opened. The hand pump turned slowly in clockwise direction.
- iv. When the required pressure was reached, the valve at the bottom of the outer phase accumulator was closed. This was responsible for stabilizing the cell pressure.

- v. The sample phase accumulator cover was opened and then oil sample was manually poured into it until inside trend mark for its maximum filling is reached. Close cover.
- vi. A continuous turning of the pump persisted to increase the gauge pressure to be above the reservoir pressure. This was done in order to develop the pressure that will be responsible for existence in the absence of air for release the drop into the cell.
- vii. The valve below the IFT cell was slowly opened with fine adjustment to control the sample drop.
- viii. To de-pressurize the cell, the heater was first turned off and the cell was allowed to gradually cool off. At room temperature, the remaining pressure was released slowly.

3.3.2.5 Experimental run/IFT measurement

- i. Dropping.exe file on the desktop was initiated, which opened a new experiment wizard option box. Surface Tension-Pendant was selected.
- ii. On clicking next, an option box to name the new experiment was displayed, and SVU_IFT was entered.
- iii. The drop phase was oil and formation water mixed with bio-surfactant was selected as the outer phase. The solid phase was steel, which refers to the tip of the needle.
- iv. This followed by setting the data for the experiment's timing. Number of experiment was selected to ten (10), and time interval of two (3) seconds. The wizard then saved the choices in new parameter and method files.
- v. The yes button was then clicked to start the experiment. The measure parameter box appeared with the crosshair lines (vertical and horizontal).
- vi. The drop was released to the near buoyant point. A picture of the drop was taken using the camera button on the tool bar. Then the crosshairs were positioned correctly on the drop for accurate readings, and the measure button was clicked to take measurements. The IFT values were recorded.
- vii. Before the readings were taken, the video setup was selected from the view option box on the main window to adjust the video properties. This was necessary for clearer viewing of the drop profile. The camera zoom was adjusted to 100%

3.3.2.6 Cleaning of the IFT Cell

A very important procedure in achieving reliable results for interfacial tension and contact angle is a thorough cleaning of the apparatus, since contamination of trace amounts can alter the measurement results.

- i. Repetition of steps 1-10 in phase 1 with Hexane as the outer phase and sample phase in order to flush out oil contaminants from the system.
- ii. The valve under the IFT cell was unscrewed using spanner (size 19) which allowed the draining of Hexane. The screwing of the valve followed immediately.
- iii. Repetition of step 1 and 2 of phase 4 were carried out with Acetone as the outer phase and sample phase to flush out Hexane.
- iv. Repetition of steps 1-3 of phase 4 were carried out with distilled water as the outer phase and sample phase to flush out the Acetone.
- v. Repetitions of step 4 phase 4 with distilled water and heating the cell to at least a temperature of 100°C for 15 mins. Temperature adjustment was achieved using the up and down arrow buttons in the Watlow temperature controller to set the needed temperature.
- vi. The system was allowed to cool down to room temperature, before repeating step 2 of phase 4 to expel the distilled water from the cell.

3.3.2.7 Precautions

Precautions must be observed since the IFT cell is a high-pressure/temperature system of which some will aid in having accurate results:

- Avoid close viewing of a high-pressure cell without protective eyewear in case of a sudden glass window failure.
- It is also advisable to place shields at each end of the window axis, especially if the cell is left unattended.
- Do not view the cell directly in line with the window: use the video system to view the cell indirectly, or use a mirror to view the cell at an angle.
- Avoid contact with exterior surfaces of the IFT Cell as it can become very hot.

- It is necessary to always change the associated fluid densities in the software. This will insure an accurate calculation.
- Cell should be cleaned periodically to remove any heavy fluid build-up.

3.3.3 Error and Accuracy

- i. For every IFT and contact angle measured, the oil film was assumed to be at equilibrium 5 minutes after film formation, before then taking the measurements.
- ii. For every single variable that was considered, the error given were calculated by the program and given by the standard deviation between 0.02 to 0.12, of the regression in the x-direction at the critical surface tension.
- iii. Calibration of the total magnification in the system was always carried whenever there was a change in optical magnification. Calibration was performed by measuring the diameter of the needle (capillary tube), which is the solid phase.
- iv. The time in which the mechanical equilibrium of the drop is reached, was highly considered before commencing any measurement. With the help of a vibration-proof table, this was achieved.

3.4 Phase-III: Qualitative Wettability Test

Qualitative wettability test will be performed on crushed rock material to check the effectiveness of the core cleaning and aging procedures as well as the effectiveness of the bio-surfactants in changing the wettability of the crude-oil aged crushed rocks.

3.4.1 Experimental Apparatus and Materials

3.4.1.1 The Soxhlet Extraction

It is important that the core be cleaned to a repeatable initial state (water-wet) that existed before oil accumulated the formation. This process follows a procedure as discussed in Section 3.4.3.1. The following are the apparatus used for the Soxhlet extraction process: soxhlet extractor tube, glass thimble, reflux condenser tube (Figure 3.16), hose for water inlet and outlet, extraction solvent – toluene, heating mantle, 500 ml round-bottom distillation flask, retort stand (Figure 3.17), and fume cupboard. The heating mantle (temperature) controller in Figure 3.18, is a single circuit, 10A 2400 Watts, 240V, that is used to manually regulate the heating mantle with an adjustable output range from 5% to 100% of the rated voltage.

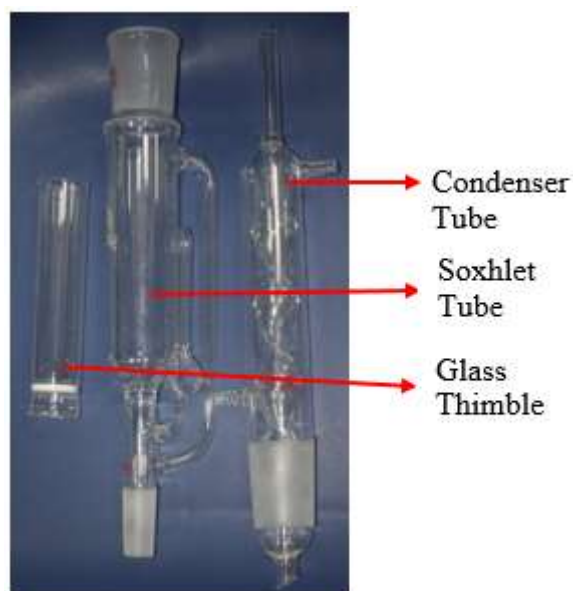


Figure 3.16: Soxhlet kit

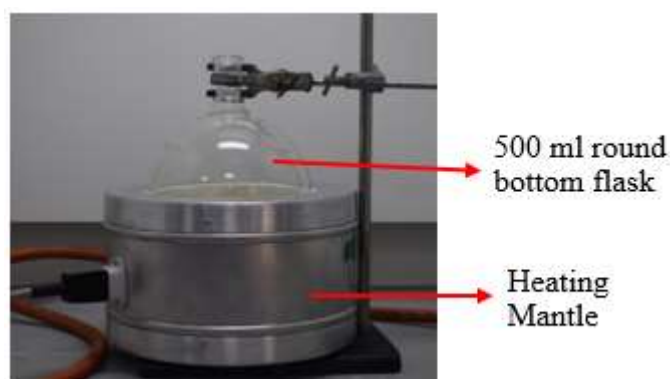


Figure 3.17: Heating mantle



Figure 3.18: Heating Mantle (Temperature) controller

3.4.1.2 Principle of the Soxhlet extraction method

A soxhlet extractor is a continuous extraction of a component from a solid mixture, and it's the most common method for cleaning samples and is routinely used by most laboratories. The core sample utilised in this study were first weighed using the analytical balance and the samples placed inside the glass thimble. Figure 3.19 shows where the samples were placed in a Soxhlet extraction tube, with the ground joint fittings tightened properly before turning on the water supply to begin circulation in the condenser.



Figure 3.19: The soxhlet extraction process

3.4.1.3 Rock Samples

The core samples used in this study are Bandera Gray and Scioto sandstones, shown in Figure 3.20. The effect of the bio-surfactants was compared between these two-sandstone sample, of which a qualitative wettability tests and core flooding experiment was conducted. The sandstone plugs utilised were 3 *in.* length, with a diameter of 1 *in.* The core characterization is listed in Table 3.6.

Table 3.6: Core Characterisation

Plug	Bandera Gray	Scioto
Average length (cm)	7.61	7.6
Average diameter (cm)	2.52	2.4
Area (cm ²)	4.98	4.52
Bulk volume (cm ³)	37.95	34.38
Pore volume (cm ³)	7.97	4.13
Porosity (%)	21%	12%

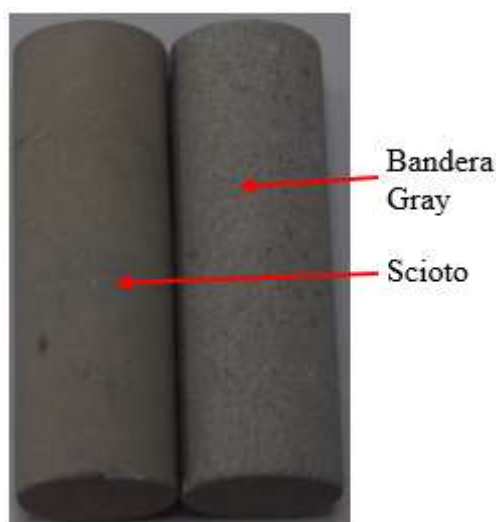


Figure 3.20: Sandstone core plugs

3.4.2 Procedure of data collection

3.4.2.1 The Soxhlet extraction/Core Cleaning

The heater was turned on and the rate of boiling adjusted bringing the toluene to a slow boil in a Pyrex flask so that the reflux from the condenser is a few drops of solvent (toluene)/per second. It boiling solvent vapours move upwards through the larger side-arm and the core becomes engulfed in the toluene vapours (at approximately 60°C). Eventually water within the core sample in the thimble will be vaporised. The toluene and water vapour then enters the inner chamber of the condenser; the cold water circulating about the inner chamber condenses both vapours to immiscible liquids.

Re-condensed toluene together with liquid water falls from the base of the condenser onto the core sample in the thimble; the toluene soaks the core sample dissolving any oil or contaminant with which it comes into contact. When the liquid level within the soxhlet tube reaches the top of the siphon tube arrangement, the liquids within the soxhlet tube are automatically emptied by a siphon effect and flow into the boiling flask.

The toluene is then ready to start another cycle. The complete cleaning was achieved after 14 cycles with close monitoring of the toluene level during the cleaning to ensure that the sample was completely submerged in the solvent. The samples were then placed in the oven at 62°C and allowed to dry for 3 days and were weighed accordingly. Drying at this low temperature was necessary to preserve and maintain the properties of the core samples.

3.4.2.2 Core Sample preparation for crude oil treatment

The core samples initially were cleaned with toluene in a soxhlet extraction device to remove all contaminant leaving it strongly water-wet. The cleaning process was carried out in a fume cupboard in a continuous process until there was no more discoloration of the solvent with contact time. They were placed in an oven and dried to a constant weight. The cleaned samples were then crushed and meshed with 300 μm and 225 μm sieve in Figure 3.21, to check the size of the distribution and remove particles. The crushed samples were submerged in crude oil in the OFTIE aging cells (Fig. 3.22) and stored in an OFITE 5 roller oven at an aging temperature of 62.2°C for two weeks. At the end of the aging period, the oil aged in the core was displaced with kerosine (pure grade paraffin) and the grains dried again in the oven for a day and were ready for bio-surfactant treatment.

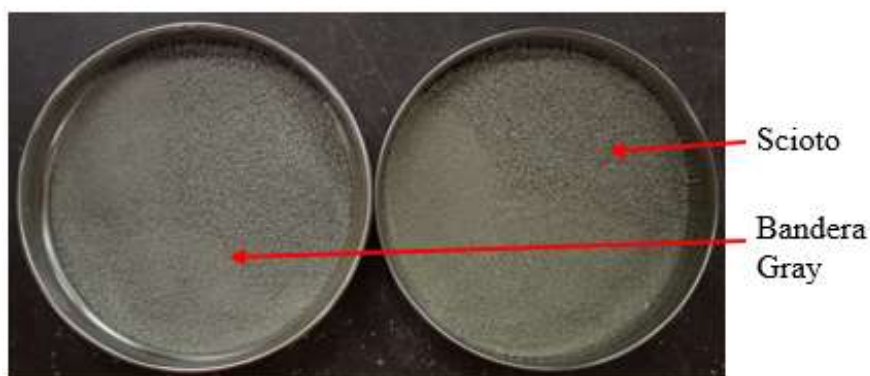


Figure 3.21: Crushed grains of sizes 300 μm and 225 μm .



Figure 3.22: Aging of the sandstone cores in crude oil

3.4.2.3 Core Sample Preparation for bio-surfactant treatments

2g of crushed the rock samples each (Bandera Gray and Scioto sandstone grains) was added into 6 bottles each of bio-surfactant solutions for cells and cell-free biosurfactants (Figure 3.23 and Figure 3.24) and allowed to saturate for a day. The samples were kept in a refrigerator and the bio-surfactants removed by successive addition of distilled water to the bottles. The grains were retrieved by filtration with the aid of unbleached filter papers, and placed onto petri dishes. The samples were dried again for a day in the oven at 32°C and were ready for qualitative wettability tests.

It is important to note here that the core samples were treated separately with the three bio-surfactants (*B. subtilis*- BS-1, *B. licheniformis*- BS-2 and *B. polymyxa*- BS-3). Aging allows the rock sample to imbibe the crude oil under high temperature. Saturation of the bio-surfactants and aging indirectly alters the degree of wettability of the grains.

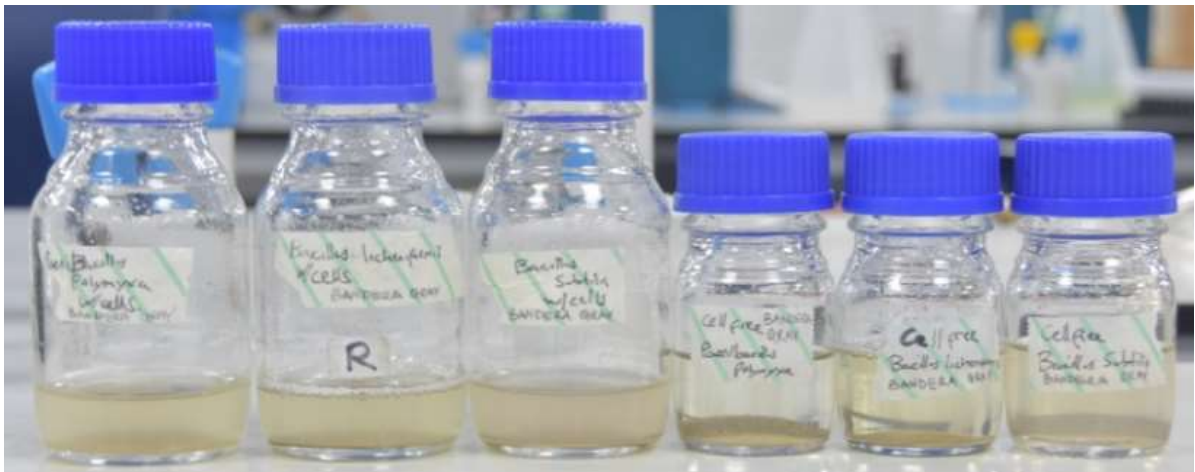


Figure 3.23: Saturation of bandera gray sandstone in BS-1 BS-2 and BS-3



Figure 3.24: Saturation of scioto sandstone in BS-1 BS-2 and BS-3

3.4.2.4 Floating test

In the floating test, the treated samples followed the same procedure and were added into distilled water. 0.2g of each sandstone sample was weighed along with twelve test tubes as represented in Figure 3.25. If the crushed rock samples float it is classified as oil-wet and if crushed rock sample sinks to the bottom it is classified as water-wet as shown below. It should be noted here that throughout the qualitative experiment, the mass of 0.2g was maintained to achieve a reliable result.

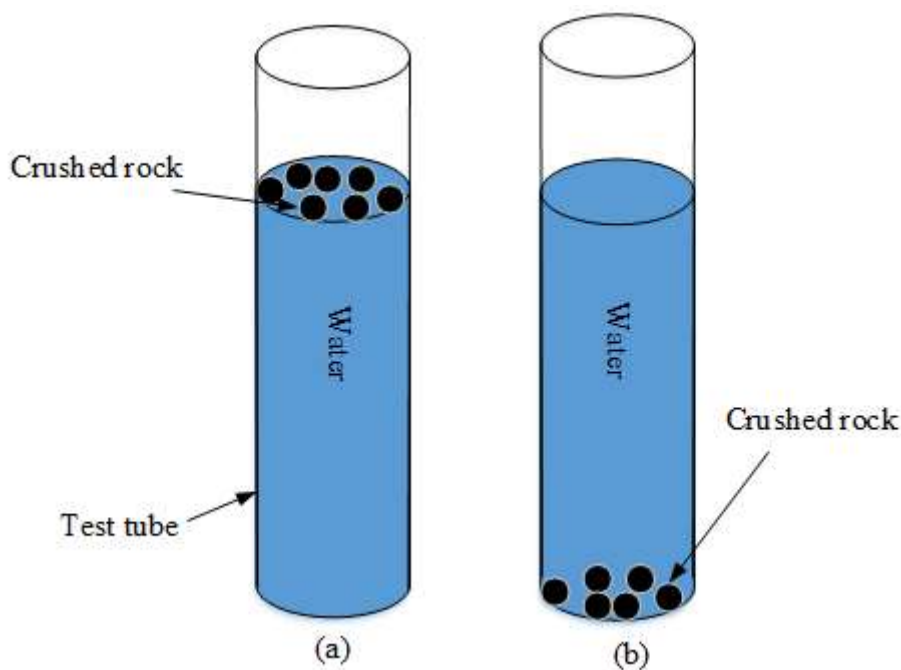


Figure 3.25: Floating test (a) oil-wet rock (b) water-wet rock

Source: (Wu, Shuler, Blanco, Tang, & Goddard, 2006)

3.4.2.5 Two phase separation test

In the two-phase separation test, 0.2g of the grains was weighed out into a 50ml test tube. In addition, 20 ml of distilled water was added to the test tube followed by the addition of 20ml of sunflower oil. The experiment was repeated by the addition of 20 ml of kerosene to the test tube. The test tubes were gently shaken and allowed some time to settle. The quantity of core material remaining in each phase gives a qualitative index of wettability, and according to (Somasundaran & Zhang, 2006) if the grains remains in the oil phase, it is strongly oil wet (Figure 3.26a) and if it sinks to the aqueous phase it is termed water wet (Figure 3.26b).

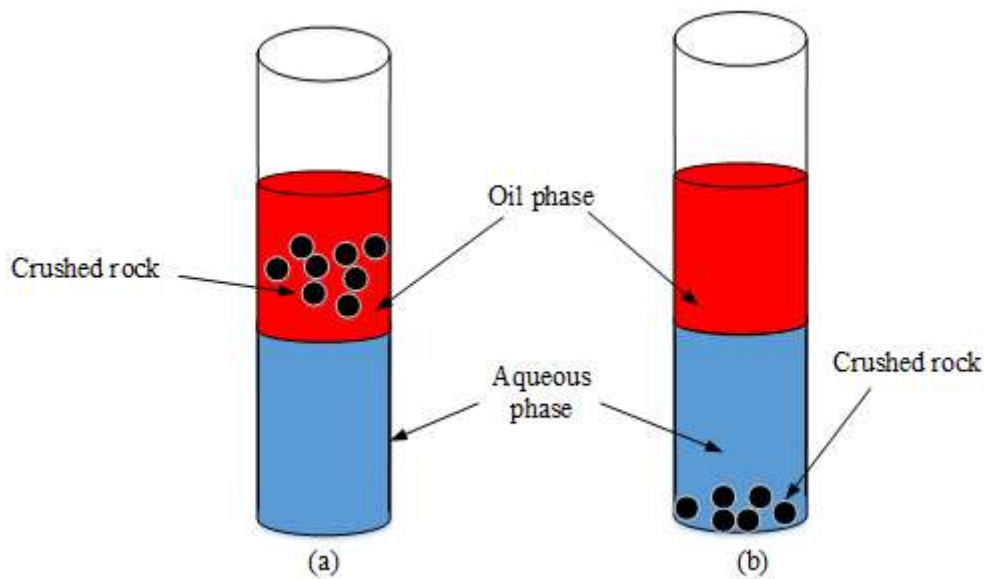


Figure 3.26: Two phase separation test (a) oil-wet rock (b) water-wet rock

Source: (Somasundaran & Zhang, 2006)

3.4.3 Error and Accuracy

- i. Sampling errors have been accounted for by repeating each set of experiment over three uniquely measured samples, following the same procedures.
- ii. The grain size and weight may have had influence on the buoyancy force of the fluid.

3.5 Phase-IV: Core Flooding

The core flooding experiment will be performed to evaluate the effectiveness of bio-surfactant treatments in altering wettability of sandstone reservoirs. Sandstone reservoir core will be used in core flood tests at simulated reservoir conditions. For a treatment to be considered for core flooding, it must be stable at ambient and reservoir conditions to avoid damaging the rock permeability. Therefore, the treatment solution should not polymerise; should not precipitate before or during injection into the core, or upon heating; and it should not cause any unwanted reaction in the core with either rock minerals or other fluid(s) initially in the core.

3.5.1 Experimental Apparatus and Materials

A major part of the experimental work related to this study was the bio-surfactant flooding, which was carried out using Figure 3.27, the CoreLab UFS-200 core flooding system student

module apparatus, located within the Department of Petroleum Engineering at The University of Salford. The equipment is configured for two phase liquid displacements under unsteady state or steady-state conditions and single phase gas steady-state experiments. For this study, the unsteady state liquid displacement method was adopted due to the displacement of each fluid utilised at a time. The flow path of the core flooding experiment can be seen in a simple schematic shown in Figure 3.28.

3.5.1.1 Description of CoreLab UFS-200

The system is rated to 5,000 psig confining pressure, 3,500 psig pore pressure at room temperature. An integral part of the system is the SmartFlood software and computer data-acquisition-and-control system hardware, which provides on-screen display of all measured values (pressures, temperatures, volumes etc.), automatic logging of test data to a computer data file, alarms, graphing, calculation of permeability, operate the pump delivery system for the start/stop of fluid flow and control of the flow rate. The major components of the core flooding apparatus is further explained in details to highlight their mode of operation and their importance in effectively performing the experiments. The entire system can be divided into four sections; to include the core holder, fluid injection system, data acquisition system and the collection tube.

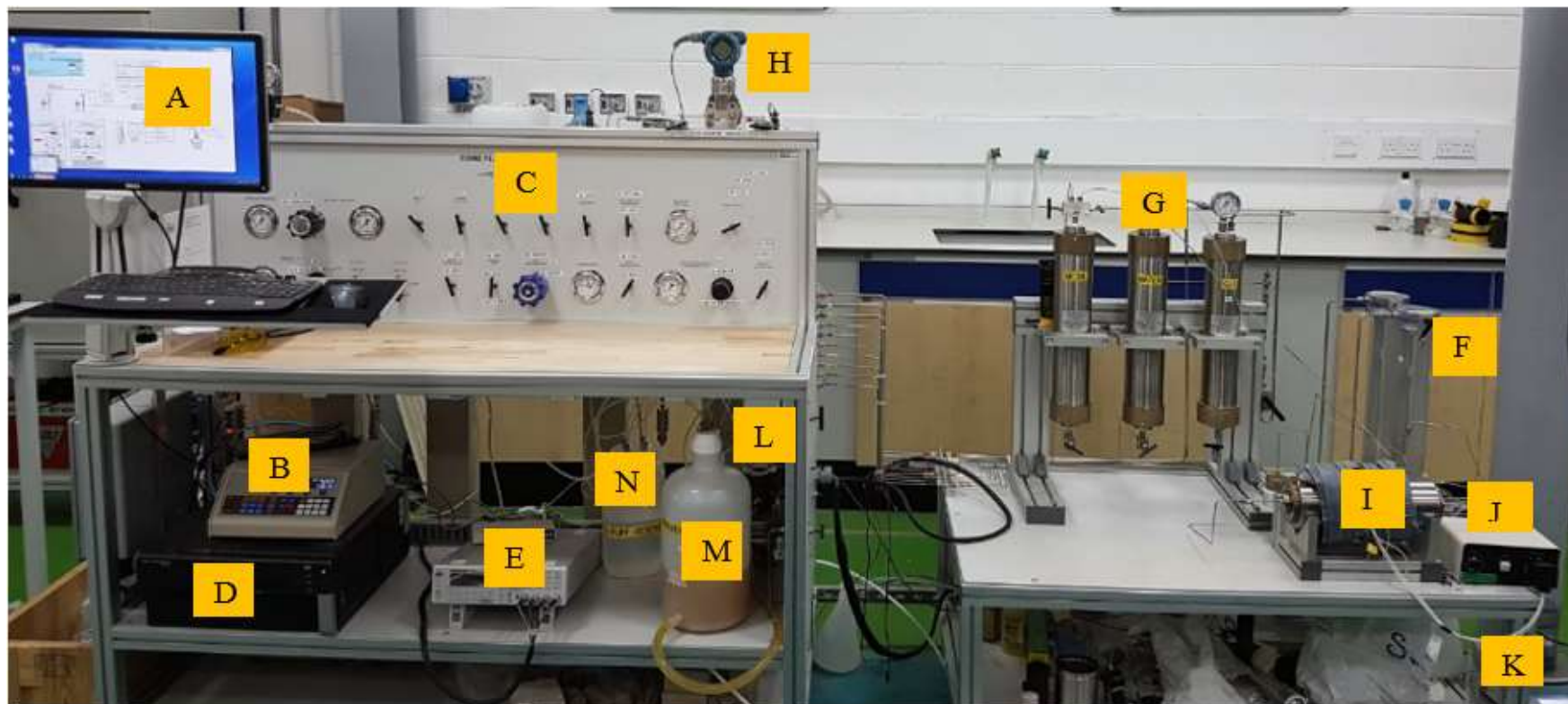


Figure 3.27: Cross-section of the UFS-200 core flooding equipment.

(A) Monitor, (B) Pump Controller, (C) Control Panel, (D) Central Processing Unit, (E) Hameg Resistivity Controller, (F). CC Cells, (G) Floating-Piston Accumulators, (H) Rosemount Transducer, (I) Core Holder, (J) Temperature Controller, (K) Hameg Balance, (L) Overburden Pump, (M) Overburden Back Pressure Oil, (N) Isco Pump Reservoir.

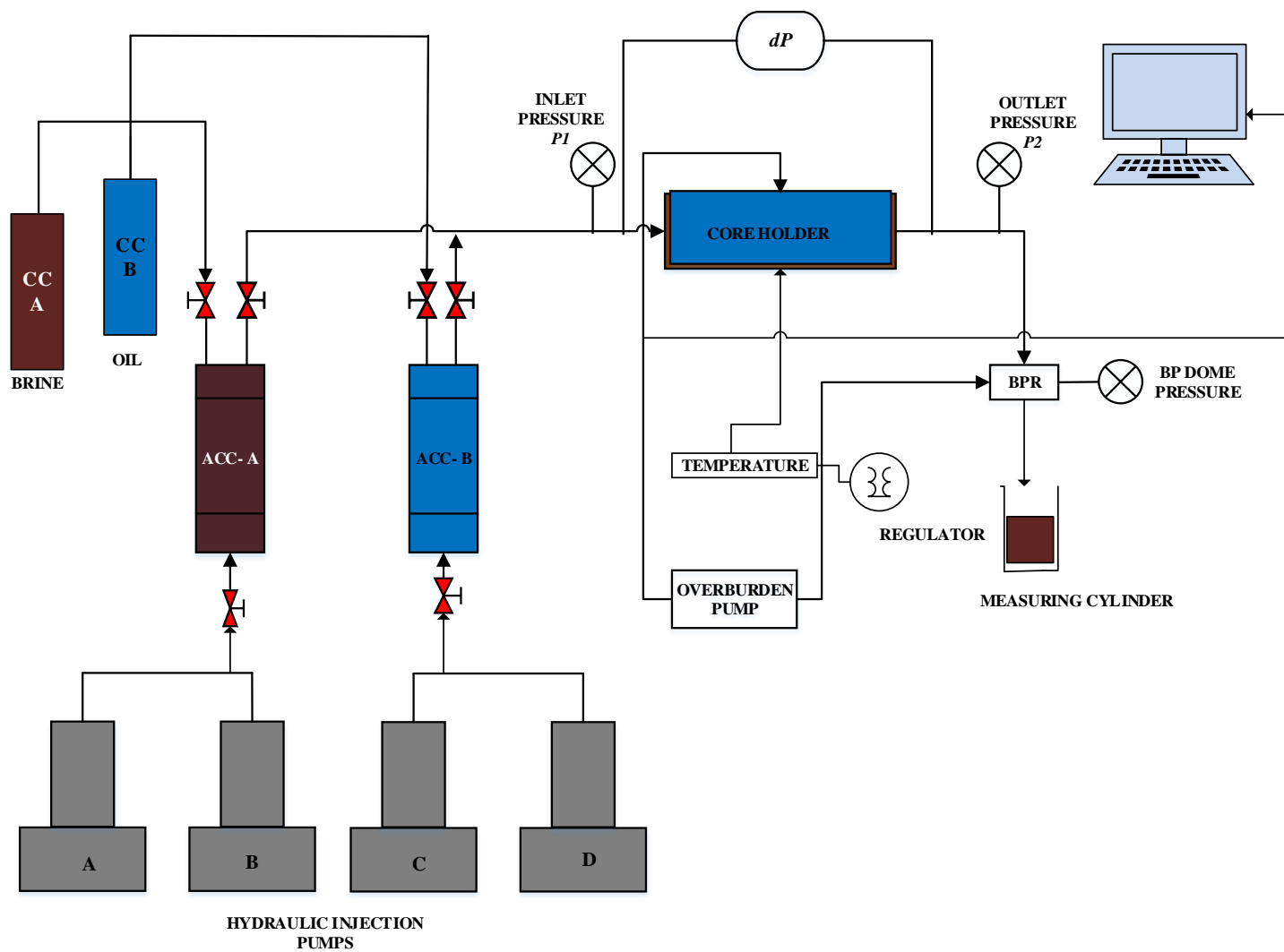


Figure 3.28: Schematic diagram of the flow path used in the core flooding experiment

(Source: Core Laboratories)

3.5.1.2 Core Holder

The core-holder used in this study was the hassler-type CoreLab's ECH-series, shown in Figure 3.29. They are routinely used for gas and liquid permeability testing, surfactant-polymer studies, water flooding experiments, other type of enhanced oil recovery studies, and for many other studies of fluid flow in porous media. The unique feature of this core-holder is that the distribution plug is able to float, and adjusts to irregular length cores. This feature ensures solid contact between the distribution plug and core sample.

The core sample is held within a rubber sleeve by radial confining pressure, which simulates reservoir overburden pressures. Figure 3.30 shows the cross-section of the core holder used in this study, with two confining pressure ports provided to fill the annulus with overburden fluid using one of the ports and expelling air with the other. The inlet and outlet distribution plugs allow fluids and gases to be injected through the core sample. The inlet pressure into the core sample and outlet pressures on the other side of each core were measured with gauge pressure transducers. Fluids produced through the core sample were collected in a sealed container on the electronic balance downstream. All flow lines and internal volumes were kept to a minimum, so that accurate flow data can be determined.

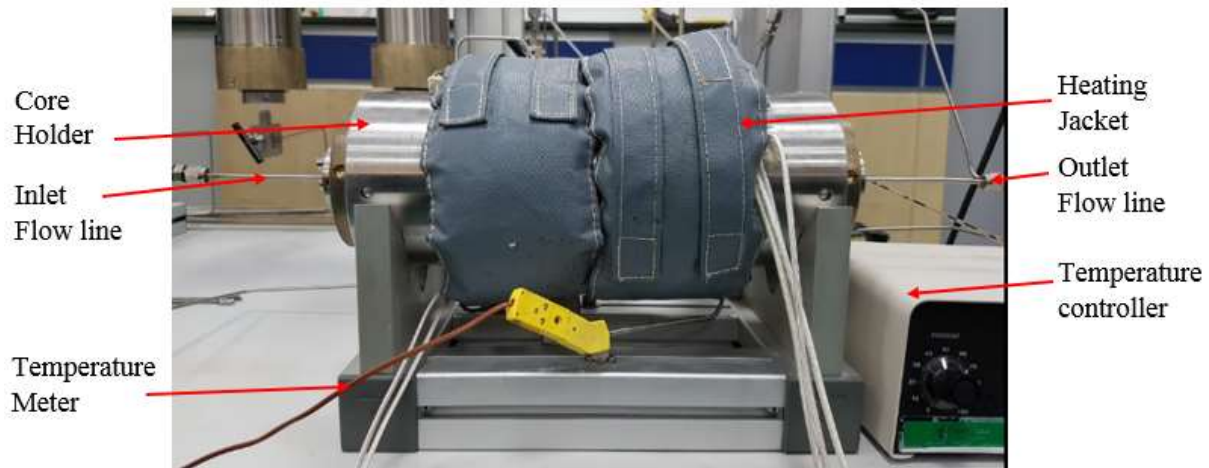


Figure 3.29: Core holder

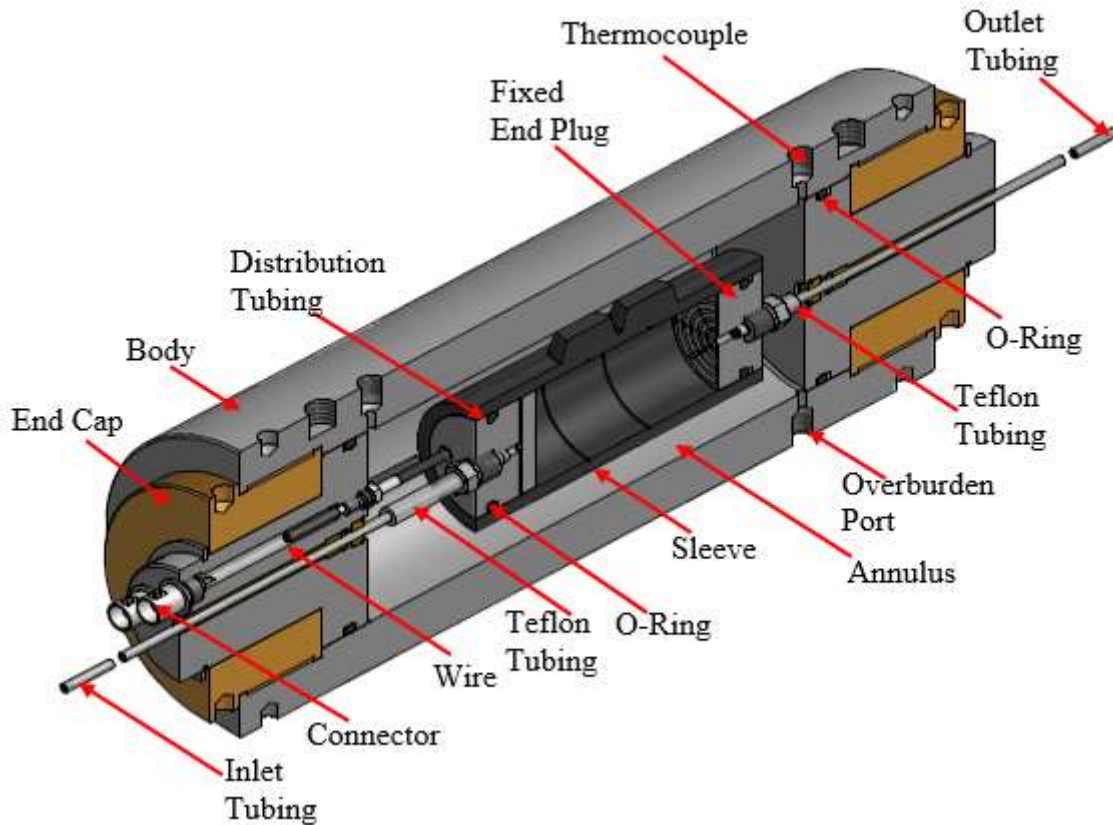


Figure 3.30: A cross-section of the Hassle core holder
(Source: Core Laboratory)

3.5.1.3 The Injection System

3.5.1.3.1 Floating-Piston Accumulators

CoreLab floating-piston accumulators are rated for 5,000 psig pressure and 350°F (177°C) temperature. The accumulator volumes are 500 cc each and provide for injecting fluids without allowing the fluid to come in contact with the metering pump (Figure 3.31). In this study, accumulator A (oil) and accumulator B (brine/bio-surfactant) were used in saturation and the flooding process. The CC-series reservoirs were used for the storage and transfer of test fluids. The test fluids of known volume were fed into the CC-cells A/B in Figure 3.32, by opening the top assembly and then opening the appropriate valve at the bottom the CC-cell, the fluid was injected into the desired accumulator with the aid of the ISCO pump.



Figure 3.31: Floating-piston accumulators



Figure 3.32: CC cells

3.5.1.3.2 Metering Pump and Overburden Pressure Pump

The ISCO model 500D is a two-barrel metering pump system which has a flow rate range adjustable from 0 to 200 ml/min and a maximum pressure rating of 3,750 psig (Figure 3.33). It's pump's limits are set to turn off itself before it reaches too high of a pressure. The ISCO pump can be controlled by the pump controller as seen in Figure 3.27-B, and can be used to inject brine or test fluid into the core sample via the floating piston accumulator. The simple procedure here is to close the valves to the confining pressure system and release the pressure in the ISCO pump. Then open the valve to accumulator and the valve at the bottom of the accumulator. Also, open the purge valve at the top of the accumulator to drain all air out of the flow lines. With a properly filled accumulator, brine or other test liquid can now be injected into the core sample.



Figure 3.33: Metering Isco pumps

Figure 3.34, represents the overburden (confining) pressure pump is a hydraulic pump, with a maximum pressure output of 10,000 psig. The maximum overburden pressure rating of the core holder and system is 5,000 psig. It functions by gradually pumping hydraulic oil into the annulus of the core holder to build up the desired overburden confining pressure as well as the back pressure.



Figure 3.34: Overburden pump and relevant reservoirs

3.5.1.4 The Collection System

As part of the process during initializing the equipment, the hameg balance is turned on and tared (zeroed). The leak-off fluids produced through the core during experimental runs can be collected by the electronic balance at the outlet of the core's BPR. The liquids flow through the back-pressure regulator (BPR) and into a sealed container on the balance (Figure 3.25). The produced fluid is then poured into a measuring cylinder and allowed to settled before taking any measurements.

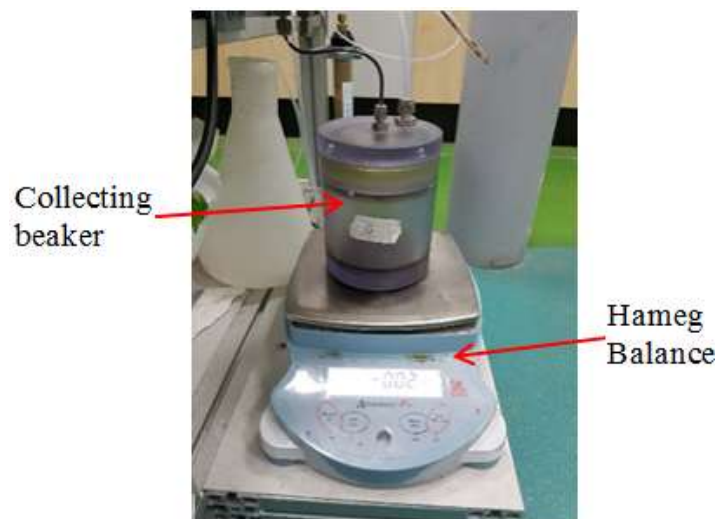


Figure 3.35: Hameg electronic balance

3.5.1.5 The Data Acquisition and Control System.

The data acquisition system consists of a personal computer and the control system SmartFlood software communicates to the UFS system through Ethernet. The entire hardware components and sensors of the system is controlled and monitored with the computer by providing on-screen display of all measured values (flow rates, pressures, temperature etc.), remote control of flow rates, automatic logging of test data to a data file, alarms, calculations and graphing as seen in Figure 3.27-A. A major advantage of this system is that it provides a means to remotely acquire and record test results. The data logging features in the software relieves the operator of much of the tedious, time-consuming setup and data recording that used to be required when running tests.

3.5.1.6 Back-Pressure Regulator, Pressure Gauges, Air Actuated Valves, and Pressure Transducers

The CoreLab back-pressure regulator controls the back (outlet) pressure. It is rated for a maximum working pressure of 5,000 psig, and is a dome-loaded type which controls the back pressure to whatever pressure is supplied to its dome. For this system, 2.5-inch-dial pressure gauges are used to monitor the Overburden Pressure and the BPR Dome Pressure. The pressure range on these gauges is 15,000-psig full scale. A 160-psi gauge is provided to monitor the main inlet air going to the pump and air actuated valves. The system uses Vindum, CV series High Pressure (10,000 psig) three-way valves, which can be operated remotely via the SmartFlood software. The Rosemount transducer measures the differential pressure across the core holder.

5.5.1.7 Materials

The following listed materials were used in successfully performing the bio-flooding/waterflooding experiments.

- i. Bandera Gray core sample, as described in Section 3.4.2.1
- ii. Crude oil sample, as described in Table 3.3
- iii. *BS-2* supernatant biosurfactant
- iv. Distilled water

3.5.2 Procedure of data collection

5.5.2.1 Initial Setup

Prior to beginning any experiment, the flow diagram was always in hand as a guide. The process follows the steps below;

- Switch on the main power, PC, Isco pumps and controllers, Hameg balance, and set air pressure between 85-95 psi. Air-pressure above 95 psi could cause leaks on the SMC manifold.
- Fill overburden/BPR pump reservoir with oil and Isco pump reservoir with distilled water.
- Open SmartFlood-51 software, select FILE-ONLINE and refill Isco pumps

3.5.2.2 Filling the Floating-Piston Accumulators with Lexan CC Cells

- In filling the accumulators with the fluid of interest, the CC Cell A/B was vented, opened, filled with the desired fluid and connected to the required accumulator by opening the valve at the bottom of the CC Cell A/B.
- Open PURGE PUMP AB/CD to distilled water container (pump fluid reservoir). This allows the fluid from the bottom of the accumulator to move back into the metering pump reservoir. When the accumulator is filled to desired volume, the PURGE PUMP valve was closed.
- Move CC Cells A or B to PRESSURIZED and regulate 20 psi air to push fluid into accumulator and then release pressure before disconnecting line.
- The accumulator volume on software was reset since the software counts down volume according to Isco pump flow rate.
- The correct FLOW OPTION part on the software was selected to count down volume.

After filling the accumulators, the core holder was then loaded with the sandstone sample. The core sample was placed inside a rubber sleeve and a hose clamp was applied on one side of the sleeve to ease installation.

3.5.2.3 Inserting Sample in the Core Holder

The core-sample was inserted into an adequate length of Telfon sleeve and placed on the core-holder's fixed end plug and fastened with a hose clamp to prevent the core from moving as shown in Figure 3.36. The sleeve is designed in such a way that the dimension's fits perfectly to accommodate the outer diameter of the core sample and thus leaving an annular space between the outer diameter of the sleeve and the inner diameter of the core-holder. The fixed end assembly was then inserted into the core holder and screwed in place. Furthermore, the adjustable end plug was carefully inserted into the other end of the sleeve already in the core holder and the end cap screwed appropriately. The adjustable end was properly adjusted to allow the core sample sit properly between the two plugs.



Figure 3.36: Adjustable and fixed end plug

3.5.2.4 Applying Overburden Pressure and Back Pressure

The overburden (OBD) pump was run long enough to fill the annular space (overburden chamber) in the core holder with hydraulic oil. While this process was ongoing, the flow lines were detached to observe that the core sample was fitted properly and that no fluid drips out of the lines otherwise there is likely a leak through the distribution plug fittings or a ruptured sleeve. The overburden pressure was set at least 500 psi higher than the pore pressure to avoid rupturing the sleeve and since pore pressure can rise rapidly, care was taken to set the ISCO pump safety pressure at least 500 psi below the overburden pressure. The steps below were employed to get the overburden pressure;

- Close PUMP TO BPR, DRAIN OVERBURDEN, AIR TO OVERBURDEN.
- Open PUMP TO OVERBURDEN, ISOLATE OVERBURDEN BPR and back off all the way on SET OVERBURDEN REGULATOR.
- The pump speed was increased with DRIVE AIR PRESSURE TO OVERBURDEN PUMP and run until air is purged (fluid will return to reservoir).
- The SET OVERBURDEN REGULATOR was turned slowly clockwise to increase overburden pressure to the desired pressure.

After setting the overburden pressure, the back pressure was set simultaneously and then the flow lines connected getting the core sample ready to be flooded with bio-surfactant. It should be noted here that temperature was applied to the core holder using heating tapes wound round it and the desired temperature was maintained with the aid of heating jackets wrapped around the core holder.

Before commencing the experiment, the pressure transducer system was filled and purged. The transducer was filled with distilled water from the pump by closing INLET dP and OUTLET dP. And then opening FILL dP SYSTEM VALVE, zero dP and purging valves on either side of the Rosemount transducer located at the top of the panel. The valve below accumulator B was closed before running Isco pump CD to flow distilled water into transducer system. After filling and purging as desired, the reverse procedure was applied on all the valves.

3.5.2.5 Fluid Injection System

With the inlet flow tubing filled up to the metering pump, and the proper fluids in the accumulators, and the overburden pressure set on the core holder, we were then ready to begin fluid injection. Figure 3.37, summarises the fluid injection process.

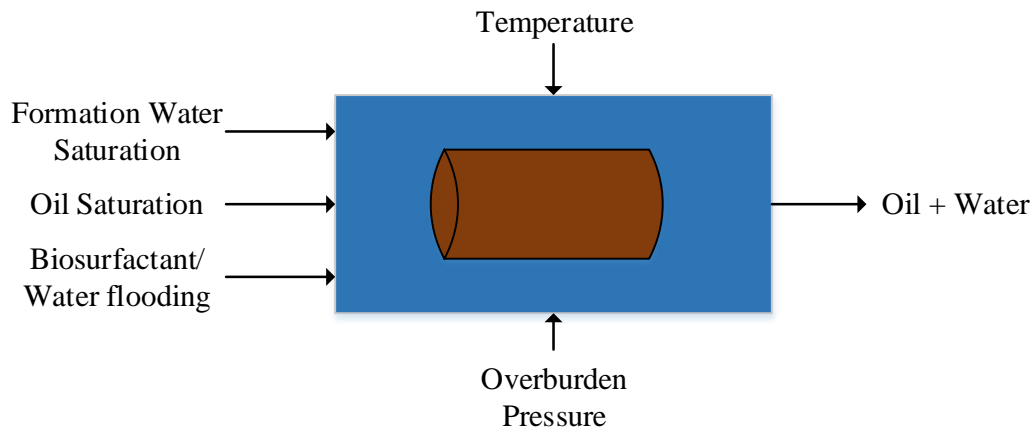


Figure 3.37: The fluid Injection process.

First, fill the core by turning on the metering pump, and opening the desired accumulator valves to inject the desired fluid into the core. After the full (desired test) inlet pressure and back pressure are reached, stop the injection metering pump and allow enough time for the pressure to equalize across the core. Re-zero the dP transducer at this test pressure, to compensate for its zero shift due to changing line pressure. This is done by adjusting the transducer Zero screw (on the Rosemount Transducer) until the front-panel display reads 0.000 psig.

3.5.2.5.1 Saturating the sample with formation water

The injection of brine was started in order to increase the sample pore pressure to the reservoir *in-situ* pore pressure. Meanwhile, the overburden pressure was also raised to full reservoir *in-situ* overburden pressure. This way both pore and overburden pressures would reach the full *in-situ* values at the same time and the sample would never be exposed to pressures exceeding the reservoir *in-situ* net effective pressure.

During saturation of the core sample with brine and aging with oil the data logging is not initiated. All pressures were closely monitored for any pressure loss which is a sign of leakage in either the lines or valves and were fixed and then the pressure readjusted before proceeding with the experiment.

3.5.2.5.2 Displacing the formation water with crude oil

By opening the valve at the top of the oil accumulator, the injection began into the core sample at a constant flow rate under the desired reservoir temperature, pore pressure, and back pressure conditions. This unsteady state condition continued to the point where the pore

pressure almost equal the back pressure thus initiating a flow. At this point, brine was produced which was collected into a measuring cylinder and with continued flow a breakthrough was achieved (a mixture of oil and brine) and then only oil started flowing. Once the breakthrough was achieved, the time and other pressure conditions were noted. The oil injection continued until 3 pore volumes were produced at which point the core should be fully saturated with oil and then the produced water measured. However, in order to be certain of full oil saturation, the sample was left for 24-hours to age under reservoir in-situ P-T conditions, while all pressures were monitored for any fluctuations and then adjusted accordingly.

3.5.2.5.3 Displacing the crude oil with distilled water (waterflooding)

This flooding process was carried out as a control measure to set a benchmark of the oil recovered while comparing the outcome with the bio-surfactant recovery. Also, it was necessary to determine the best flow rate that would give the maximum oil recovery by carrying out repetitive test runs at different flow rates. During the injection of distilled water, the overburden pressure and back pressure was maintained. The pore pressure however increased to a point where flow was initiated until there was a breakthrough of water. The low flow rate was necessary to avoid a viscous fingering through the core, therefore displacing more of the oil. The amount of oil recovered was then measured and the residual oil left behind was calculated and used as the benchmark for this study.

3.5.2.5.4 Displacing the crude oil with bio-surfactant (bioflooding)

At the start of the distilled water/bio-surfactant flooding, the data logging is initiated with 10 seconds logging interval. To be able to achieve one of the aims of this study, the basic flooding procedure was slightly modified and extended with repeatability experiment carried during the procedure above, certain parameters which would be used during data analysis/interpretation, were recorded against time. These parameters included the brine and oil production and/or injection volumes and flowrates, core holder inlet and outlet pressures, breakthrough time and stabilised conditions e.g. differential pressure.

3.5.2.6 End Test

- The back pressure was released by opening BPR VENT

- Release (back off on SET OVERBURDEN regulator) and drain overburden to remove the core (open AIR TO OVERBURDEN and DRAIN OVERBURDEN).

All the lines were then cleaned by flowing through with either distilled water and/or soap as needed.

3.5.3 Errors and Accuracy

- Re-zero the dP transducer at the test pressure, to compensate for its zero-shift due to changing line pressure. This is done by adjusting the transducer Zero screw (on the Rosemount Transducer) until the front-panel display reads 0.000 psig.
- All measurements were made in triplicate at elevated temperature (60 ± 2)°C and flowrate (0.25 ml/min), and the average values were reported.

3.6 Chapter Summary

The main points of the experimental process of this chapter may be summarised as follows:

The recovering of pure cultures:

- Three selected microbial strains were retrieved from freeze dried condition.
- These microbes were grown on selected media and LB agar
- The growth was carried out on different temperatures, and a phenotypic characteristic which is gram-stain was performed to determine if the microbes were gram-positive bacterial.

Quantitative screening:

- Heavy oil was utilised in a pendant drop system, comprising of synthetic formation water and the produced biosurfactants, to observe for reduction in IFT and contact angle, in the liquid-liquid phase.
- This sets of experiments were performed at varying temperatures and pressures, for both supernatant biosurfactants and biosurfactants with cells.

Qualitative analysis:

- Two sandstones of different permeability's were used here to see how effective these microbes could be in affecting their pore spaces.

- Two qualitative tests (floating and two-phase separation) were used here, to determine the effectiveness of the core cleaning, as well the effectiveness of the biosurfactants in changing the wettability of the crude oil aged crushed rock.

Core flooding:

- The core flood test was carried out on Bandera Gray sandstone at simulated reservoir conditions, using supernatant *BS-2* biosurfactant, and also waterflooding was performed, for a direct comparison of the oil recovered.

The next chapter describes the experimental analysis and results obtained from this study.

Chapter 4

4 Result and Discussions

4.1 Overview

This chapter introduces the results obtained from the experimental investigation conducted according to the equipment, material selection and procedure, set out in Figure 3.1, which is in line with the original target of this investigation in utilising microbial surfactants to mobilize residual oil from mature reservoir and increase production. The results are categorised into four phases in which the experimental sequence followed.

- **Phase I:** Microbial culture: Section 4.2 highlights the condition for effectively growing the strains in producing the required biosurfactant and determination of phenotypic characteristics of the strains to verify that they are gram-positive bacteria as will be detailed in Section 4.2.1. The extraction of the produced biosurfactants is given in Section 4.2.3. The qualitative results have been illustrated in relation to the microbial culture.
- **Phase II:** Interfacial tension/contact angle measurements were conducted quantitatively using Pendant DROPImage technique as detailed in Section 3.3.3.2 for both cells and cell-free cultures of *BS-1*, *BS-2* and *BS-3*. The measurement of the effect of biosurfactants in reducing the IFT/contact angle of heavy crude oil is a first step towards achieving enhance recovery.
- **Phase III:** Qualitative wettability tests. In Section 4.4 the effects of the biosurfactants can be seen on how it has been able to effectively change the rock chemistry, thus altering the wettability of the crude oil aged crushed rock. This qualitative process follows the principle of floatation in two forms, which includes the floating test in Section 4.4.2 and two-phase separation test in Section 4.4.3.
- **Phase IV:** Coreflooding in enhancing recovery in heavy oil reservoirs. In Section 3.5, the unsteady state liquid displacement was utilised during the bioflooding process, and the biosurfactant that gave the best IFT reduction was then used to perform the tertiary recovery, since it could be a potential candidate for EOR.

4.2 Phase I - Microbial Culture

4.2.1 Culture and Growth

The isolation of pure cultures from freeze dried condition to recover the cells is summarized in Figure 4:1 below, showing the growth of bacteria on nutrient agar and liquid broth. The strains used were grown for 48 hours at 30°C and 37°C respectively. It was observed that there was faster growth at 37°C in the first 24 hours for all three strains, and more visible growth was seen at both temperatures after 48 hours. However, the growth of type strain DSM 740, was minimal, even after 2 days, and the weak observation of growth was taken as a positive result as shown in Figure 4.2 and Figure 4.3.

4.2.2 Phenotypic Characteristics

The observable physical characteristics of the microbes used in this study were determined to confirm that the selected bacterial were gram positive.

4.2.2.1 Colony Morphology of Microorganisms

In this study, the strains used were proven to be gram-positive bacterial, *B. subtilis* (Perez, Abanes-De Mello, & Pogliano, 2000), *B. licheniformis* (Jeong et al., 2011), and *B. Paenibacillus polymyxa*. The colonies of *B. licheniformis* appeared whitish at 37°C like lichens or a big wad of snot that grow on rocks, about 1 µm in diameter. After 48 hours of incubating *B. subtilis* at 37°C, the cream-colored colonies formed appeared thick and opaque with lobate margins about 2.0-3.0/0.7-0.8 µm. In addition, *P. polymyxa*, 0.3 by 0.6 µm in size produced thin-pale colonies on agar. These strains are motile by peritrichous flagella (containing protein) and their vegetative cell were not destroyed because they form a sub-terminal or paracentral spore. These features can be seen in Figure 4.3.

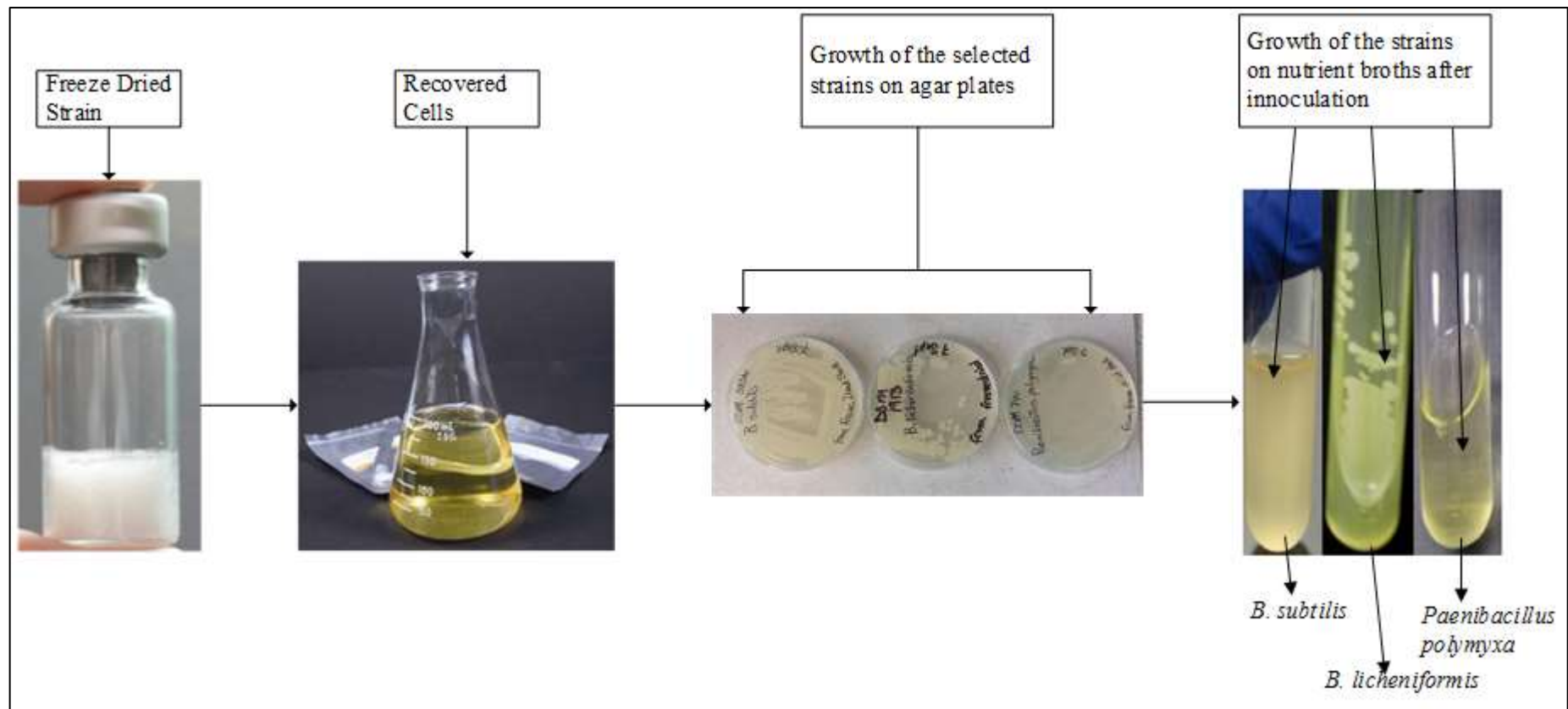


Figure 4.1: Isolation of pure cultures and growth of bacteria



Figure 4.2: Bacteria growth after 48 hours, stores at 30°C.



Figure 4.3: Bacteria growth after 48 hours, stores at 37°C.

4.2.2.2 Gram Staining

It was observed that all three strains of bacteria selected for this study were not decolorised by alcohol and remained purple, when the cells were observed under light microscope, as seen in Figure 4.4. This procedure has helped to determine the presence of bacteria in the selected strains, and has proven that, all three strains are gram-positive bacteria, and accepted to be gram-positive cells. The bacteria were able to retain the crystal violet dye that was used to stain the cells, because the gram-positive bacteria have a very thick cell wall made of protein called peptidoglycan.

4.2.3 PCR Amplification

PCR is sometimes referred to as molecular photocopying, which is used to amplify small segments of DNA into larger ones. It was necessary to carry out this process, due to the sample strains having small amount of DNA to characterise it by sequencing. Larger amounts of DNA mean more accurate and reliable results.

The sequence of each of the bacterium was compared with the 16S rRNA sequence in the Genious R9 library (v 9.15). Upon comparison, the software provided a potential ID for the unknown bacterial species. The Genious R9 ID 16S rRNA library (v 9.15) included over 1489 validated 16S rRNA sequences for each bacterium (NCBI, 2016). All sequences and strains were carefully checked and quality controlled to achieve maximum reliability. Identically colored boxes as seen in Figure 4.5, indicates the selected bacterial belonging to the same gene family in which they were compared with. The different colors represents the different sequence identities which can easily be observed by the broken portions. The complete sequence alignment and comparison between the the strains and the reference strains can further be seen in Appendix B.

4.2.4 Serial Dilutions

The sequential dilutions were used to reduce the dense culture of the cells to a more usable concentration. It helped to determine the number of bacteria per unit volume in the original culture, and determination of the culture density in cells per ml. *B. subtilis* strain as a representative example and were formed in 10^{-1} to 10^{-6} dilutions after 48 hours of incubation as seen in Figure 4.6. Each countable colony contains thousands of individual bacteria. The simple calculation is thus presented below.

The concentration of microscopic cells in a sample of *B. subtilis* can be calculated thus;

$$\text{Number of colonies on plate} \times \text{reciprocal of dilution of sample} = \text{number of bacteria/ml} \quad (4.1)$$

For example, there are 52 colonies on the plate of 1/1,000,000 dilution, then the count is:

$$52 \times 1000000 = 52,000,000 \text{ bacteria/ml in sample}$$

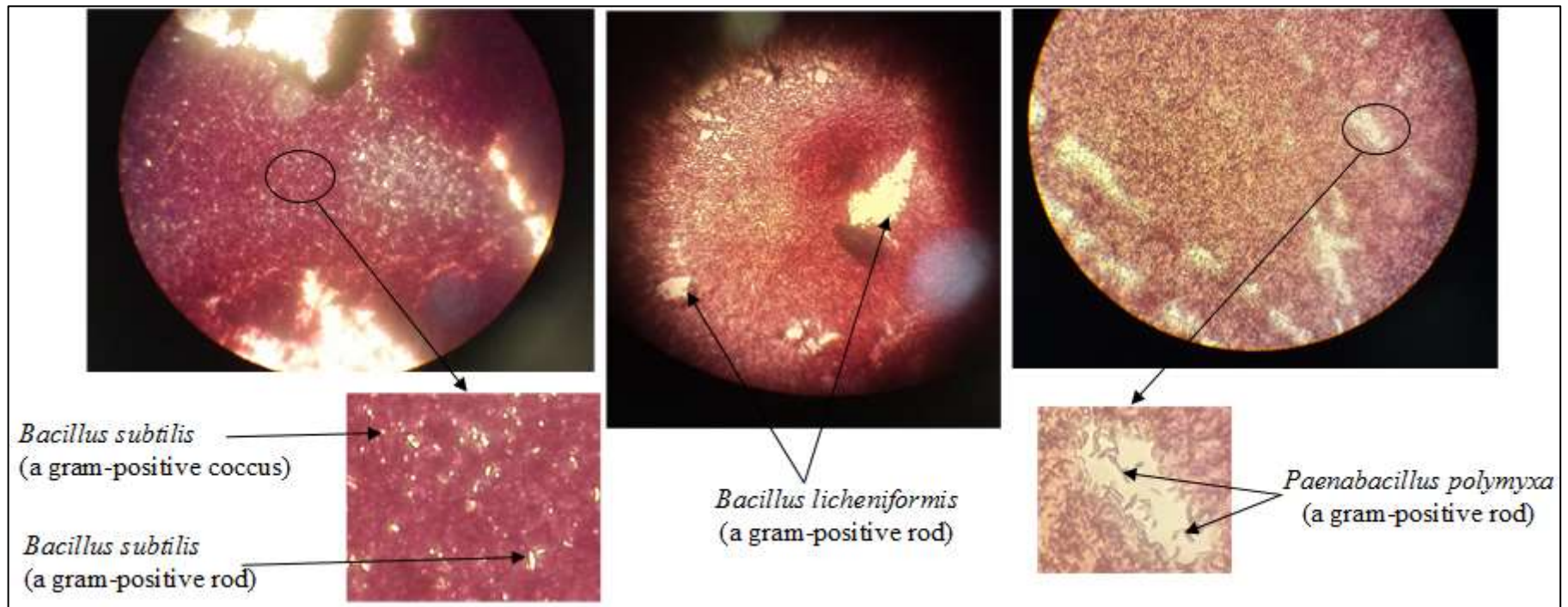
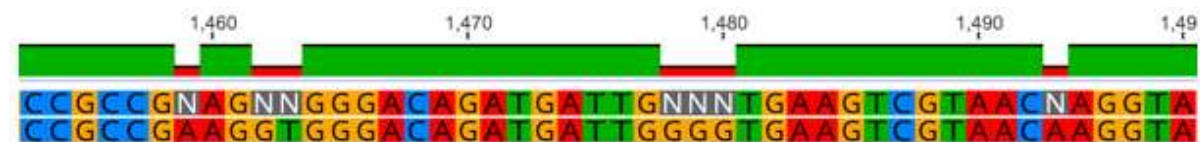
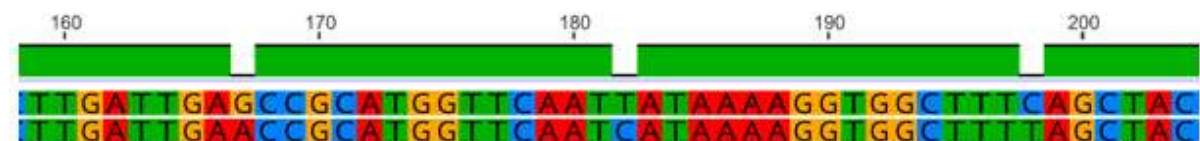


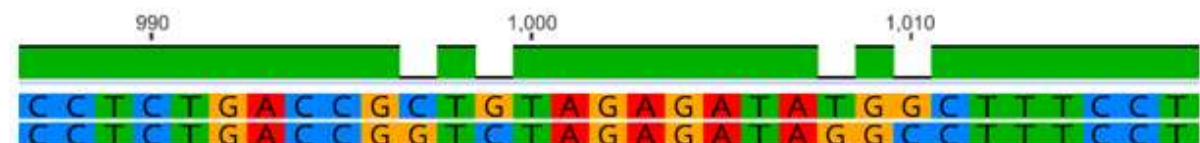
Figure 4.4: Appearance of gram-positive cells of the selected strains



1. DSM 3256 sequence
2. *Bacillus subtilis* gene for 16S rRNA, complete sequence



1. DSM 1913 sequence
2. *Bacillus licheniformis* strain DSM 13 16S ribosomal RNA gene, complete sequence



1. DSM 740 sequence
2. *Paenibacillus polymyxa* SC2 strain 16S ribosomal RNA gene, complete sequence

Figure 4.5: Sequence alignment for the selected strains.

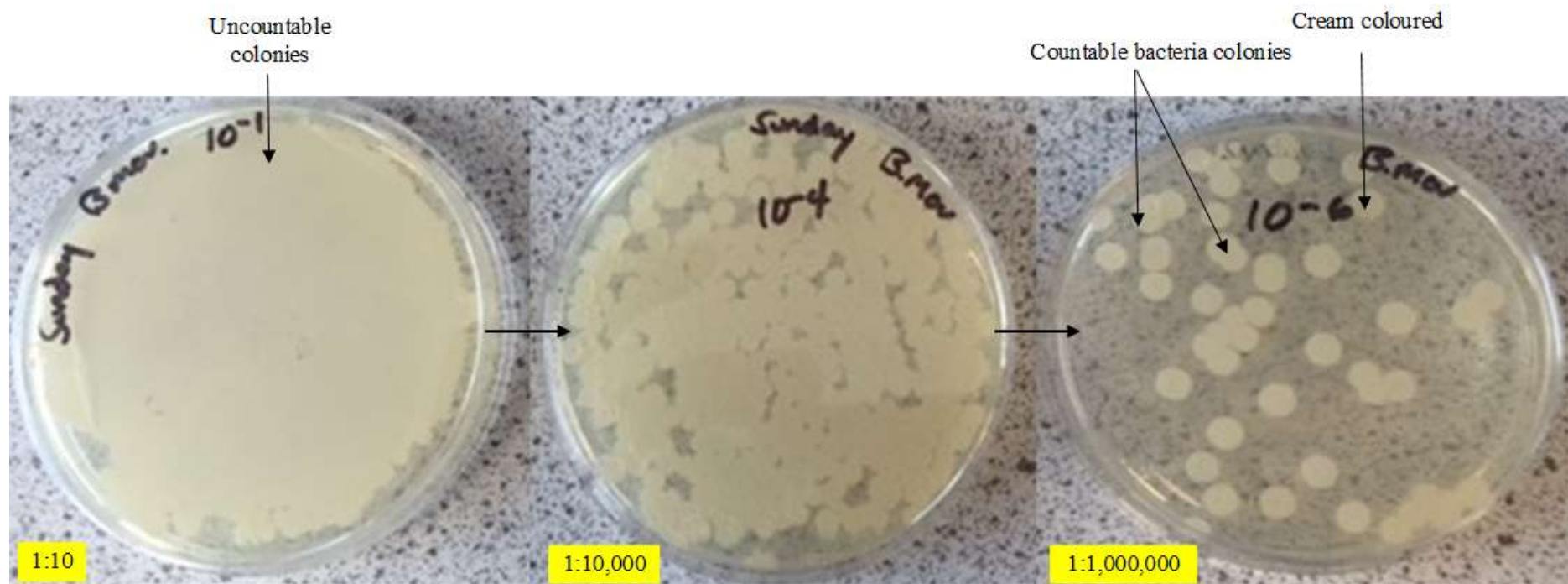


Figure 4.6: View of bacteria colonies from *Bacillus subtilis* at different dilutions

4.2.5 Measurement of the Cell Concentration by Optical Density (OD)

Below is the process of working out the required volume of biosurfactant culture needed to be mixed with the synthetic formation water, for the interfacial and contact angle experiment. BS-2 supernatant was used to explain the process.

$$\text{Absorbent}; 0.910 \times 2 \quad (4.2)$$

When working out concentration of solutions upon dilution or making a fixed amount of dilute solution from a stock solution, the dilution equation is usually applied.

$$C_1 V_1 = C_2 V_2 \quad (4.3)$$

C_1 , concentration of the bacteria culture = 1.820

V_1 , final volume of minimal salt concentration mixed with bacteria culture =?

$C_2 = 0.1$

V_2 , volume of minimal salt concentration, needed to make the new solution = 200 ml

$$V_1 = \frac{C_2 V_2}{C_1} \quad (4.4)$$

$$V_1 = \frac{0.1 \times 200}{1.820} \quad (4.5)$$

V_1 , volume of bacteria culture that will be added to the minimal salt concentration = 10.99 ml. Therefore, the final volume V_1 , was obtained by subtracting 10.99 ml from the minimal salt concentration (189.01 ml) and adding 10.99 ml of the bacteria culture to it, to make the final volume of 200 ml.

The next phase will detail the investigations of temperature and pressure variations with time, with regards to microbes and their behaviour in actual oil field application.

4.3 Phase II - Interfacial Tension and Contact Angle

4.3.1 Interfacial Tension Measurements

The measurement of interfacial tension is an integral part of this investigation as the application of biosurfactant can aggregate at the interfaces between fluids having different polarities, such as water and oil, leading to the reduction in interfacial tension (El-Sheshtawy, Aiad, Osman, Abo-ELnasr, & Kobisy, 2015; Fang et al., 2007). One of the major considerations, with enhanced oil recovery, is how much the injected bacteria can stimulate the production of additional oil from reservoirs. Usually, this is achieved by the addition of nutrients during water injection. The reduction in interfacial tension is possible by stimulating the growth of bacteria at an oil/water interface, which in turn can aid the recovery of oil. The effects of temperature and pressure on interfacial activity helps to show the behaviour of liquids during interfacial tension measurements. And with the help of density difference between liquids, interfacial tension is easily calculated by the pendant drop method.

Previously, Lin, Chen, Xyu, & Wang, (1995) concluded that after experimenting with air/water and fluid/fluid interfaces, the measured IFT is drop dependent. In this present study, it is demonstrated that there is a reasonable and clear impact of the drop size on the measurement of the IFT. The bigger the drop the more reasonable it is in estimating the IFT by the pendant drop technique, in light of the fact that with this there is higher accuracy, in the image edge detection process. This perception concurs with Yang, Wei, & Lin, (2007) who likewise contemplated the impact of drop size on the IFT and adsorption of surfactants, and it demonstrates the high accuracy with which the drop coordinates, must be resolved and not just rely upon the numerical treatment of the data, but also on the experimental data itself.

In this present study, a total of three hundred and thirty nine (285) IFT measurements were performed at different temperatures and pressure ranges from 0.15 MPa to 13.89 MPa. The interfacial tension data generated from the analysis are discussed below.

The control experiment for crude oil/distilled water system was conducted using the equipment and procedure that were described in the previous Chapter 3. The results shows that there are variations between the interfacial tension with the temperatures. The expected decrease of interfacial tension from 56.95 to 29.47 mN/m, between 26°C and 75°C, for raw crude oil/distilled water system is typified in Figure 4.7. A similar trend was also reported by

(Hamouda & Karoussi, 2008) for 0.005M SA in n-decane/water system. As can be seen, the IFT measurements are shown to be lower at higher pressure of 12.51 MPa. Interfacial activity from this present study shows that the IFT value of 45.25 mN/m at 42°C, can be compared with the 46.8 mN/m that was previously reported by McCaffery, (1972), with n-octane/distilled water at 40°C and 1.38 MPa. The effect of temperature on the pure grade hydrocarbon this author used provided, in most cases, a linear decreasing trend in IFT with increasing temperature over the range that were investigated.

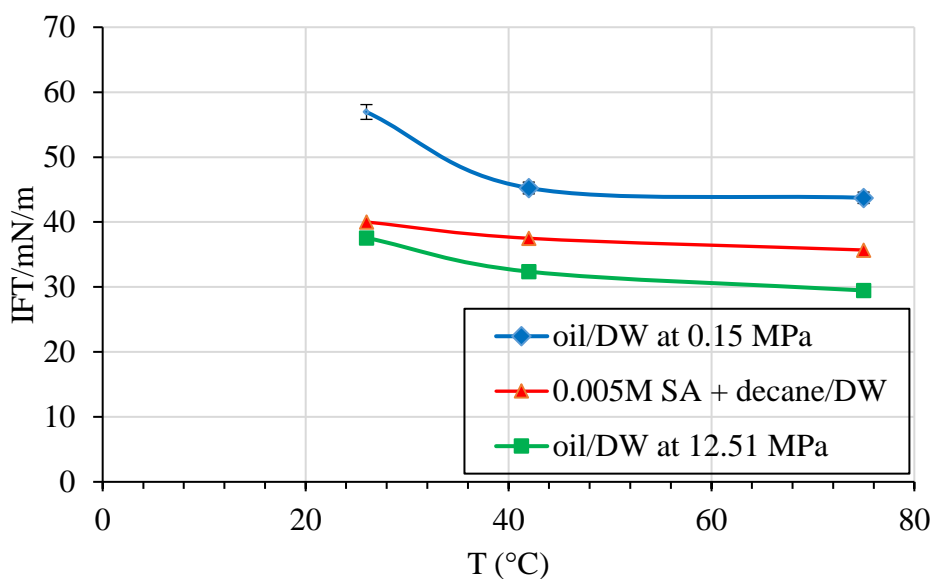


Figure 4.7: Effect of temperature on IFT for crude oil/distilled water system

In the following Sections, the biosurfactants that were used in this investigation are discussed and the corresponding results are presented accordingly.

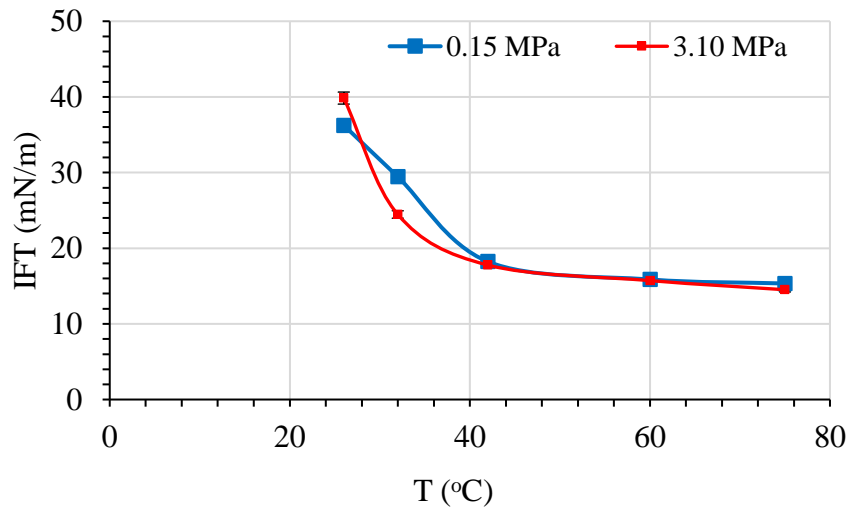
4.3.1.1 *Bacillus subtilis* (BS-1) cells

In a typical laboratory setting, difficulty is usually experienced in the measurement of interfacial tension in bacterial systems. This is mainly due to a growth period of several days that is required to reach a sufficiently large bacterial population. In this study, analysis was carried out in real-time, which lasted about 6 hours. The density of the external phase was 0.9863 Kg/m³. The biosurfactant reduced the Interfacial Tension (IFT) by accessing the oil droplets from the water phase. IFT was measured for heavy crude oil using synthetic formation water and a lipopeptide biosurfactant produced by *Bacillus subtilis* (BS-1) over a pressure range of 0.15 MPa to 13.89 MPa and at temperatures of 26°C to 75°C. Within this

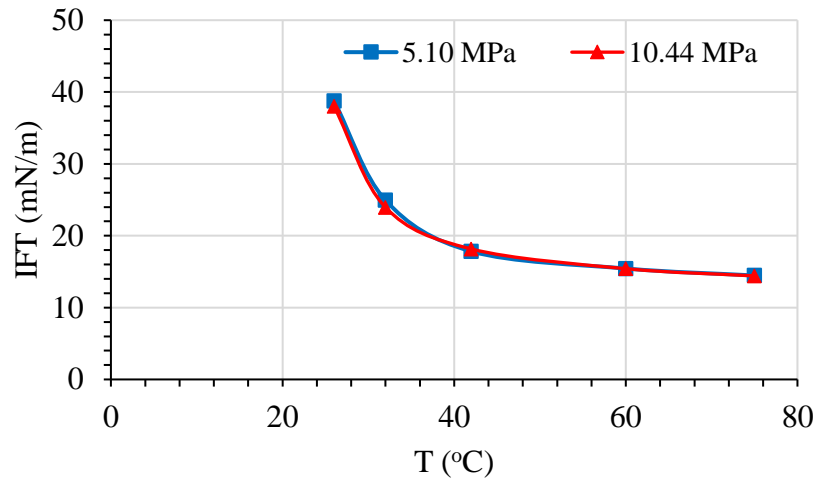
reservoir conditions, IFT was varied with time up to 15 minutes at three selected set pressures.

Further IFT data obtained from biosurfactant with cells from *BS-1* is also represented in Appendix D. The results tabulate the average analysed IFT values at varying pressures and temperatures. The reduction in interfacial tension followed a similar pattern for all pressures but for 0.15 MPa that fluctuated slightly.

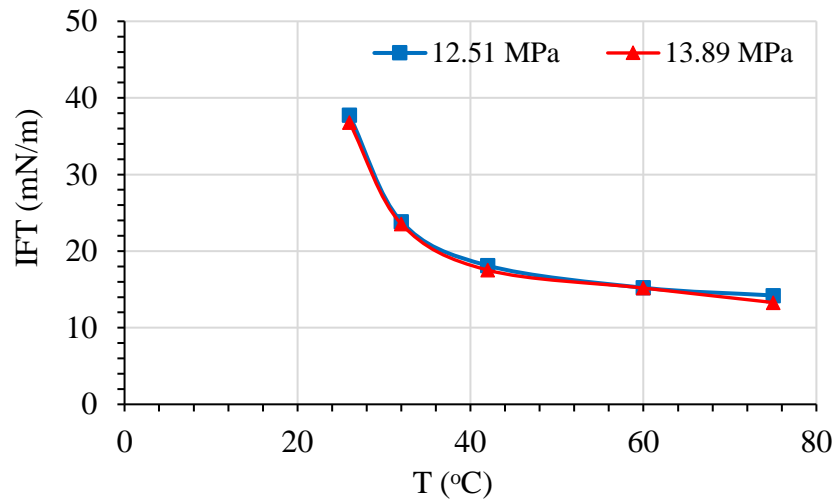
Figure 4.8 shows the IFT of *Bacillus subtilis* (*BS-1*) biosurfactant and heavy oil at different reservoir conditions. The data analysed between 26°C and 32°C (0.15 MPa), may indicate the system probably had not attained equilibrium when the first two measurements were taken 5 minutes after the oil film was formed. The subsequent analysed data lowered the IFT value from 39.85 mN/m (2°C) to 13.29 mN/m (75°C) which corroborates the effect of high temperature in reducing interfacial tension Figure 4.8 (c). There was however a slight reduction in the size of the drop volume from 39.74 µl (26°C) to 38.56 µl (75°C) which may have resulted due to high oil viscosity.



(a)



(b)



(c)

Figure 4.8: Experimental of IFT data with temperature for *Bacillus subtilis* cells

Figure 4.9 is a plot of the variation of IFT with pressure for *BS-I* cells. An increase in pressure did not show any significant reduction in interfacial tension except at 3.10 MPa (26°C and 32°C) where minimal increase and decrease of IFT was seen. This conforms to conclusion made by Cai, Yang, & Guo, (1996), that IFT is weakly dependent on pressure.

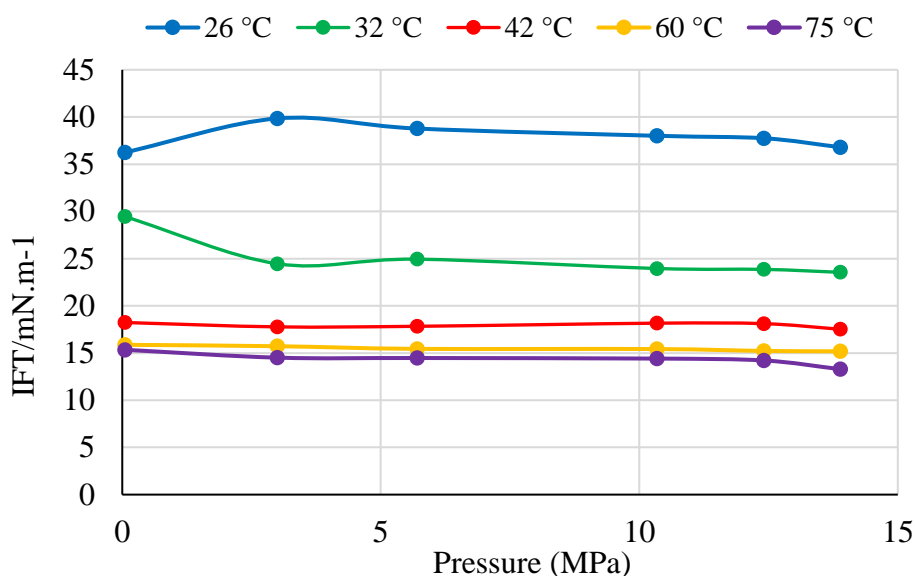
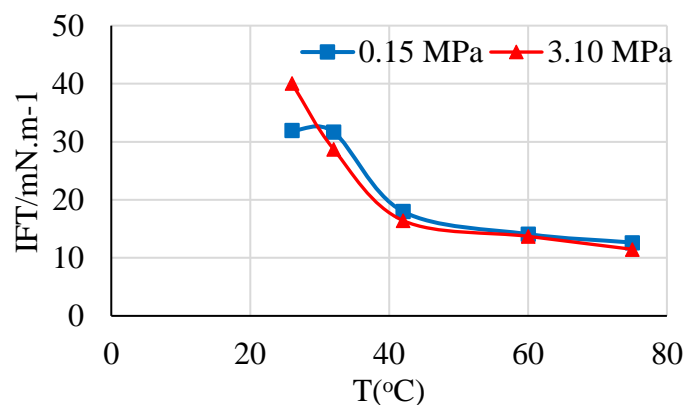


Figure 4.9: Pressure effect on IFT for *BS-I* cells

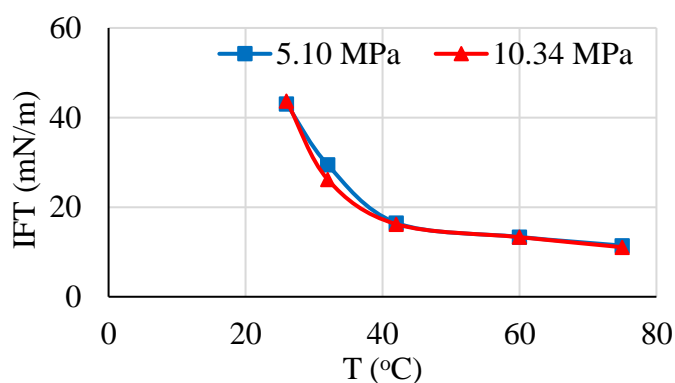
The Figure and data of a series of IFT trend with time obtained at three different temperature and pressures is presented in Appendix E. Measurement at a given temperature and pressure were always taken at intervals up to 3 minutes aging time, and often to 15 minutes. In Appendix E-1, the biosurfactant capacity to reduce interfacial tension had negligible effect at 12.51 MPa (32°C) may be attributed to less microbial activity. The activity of the biosurfactant was clearly seen in Appendix E-2 at 0.15 MPa (42°C) where the IFT reduced from 18.23 mN/m to 17.73 mN/m and then increased across other selected pressures. This reduction may well be due to the fact that there was a significant growth of microbial population at that temperature and pressure. Recalling that *Bacillus subtilis* grow optimally between temperatures of 37°C and 55°C. In Appendix E-3 there was a significant decrease in IFT indicating a strong activity of the biosurfactant. However, after nine minutes of incubation at 5.10 MPa (75°C) IFT increased for the remaining aging time.

4.3.1.2 *Bacillus subtilis* (BS-1) cell-free

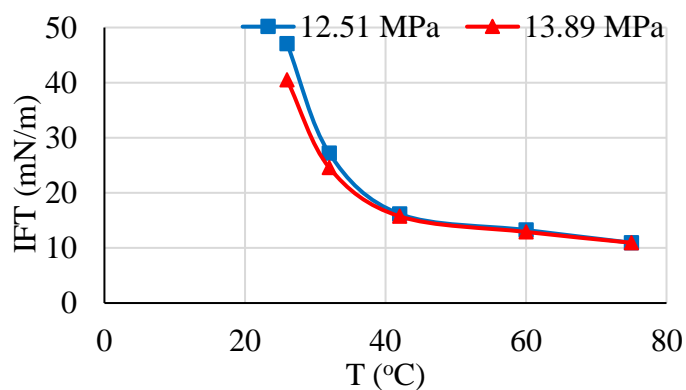
The effect of *BS-1* cell-free biosurfactant was adequately noticed in the reduction of IFT investigated under thermophilic conditions. In Figure 4.10, the variation of IFT is seen to decline in a similar trend that the isotherms overlap. In this analysis, IFT significantly decreased from 47.06 mN/m to 10.94 mN/m (see also Appendix F) which was expected since the effect of temperature dependence on IFT reduction is highly effective.



(a)



(b)



(c)

Figure 4.10: Temperature effect on IFT for *BS-1* cell-free biosurfactant.

The pattern in Figure 4.11 indicates that the effect of pressure does not show a definite tendency even at high temperatures. The influence of pressure on the IFT is not clearly defined, showing that temperature has greater effect on the IFT than does the pressure. This behaviour likewise concurs with Michaels & Hauser, (1951) who examined decane/water systems and inferred that the impact upon the IFT is moderately little, the greatest change being fairly more than 2 mN/m over a pressure range of 70 MPa in their study. The increasing trend of IFT at 26°C maybe in agreement with that obtained by Okasha & Alshiwaish, (2009) and Wang & Gupta, (1995).

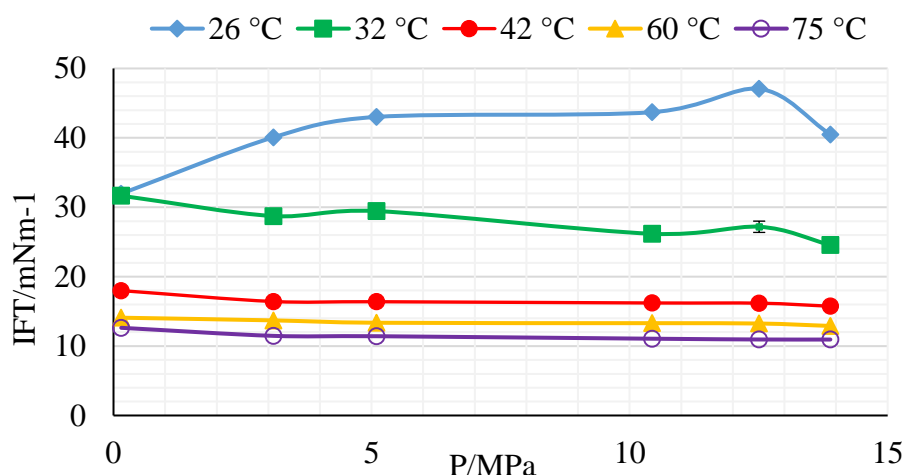


Figure 4.11: Effect of pressure on IFT for cell-free *BS-1*-biosurfactant

The pattern of biosurfactant production is presented by the interfacial behaviour of the bacterium, i.e. the interfacial tension reduction of cell free supernatants. The time variation of IFT data (Appendix G) for *BS-1* cell-free supernatant are shown in Appendix G-1 to G-3. A noticeable decrease in interfacial tension was observed after six (6) and nine (9) minutes of aging at 75°C (0.15 MPa). The appearance of the interfacial tension summary for this case did not show a significant reduction as IFT trended more with a horizontal slope in most of the three temperatures conducted.

4.3.1.3 *Bacillus licheniformis* (BS-2) with cells

The experimental results of the variation of IFT with pressure and temperature for *Bacillus licheniformis* cells in formation water/crude oil sample shows no significant declining effect on IFT with increasing pressure, Figure 4.12.

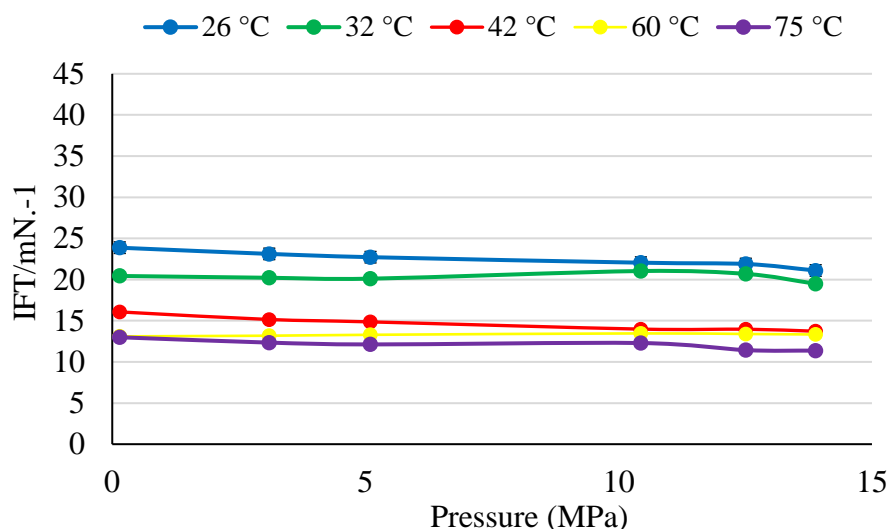
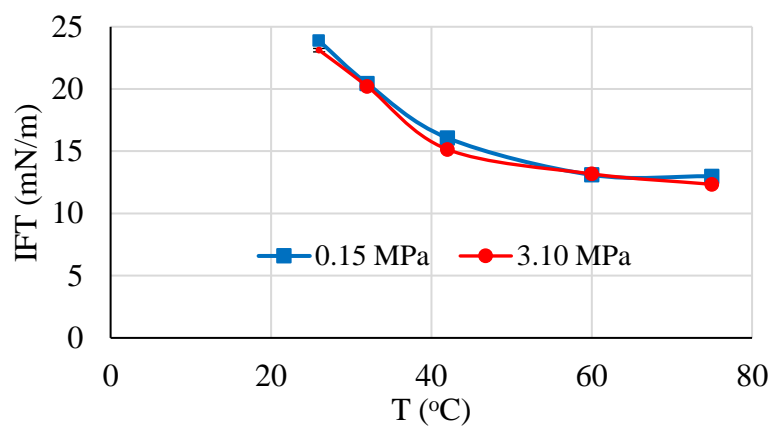
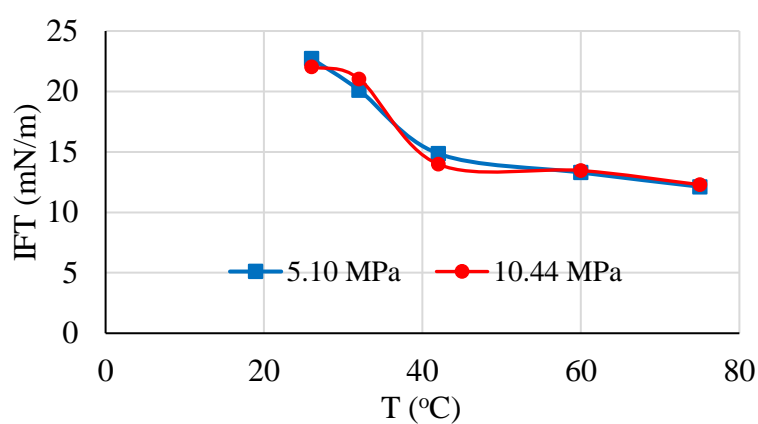


Figure 4.12: Pressure effect on IFT for *BS-2* biosurfactant cells

The analysis further revealed that under the same conditions of pressure, increasing temperature and microbial activity, IFT decreases and is changing with a lower slope, Figure 4.13 (a). For IFT values of 13.10 mN/m (60°C) and 12.99 mN/m (75°C) respectively may indicate that the concentration and activity of the biosurfactant (*B. licheniformis* cells) molecule is approaching a stable value Appendix H. More interestingly as the interface ages, it was observed in Figure 4.13 (b, c), that IFT showed a stable trend between 42°C and 60°C, but further decreased down the slope. This may have resulted to abrupt changes in the physical properties such as osmotic pressure and turbidity as the liquids (crude oil and formation water) react with the biosurfactant concentration. It can therefore be inferred here that the rate at which the osmotic pressure increases with microbial concentration turns out to be unusually low, and the rate of increase of turbidity with concentration is highly improved, which suggests that considerable association was taking place. Turbidity in the IFT cell will look like the reaction in a broth culture which occur due to increase in the bacterial population after growth.



(a)



(b)

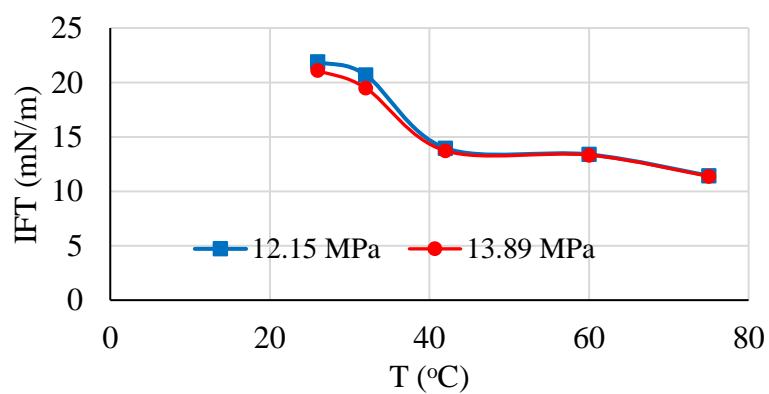


Figure 4.13: IFT with temperature at varying pressures for *BS-2* with cells.

Figure 4.14 and 4.15 shows IFT as a function of time at reservoir conditions, 42°C and 75°C (0.15 MPa, 5.10 MPa and 12.51 MPa). The data is fully presented in Appendix I. It can be noted from Figure 4.14 that as the interface ages, stable values of interfacial tension resulted

after 3 minutes for 0.15 MPa (42°C), while a gradual decline of interfacial tension value occurred between the two other pressures. We found out that at a given temperature and pressure, IFT didn't show a significant decrease with time at 12.51 MPa (75°C), as IFT initially was increasing (Figure 4.15). The uncommon decrease of IFT with time may be the result of mutual solubility changes of the system with pressure, which may have resulted to changes in the physical properties such as osmotic pressure and turbidity. However, no literature was found to support this unusual effect.

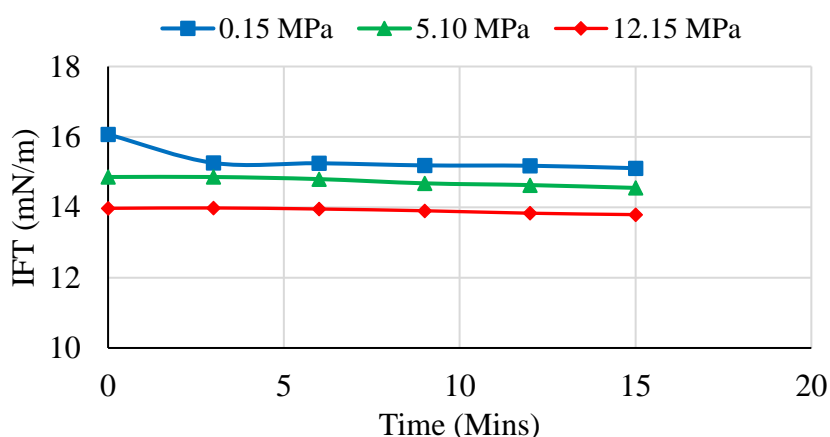


Figure 4.14: IFT with time for *BS-2* biosurfactant at 42°C

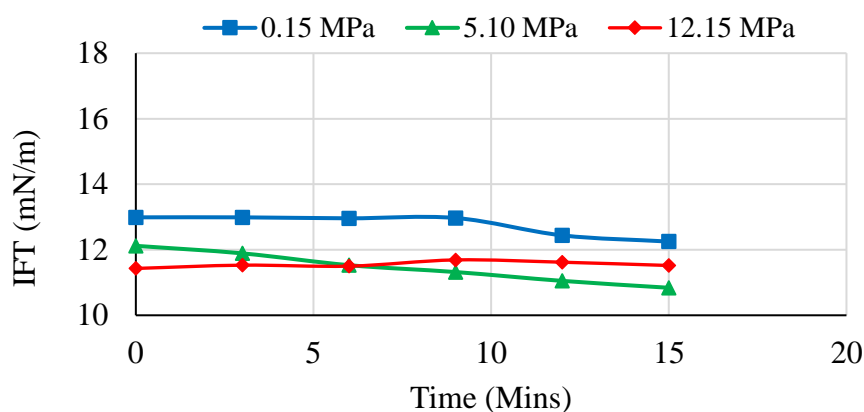
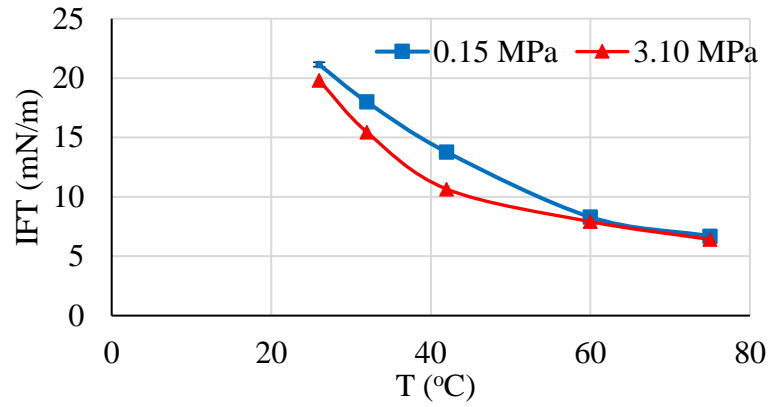


Figure 4.15: Variation of IFT with time for *BS-2* biosurfactant at 75°C

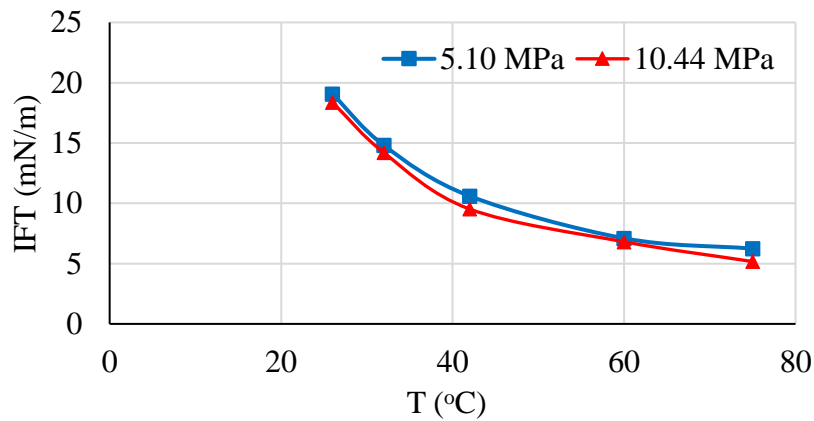
4.3.1.4 *Bacillus licheniformis* (BS-2) cell-free

Cell-free biosurfactant of *Bacillus licheniformis* gave the greatest reduction values of IFT as, also seen in the data generated in Appendix J. It was assumed that equilibrium between the liquids was reached after five minutes of forming the oil film before the measurement were taken to observe the effect of the biosurfactant concentration . This is in conformity with

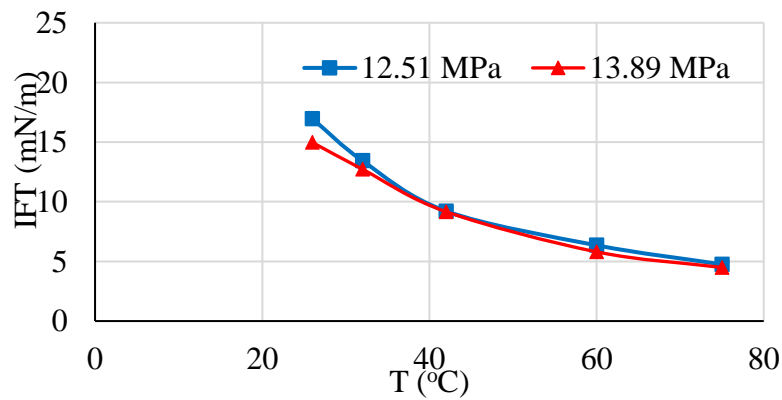
reports of Wang & Gupta, (1995) where oil drops were equilibrated for five minutes in order to get reliable results. The series of pressure measurements from lowest to highest shows a consistent reduction of the interfacial tension value. At 75°C, Figure 4.16(c), IFT value of 4.49 mN/m was lowest at a constant pressure of 13.89 MPa.



(a)



(b)



(c)

Figure 4.16: IFT with temperature at varying pressures for *BS-2* biosurfactant cell-free

This is an evidence to demonstrate the importance of screening biosurfactants to isolate the most profitable and versatile amphilic surface compounds to be used for EOR applications, since environmentally friendly biosurfactants of the same family have different surface active strenght behaviours. This result may potentially be applicable to an in situ microbial enhanced oil recovery operation.

The effect of varying IFT with aging time at given temperature was clearly observed at varying pressures at intervals of 3 minutes and often to 15 minutes (see also Appendix K). In Figure 4.17, 4.18 and 4.19 for 12.51 MPa, the IFT value decreased insignificantly by considerable small amounts that could indicate that the biosurfactant concentration reached its critical point at the beginning of time variation, thus lowering the free energy of the system. The CMC can be clearly seen as the IFT approached a constant value across the three temperatures observed between twelve and fifteen minutes, with the lowest recorded values of 12.89 mN/m, (32°C). 19.16 mN/m (42°C), 4.52 mN/m (75°C). These gradual decrease or aging effect is typical of crude-oil/brine systems and can be attributed to the collection of surface-active materials at the interface.

The effect of increasing time of IFT reduction between oil/biosurfactant with formation water followed the trend investigated by Dunlap, Schisler, Price, & Vaughn, (2011), following the isolation of biosurfactant strains for the purpose of anti-fungal of fusarium head blight virus with wheat.

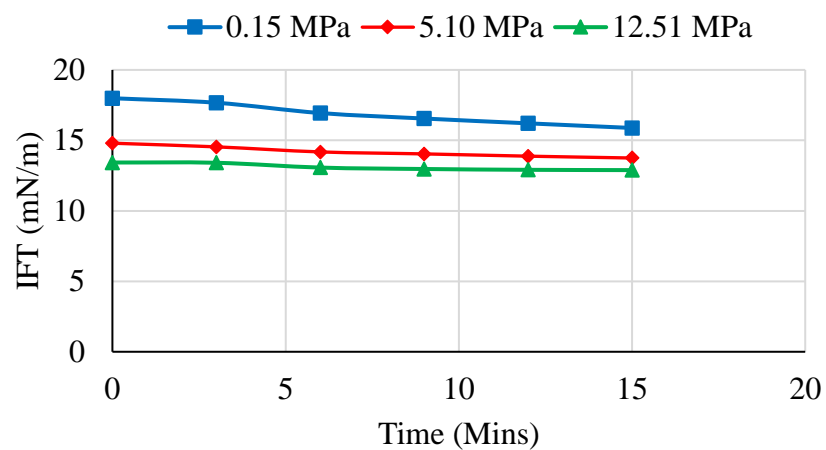


Figure 4.17: IFT with time for *BS-2* biosurfactant cell-free at 32°C

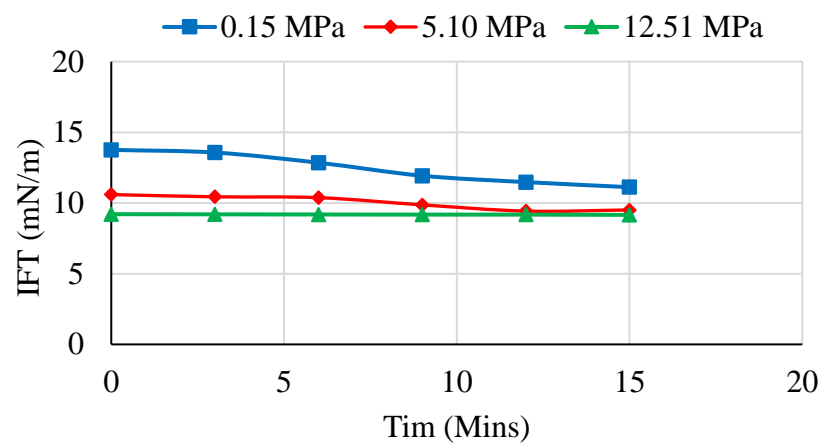


Figure 4.18: IFT with time for *BS-2* biosurfactant cell-free at 42°C

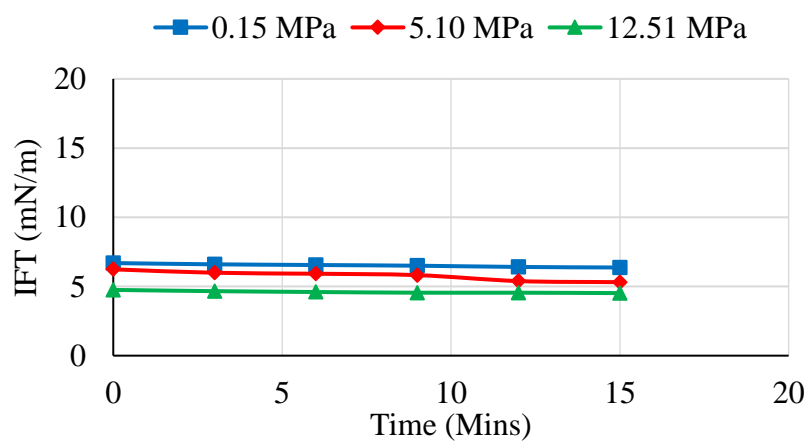
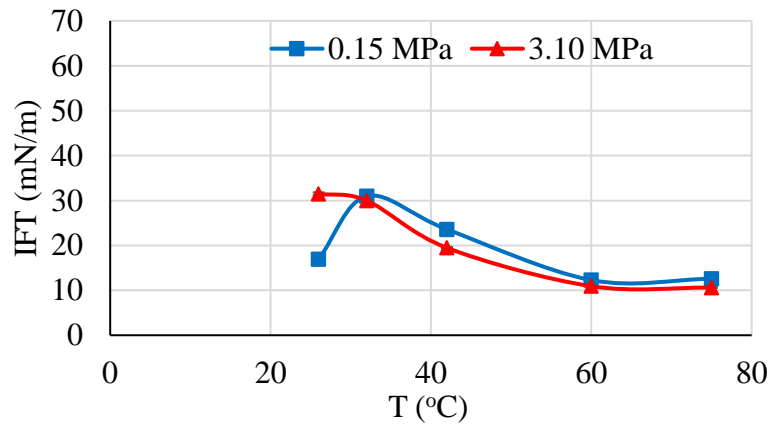


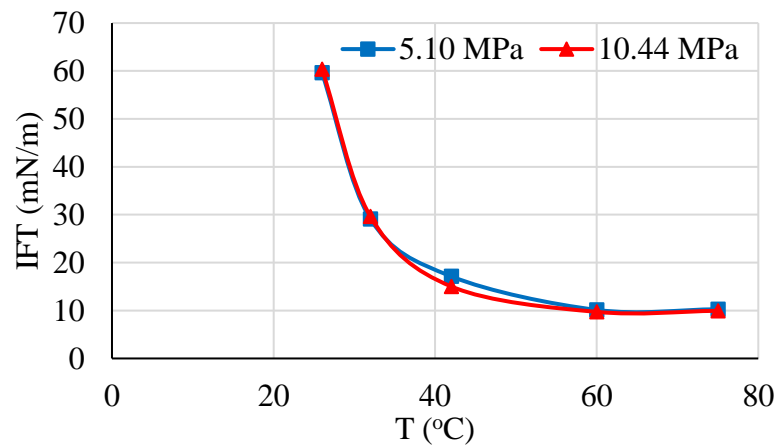
Figure 4.19: IFT with time for *BS-2* biosurfactant cell-free at 75°C

4.3.1.5 *Paenibacillus polymyxa* (BS-3) Cells

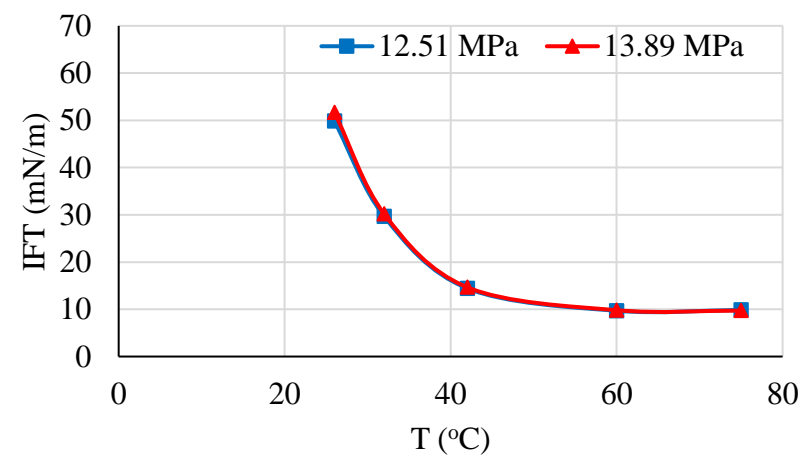
The impact of *P. polymyxa* (BS-3-cells) is observed as IFT reduced through Figure 4.20 to reach its maximum reduction of 9.73 mN/m (75°C, 13.89 MPa).



(a)



(b)



(c)

Figure 4.20: IFT with temperature at varying pressures for BS-3 with cells

This value remains closely compared to 9.75 mN/m (42°C, 10.44 MPa) for *BS-3* cell-free, of which the IFT reduction was only about half way through the investigation. This indicates that the endospore forming bacterium has a better effect on interaction with the crude oil if the cells are extracted out from the biosurfactant. The full experimental data is also represented in Appendix L.

4.3.1.6 *Paenibacillus polymyxa* (BS-3) cell-free

IFT measurements for cell-free cultures of *BS-3* at pressure ranges up to 2000 psi was investigated. Figure 4.21 is a plot of microbial effect on crude oil for a 37.5 w/v biosurfactant solution diluted in a 62.5 w/v formation water. No effect was seen yet again for pressure except for 0.15 MPa (32°C) where their was a minimal decrease of IFT.

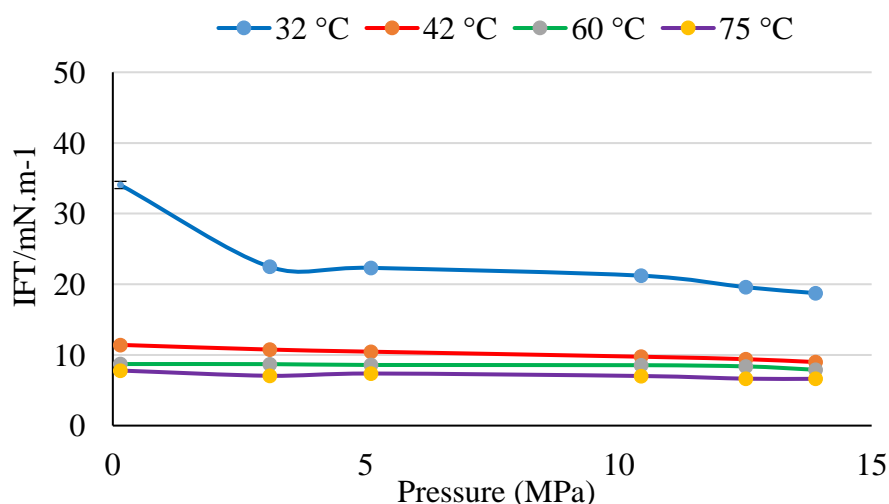
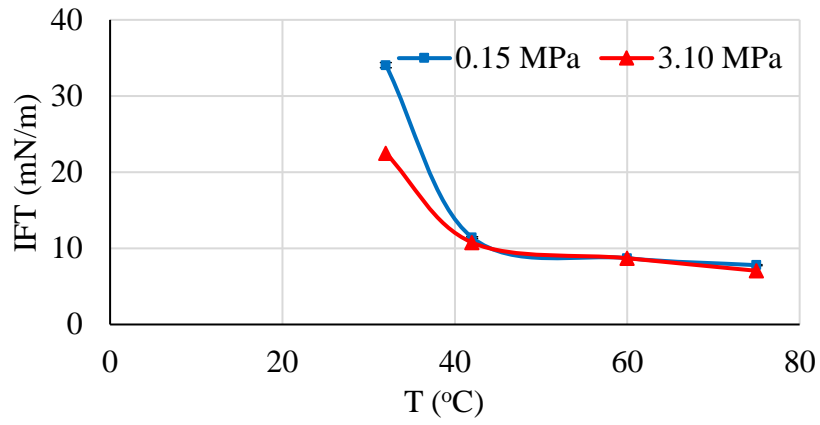
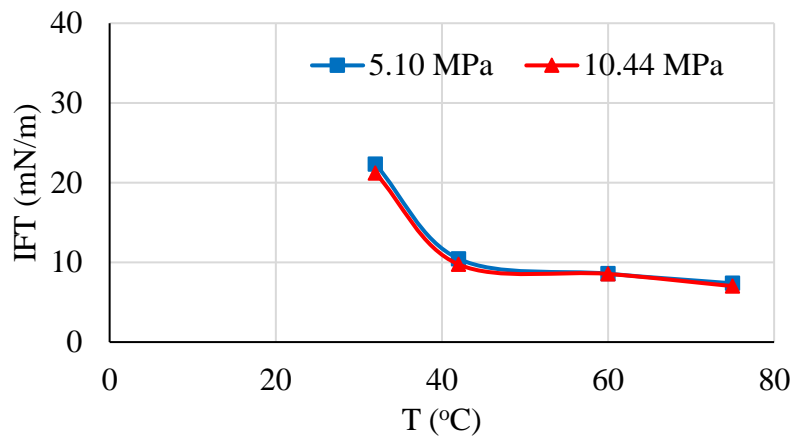


Figure 4.21: Pressure effect on IFT for *BS-3* cell-free at varying temperatures

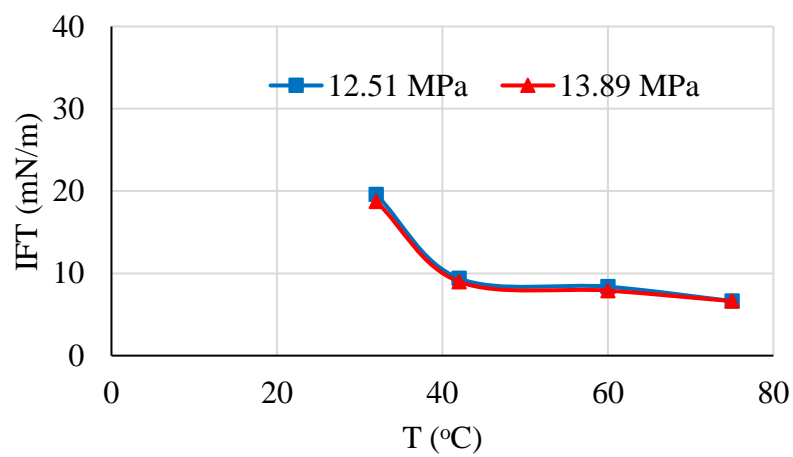
Investigations were further carried out on the heavy crude oil using *BS-3* cell-free biosurfactant to determine the effect of the microbial activity and interfacial tension, as represented in Appendix M. Measurements was not taken at 26°C since the room temperature was very high up. In Figure 4.22(a), IFT reduced significantly from 34.05 mN/m (32°C) to 11.42 mN/m (42°C) which may relate to multiple bacteria growth and interactions between the two interface. Although at varying temperatures and pressures, the pattern in which the IFT is reducing followed a similar trend and declined to a final reduction of 6.6 mN/m (75°C).



(a)



(b)



(c)

Figure 4.22: Temperature effect on IFT for *BS-3* cell-free at varying pressures.

The plot for IFT with time at constant pressure in 32°C and 42°C for *BS-3* cell-free supernatant is presented in Appendix N-1 and N-2. The lowest reduction recorded at 42°C was 10.07 mN/m, and it was observed that this reduction was the same at 12 mins and 15 mins of the time measured. This reduction followed a similar pattern by (H. S. Al-Sulaimani et al., 2010), where strain W19 gave a maximum IFT reduction to 3.28 mN/m in 16 hours of incubation.

4.3.1.7 Comparison of IFT with temperature and time for *BS-1*, *BS-2* and *BS-3* Biosurfactants with Cells

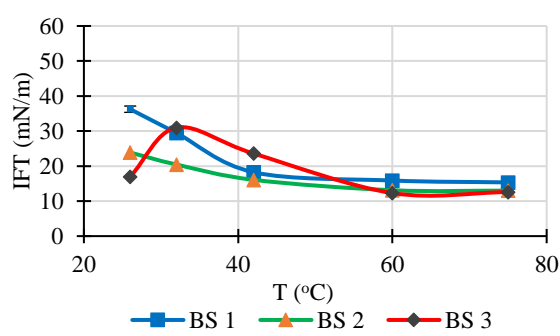
In aqueous surfactant solutions, there is a large body of data on the surface and interfacial tension which demonstrates that the structure of the surfactant molecule has a pronounced capacity to reduce these tensions (Möbius, Miller, & Fainerman, 2001). However, this study was not able to verify the biological structures of these produced biosurfactants, since it was a costly process to undertake a mass spectrometry of the lipopeptide. I however assumed their structures to be like that of surfactin, since they belong to the same family of lipopeptide.

Comparison of the cultured biosurfactants with cells in terms of IFT and contact angle reduction, showed higher values when compared to interactions with cultured cell-free biosurfactants at constant pressures as shown in Figure 4.23. Measurements of interfacial tension reduction by these three biosurfactants with cells showed that *Paenibacillus polymyxa* (*BS-3*) gave the greatest IFT reduction of 9.73 mN/m. This could be because *BS-3* was isolated from an oil field, which explains this interfacial activity. However, at the start of the experiment, Appendix O, IFT can be seen to be constantly increasing, and may have resulted due to a slow interaction of *BS-3* cells with the oil, since further down, the effect was significantly noticed.

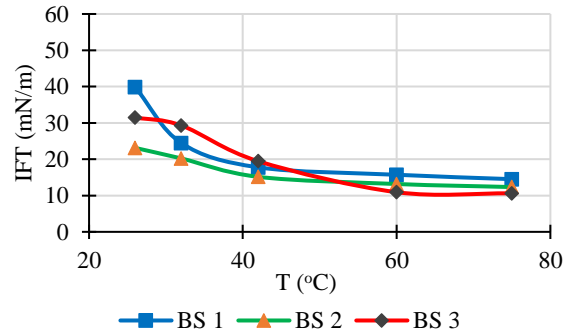
The influence of pressure on the IFT is not clearly defined and did not indicate any significant reduction in interfacial tension, showing that temperature has a greater effect on the IFT than does the pressure. This behaviour likewise concurs with conclusion made by Cai et al., (1996), that IFT is weakly dependent on pressure. Michaels and Hauser, (1951) who examined decane/water systems and inferred that the impact upon the IFT is moderately little, the greatest change being more than 2 mN/m over a pressure range of 70 MPa in their report. However, the sharp increase of IFT at 26°C for cell-free *BS-1*, maybe in agreement

with results obtained by Wang and Gupta, (1995) and Okasha and Alshiwaish, (2009) when IFT increased with pressure at constant temperature.

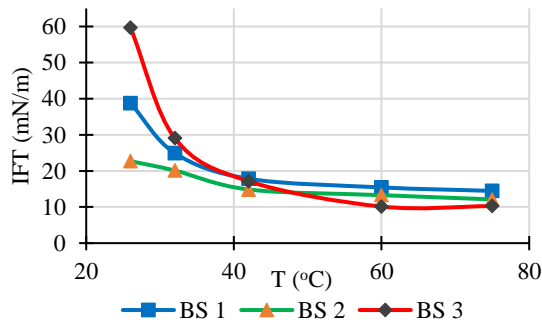
Further data are also shown in Appendix P that there was an insignificant reduction in IFT with time for all three biosurfactants as the trend followed a reduction parallel to each other.



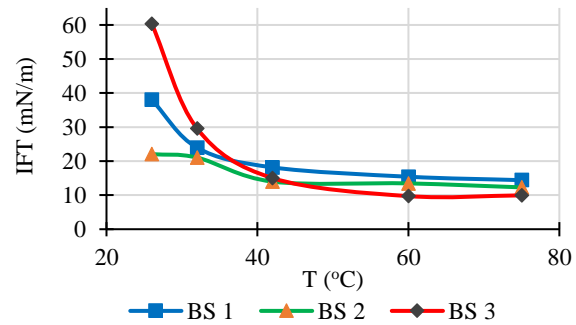
(a) At constant pressure of 0.15 MPa



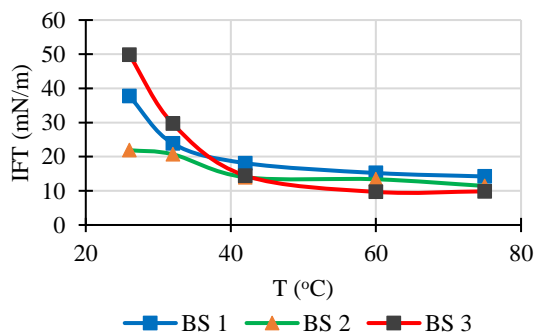
(b) At constant pressure of 3.10 MPa



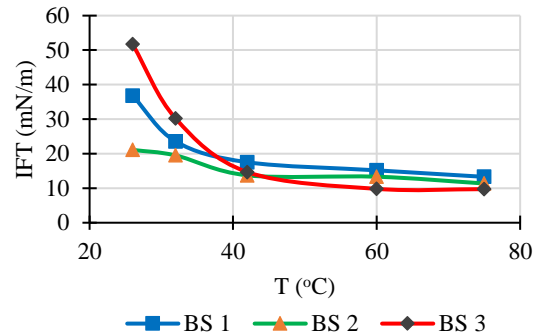
(c) At constant pressure of 5.10 MPa



(d) At constant pressure of 10.44 MPa



(e) At constant pressure of 12.51 MPa



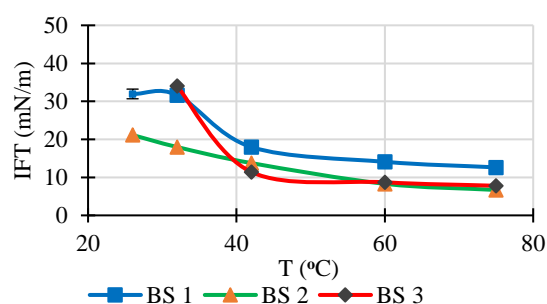
(f) At constant pressure of 13.89 MPa

Figure 4.23: Comparison of IFT with temperature for biosurfactants with cells

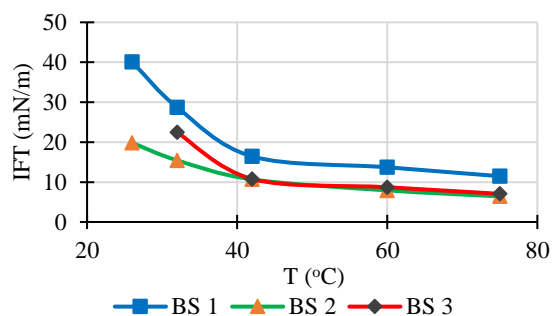
4.3.1.8 Comparison of the effect of IFT with temperature for supernatant *BS-1*, *BS-2* and *BS-3* Biosurfactants

In a typical laboratory setting, difficulty is usually experienced in the measurement of interfacial tension in bacterial systems due to a growth period of several days, to reach a sufficiently large bacterial population. In this study, analysis was carried out in real-time, which lasted about 6 hours. The densities of the external phases were duly calculated. To be able to understand and predict their action in practical reservoir field application, it is important to know the general relationships between structure and performance, mechanisms of interactions among amphiphiles and other species as well as their behaviour in complex systems. In comparison, the three produced biosurfactants were analysed to estimate, which has the greatest impact on IFT reduction that could give the best outcome in enhancing oil recovery. The trend in the reduction of interfacial tension followed a similar pattern as it can be seen from the plot of Figure 4.24 and tabulated in Appendix Q. The effect of biosurfactant concentration was almost approximate between *BS-2* and *BS-3* at 42°C (3.10 MPa and 5.10 MPa), with the greatest reduction being 4.49 mN/m for cell-free *BS-2*-biosurfactant.

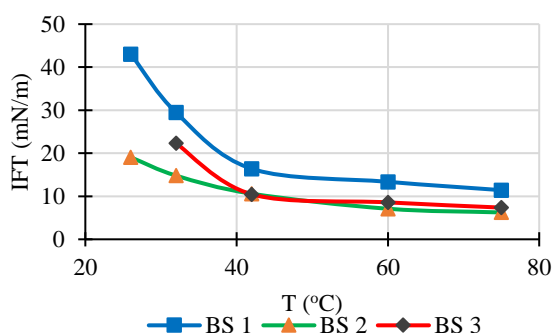
A secreted, extracellular biosurfactant, that was produced by *BS-2*, gave the greatest reduction values of IFT as seen in Figure 4.24-f. The effectiveness in interfacial tension reduction by biosurfactant in a liquid-liquid system can be characterised by the biosurfactant concentration in the entire system, which is required to produce a given interfacial tension (Attwood and Florence, 2012, Möbius et al., 2001). It was assumed that equilibrium between the liquids was reached after five minutes of forming the oil film, before the measurement were taken to observe the effect of the biosurfactant concentration. This is in conformity with the reports of Wang and Gupta, (1995), where oil drops were equilibrated for five minutes to get reliable results. The interactions between the intermolecular forces between the crude oil and biosurfactants is highly effected by the size of the film and was more pronounced at higher temperatures and thus decreasing the oil viscosity by reducing the forces of attraction between the molecules of the crude oil. At 75°C the IFT value of 4.49 mN/m was lowest at a constant pressure of 13.89 MPa. This is evidence to demonstrate the importance of screening biosurfactants to isolate the most profitable and versatile amphilic surface compounds to be used for EOR applications, since environmentally friendly biosurfactants of the same family have different surface active strength behaviours. This result may potentially be applicable to an *in situ* microbial enhanced oil recovery operation.



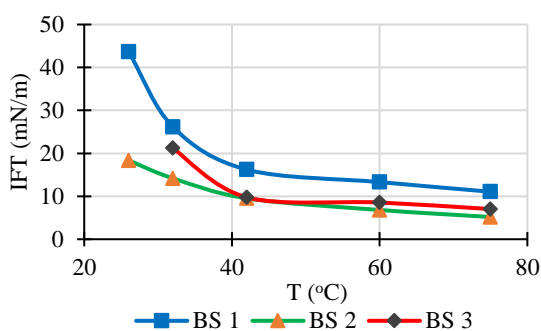
(a) At constant pressure of 0.15 MPa



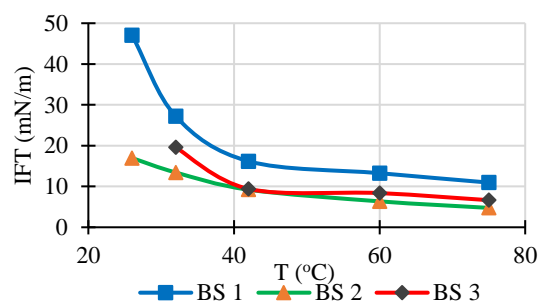
(b) At constant pressure of 3.10 MPa



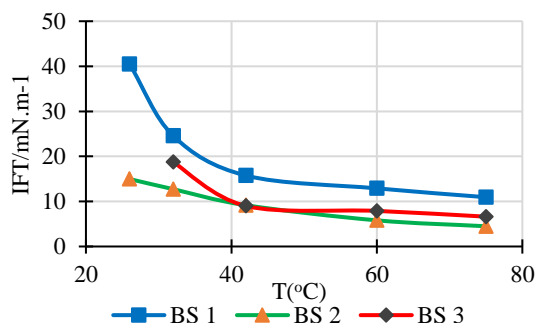
(c) At constant pressure of 5.10 MPa



(d) At constant pressure of 10.44 MPa



(e) At constant pressure of 12.51 MPa



(f) At constant pressure of 13.89 MPa

Figure 4.24: Comparison of IFT with temperature for supernatant biosurfactants

Accurate density measurements are essential to the pendant drop method since IFT calculations depend on the density difference between the two fluids. The tabulated results of IFT measurements with time for cell-free biosurfactants can be seen in Appendix R and shown graphically in Appendix R-1 to R-3.

The data displayed a time variation of 15 minutes at selected pressures. No meaningful reduction of interfacial tension occurred except for *BS-3* at 32°C (0.15 MPa) where a steep decrease of IFT from 36.74 mN/m - 18.82 mN/m was observed. This pattern however, indicated that IFT was weakly dependant on time, which could have resulted due to short time variation in which the measurements were taken.

4.3.2 Contact Angle Measurements

Contact angle is the most acceptable measure of the natural wettability of a reservoir rock. When a drop of liquid is placed on a surface immersed in another liquid, a contact angle is formed which can range from 0° to 180°. A contact angle of 0° means total hydrophilicity, which indicates completely water-wet, whereas and an angle of 180° means the surface is totally hydrophobic, completely oil-wet. Wettability evaluation in the form of contact angle estimation is a difficult type of measurement, since it is so sensitive to the surrounding environment. In addition, Young's equation (Eqn. 4.6) describes the sensitivity in the measurement of a drop by considering the equilibrium between forces factors at the three-phase-contact for oil/water/rock system.

$$\sigma_{os} = \sigma_{ws} + \sigma_{ow} \cdot \cos\theta \quad (4.6)$$

Where θ , is the contact angle at the oil/water/solid contact line, σ_{os} , oil-solid (N/m), σ_{ws} , oil-water (N/m), σ_{ow} , water-solid (N/m)

When the contact angle is greater than 90°, it is said to be oil-wet. If the angle is below 90° it indicates water-wet surface, with a higher affinity for water than oil. If the surface shows affinity for both phases, it is called intermediate-wet with an angle close to 90°. Since the measurement techniques influence the value of contact angle, the angles measured by different techniques may not be comparable. The generally accepted wetting classification is given by (Anderson, 1986): 0°-75°, water-wet; 75°-115°, intermediate-wet; 115°-180°, oil-wet. In this study, 95°-115° was defined as weakly intermediate-wet and 115°-135° was defined as weakly oil-wet.

The results obtained from this study for the contact angle investigation was summarised and presented with the lowest reductions for all the biosurfactant applied to the system. The contact angle of the oil film reduced from 147.04° to 111.84°. Table 4.1, represents a

summary of this reductions which was recorded at different pressures and at elevated temperature of 75°C.

Table 4.1: Greatest contact angle reduction of all produced biosurfactant

Parameters	Temperature (°C)	Pressure (MPa)	Contact Angle (°)
Formation water	75	12.51	147.04
<i>BS-1</i> Cells	75	13.89	135.86
<i>BS-1</i> Cell-free	75	5.10	131.35
<i>BS-2</i> Cells	75	10.44	125.11
<i>BS-2</i> Cell-free	75	0.15	111.84
<i>BS-3</i> Cells	75	12.51	133.36
<i>BS-3</i> Cell-free	75	13.89	130.66

As the pressure increased, the contact angle became smaller and for most of the biosurfactant applied to the system, the contact angle remained weakly oil-wet, mostly ranging between 125° to 136°. Although, the effect of *BS-2* cell-free biosurfactant was significant enough to reduce the contact angle to 111.84°, a weakly intermediate-wet state as seen in Figure 4.25. However, none of the biosurfactants could reduce the contact angle enough to alter the wettability of the oil film into a water-wet state. Although, the low salinity of the formation water which influenced the preparation of the MSM used during the bacteria culture, could have affected the outcome of the results. Thus, for each scenario investigated in this study, the contact angle decreases as the temperature was increased, which means that the system was greatly influenced at elevated temperature.

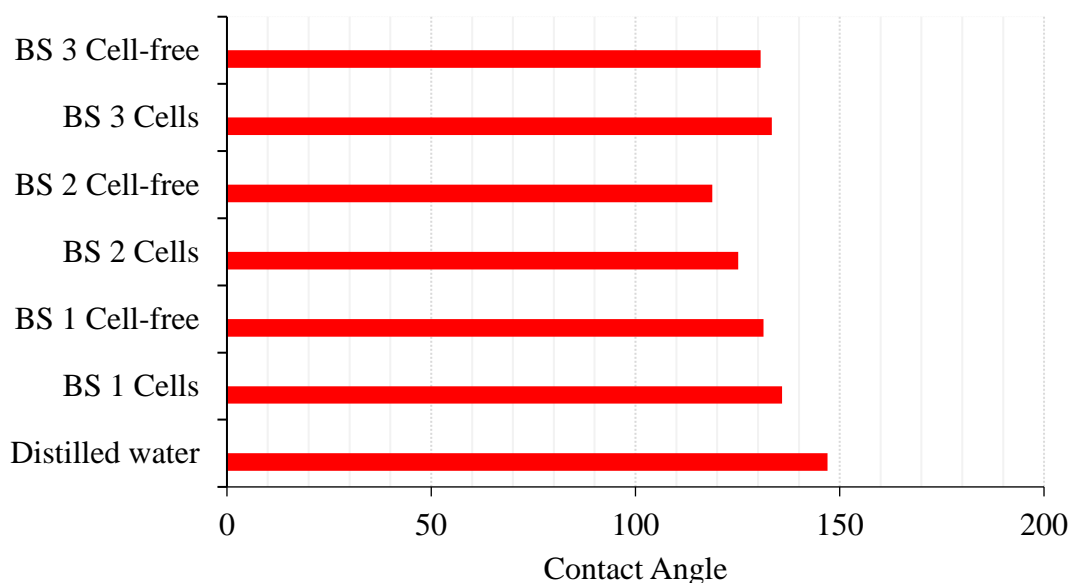


Figure 4.25: Effect of drop size on contact angle values for different pressures at 75°C

4.3.2.1 Film (oil-drop) formation

The tendency to form rigid interfacial films is temperature - dependent. Higher concentrations of the molecules responsible for these films accumulate at the formation water/oil interface at low temperatures. It was observed that the film formation decreased with increasing temperature as seen in the Figures 4.26 - 4.30, for cells/cell-free biosurfactant. Notice here that the size of the drop is much bigger at 26°C for the entire experiment performed, which could suggest that a larger quantity of film-forming material is present at the oil/biosurfactant/formation water interface. As the volume of the film gets bigger the interfacial tension becomes higher and closer to the literature value of 72 mN/m at 25°C for air-water system (Friberg & Ahmad, 1971).

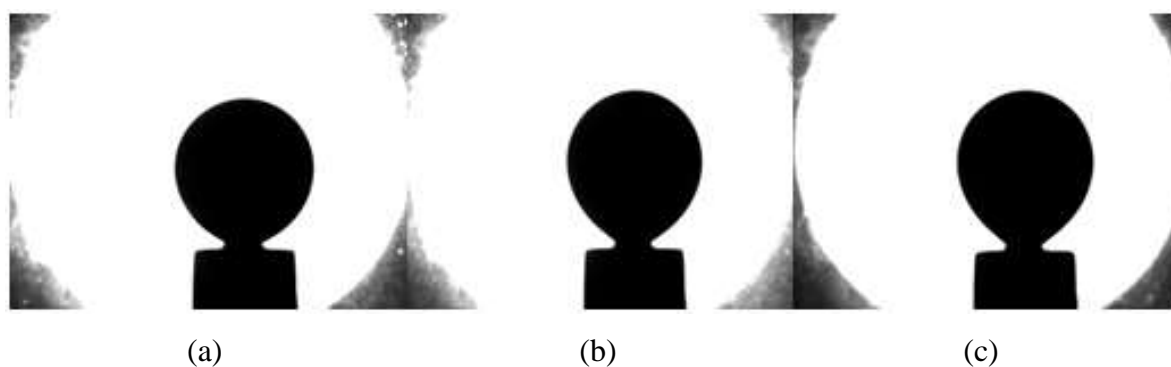


Figure 4.26: Film formation of oil with *Bacillus subtilis cells* biosurfactant at; (a) 26°C, 0.15 MPa (b) 42°C, 0.15 MPa (c) 60°C, 13.89 MPa

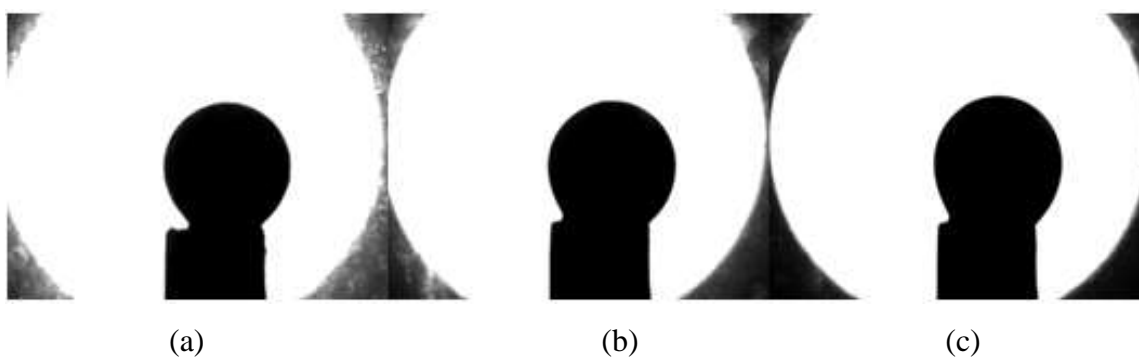


Figure 4.27: Film formation of oil with *Bacillus licheniformis* biosurfactant cells at 0.15 MPa; (a) 26°C, (b) 42°C, (c) 75°C

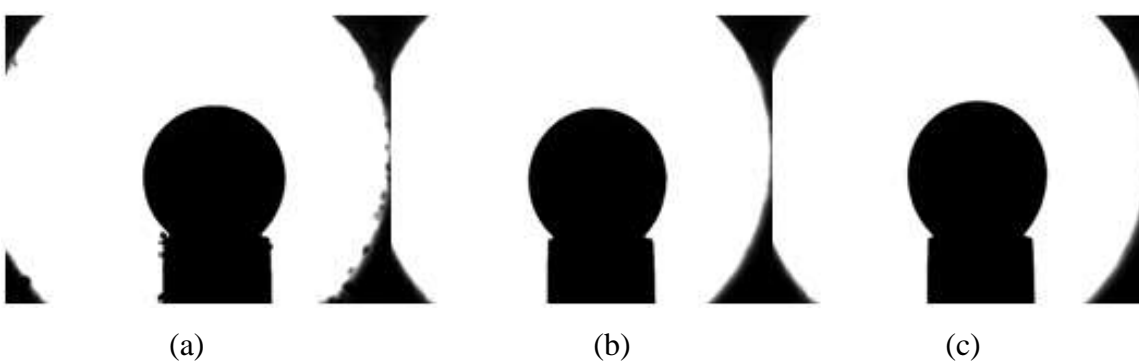


Figure 4.28: Film formation of oil with *Bacillus subtilis* cell-free biosurfactant at; (a) 26°C, 0.15 MPa (b) 42°C, 12.51 MPa (c) 75°C, 10.44 MPa

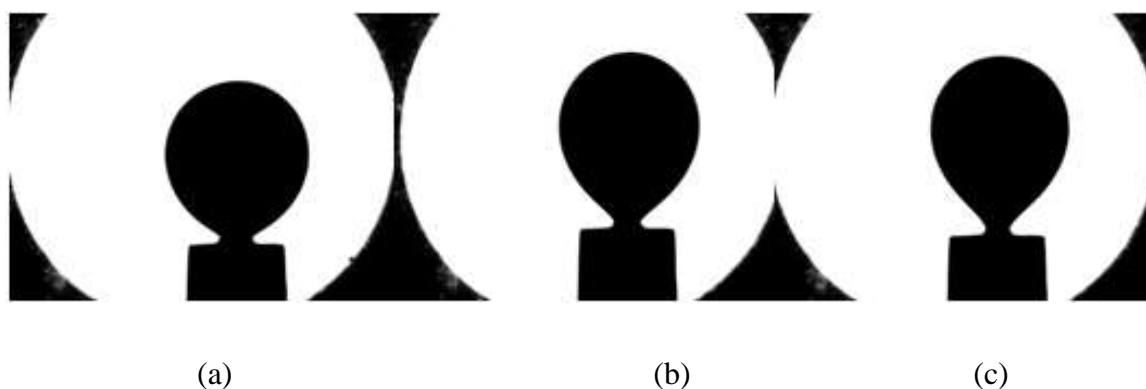


Figure 4.29: Film formation of oil with *Bacillus licheniformis* cell-free biosurfactant at 3.10 MPa; (a) 26°C, (b) 42°C, (c) 75°C

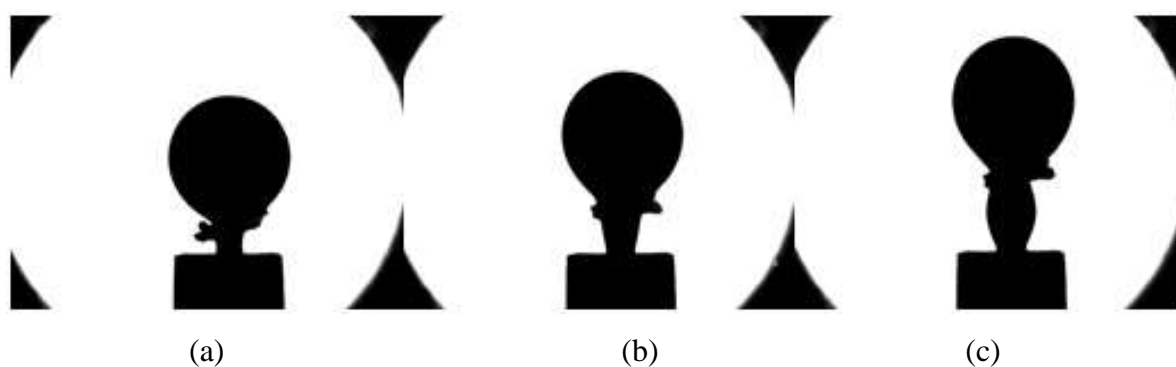


Figure 4.30: Film formation of oil with *paenibacillus polymyxa* cell-free biosurfactant at 10.44 MPa (a) 32°C, (b) 42°C, (c) 75°C

The ability to form interfacial films, as well as the type of film, has been shown to be closely related to the amount of polar compounds (i.e. asphaltenes and resins) in the crude oil as well as brine pH (Hasiba & Jessen, 1968; Strassner, 1968). In this study, the impact of pH on interfacial tension was not examined. The transition of a rigid film into a liquid expanded film may explain the reduction of film size with temperature Davies & Rideal, (1963). In all the oil film framed in this study, the shape was spherical with a clearly formed neck, except for *BS-2* cells and *BS-3* cell-free that did not form a clear neck. Subsequently, measures were taken into consideration, by adjusting the horizontal cross-hair line to the point of convergence before taking the IFT measurements.

4.4 Phase III - Qualitative Wettability Tests

It is essential to maintain the correct reservoir wettability conditions if special core analysis tests are to give dependable results. Qualitative wettability tests were thus performed on crushed rock grains, which followed the equipment and procedures that were already described in the previous Chapter (3). The testing was to check the effectiveness of the core cleaning and aging procedures, as well as the effectiveness of the biosurfactant in changing the wettability of the crude-oil aged crushed rocks.

The crushed rock grains were added into a test tube of distilled water after cleaning with toluene. An initial control tests were carried out with the untreated samples by the addition of the grains into distilled water. If the crushed rock sample sink to the bottom of the tube it is then completely water-wet, otherwise, it is oil-wet if it floats. The outcome for both sandstones gave a completely oil-wet characteristic as can be seen in Figure 4.31, since the grains were floating and remained that way even after several hours.

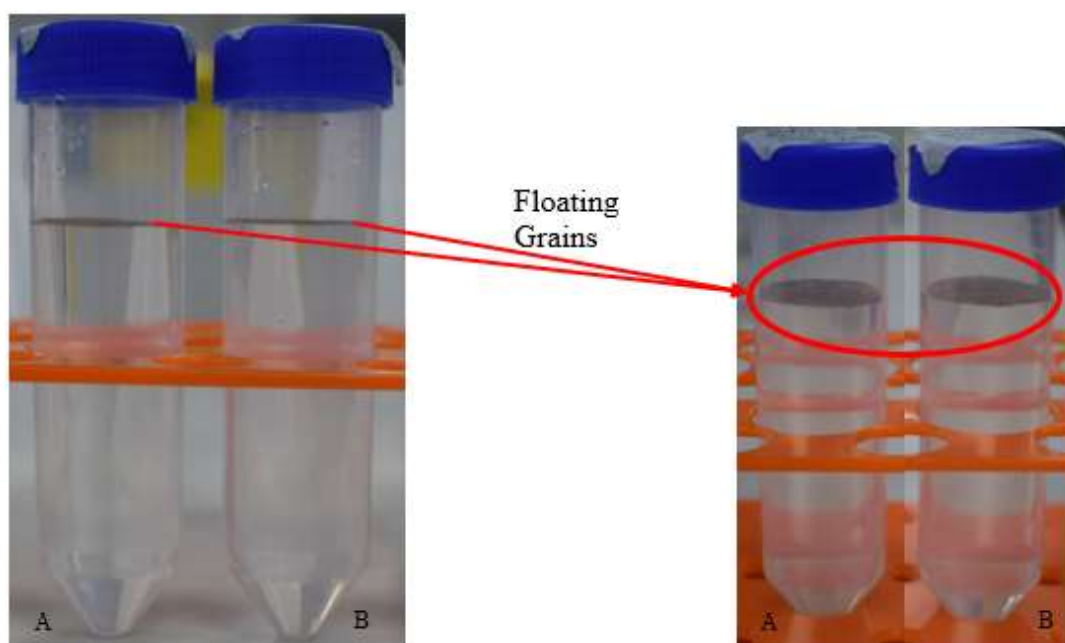


Figure 4.31: Control test for distilled water and untreated grain samples without biosurfactant
(a) Scioto, (b) Bandera gray

4.4.1 Floating Test

The floating test was initiated after treatment with the oil and with the different biosurfactants. 0.2g of each grain samples were weighed and used for the floating test. Treated samples were added into 12 test-tubes for both the cell and cell-free cultures. The

impressive performance of the effect of these biosurfactants was observed as the samples were added into distilled water. Interestingly most of the outcome gave a positive effect in altering the degree of wettability as can be seen in Figure 4.32 to 4.35. These results can be compared to the floatation experiment conducted by Wu et al., (2006), where different surfactants and naphthenic acids, treated with calcite powder, provided information about the mechanisms responsible for the reversal to a water-wet state. The polar compounds in resins and asphaltenes both combine hydrophilic and hydrophobic characteristics. Most of the grains, treated with the biosurfactants, showed alteration in wettability from hydrophobic to a slightly intermediate wet, rather than to a water-wet state, throughout the pore system for this test. A summary of the results is presented in Table 4.2.

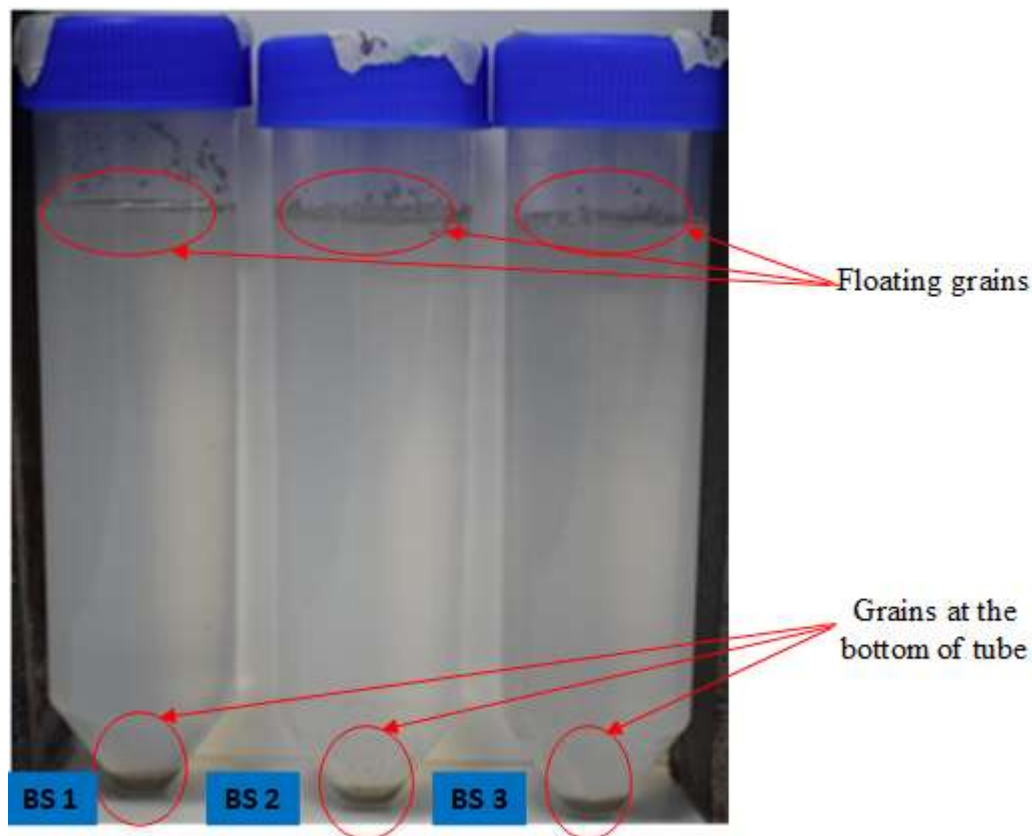


Figure 4.32: Distilled water and treated scioto grain sample in biosurfactant with cells

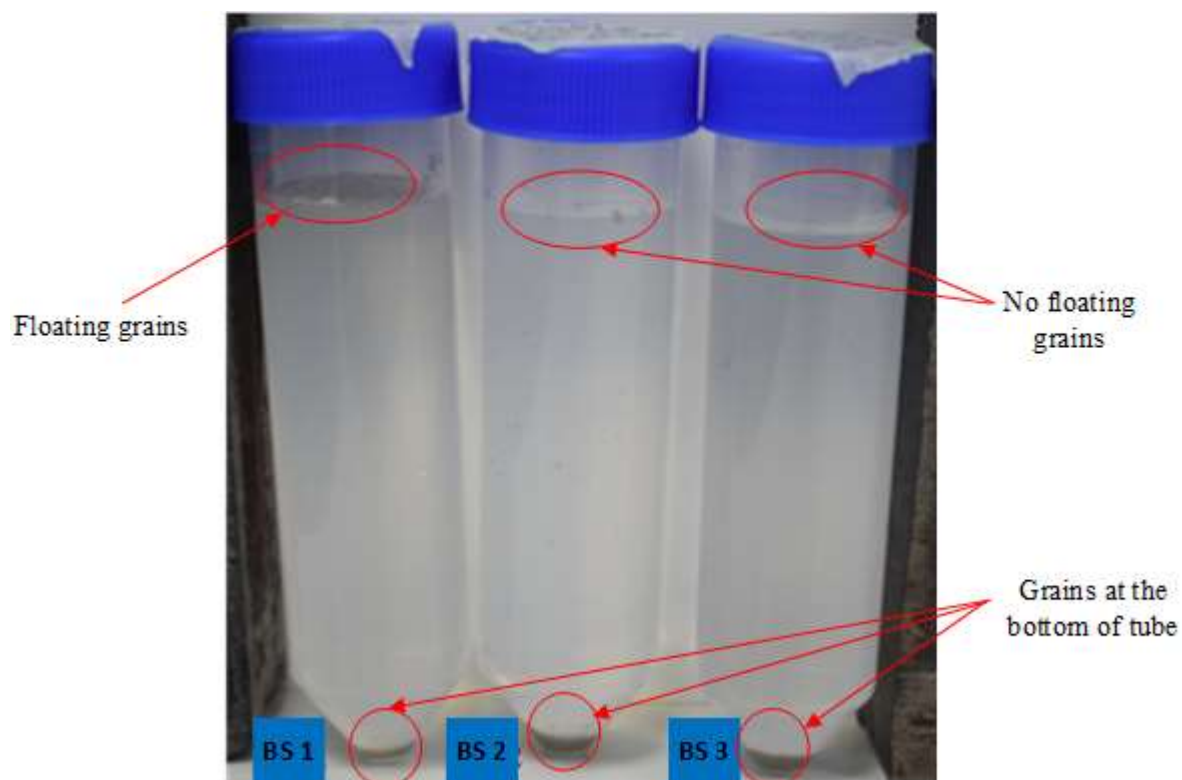


Figure 4.33: Distilled water and treated bandera gray grain sample in biosurfactant with cells

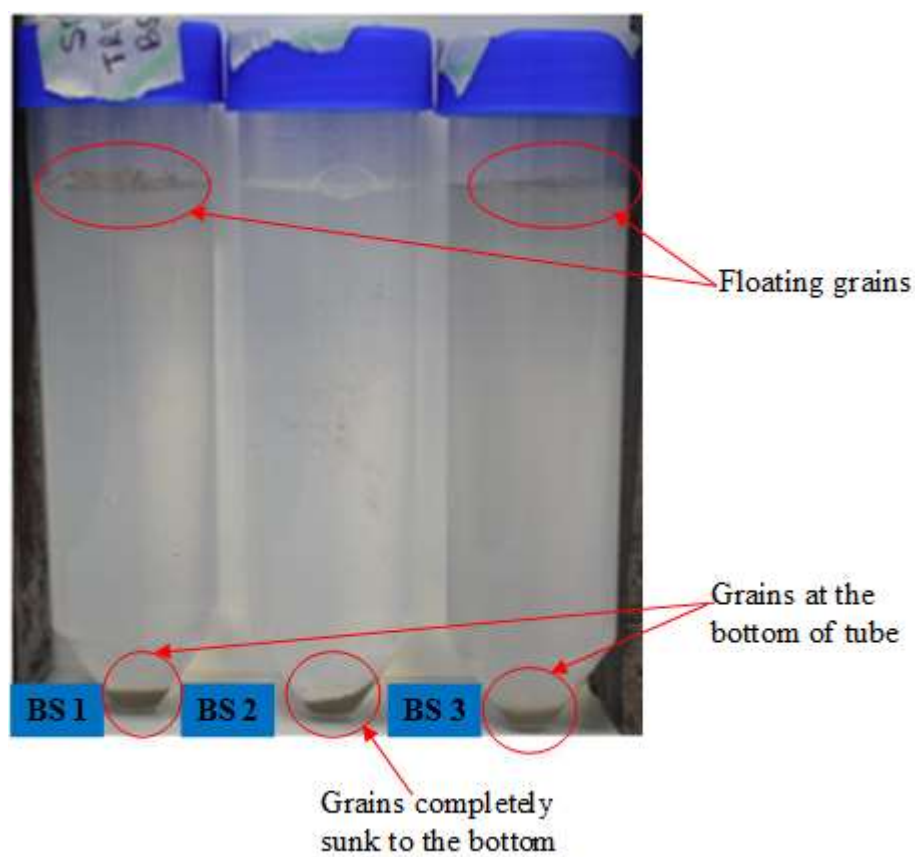


Figure 4.34: Distilled water and treated scioto grain sample in cell-free biosurfactants

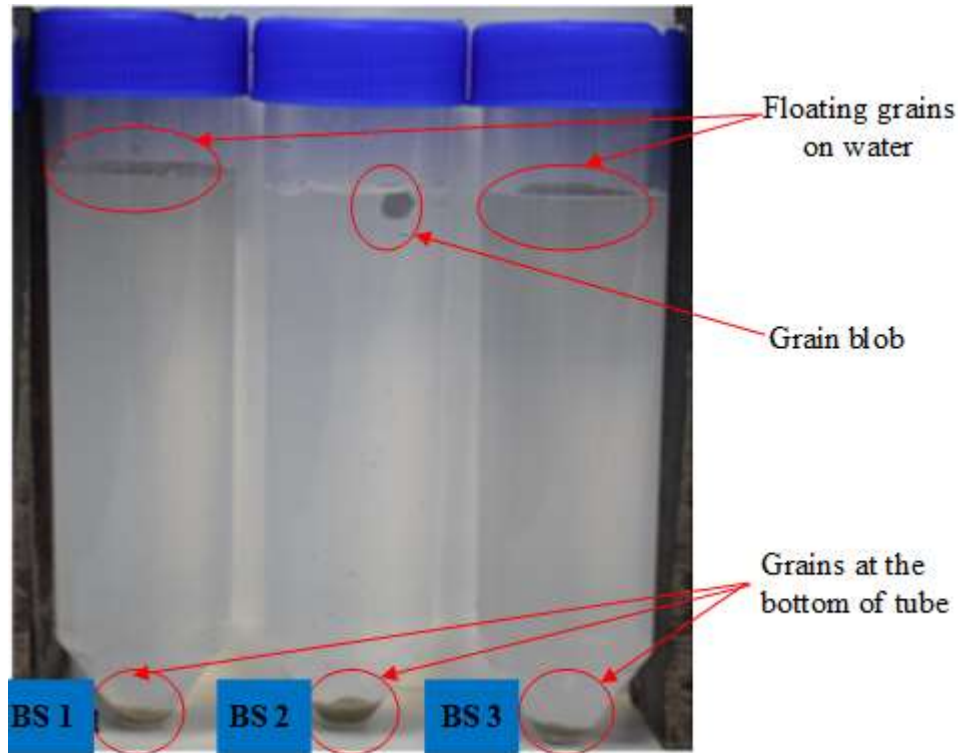


Figure 4.35: Distilled water and treated bandera gray grain sample in cell-free biosurfactants

Table 4.2: Wettability effect on sandstone grains after treatment with biosurfactants

Bio – surfactants	Wettability Effect	
	Scioto	Bandera Gray
<i>BS-1 Cells</i>	Intermediate-wet	Intermediate-wet
<i>BS-2 Cells</i>	Intermediate-wet	Water -wet
<i>BS-3 Cells</i>	Intermediate-wet	Water - wet
<i>BS-1 Cell-free</i>	Intermediate-wet	Intermediate-wet
<i>BS-2 Cell-free</i>	Water - wet	Water - wet
<i>BS-3 Cell-free</i>	Intermediate-wet	Intermediate-wet

4.4.2 Two-phase separation test

In the separation tests, grains were added into a mixture of distilled water plus kerosene (see Figure 4.36) and sunflower oil (see also Figure 4.37 and 4.38) in twelve (12) test tubes after treatment with biosurfactants. The treated rock grains remained completely in the water phase throughout the experiment for both kerosene and the sunflower oil, signifying a complete water-wet state. The quantity of rock grain remaining in each phase gives a qualitative index

of its wettability, and according to (Somasundaran & Zhang, 2006), if the grains remain in the oil phase, it is strongly oil wet, otherwise it is water wet.

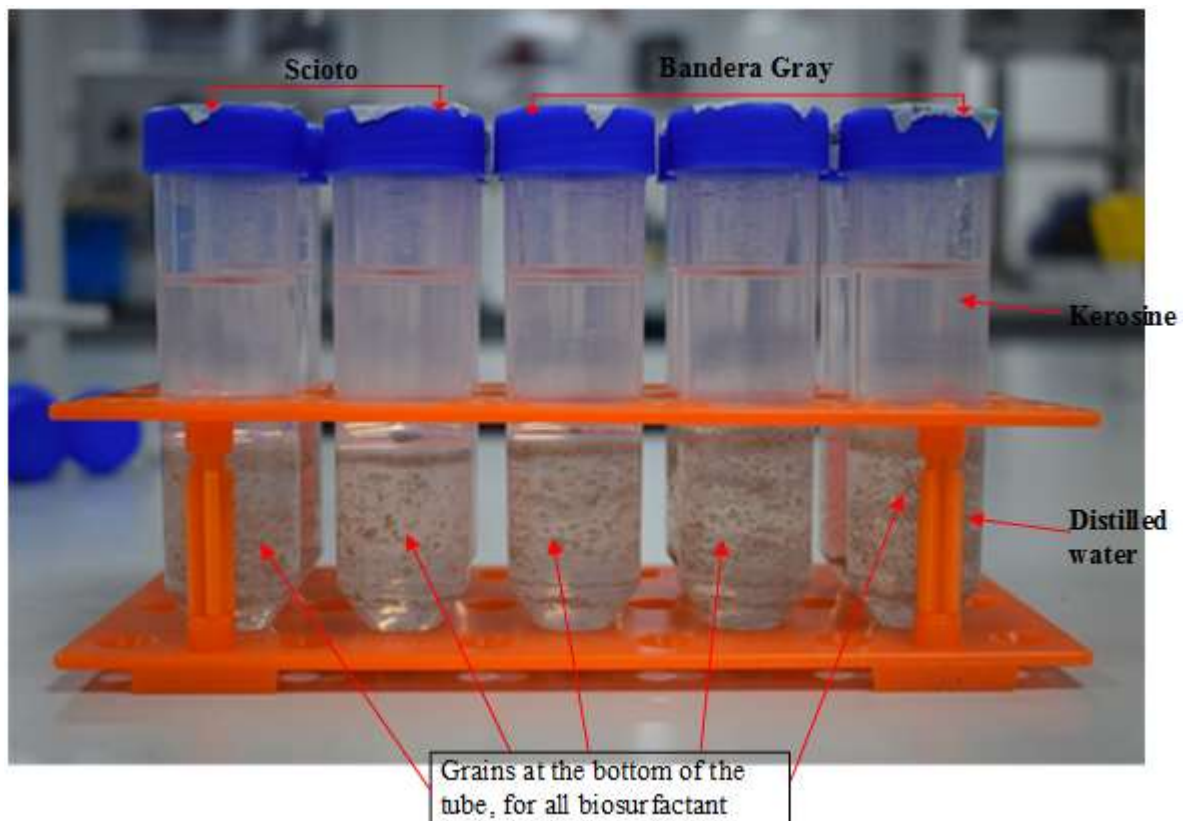


Figure 4.36: Distilled water with kerosene plus treated grain samples in biosurfactants for both cells and cell-free

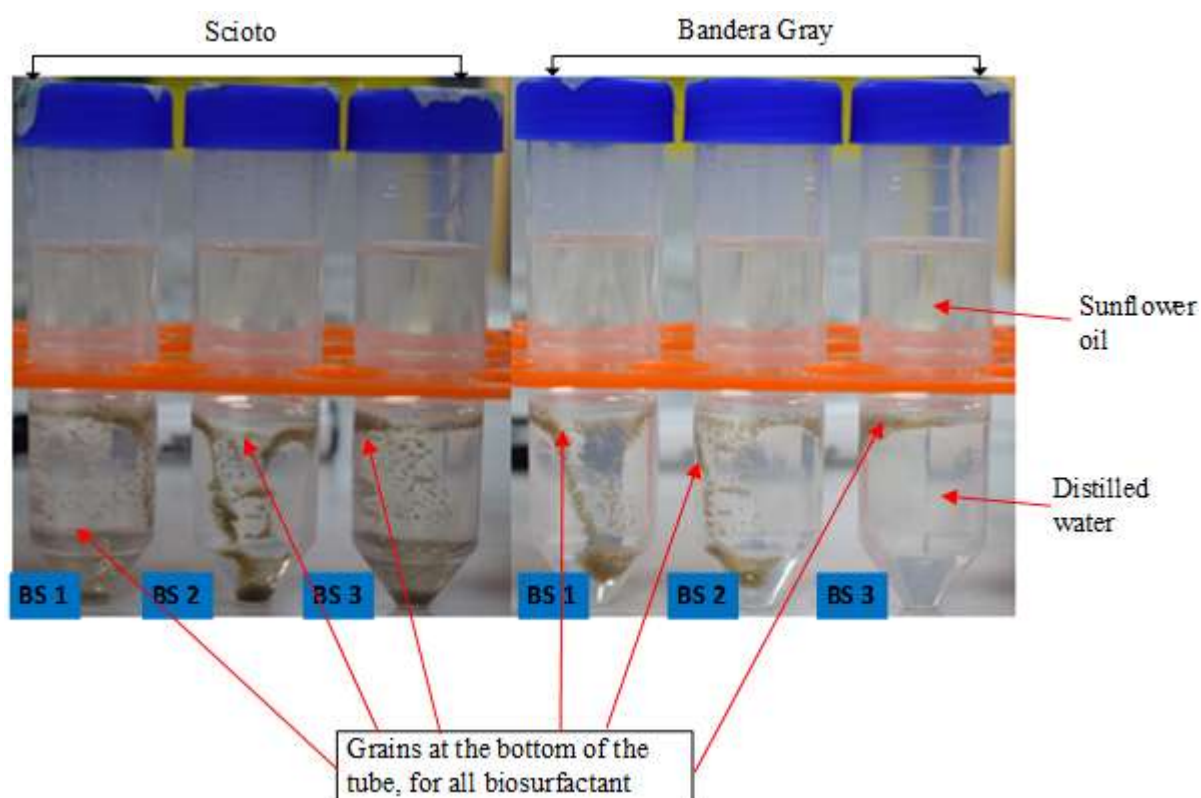


Figure 4.37: Distilled water with sunflower plus treated grain sample in biosurfactant with cells

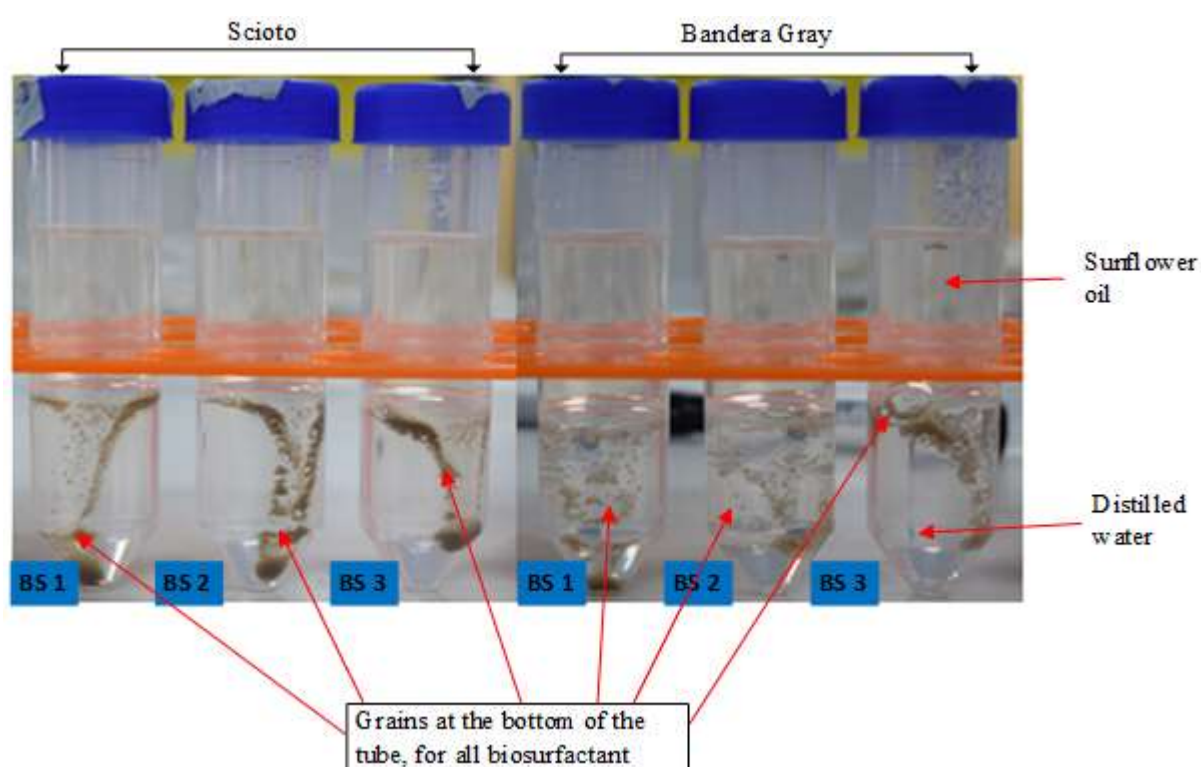


Figure 4.38: Distilled water with sunflower plus treated grain sample in cell-free biosurfactants.

Most sandstone reservoirs in the Niger Delta are not strongly water-wet, but are recognised generally to exhibit a largely intermediate to slightly oil-wetting behaviour (McPhee, Reed, & Zubizarreta, 2015). The wettability for Scioto and Bandera Gray, treated with these biosurfactants, displayed an alteration in wettability from hydrophilic to hydrophobic, characterised by the grains completely remaining in the aqueous phase. The crude oil utilised, while preparing the grains, showed that it is a poor solvent for the biosurfactants, thus having a greater propensity to change wettability (Al-Maamari & Buckley, 2003).

4.5 Phase - IV: Core flooding

The bio-flooding trials were conducted with a specific focus of investigating the effect of biosurfactant injection on unsteady state flow behaviour of rock-fluids systems in changing the wettability of the rock grain to further enhance oil recovery. These experiments were run on a selected sandstone sample as described in Chapter-3, having same porosity and permeability. All experiments were carried out using the core-flooding tests described according to the procedures that were outlined in the previous Chapter (3).

One of the main objectives of this investigation was also to produce biosurfactant that can ultimately improve oil recovery when compared with the conventional water flood. In order to achieve this goal, the produced biosurfactant that gave the best outcome, (*BS-2* supernatant), from the results obtained in IFT (Phase-II) and wettability experiments (Phase-III) was selected. Also, the parameters needed to be established were, flowrate and pore volume. This was necessitated to serve as a control for the initial conditions that will give an ultimate recovery. Hence, 15 sets of core-flooding trials were conducted at different repeatability runs, at flow rates of 0.75 ml/min, 0.5 ml/min and 0.25 ml/min, out of which 3 trials generated acceptable results which formed the basis of these series of experiments. These different flow rates were ideal to obtain the optimum flowrate that gives the best recovery prior to the injection of the biosurfactant. The best recovery was recorded at a flow rate of 0.25 ml/min, with a breakthrough time of 246 minutes as shown in Figure 4.39. During each of the injection cycle (preliminary and actual runs), on the average, about 13 pore volumes of biosurfactant/distilled water were injected into the core sample before reaching stabilised conditions i.e. the displaced phase was no longer produced and reaching a stable pressure drop across the sample.

In Figure 4.40, the performance of *BS-2*- supernatant flooding showed a significant amount of oil was produced at a reduced breakthrough time with decrease in pore volume (PV) compared to the water flooding, leading to a higher recovery rate.

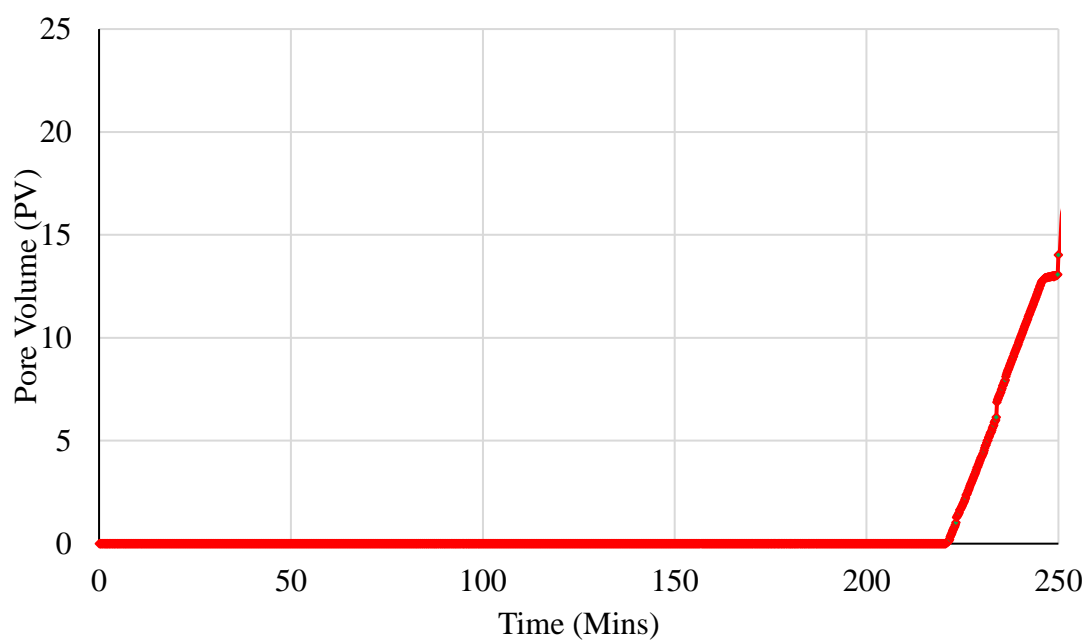


Figure 4.39: Distilled water flooding versus time

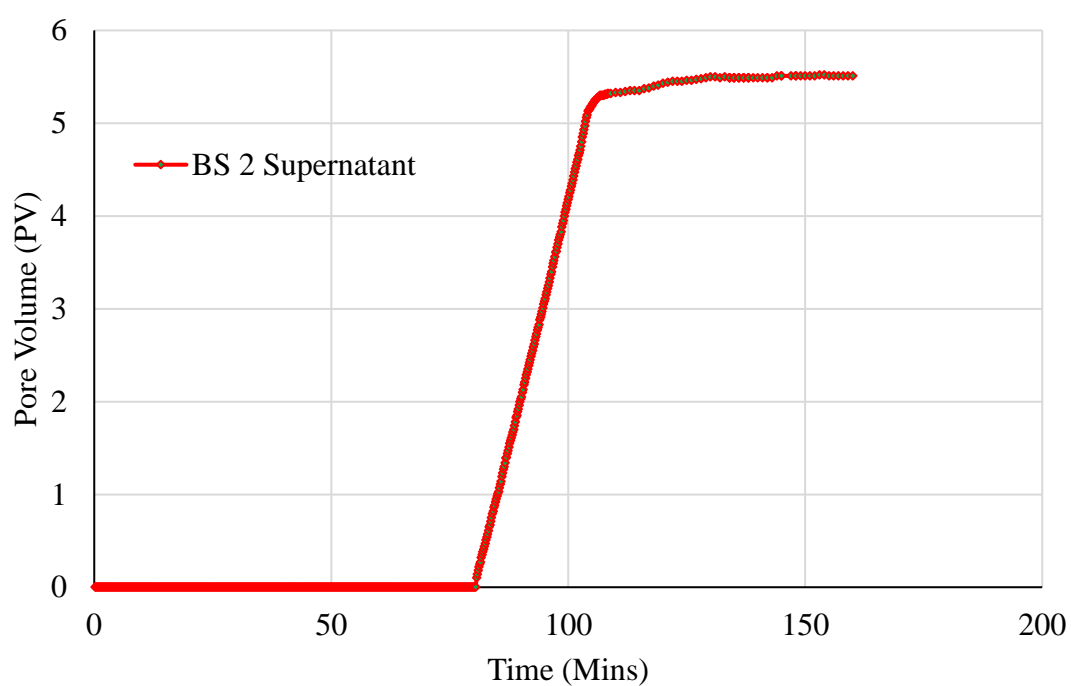


Figure 4.40: Biosurfactant flooding versus time.

4.5.1 Oil Recovery

Figure 4.41 and 4.42 are the differential pressures across the sample versus time for the water flooding and the bio-flood experiment, whose oil production profiles were reported above. In addition, most the differential pressure profile for the imbibition cycles show a stable pressure drop at the point of oil breakthrough for the bio-flooding and a sudden steep decline for the water flooding close to the conclusion.

At the beginning of injection during the water flooding, it can be seen from Figure 4.41 that the differential pressure was stable with a sudden fluctuation, even with a negative differential. This seemed to be due to the back pressure that had already been applied prior to the injection process, which may have resulted in the fluctuations. However, after passing through thirteen pore volumes, stabilised conditions were established and at which point the production of oil began. Although the differential pressure remained within reasonable range and was not actually constant, which also, could be attributed to the automated pressure transducer of the equipment.

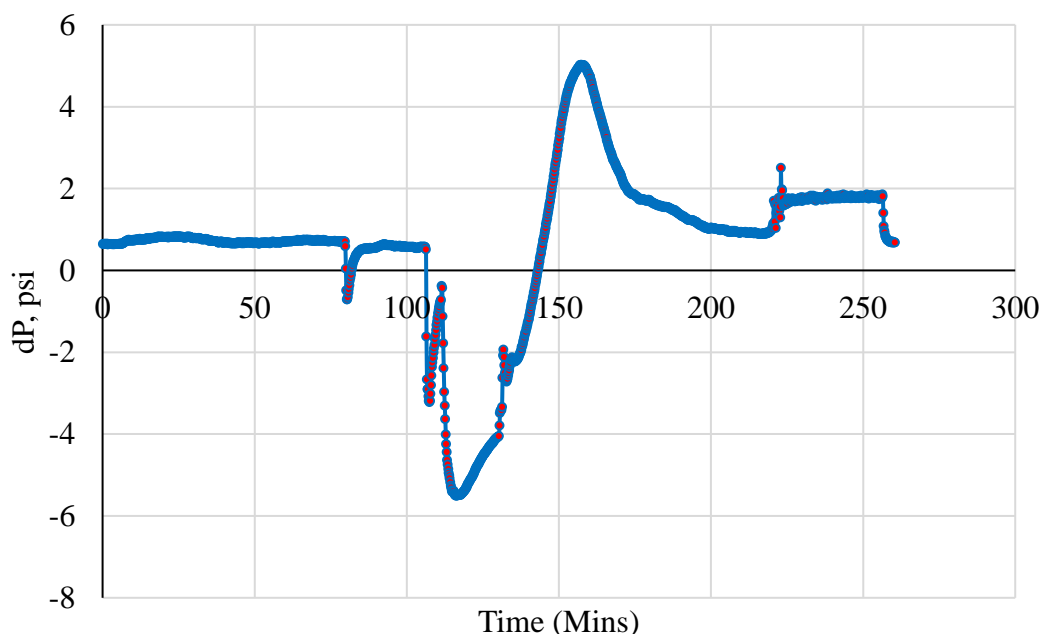


Figure 4.41: Differential pressure across the sample versus time for the water flooding cycle

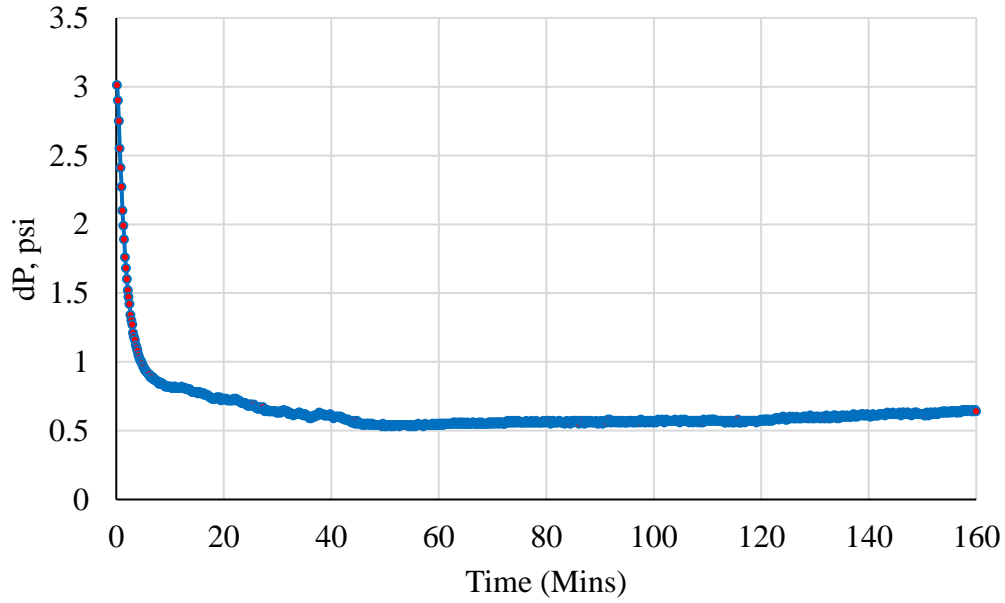


Figure 4.42: Differential pressure across the sample versus time for the biosurfactant flooding cycle.

An important objective of enhanced oil recovery is to increase the recovery factor. The oil recovery factor (RF), is the amount of original in place (OOIP), normally expressed as a percentage in Eqn (4.7).

$$RF = \frac{QO}{OOIP} \quad (4.7)$$

where;

QO is the produced oil

The recovery factor is a function of the displacement mechanism. While water cut (FW) as shown in Eqn (4.8), is the ratio of water produced (QW) to the volume of total liquids produced (Qtotal). Table 4.3, details the data generated for the oil recovery and recovery factor, after performing the flooding process for both bio/water flooding.

$$FW = \frac{QW}{Q_{total}} \quad (4.8)$$

Table 4.3: Data analysis for recovery factor

Parameters	Distilled Water	Biosurfactant
	Flooding	flooding
Flow rate, ml/min	0.25	0.25
Inlet Pressure, psia	591.7	736.7
Outlet Pressure, psia	590.7	734.7
Oil Saturation, ml	5.3	5.3
Water Saturation, ml	4.57	4.57
Total pore volume, ml	7.97	7.97
Oil Production, ml	1.5	1.9
Oil recovery, %	30	38
Water cut, %	0.10	0.96
Breakthrough, mins	246	105

Figure 4.43 shows the relationship between recovery and injected pore volume. The oil recovery increases from 30% to 38% in less time from initial flooding with water. The increase in oil recovery is proposed to be due to the biosurfactant changing the wettability of the rock around the production well. As observed in the floating qualitative test in Phase - III, when crushed samples were treated with *BS-2* supernatant, water-wet wettability effect was developed. Therefore, the wettability within the core would also have changed from its initial oil-wet state to a complete water-wet state.

Thus, at the start of flooding, the injected biosurfactant will displace the oil bank continuously at a flow rate low enough to avoid a viscous fingering around the core. Since the wettability within the core sample is assumed to have change to a more water-wet condition, the displaced oil will travel through the larger pores. Increase in oil recovery may be aided by an additional process of lowering the interfacial tension and wettability alteration throughout the rest of the core due to the biosurfactant diffusing through the rest of the core.

A close observation at Figure 4.43 indicates that there was a significant recovery between the bio-flooding and conventional waterflood. This was an interesting result since the experiment was conducted in real time. The biosurfactant flooding gave an incremental recovery of about 8% when compared to the waterflooding, and occurring at a shorter time with less pore

volume. This indicates that the biosurfactant was effective in real time, and could be attributed to its concentration and rich nutrient present, which will allow for the bacterial growth and diffusion through the rest of the core. A very important observation made by analysing the recovery trends is that the longer the saturation period is, the more time available for the biosurfactant to redistribute in the core, and therefore more volume of oil that will be produced.

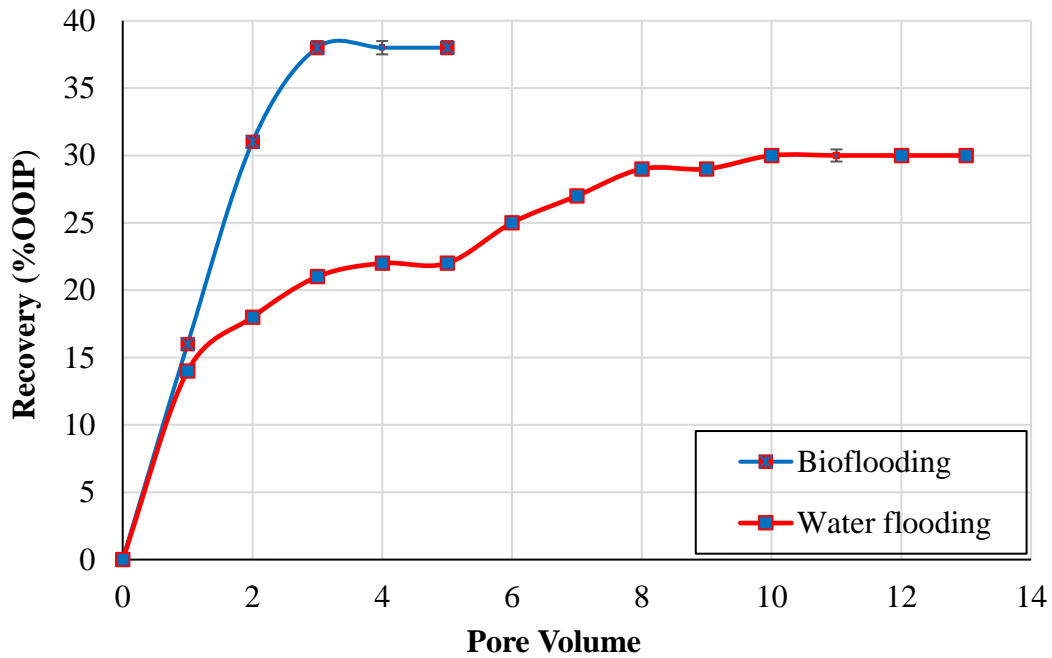


Figure 4.43: Oil recovery curves with injected pore volumes

Al-Sulaimani et al., 2012 reported that biosurfactant had a potential for MEOR technology because it yielded a total production of 23% of residual oil when treated with 0.25% (w/v) biosurfactant. In this study, a total of 38% of residual oil was recovered when injected with pure biosurfactant (*BS-2*) of 174.17 ml/L (w/v). In both cases, the biosurfactant used for the core flooding were produced from a *B. subtilis* strain, W19 and *BS-2* respectively. The core flood experiments were also conducted at 60°C, to mimic the average reservoir temperature of the field of interest. Oil production however, increased to 30% when injected with pure chemical surfactant (Al-Sulaimani et al., 2012). Figure 4.44 presents a summary of these core flooding results.

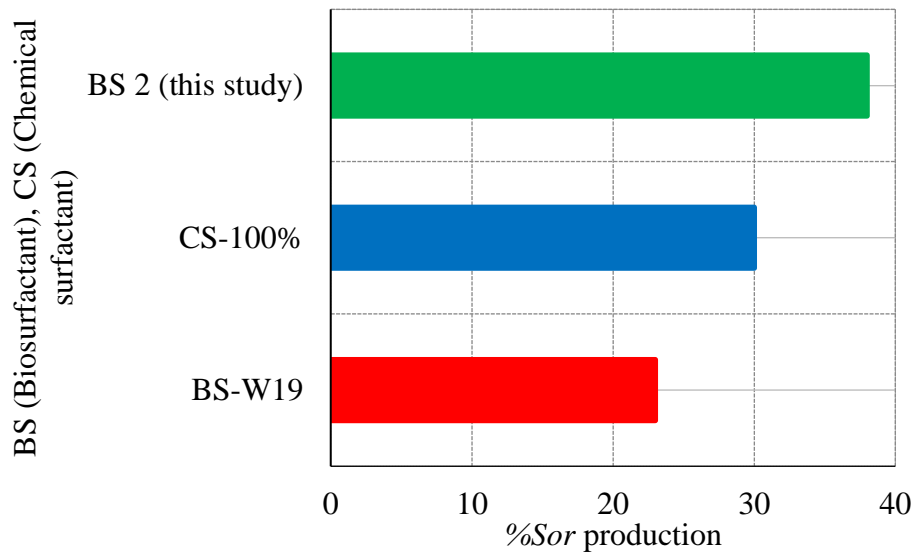


Figure 4.44: Comparison between surfactant solutions in residual oil recovery

4.6 Summary

The preceding Chapter can be summarised as follows:

Phase - I: Microbial Culture

- Phenotypic characteristics were determined and the results were positive, which validates the choice of the selected bacteria's.
- Three biosurfactants (*BS-1*, *BS-2* and *BS-3*) were produced after culturing, a process of filtration and centrifugation.

Phase - II: IFT and contact angle measurements

- IFT of the selected heavy oil decreased significantly when tested with the produced biosurfactants.
- The contact angle reduction was minimal and was considered to be positive in terms of the corresponding obtained results.
- The supernatant *BS-2* biosurfactant, gave the best IFT/contact angle results.

Phase - III: Qualitative wettability

- The results of the floating test showed that supernatant *BS-2* biosurfactant had same effect on both selected sandstones, by altering their wettability to a water-wet state.
- The treated grains in the two-phase separation test, completely remained in the water phase.

Phase – IV: Core Flooding

- After flooding bandera gray with supernatant *BS-2* biosurfactant, 38% of the residual oil was recovered, which was a better outcome when compared with water flooding in the same core system.

The next chapter will discuss the environmental risk assessment of the microbes selected to produce the biosurfactants in this study.

Chapter 5

5 Risk Assessment in Utilising Biosurfactant produced from the *Bacillus* Genus

5.1 Introduction

The environment is a broad concept that describes our biophysical surroundings. It includes air, water, land and living organisms such as plants and wild life. Environmental risk assessment is a scientific process that identifies and evaluates treats to the environment in particular to living organism, habitats and ecosystems (Raz & Hillson, 2005). The causes of environmental treats are diverse, some are natural, for example earthquake or volcanic eruptions, whilst others might be as a result of human activities such as industrialization and urbanisation. For instance, air pollution, toxic chemicals in food and water and sanitation. In the petroleum industry, individual companies are responsible for carrying out risk assessment for chemicals utilised during a recovery process that do not follow the natural production process. This is because the use of these products may pose a risk to the environment.

This study evaluates the risk assessment in the following generalised areas to include, human risk assessment and ecological risk assessment. The purpose of this assessment is to access the seriousness and the likelihood of harm to the environment, which might arise following a specific activity such as, inadequate controlled environment during bacteria culture and non-treatment of wastewater. These assessments follow several stages as presented in Figure 5.1 beginning with the problem formulation. This is the first critical step because it defines the scope of the environment risk assessment, by specifying what needs to be protected from harm and by identifying potential harmful effects. This is then followed by a hazard and exposure characterisation. In hazard characterisation, potential hazards and the seriousness of potential harm are examined, while the exposure characterisation considers the likelihood and the level of exposure to the hazards and thus how likely is it that harm will occur. The final step involves the characterisation of risk. Here the seriousness and the likelihood of harm are combined to estimate the level of risk. In some cases, the environmental risk assessment also includes risk mitigation measure, such measures aim to reduce and identify risk to an acceptable level or level of no concern (AIRMIC, 2002). This risk assessment is carried out to ensure that the produced biosurfactant in Chapter-3, if used in an actual field in-situ operation, do not cause an unacceptable harm to the environment.

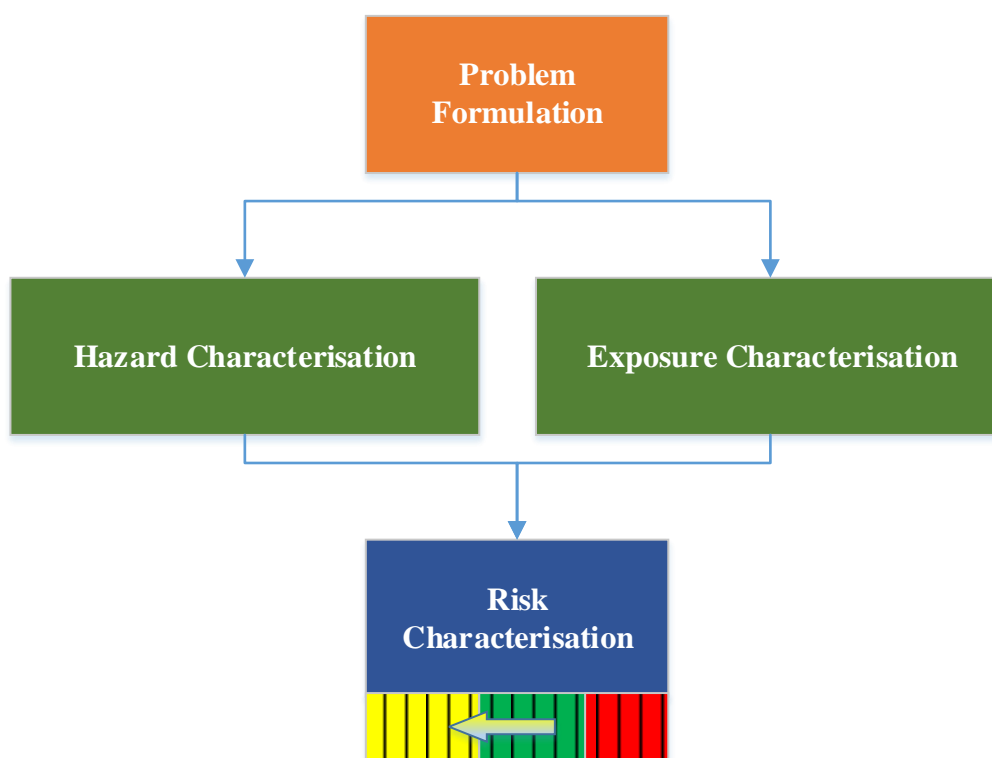


Figure 5.1: Stages of risk assessment

5.2 Oil and gas production wastewater

With the development of oil the industry, the general environment and in particular wetland ecosystem has become extremely vulnerable to damaging effects of wastewater pollution. The multidisciplinary nature of produced water is so complex that there has been less emphasis and focus on water treatment since it is not usually a revenue stream. Water quality is one important factor of an aquatic environment, therefore contamination of aquatic environment by wastewater constitute an additional source of stress to aquatic organisms (Omorie, Ufodike, & Onwuliri, 1997). Water analysis consists of an assessment of the condition of water in relation to set goals. Toxic pollutants in water refer to a whole array of chemical which are leached into ground water or which are discharged directly into rivers.

Environmental assessment is a very important factor to consider before embarking on any project. This is necessary to be able to identify any possible negative impact that could cause drawbacks, and subsequently putting in place measures to mitigate them.

5.3 Produced water

Almost all offshore oil produces large quantities of contaminated water that can have significant environmental effects if not handled appropriately (Wills, 2000). As oil and gas

production proceed, formation water eventually reaches the production well, and water begins to appear alongside the hydrocarbons. This produced water is a mixture of injected water, formation water, biosurfactants, and hydrocarbons (Pichtel, 2016). Tertiary oil-recovery processes that uses water injection result in the production of even more water with the oil. Most offshore platforms dispose of their produced water directly into the ocean, but have to meet increasingly stringent regulations on the entrained and dissolved oil and other chemicals that are in the produced water. Some offshore operators are considering produced-water reinjection to avoid meeting these expensive ocean-disposal requirements. The product of the formation and injected water is referred to as produced water.

This chapter is primarily focused on the environmental impact of the biosurfactants used in this study for enhancing production. Thus, this evaluation will be in line with the US Environmental Protection Agency (EPA), Canadian Environmental Protection Agency (CEPA), the European Federation of Biotechnology guidelines, and other guidelines. The three-produced bio-surfactant in Chapter-3, will be discussed to evaluate the likelihood of harm, identify the risks of being exposed to them, and provide possible ways of mitigating such risk to prevent it from occurring.

5.4 Risk Matrices

Risk matrices are probably one of the most commonly used tools of evaluating risk. They are mainly used to determine the size of a risk and whether or not the risk is sufficiently controlled. Figure 5.2, a bowtie diagram was adopted for this assessment to explain the use of the risk matrices in the most common three areas, which include;

- The low probability or insignificant impact (usually green) which indicates the risk of an event is sufficiently controlled, or not high enough. No action is usually required with this.
- The high or extreme probability, high impact (usually red) that is not acceptable and which indicates work should not be started or continued until risk has been mitigated. In the event, significant resources or more control measures is needed to bring the probability or impact down.
- In the medium category (usually yellow), efforts should be made to mitigate the risk within a pre-defined time period. Events should be monitored and controlled as low as

reasonably practicable, which implies that if the risk is kept at that level, it will be accepted. However, the cost of prevention should be carefully considered.

Extremely Harmful	Medium Risk	High Risk	Extreme Risk
Harmful	Low Risk	Medium Risk	High Risk
Slightly Harmful	Insignificant Risk	Low Risk	Medium Risk
	Highly Unlikely	Unlikely	Likely

Figure 5.2: Adopted 3 × 3 impact matrix

5.5 Microbial Pesticide Name: *Bacillus licheniformis* strain DSM 1918

5.5.1 Identification and Overview

Bacillus licheniformis is a ubiquitous saprophytic bacterium that is wide spread in nature and thought to contribute to nutrient cycling and displays antifungal activity (Claus and Berkeley, 1986). It has been used in the fermentation industry for production of proteases, amylases, antibiotics, and specialty chemicals for over a decade with no known reports of adverse effects to human health or the environment. This species is easily differentiated from other members of the genus that are pathogenic to humans and animals.

A series of literature searches have been conducted to determine whether any adverse effects from *B. licheniformis* have been reported. There are no indications that *B. licheniformis* is pathogenic to plants and estuarine marine species. However, reports in literature indicating human infections with *B. licheniformis*, occurred in immunosuppressed individuals or following trauma. Also, there are reports links *B. licheniformis* and abortions in livestock. In most reports, there were predisposing factors which may have resulted in immunosuppression of the affected animals.

Since *B. licheniformis* is ubiquitous in the environment and appears to be an opportunistic pathogen in compromised hosts, the potential risk associated with the use of this bacterium in fermentation facilities is low.

5.5.2 Physical/Chemical Properties Assessment

B. licheniformis does not produce significant quantities of extracellular enzymes or other factors that would predispose it to cause infection. Unlike several other species in the genus, *B. licheniformis* does not produce toxins. Overall, *B. licheniformis* has a low degree of virulence. Although the possibility of human infection is not non-existent, it is low in the industrial setting where highly immunocompromised individuals would not be present. Infection might be a possibility following trauma, but in the industrial setting with the use of proper safety precautions, good laboratory practices, and proper protective clothing and eyewear, the potential for infection of workers should be quite low.

5.5.3 Ecological Risk Assessment

Likewise, the ecological hazards associated with the use of *B. licheniformis* are low. There are various reports in the literature suggesting that *B. licheniformis* is a cause of abortion in livestock. However, Koch's postulates have not been satisfied demonstrating that this microorganism was the causal agent. In most of these cases, infections with *B. licheniformis* occurred in animals already in an immunocompromised state resulting from either infection with other organisms or poor nutrition. Apparently, there is immunosuppression

associated with maternal and fetal placentas in pregnant livestock, whereby opportunistic microorganisms are capable of causing infection and lesions in fetuses. Although *B. licheniformis* has not been shown to be an etiological agent of livestock abortion, it has been associated with a number of cases. Even so, the association of *B. licheniformis* with livestock abortion is quite small compared to the total number of abortions in livestock caused by all other microorganisms, particularly viruses and fungi.

5.5.4 Human Health Risk Assessment

The use of *B. licheniformis* for industrial production of enzymes should not pose environmental hazards. First, the number of microorganisms released from the fermentation facility is low. In addition, *B. licheniformis* is ubiquitous in the environment, and the releases expected from fermentation facilities operating under the conditions of this exemption will

not significantly increase populations of this microorganism in the environment. Therefore, although *B. licheniformis* may be associated with livestock abortions, the use of this microorganism in fermentation facilities will not substantially increase the frequency of this occurrence, even if a scenario for high exposure to *B. licheniformis* released from the fermentation facility to livestock could be envisioned.

In conclusion, the use of *B. licheniformis* in fermentation facilities for production of enzymes, biosurfactants or specialty chemicals presents low risk. Although not completely innocuous, *B. licheniformis* presents low risk of adverse effects to human health or the environment. This assessment thus, justifies the use of *B. licheniformis* in producing BS-2 biosurfactant, that resulted in a positive experimental outcome as discussed in Chapter-4, without causing any harm.

The probability of risk occurrence is used to estimate the likelihood of risk occurrence and impact on positive events and decrease the likelihood and negative events in a project as seen in Table 5.1.

Table 5.1: Probability of occurrence

Descriptor	Frequency
Insignificant	<p>Could only occur as the result of multiple, independent system or control failures.</p> <p>Occurrence is thought most unlikely and does not produce toxins. No comparable occurrence is known.</p>
Low	<p>Could occur in immunosuppressed individual or following trauma. Environmental hazard occurrence is unlikely as the number of microorganisms released from fermentation facility is low.</p> <p>Would probably occur from high level of exposure during fermentation operation.</p> <p>Comparable reports of infections are known to have occurred in the past.</p>
Medium	<p>Could result from predisposing factors in immunosuppression of the affected animals.</p> <p>Could be expected to occur in animals already in an immunocompromised state resulting from either infection with other organisms or poor nutrition. Comparable reports in association with abortion in livestock is quite small.</p>
High	<p>Occurrence is highly unlikely to occur.</p>

The final risk writing is made up from the likelihood writing and overlaid against the consequence or impact writing. This risk matrix rating presented here is specific only for this study as represented in Table 5.2 and Figure 5.3.

In the event of likelihood of a risk to occur, response strategy to avoid such risk should be put in place to avoid and decrease the likelihood of such impact, which is presented in Table 5.3 as a mitigation plan.

Table 5.2: Risk rating matrix

	Type of Impact	Probability or Likelihood	Potential Consequence/Impact
1.	Human Health	I	L
2.	Virulence	L	L
3.	Soil	L	L
4.	Hazard to animal	L	M
5.	Air	L	L
6.	Environment	I	L
7.	Hazard to plant	I	I
8.	Water	L	L
9.	Worker Exposure	I	L

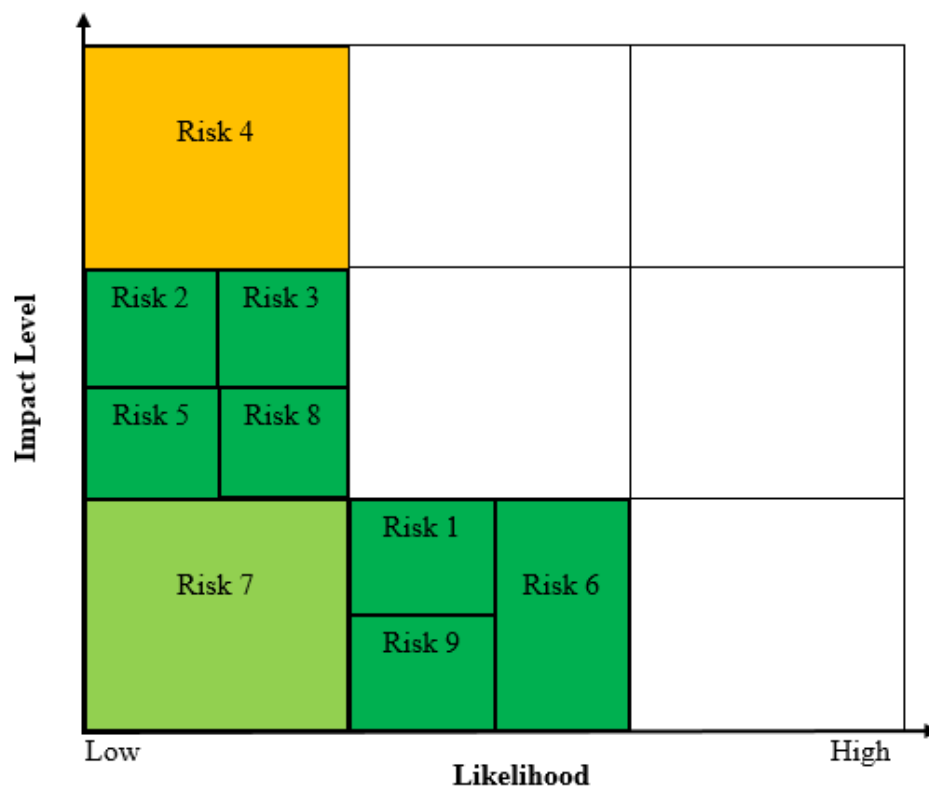


Figure 5.3: Probability impact grid

Table 5.3: Planned response (mitigation)

Risk Probability	Mitigation Plan
Low	<p>The use of proper safety precautions, good laboratory practices, and proper protective clothing and eyewear in industrial settings can influence impact on workers.</p> <p>Risk reduction measures are unlikely to be cost-effective.</p>
Medium	<p>Avoid high level of inhalation exposure due to point source releases.</p> <p>Risk reduction measures will be roughly cost-neutral.</p>

5.6 Microbial Pesticide Name: *Bacillus subtilis* strain DSM 3256

5.6.1 Identification and Overview

Bacillus subtilis is a ubiquitous, saprophytic, soil bacterium which is thought to contribute to nutrient cycling due to its ability to produce a wide variety of enzymes. This latter feature of the microorganism has been commercially exploited for over a decade and has been used for industrial production of proteases, amylases, antibiotics, and specialty chemicals. The US EPA agency (1997) has reviewed the production of enzymes using genetically modified *B. subtilis* and found no unreasonable risks to human health or the environment from the use of this microorganism in fermentation facilities. It is not considered pathogenic and does not possess traits that cause disease.

Historically, *B. subtilis* was a term given to all aerobic endospore-forming bacilli. Later, *B. subtilis* and two closely related species, *B. licheniformis*, and *B. pumilus*, were grouped taxonomically into what was known as the subtilis-group. However, recently methods have been developed that allow *B. subtilis* to be distinguished from these other species. *B. subtilis* is not a frank human pathogen, but has on several occasions been isolated from human infections.

Infections attributed to *B. subtilis* include bacteraemia, endocarditis, pneumonia, and septicaemia. However, these infections were found in patients in compromised immune states. There must be immunosuppression of the host followed by inoculation in high

numbers before infection with *B. subtilis* can occur. There also have been several reported cases of food poisoning attributed to large numbers of *B. subtilis* contaminated food. *B. subtilis* does not produce significant quantities of extracellular enzymes or other factors that would predispose it to cause infection. Unlike several other species in the genus, *B. subtilis* is not considered toxigenic. *B. subtilis* does produce the extracellular enzyme subtilisin that has been reported to cause allergic or hypersensitivity reactions in individuals repeatedly exposed to it (Edberg, 1991).

5.6.2 Human Health Risk Assessment

B. subtilis is considered a Class 1 containment agent under the National Institute of Health (NIH) guidelines for research involving recombinant DNA molecules (USHHS, 1986). This microorganism also falls under the Class 1 containment under the European Federation of Biotechnology guidelines (Frommer et al., 1989)

In an industrial setting with the use of proper safety precautions, good laboratory practices, and proper protective clothing and eyewear, the potential for infection of workers should be quite low, as further explained in Table 5.4. The only human health concern for workers in the fermentation facility is the potential for allergic reactions with chronic exposure to subtilisin. Overall, *B. subtilis* has a low degree of virulence (Edberg, 1991; Ihde & Armstrong, 1973). Although the possibility of human infection is not non-existent, it is low in the industrial setting where exposure to the bacterium is expected to be low, and where highly immunocompromised individuals would not be present.

5.6.3 Ecological Risk Assessment

Likewise, the ecological hazards associated with the use of *B. subtilis* are low. There are several reports in the literature on the association of *B. subtilis* with abortions in livestock (Fossum, Herikstad, Binde, & Pettersen, 1985). However, these few reports indicate that this association must be fairly rare, and typically, the animals were immunocompromised. In addition, *B. subtilis* has not been shown to be a causal agent and is not considered an animal pathogen (Logan, 1988). Likewise, *B. subtilis* is not considered a plant pathogen. Although it produces enzymes such as polygalacturonase and cellulase that are sometimes associated with the ability to produce soft rot in plant tissue, there are many organisms that are capable of producing a soft rot when injected beneath the outer protective epidermal layers. The use of *B. subtilis* in an industrial setting should not pose an unreasonable risk to human health or

the environment as rated in Table 5.5. First, human health and environmental hazards of *B. subtilis* are low. Second, the number of microorganisms released from the fermentation facility is low. In addition, *B. subtilis* is ubiquitous in the environment, and the releases expected from the fermentation facilities will not significantly increase populations of this bacterium in the environment.

Specific data which indicate the survivability of *B. subtilis* in the atmosphere after release are currently unavailable. Air releases from fermentor off-gas could potentially result in non-occupational inhalation exposures due to point source releases. The natural habitat for *B. subtilis* is the soil. Therefore, long-term survival in soil may be expected to occur.

In conclusion, the use of *B. subtilis* in fermentation facilities to produce *BS-1* biosurfactants or specialty chemicals has a low risk. Although not completely innocuous, the industrial use of *B. subtilis* presents low risk of adverse effects to human health or the environment. This is represented in the risk matrix of Figure 5.4 with a response plan in Table 5.6.

Table 5.4: Probability of occurrence

Descriptor	Frequency
Insignificant	<p>Could only occur as the result of multiple, independent system or control failures.</p> <p>Occurrence is thought most unlikely and does not produce toxins.</p> <p>No comparable occurrence is known.</p>
	<p>Infection could occur in immunosuppressed individual or following exposure to the bacterium. It has a low degree of virulence.</p> <p>Environmental hazard occurrence is unlikely as the number of microorganisms released from fermentation facility is low.</p> <p>Concerns for workers in the fermentation facility is the potential for allergic reactions or hypersensitivity with high level of exposure is low.</p> <p>Comparable reports of food poisoning attributed to large number of <i>B. subtilis</i> contaminated food..</p>
Medium	<p>Could result from predisposing factors in immunosuppression of the affected animals.</p> <p>Could be expected to occur in animals already in an immunocompromised state resulting from either infection with other organisms or poor nutrition.</p> <p>Comparable reports in association with abortion in livestock are fairly rare.</p>
High	<p>Occurrence is highly unlikely to occur.</p>

Table 5.5: Risk rating matrix

	Type of Impact	Probability or Likelihood	Potential Consequence/Impact
1.	Human Health	L	L
2.	Virulence	L	I
3.	Soil	L	I
4.	Hazard to animal	L	M
5.	Water	L	L
6.	Environment	I	L
7.	Hazard to plant	L	I
8.	Food poison	L	M
9.	Worker Exposure	L	L

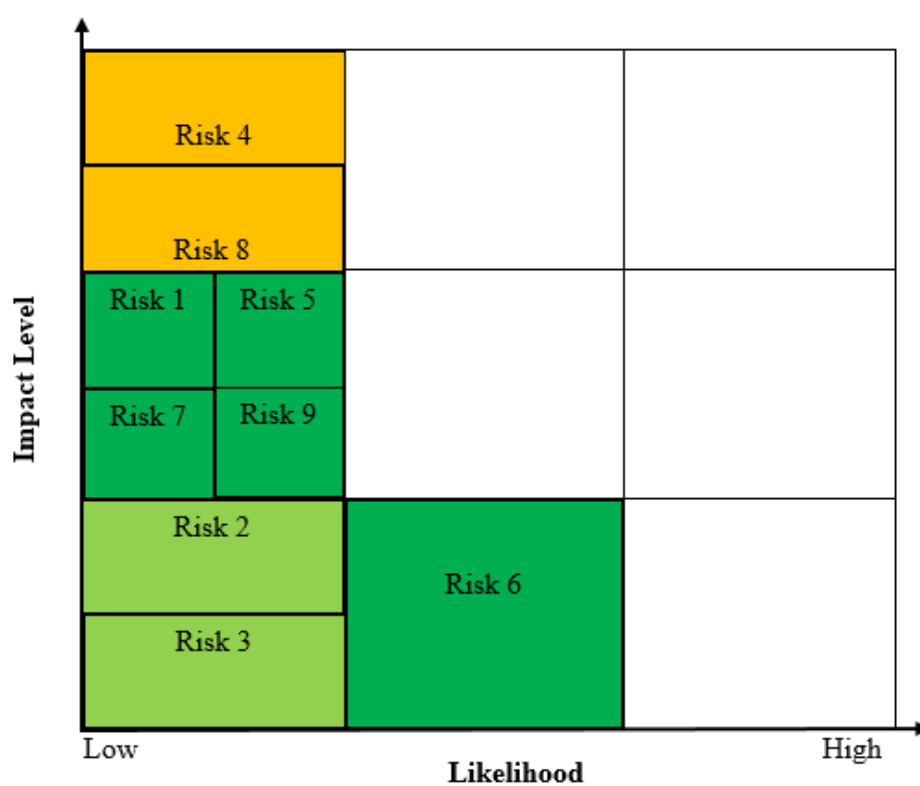


Figure 5.4: Probability impact grid

Table 5.6: Planned response (mitigation)

Risk Probability	Mitigation Plan
Low	<p>The use of proper safety precautions, good laboratory practices, and proper protective clothing and eyewear in industrial settings can influence impact on workers.</p> <p>Risk reduction measures are unlikely to be cost-effective.</p>
Medium	<p>Avoid high level of inhalation exposure due to point source releases.</p> <p>Risk reduction measures will be roughly cost-neutral.</p>

5.7 Microbial Pesticide Name: *Paenibacillus polymyxa* strain DSM 3256

P. polymyxa is a facultatively anaerobic bacterium that is present in many environments and it's not known as an animal, plant or human pathogen. *P. polymyxa* strain DSM 740 share characteristics with other *P. polymyxa* strains that occur in the environment. This assessment will consider the environmental and human health effects associated with this product use and industrial processes subject to (CEPA, 1999), including releases to the environment through waste streams and incidental human exposure through environmental media.

5.7.1 Biological and ecological properties

P. polymyxa is a spore-forming bacterium (Priest, 2015). As a facultative anaerobe, it can be active under anaerobic conditions and thrives in semi-anaerobic environments, and has a broad host range as a plant growth-promoting bacterium. It is present in many environments occurring naturally in marine sediments (Lal & Tabacchioni, 2009), and has also been isolated from various soils and from cultivated olive trees in an organic orchard farm (Blibech 2012), and other plant and crops (Lal & Tabacchioni, 2009; Raza, Yang, & Shen, 2008).

5.7.2 Effects on the environment

In agricultural ecosystems in spite of the well-accepted role of *P. polymyxa* as a plant growth-promoting bacterium, a few studies have shown that it can also act as a deleterious rhizobacterium under certain circumstances which resulted in reduction of plant growth and stunted root system (Timmusk, 2003; Timmusk & Wagner, 1999). It is also known to cause

blight in tomato seedlings (Caruso, Zuck, & Bessette, 1984). A comprehensive scientific literature search did not reveal any further reports of *P. polymyxa* or other *Paenibacillus* species in association with aquatic plants.

5.7.3 Effects on human health

Thus far, there are only two reports associated with human infection involving *P. polymyxa*, one involving self-injection of a polymicrobial product containing *P. polymyxa* and the other involving a serious comorbidity (pre-existing health condition or disorder) (Galanos et al., 2003; Nasu et al., 2003). Taken together with the ubiquity of this organism, the significance of these two cases appears to be negligible. In the unlikely event of *P. polymyxa* infection, there are effective antibiotic treatments available (Galanos et al., 2003). However, other *Paenibacillus* species occasionally cause disease in humans or are isolated from clinical samples (K. K. Kim et al., 2010; Ouyang et al., 2008).

5.7.4 Hazard severity

There is little information in the literature to suggest that *P. polymyxa* is pathogenic to aquatic or terrestrial plants, vertebrates or invertebrates, in spite of its widespread distribution in the environment. No reports of animal or plant diseases are attributed to *P. polymyxa* strains DSM 740. As discussed previously, *P. polymyxa* appears to have a history of safe use based on the range of products known to be in commerce and on an absence of reports of adverse effects. A few experimental challenge studies have suggested some potential for adverse effects in plants when directly inoculated with high concentrations of *P. polymyxa* (Timmusk (El-Hadad et al., 2011; Liu, Dai, Wu, Li, & Liu, 2012; Timmusk, Grantcharova, & Wagner, 2005), Blibech et al. 2012. The environmental and human hazard severity for *P. polymyxa* strains is therefore estimated to be low.

5.7.5 Sources of exposure

Based on disposal of produced water into the sea, it could likely introduce the strain into aquatic and terrestrial ecosystems. The magnitude of plant and animal exposure to *P. polymyxa* will depend on their persistence and survival in the environment. *P. polymyxa* is an endospore-forming facultative anaerobe, capable of thriving in environments with limited oxygen availability. This explains its ubiquity in soils and in the rhizosphere of various plants as well as in deeper sub-surface zones in marine sediments. Although this evidence suggests that *P. polymyxa* strains introduced to soil and water will likely decrease to background levels

over time. Under sub-optimal conditions the spores of *P. polymyxa* strains are likely to persist and could accumulate in the environment (Providenti et al., 2009).

Human exposure is expected primarily through direct contact with consumer products containing *P. polymyxa*. Secondary to product application, residual *P. polymyxa* DSM 740 on surfaces and in reservoirs such as treated drains could result in dermal exposure, as well as exposure through inadvertent ingestion where the organism persists on food preparation surfaces and through inhalation where aerosols are generated.

Indirect exposure to *P. polymyxa* in the environment subsequent to its use in water and wastewater treatment or produced water disposal, or disposal of waste from its use in the production of enzymes is also likely to occur in the vicinity of application or disposal sites. In the event that the organisms enter municipal drinking water treatment systems through release from potential uses, the water treatment process, which includes coagulation, flocculation, ozonation, filtration and chlorination, is expected to effectively eliminate these micro-organisms from drinking water.

5.7.6 Risk Characterization

In this assessment, risk is characterized according to a model embedded in section 64 of CEPA 1999, that a hazard and exposure to that hazard are both required for there to be a risk. The risk assessment conclusion is based on the hazard, and on what is known about exposure from current uses. Hazard has been estimated for *P. polymyxa* DSM 740 to be low for the environment and low for human health. Exposures to *P. polymyxa* DSM 740 from its deliberate use in industrial processes or consumer or commercial products is not currently expected (low exposure), so the risk associated with current uses is estimated to be low for both the environment and human health. The determination of risk from current uses is followed by consideration of the estimated hazard in relation to foreseeable future exposures.

P. polymyxa DSM 740 have useful properties that make them of interest for use in additional industrial processes or consumer or commercial products. In the event that potential consumer, commercial or industrial uses of *P. polymyxa* is realized, the level of environmental and human exposure to this strain could increase. Nevertheless, the risk from foreseeable potential uses of *P. polymyxa* remains low, given that there is no evidence of effects on human health or adverse ecological effects at the population level for

environmental species, despite widespread distribution of *P. polymyxa* in the environment and the history of industrial, environmental and commercial uses of strains DSM 740.

The release of these strains into the environment is not expected to adversely affect ecosystems. Therefore, in conclusion, based on the information presented in this assessment, *P. polymyxa* strains DSM 740 is not entering the environment in a quantity or concentration or under conditions that:

- have or may have an immediate or long-term harmful effect on the environment or its biological diversity;
- constitute or may constitute a danger to the environment on which life depends; or
- constitute or may constitute a danger to human life or health.

Therefore, it is concluded that this substance does not meet the criteria as set out in section 64 of CEPA 1999, and therefore, the use of *BS-3* biosurfactant in Chapter-4 did not result in any human risk.

Table 5.7: Probability of occurrence

Descriptor	Frequency
Insignificant	Could only occur as the result of multiple, independent system or control failures.
	Occurrence is thought most unlikely, does not produce toxins and is not a pathogen to aquatic and terrestrial plants.
	Comparable reports of human infections are known but the significance of the case appears negligible.
Low	Subsequent to waste water, organisms could enter municipal drinking water in the vicinity of disposal sites.
	In agricultural ecosystems, it could be harmful to plants under certain circumstance resulting in reduction of plant growth.
	Hazard occurrence is unlikely as the number of microorganisms entering the environment is low.
Medium	Occurrence is highly unlikely to occur
High	Occurrence is highly unlikely to occur.

The final risk writing is made up from the likelihood writing and overlaid against the consequence or impact writing. This risk matrix rating presented here is specific only for this study, as represented in Table 5.8 and Figure 5.5.

In the event of likelihood of a risk to occur, response strategy to avoid such risk should be put in place to avoid and decrease the likelihood of such impact, which is presented in Table 5.9 as a mitigation plan.

Table 5.8: Risk rating matrix

	Type of Impact	Probability or Likelihood	Potential Consequence/Impact
1.	Human Health	I	L
2.	Virulence	L	L
3.	Soil	L	L
4.	Hazard to animal	I	I
5.	Air	I	I
6.	Environment	I	L
7.	Hazard to plant	I	L
8.	Water	L	L
9.	Worker Exposure	I	L

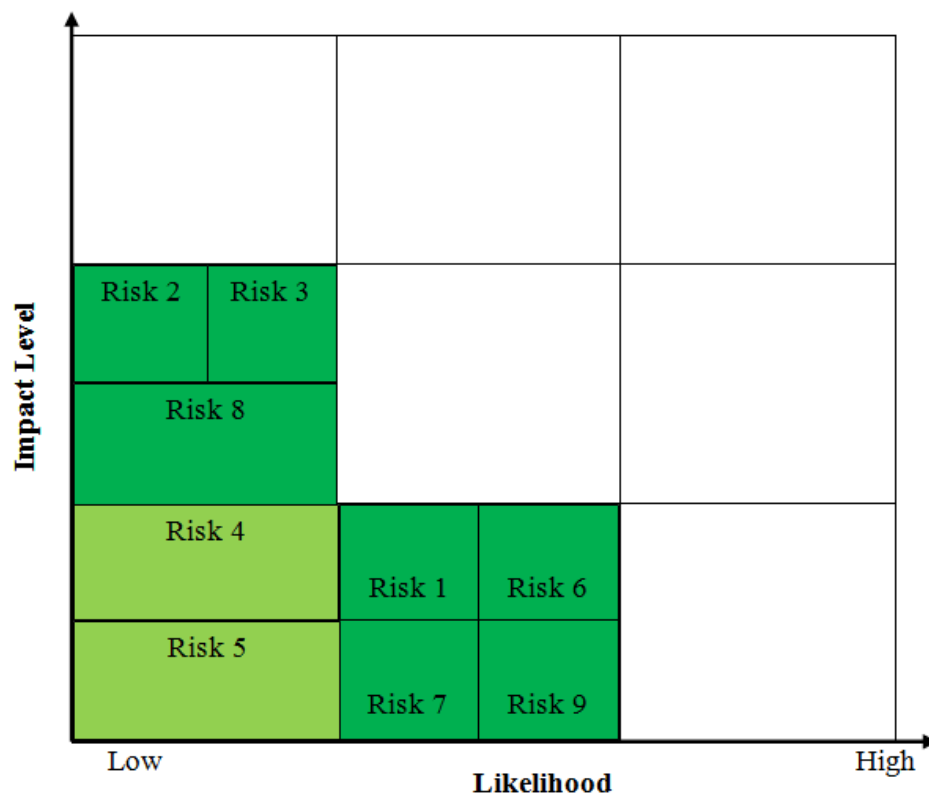


Figure 5.5: Probability impact grid

Table 5.9: Planned response (mitigation)

Risk Probability	Mitigation Plan
Low	<p>In the event of drinking water pollution, water treatment process, which includes coagulation, flocculation, ozonation, filtration and chlorination, is expected to effectively eliminate these micro-organisms.</p> <p>Risk reduction measures are unlikely to be cost-effective.</p>

5.8 Summary

The advantage of the selected strains for their laboratory production and application was carefully considered. Besides the beneficial effects, they do not show any marked toxicity and cannot cause any risk to health and environmental pollution based on what the guidelines used in this study revealed. The probability of risk occurrence of any of the strains is thought most unlikely as they do not produce toxins. Previous studies revealed that, immunosuppressed individuals following trauma, could be affected when prone to high level of exposure during a fermentation operation, and animals already in an immunocompromised state resulting from either infection with other organisms or poor nutrition.

In this present study, the significance of the outcome of this assessment based on the guidelines used is highlighted thus;

- The selected strains were of low concentrations and do not have potential of toxicity.
- Exposure to the strains during the culture process and use of the biosurfactants during the laboratory investigations conducted in Chapter-4 was therefore safe from risk.
- In direct comparison to synthetic surfactant, these three microbial surfactants produced can be said to be less toxic than the former.
- The produced biosurfactant from these strains, resulted in maximal beneficial output
- A mitigation strategy was put in place to decrease the likelihood of any impact especially at the fermentation stage resulting in risk reduction measures which are unlikely to be cost-effective.

The next chapter will evaluate the economics of utilising one of the produced biosurfactants for an EOR process, which will involve drilling an injection well.

Chapter 6

6 Economic Analysis Using *BS-2* Biosurfactant to Enhance Residual Oil in Nembe field, Niger delta.

6.1 Introduction

Economic optimisation is the ultimate goal of any reservoir engineering management, leading to the main objective of any business project, which is to evaluate the project economic value, to estimate the return of investment. This is achieved by firstly carrying out a financial analysis and secondly the economic analysis quantifying all factors to determine whether the project is profitable or not. In essence, the purpose of any project economics is to determine the economic value of the project and to support decision-making. Most projects are prioritised according to investment alternatives whether there is a need to revise, postpone or even reject the proposal for financial reasons or other intangible considerations.

The majority of oil companies today are focusing on maximizing the recovery factor (RF) from their oilfields as well as maintaining an economic oil rate. This is because it is becoming increasingly difficult to discover new oilfields. The average RF from mature oilfields around the world is somewhere between 20% and 40% (OECD/IEA, 2008; Sandrea & Sandrea, 2007). This contrasts with a typical RF from gas fields of between 80% and 90%. At current production rates existing proven oil reserves will last 54 years (Dudley, 2012). This is probably as good as it has ever been. Improving oil recovery to that typical of gas fields could more than double the time for which oil is available or alternatively allow for increased production rates. This would provide more time for an increasingly energy-hungry world to develop alternative energy sources and technologies (Muggeridge et al., 2014).

The oil market has been at the centre of economic news over much of the past year: what should we make of the US shale revolution; how will the rebalancing of the Chinese economy affect demand; and most obviously, what are the implications of the dramatic fall in oil prices over the past year or so? The implications of these developments are far reaching. For policymakers, responding to their impact on the prospects for demand and inflation; for financial markets, involved in the trading and financing of oil flows; and most fundamentally of all, for businesses and families across the world that rely on oil to fuel their everyday businesses and lives. As economists, when faced with questions about the oil market and oil prices, a natural instinct is to revert to the key principles and beliefs that we think underpin the operation of the oil market (Dale, 2015).

Economic evaluation consists of comparing the costs of a project and the effort needed to finance it, with the value of the expected benefits, which may not be necessarily monetary in nature, but non-monetary benefits such as social and environmental benefits are also considered. To make this comparison as many factors as possible are measured in the same cash units, this evaluation uses the dollar (US\$), since most international business in oil and gas are quoted in dollar.

6.2 Consideration of Economic Parameters and Assumptions

In order to conduct the economic analysis for drilling the injection well, the following economic parameters and assumptions were considered in this research based on a case study.

- Amount of biosurfactant required for injection is 5,000 gals
- Estimated project life is 5 years
- Oil price is US\$54.89 per barrel flat, Brent Oil (19/04/2017)
- Estimated recoverable reserve, 48 million barrels
- Uptime 90%, meaning productivity is $0.9 * 365$ days
- Depreciation follows a straight-line model
- A salvage value of zero is assumed
- Cooperate taxes rate, 75%
- Cost escalation (Inflation rate) 3% every year
- Annual production increased by 2.9%
- Real discount rate taken to be 10 %
- Royalty taken as zero
- Capital Expenditure acquired at year 0, while production starts from year 1

6.2.1 Total Capital Cost for Drilling the Injection Well

Although various studies have taken different approaches to calculating the capital cost associated with drilling and maintaining wells (Godec, 2011), therefore, for the purpose of targeting enhanced oil recovery in depleted oil reservoirs, this study used the capital cost estimate based on a case study of Nembe field, within the Niger Delta, Nigeria. Drilling costs are somewhat dependent upon the type of formations that must be drilled through in order to reach the target zones; however, that level of detail is not applicable in this study. The estimated recoverable reserve is 48 million barrels and current production rate is 31,285.62

barrels per day. Although, the well production rate was initially 51,530.68 barrels per day before depleting to its current rate, hence the need for enhanced recovery. The breakdown of drilling the injection well or capital expenditure (CAPEX) is shown in Table 6.1.

Table 6.1: Typical cost estimate for drilling an injection well

Unit	Total Cost	Cost \$
	(%)	(Millions of Dollar)
Biosurfactant Production	10	4.52
Pump	10.4	4.17
Surface Equipment	44.5	20.17
Plugging Costs	0.6	0.27
Drilling/Pipping	13.4	6.07
Biosurfactant Storage Plant	6.7	3.04
Power Plant	8.2	3.72
Miscellaneous	6.2	2.81
Total Cost	100.0	45.32

6.2.2 Estimation of operating expenditure (OPEX)

As it is imperative to incur a daily operating expenditure of running the injection well, the significance of OPEX has no future benefits, and thus needs to be managed not to consume the profits made. The use of inexpensive and waste substrate for the formulation of fermentation media, which lower the initial raw material costs involved in the process of biosurfactant production, needs to be harnessed. A series of financial assumptions was incorporated that affected the price estimates. The OPEX for this recovery process are divided into two separate costs. Firstly, the cost of raw materials (feed costs) and secondly, non-feed costs.

6.2.2.1 Preparation of Biosurfactant

The production of biosurfactant requires the formation media for bacterial cultures and the broth nutrient agar for growing the bacterial. The main raw materials used for this process are substrates, microorganism, Luria Broth (LB) and Minimal Salt Medium (MSM). However, there is difficulty in estimating the individual cost of these raw materials, since the LB and MSM contain several chemical compounds in g/L. Therefore, a lump estimate of 9.5% of the

total capital cost of drilling the injection well was taken as the cost of the raw materials. When we consider the cost of \$45.32 million US dollars in drilling the injection well, the feed cost is then estimated to be **\$4,305,400** per year.

The non-feed cost includes expenses like maintenance, wages, utilities and miscellaneous costs. In the absence of itemized costs, the non-feed cost was taken to be 4.05% of the capital expenditure and it is estimated to be **\$1,835,460** per year.

Hence the total operating cost for the entire injection process to enhance oil recovery is the addition of both the feed (raw materials) and non-feed costs as shown in Table 6.2.

Table 6.2: Annual operating costs

Items	Total annual Cost (\$)
Raw-material	4,305,400
Non-feed cost	1,835,460
Total	6,140,806

6.2.3 Revenue generated from the sales of Oil produced

Cash inflows are generated by the production of oil. The well of interest has the current capacity of producing 31,285.62 barrels per day. The well was injected with *BS-2* supernatant biosurfactant and shut-in for a two-month period before commencing production again, (Kuznetsov, 1963). The choice of the biosurfactant for this analysis, is due to the results obtained in Chapter-4 for *BS-2* supernatant biosurfactant, which gave the best outcome in all experimental phase. The essence of closing the well for the time period, was to allow for adequate reaction between the biosurfactant and oil in the pore spaces, of the formation to take place, to enable an added recovery. With the current oil price and the additional product yield, the annual sale of the oil produced is estimated as shown in Table 6.3.

Table 6.3: Annual sales of oil produced

Oil Produced	Production (Bbl/day)	Price (\$/Bbl)	Annual Sales (\$)
Current Recovery, Excluding Biosurfactant	31,285.62	54.89	564,122,433.5
Total Recovery, Including Biosurfactant	34,005.62	54.89	613,167,746.3
Enhanced Recovery (results from biosurfactant addition)	2,720.00	54.89	49,045,312.8

6.2.4 Estimation of Depreciation Cost/Tax

An analysis of costs and profits for any business operation requires recognition of the fact that physical assets decrease in value with age. This decrease in value may be due to physical deterioration, technological advances, economic changes, or other factors which ultimately will cause retirement of the property. The reduction in value due to any of these causes is a measure of the depreciation (Max, Klaus, & Ronald, 1991). The depreciation allowance, or fiscal depreciation, is not itself an element of the cashflow. Its only role is in the calculation of tax. Since depreciation reduces taxable income, fast depreciation leads to a lower tax bill in the early years of a project, thus improving its early cashflow at the expense of its later cashflow. This has a beneficial effect on the economics of the project.

In this study, the straight-line depreciation method was adopted, based on the available economic parameters that is considered. It distributes the cost of the asset uniformly over its depreciable life. Mathematically, expressed as:

$$D = \frac{C - S}{n} \quad (6.1)$$

Where,

D = depreciation (US\$/year)

C = initial asset cost (US\$)

S = expected salvage value at the end of useful life of asset (US\$)

n = estimated useful life of asset (year)

At the end of the project some salvage value can be recovered. The salvage value is a net amount, net of any removal or dismantling costs but may be very difficult to forecast. If the net salvage value is small, it can be excluded from the cash flow analysis. Salvage value is usually positive, which means it is a cash inflow. But there can be cases when the dismantling and removal costs outweigh the returns from the salvaged asset, thereby rendering the net salvage value negative. The usual practice is to assume zero salvage value (Perry & Green, 1999). Hence this value assumed in this study.

For the initial capital investment of \$45.32 million and estimate plant life of 5 years, the depreciation cost is estimated as:

$$D = \frac{45.32 - 0}{5} \quad (6.2)$$
$$= \$9.064 \text{ Million}$$

The effect of tax on capex/opex/production trade-offs can be very significant. It tends to make capex more difficult to justify, because the tax relief (through the depreciation allowance) is deferred and loses Present Value by comparison with the immediate relief on operating expenditure and the immediate tax on revenue.

6.3 Cash Flow Model

A project or business cash flow is an important financial statement because cash is important to the survival of a business. This statement reveals the movements of cash over a period and the effect of these movements of cash position with regards to the economic performance of the project (McLaney & Atrill, 2015).

A company typical flow of funds is illustrated in Figure 6.1. The excess of sales over operating costs is called gross profit. From this point, depreciation is deducted, leaving the taxable income. The taxable income is subjected to state, federal and other fiscal taxes. The profit remaining after taxes, combined with depreciation is termed cash flow of the venture. This is the amount of money that goes to the account of the company.

The cash flow model was developed based on the following cost models:

$$\text{Revenue} = \text{Price per barrel} * (\text{Number of barrels of Enhanced Oil produced per year}) \quad (6.3)$$

$$\text{Taxes} = \text{Tax rate} * (\text{Revenue} - \text{Opex} - \text{Depreciation}) \quad (6.4)$$

$$\text{Net Cash Flow} = \text{Revenue} - \text{Capex} - \text{Opex} \quad (6.5)$$

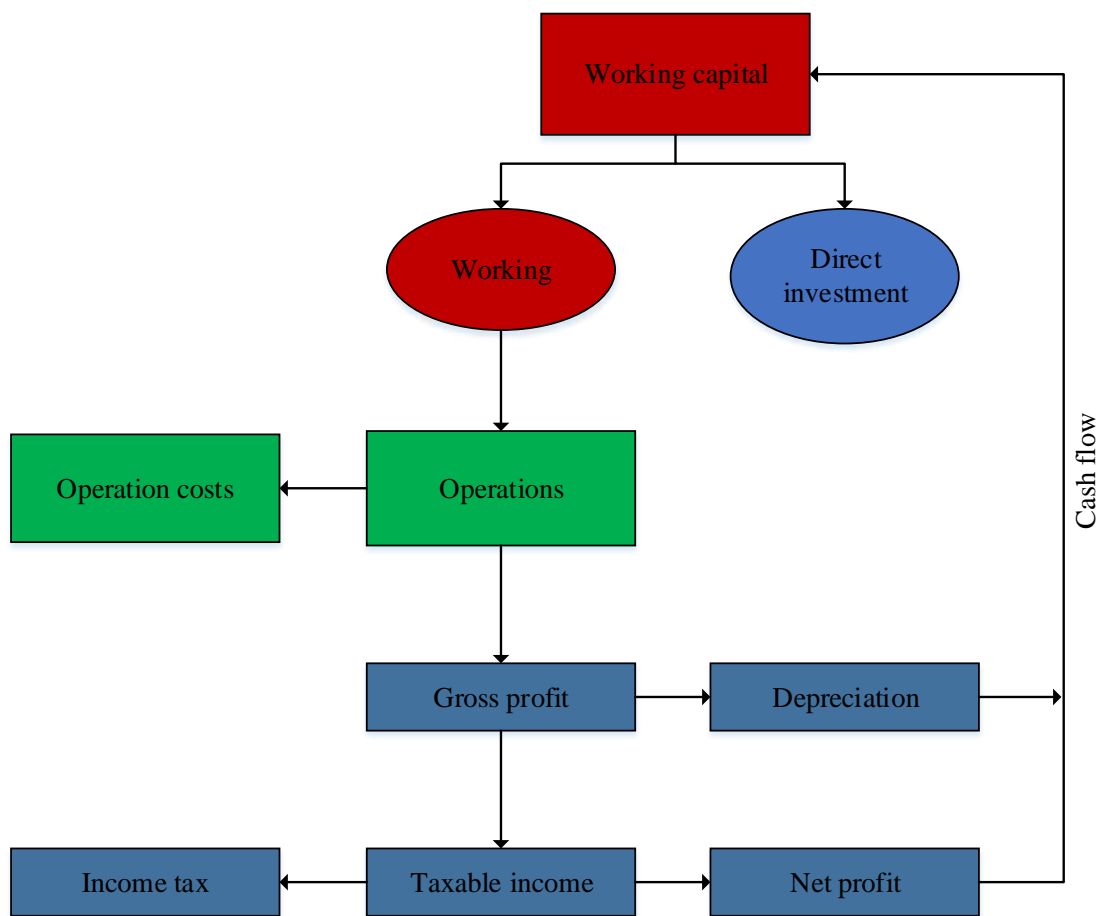


Figure 6.1: Cooperate cash flow diagram

Source: (Ikoku, 1985)

Equations 6.3 – 6.5 were used to calculate the Net Cash Flow in drilling the injection well. Two project evaluation and selection models were used to measure the acceptability of the

proposed well in this study. The first was after-tax Net Present Value (NPV) and the later the Payback period.

6.4 Net Present Value (NPV) Analysis

A project net present value, or alternatively called its present value cash surplus, is the sum over the years of the project of its discounted cashflow. This represents the value of the project to the investor. When a project has a positive NPV, it becomes more economically attractive and the project is likely to be accepted. However, where capital is limited, the project with the highest NPV is usually accepted. The economic aim in considering alternatives it to reduce the negative NPV to as low as can be possible.

The net present value realistically predicts the future cash flows against the initial investment. Mathematically, expressed in Eqn. (6.6). If the project is affected by the impact of inflation/deflation, then Eqn. (6.6) is modified into Eqn. (6.7) to take care of the impact.

$$NPV (project) = A_o + \sum_{t=1}^n \frac{F_t}{(1 + k)^t} \quad (6.6)$$

$$NPV (project) = A_o + \sum_{t=1}^n \frac{F_t}{(1 + k + p_t)^t} \quad (6.7)$$

Where,

F_t = the net cash flow in period t

A_o = initial cash investment (it is negative because it is outflow)

k = the discount rate

p_t = predicted rate of inflation/deflation during period t (*only if applicable*)

t = year of evaluation

n = total number of years of the project life

Investment decisions are based on capital availability; predictions of costs, revenues tax, inflation, etc.; alternative investments available, attitude to the risks involved. Therefore,

appraisal should assess cash flow related to the reject, degree of risk involved and expected return on investment. Thus, decision-making criteria using NPV are as follows:

- where NPV is equal zero or positive, accept the project.
- where, NPV is less than zero, reject the project.

In the early life of a project, the net cash is likely to be negative, since the major cash outflow is the initial investment in the project, A_0 . The cash flow will be positive if the project is successful.

6.5 Net Cash Flow of Oil Recovery

Cash flow helps to predict whether the sales or income you forecast will cover the costs of operation. It also allows you to analyse whether a project will be sufficiently profitable to justify the effort put into it.

Table 6.4, shows the discounted cash flow generated from drilling the injection well for enhancing oil recovery using *BS-2* supernatant biosurfactant, at 10% discount rate, using equations 6.3 – 6.7. It can be seen from Table 6.4, that at the end of a five-year period, the NPV of the project at the discount rate of 10% is \$28.340 million, while the cumulative cash flow was \$75.868 million.

Table 6.4: Cash flow at 10% discount rate of drilling an injection well

Year	Annual Revenue (\$)	Capex (\$)	Opex (\$)	Depree	Tax	Net Cash Flow (%)	Inflation Rate (%)	NPV (\$)	Cum. Cash Flow (\$)
0	0	0	0	0	0	0	0	0	0
1	0	45.32	0	0	0	-45.32	0	-41.2	-45.32
2	49.045	45.32	6.14	9.064	22.587	29.382	0.03	23.010	-15.938
3	50.467	45.32	6.14	9.064	22.587	30.804	0.06	19.735	14.866
4	50.496	45.32	6.14	9.064	22.587	30.833	0.09	15.375	45.699
5	50.525	45.32	6.14	9.064	22.587	30.862	0.12	11.419	76.561
Total	200.533					76.561		28.340	75.868

6.6 Payback (Payout) Period

The payback of a project is the exact period in years in which it takes for the projects net cash flow to recoup the original capital investment. The payback period therefore measures the speed with which invested funds are recovered in a business. The project with the shortest payback is accepted. A common rule of thumb is 2-4 years subject to the conditions of the cash flow (Lyons & Plisga, 2011). It is important to measure payout using only the incremental cash flow created by the investment, not cash flow that would have been obtained anyway.

The plot of the cumulative annual cashflow of the enhanced recovery in Table 6.4 against time will give the payback period. Figure 6.1 shows the payback period obtained from drilling the injection well for enhanced oil recovery. The payback period is estimated to be 2.54 years.

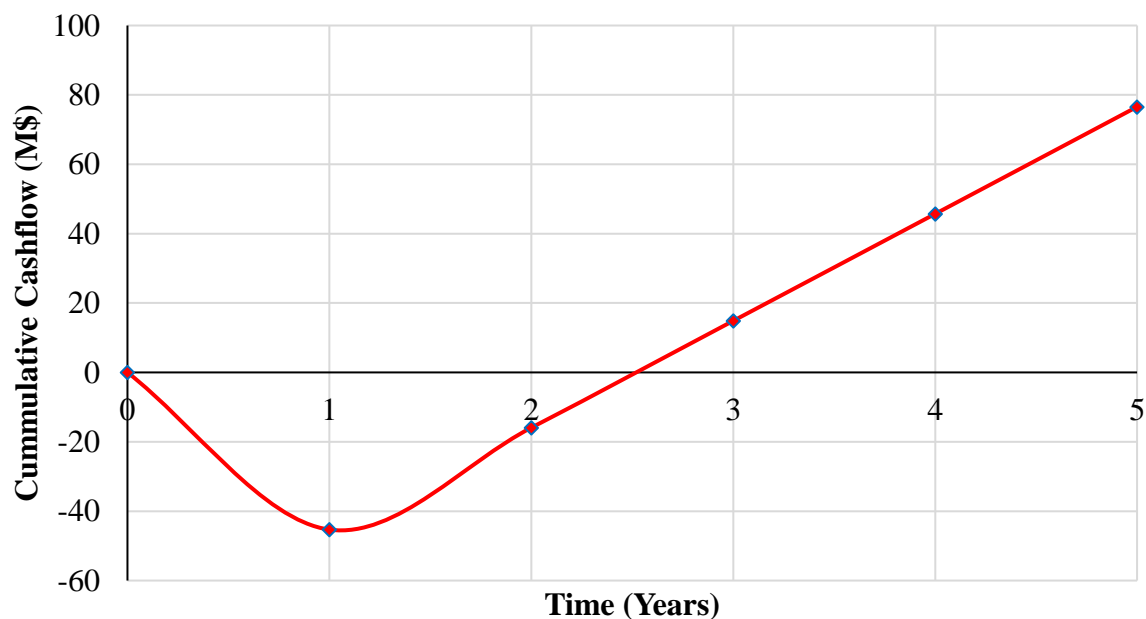


Figure 6.2: Payback period for drilling the injection well

6.7 Break-even point for the Injection Well

This analysis is useful in the determination of the level of production or in a targeted desired sales mix. Break-even analysis looks at the level of fixed costs relative to the profit earned by the additional unit produced or sold. Establishing the break-even point helps a firm to plan

the levels of production it needs to be profitable, by working out the minimum sales needed to avoid losses.

For the injection well that was drilled in Nembe oil field, at a cost of \$45.32 million, 30% of the total capital cost was used to estimate the plant fixed cost, which amounted to **\$13,596,000**. The variable cost was already estimated in Table 6.2 as **\$6,140,806** and revenue from the product sales in Table 6.3 amounted to **\$49,045,312.8**.

The two components of the total cost of goods and services are the fixed and variable costs. Table 6.5 gives the summary of all the costs discussed in this section for a production rate of 2,720 barrel of crude oil per day.

Table 6.5: Cost Summary of Drilling Injection Well.

Sales Volume (Barrels)	Million Dollars			
	Fixed cost	Variable costs	Total costs	Product Sales
0	13.596	0	13.596	0
2720	13.596	6.14	19.736	49.045

The plot of various cost is plotted in Figure 6.2. The vertical distance between the total cost and product sales revenue lines, gives the break-even point. Below this point a loss is made, above it a profit. Therefore, to sustain the expenses of drilling the injection well, the daily production rate of the enhanced recovery must be 865 bbl/day.

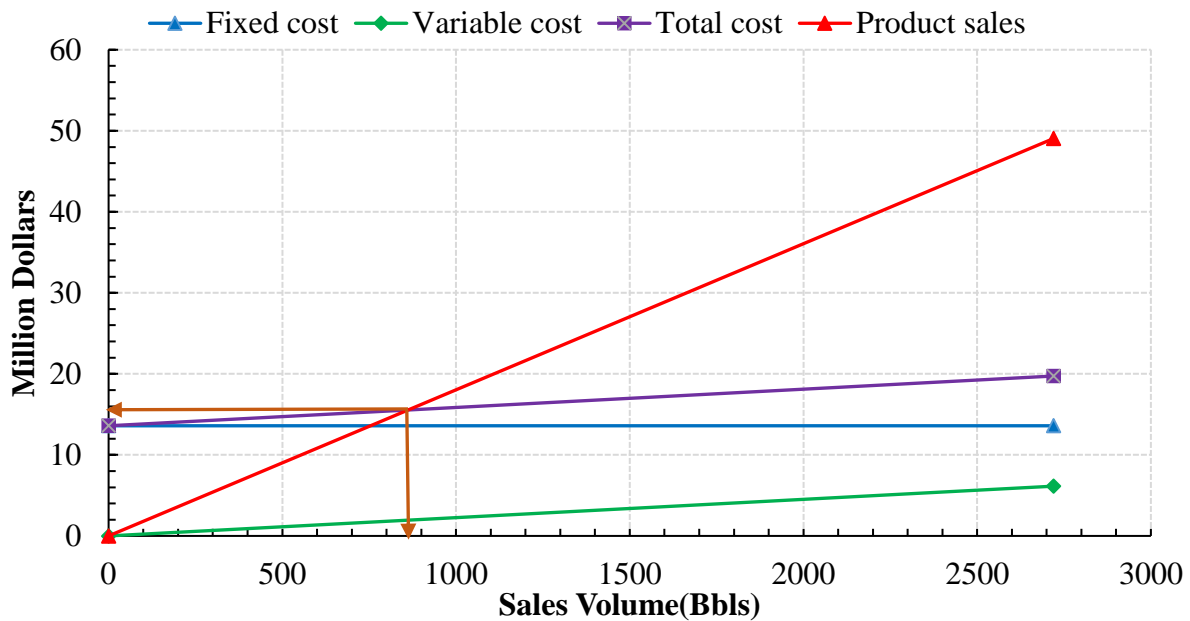


Figure 6.3: Break-even graph of enhanced recovery using *BS-2* biosurfactant

6.8 Chapter summary

The economic parameters and assumption were established to perform the viability of using the *BS-2* supernatant biosurfactant in an EOR process. All the financial parameters utilised as a part of this present study, demonstrated that the proposed technique which entails drilling an injection well for enhancing recovery, is monetarily better and environmentally safe when used to the oil industry.

A cash flow for the enhanced oil recovered was established, to forecast if the income generated will cover for the cost of operation. The outcome indicated a payback period of 2.54 years, which may be acceptable for this project.

The cumulative cash flow of US\$75,868,000 million dollars was generated by the proposed injection well. The results also showed that the generated revenue at the end of the estimated project life, has over 75% influence on the profitability of the project.

The next chapter will give comprehensive conclusion on the findings of this research and give some future recommendation that could be further studied.

Chapter 7

Conclusions and Future Works

7.1 Conclusions

The experimental methodology utilised in this study gave the main impact and outcome, and the proposed biosurfactant has been demonstrated to be capable of enhancing residual oil in a heavy oil reservoir.

A detailed review and discussion of the main mechanisms of MEOR was presented in Chapter 2, and the significance of wettability in EOR was also discussed. Furthermore, discussed in Chapter 2 was theoretical background of the pendant drop interfacial tension tool that was used to quantitatively investigate the effect of the biosurfactants on IFT and contact angle. Chapter 3 provided a detailed description of the experimental equipment, materials and procedure used during this experimental work. These procedures followed the conventional and widely accepted standard protocols outlined in the literature, and at the same time were modified to achieve the objectives set for this study.

The results of the various concluded experiments were included, interpreted and analysed in Chapter 4. The effects of the main MEOR mechanisms were also discussed in-line with the results obtained. Chapter 5, provided a detailed risk assessment of the three strains utilised in this study in producing the biosurfactants, based on some specific guidelines. The economic analysis of the proposed injection well was also carried out in Chapter 6, to determine the profitability of the proposed method.

Based on the findings from this present study, it can be stated that the potential to enhance oil recovery by these biosurfactants are considerable. All the above work led to the conclusion that are listed in the different phases below.

Phase – I (Microbial culture)

The selected bacteria strains were successfully extracted from freeze dried conditions, cultured, inoculated and grown at different temperatures to produce biosurfactants. The phenotypic characteristic of the bacteria were initially determined, and further sequencing of the strain using PCR to amplify their DNA, using the forward and reverse primers. The biosurfactants produced in this present study were named; *BS-1*, *BS-2* and *BS-3* respectively.

Phase – II (Interfacial tension and contact angle)

The experimental findings of decreasing IFT and contact angle indicated that there was a considerable reaction between the oil-formation water-biosurfactant interface, which led to the reduction of intermolecular forces between the oil and formation water at increasing temperatures.

The produced biosurfactant *BS-2* cell-free supernatant gave the best outcome in IFT reduction and contact angle, against the *BS-1* cells with the least performance.

Phase – III (Qualitative wettability tests)

The findings of the qualitative wettability tests revealed that the produced biosurfactants can decrease the oil wetting of strongly oil-wet Scioto and Bandera Gray sandstones, by changing the wettability of the surface chemistry of the rock grain to being both water-wet and intermediate-wet, respectively.

Phase – IV (Core flooding)

The oil recovery increased from 30% to 38% in lesser time from initial water flooding, giving a recovery factor of 8% after flooding with *BS-2* biosurfactant. The increase in oil recovery is proposed to be due to the biosurfactant changing the wettability of the rock around the production well.

Chapter 5

Increased environmental awareness has been the main driver for the search for a replacement to the chemical surfactants. Sucrose, which is a hydrophobic carbon source, was selected as a suitable carbon nutrient supplement to produce the three biosurfactants. And according to research findings in the last decade, decomposition property of sucrose makes it eco-friendly for biosurfactant production.

Chapter 6

The cashflow was discounted at a rate of 10%, which gave a payback period for the proposed injection well to be 2.54 years. A good knowledge of break-even point for a project can be a basis for risk assessment. In this analysis, the break-even point has aided to see the volume of

daily oil production rates (865 bbl/day), to cover the variable costs and contributing to the payment of the fixed costs.

7.2 Future Works

- The physical characteristics and chemical structure of the biosurfactant produced by the different strains of *Bacillus subtilis* BS-1, *Bacillus licheniformis* BS-2 and *paenibacillus polymyxa* BS-3, needed to be determined or identified using mass spectrometry on each of the samples.
- The process for identifying the Critical Micelle Concentration (CMC) is to take multiple different concentrations of purified surfactant, and measure the surface tension at each concentration. This process required the use of a DeNouy ring which was not available and expensive to rent. At the point that the surface tension does not reduce any lower, this is the point where micelles begin to form and as such is classified as the CMC using regression analysis. Furthermore, due to the amount of cell suspension (volume) the equipment requires (reservoir), it would require to make masses of culture to make enough to create each CMC concentration.
- Consideration of the thermal stability and salinity tolerance of the produced biosurfactants, which also involves the alterations of CMC at different salinities, temperatures and mineral concentrations of waters. When the CMC increases, the tolerance is lost at that specific concentration of ion or temperature.

References

- Abdallah, W., Buckley, J. S., Carnegie, A., Edwards, J., Herold, B., Fordham, E., . . . Signer, C. (1986). Fundamentals of Wettability. *Technology*, 38, 1125-1144.
- Afrapoli, M. S., Crescente, C., Alipour, S., & Torsaeter, O. (2009). The effect of bacterial solution on the wettability index and residual oil saturation in sandstone. *Journal of Petroleum Science and Engineering*, 69(3-4), 255-260. doi:10.1016/j.petrol.2009.09.002
- AIRMIC, A. (2002). *IRM," A Risk Management Standard," The Institute of Risk Management*. Paper presented at the The National Forum for risk Management in the Public Sector, The Association of Insurance and Risk Managers, London, UK.
- Al-Bahry, S., Al-Wahaibi, Y., Elshafie, A., Al-Bemani, A., Joshi, S., Al-Makhmari, H., & Al-Sulaimani, H. (2013). Biosurfactant production by *Bacillus subtilis* B20 using date molasses and its possible application in enhanced oil recovery. *International Biodeterioration & Biodegradation*, 81, 141-146.
- Al-Hattali, R. (2012). *Microbial Biomass for Improving Sweep Efficiency in Fractured Carbonate Reservoir Using Date Molasses as Renewable Feed Substrate*. Paper presented at the SPE Annual Technical Conference and Exhibition, 8-10 October, San Antonio, Texas, USA.
- Al-Maamari, R. S., & Buckley, J. S. (2003). Asphaltene precipitation and alteration of wetting: the potential for wettability changes during oil production. *SPE Reservoir Evaluation & Engineering*, 6(04), 210-214.
- Al-Sulaimani, H., Joshi, S., Al-Wahaibi, Y., Al-Bahry, S., Elshafie, A., & Al-Bemani, A. (2011). Microbial biotechnology for enhancing oil recovery: current developments and future prospects. *Biotechnol. Bioinf. Bioeng*, 1(2), 147-158.
- Al-Sulaimani, H. S., Al-Wahaibi, Y. M., Al-Bahry, S., Elshafie, A., Al-Bemani, A. S., Joshi, S. J., & Zargari, S. (2010). *Experimental investigation of biosurfactants produced by Bacillus species and their potential for MEOR in Omani oil field*. Paper presented at the SPE EOR Conference at Oil & Gas West Asia.
- Alvarado, V., & Manrique, E. (2010). *Enhanced oil recovery: field planning and development strategies*: Gulf Professional Publishing.
- Anderson, W. (1986). Wettability literature survey-Part 1: Rock/oil/brine interactions and the effects of core handling on wettability. *J. Pet. Technol.:(United States)*, 38(11).
- Anderson, W. (1986). Wettability literature survey-part 2: Wettability measurement. *Journal of petroleum technology*, 38(11), 1,246-241,262.
- Anderson, W. G. (1987a). Wettability literature survey-part 4: Effects of wettability on capillary pressure. *Journal of petroleum technology*, 39(10), 1,283-281,300.
- Anderson, W. G. (1987b). Wettability literature survey-part 6: the effects of wettability on waterflooding. *Journal of petroleum technology*, 39(12), 1,605-601,622.

- Aronofsky, J. (1952). Mobility ratio-Its influence on flood patterns during water encroachment. *Journal of petroleum technology*, 4(01), 15-24.
- Ash, C., Priest, F., & Collins, M. (1994). *Paenibacillus* gen. nov. and *Paenibacillus polymyxa* comb. nov. *Validation of the publication of new names and new combinations previously effectively published outside the IJSB, List*(51).
- Bachmann, R. T., Johnson, A. C., & Edyvean, R. G. (2014). Biotechnology in the petroleum industry: an overview. *International Biodeterioration & Biodegradation*, 86, 225-237.
- Banat, I., Franzetti, A., Gandolfi, I., Bestetti, G., Martinotti, M., Fracchia, L., . . . Marchant, R. (2010). Microbial biosurfactants production, applications and future potential. *Applied Microbiology and Biotechnology*, 87(2), 427-444. doi:10.1007/s00253-010-2589-0
- Bento, F. M., de Oliveira Camargo, F. A., Okeke, B. C., & Frankenberger, W. T. (2005). Diversity of biosurfactant producing microorganisms isolated from soils contaminated with diesel oil. *Microbiological research*, 160(3), 249-255.
- Beveridge, T. J. (2001). Use of the Gram stain in microbiology. *Biotechnic & Histochemistry*, 76(3), 111-118.
- Bond, D. C. (1961). Bacteriological method of oil recovery: Google Patents.
- Brown, L. R. (2010). Microbial enhanced oil recovery (MEOR). *Curr Opin Microbiol*, 13(3), 316-320. doi:<http://dx.doi.org/10.1016/j.mib.2010.01.011>
- Bryant, R. S., & Burchfield, T. E. (1989). Review of Microbial Technology for Improving Oil Recovery. *SPE Reservoir Engineering*, 151-154. doi:10.2118/16646-PA
- Bryant, R. S., & Douglas, J. (1988). Evaluation of microbial systems in porous media for EOR. *SPE Reservoir Engineering*, 3(02), 489-495.
- Buckley, J., Liu, Y., & Monsterleet, S. (1998). Mechanisms of wetting alteration by crude oils. *SPE journal*, 3(01), 54-61.
- Cai, B.-Y., Yang, J.-T., & Guo, T.-M. (1996). Interfacial tension of hydrocarbon+ water/brine systems under high pressure. *Journal of chemical & engineering data*, 41(3), 493-496.
- Campos, J. M., Montenegro Stamford, T. L., Sarubbo, L. A., de Luna, J. M., Rufino, R. D., & Banat, I. M. (2013). Microbial biosurfactants as additives for food industries. *Biotechnology Progress*, 29(5), 1097-1108.
- Caruso, F., Zuck, M., & Bessette, A. (1984). Bacterial seedling blight of tomato caused by *Bacillus polymyxa*. *Plant disease*, 68(7), 617-620.
- CEPA. (1999). *Paenibacillus polymyxa* <https://www.canada.ca/en/environmental-assessment-agency.html>.
- Chester, F. D. (1901). *A manual of determinative bacteriology*: Macmillan Company.

- Dake, L. P. (2001). *The practice of reservoir engineering (revised edition)* (Vol. 36): Elsevier.
- Dale, S. (2015). *New economics of oil*.
- Davies, J., & Rideal, E. (1963). *Interfacial Phenomena*, Acad. Press, NY.
- Davis, J. B., & Updegraff, D. M. (1954). Microbiology in the petroleum industry. *Bacteriological reviews*, 18(4), 215.
- De Almeida, D. G., Rita de Cássia, F., Silva, J. M. L., Rufino, R. D., Santos, V. A., Banat, I. M., & Sarubbo, L. A. (2016). Biosurfactants: Promising Molecules for Petroleum Biotechnology Advances. *Frontiers in Microbiology*, 7.
- de Guertechin, L. O. (2001). Classification of Surfactants. *Handbook of Cosmetic Science and Technology, Third Edition*, 431-450.
- de Lima, A. M., & de Souzaa, R. R. (2014). Use of Sugar Cane Vinasse as Substrate for Biosurfactant Production Using *Bacillus subtilis* PC. *CHEMICAL ENGINEERING*, 37.
- Desai, J. D., & Banat, I. M. (1997). Microbial production of surfactants and their commercial potential. *Microbiology and Molecular Biology Reviews*, 61(1), 47-64.
- Deshpande, M., & Daniels, L. (1995). Evaluation of sophorolipid biosurfactant production by *Candida bombicola* using animal fat. *Bioresource Technology*, 54(2), 143-150. doi:[http://dx.doi.org/10.1016/0960-8524\(95\)00116-6](http://dx.doi.org/10.1016/0960-8524(95)00116-6)
- Dubey, K., & Juwarkar, A. (2004). Determination of genetic basis for biosurfactant production in distillery and curd whey wastes utilizing *Pseudomonas aeruginosa* strain BS2. *Indian Journal of Biotechnology*, 3(1), 74-81.
- Dudley, B. (2012). BP statistical review of world energy. June 2012. London, UK.
- Dunlap, C., Schisler, D., Price, N., & Vaughn, S. (2011). Cyclic lipopeptide profile of three *Bacillus subtilis* strains; antagonists of *Fusarium* head blight. *The Journal of Microbiology*, 49(4), 603-609. doi:10.1007/s12275-011-1044-y
- Dusseault, M. (2001). *Comparing Venezuelan and Canadian heavy oil and tar sands*. Paper presented at the Canadian International Petroleum Conference.
- Edberg, S. (1991). US EPA human health assessment: *Bacillus subtilis*. Unpublished, US Environmental Protection Agency, Washington, DC.
- Edwards, U., Rogall, T., Blöcker, H., Emde, M., & Böttger, E. C. (1989). Isolation and direct complete nucleotide determination of entire genes. Characterization of a gene coding for 16S ribosomal RNA. *Nucleic Acids Research*, 17(19), 7843-7853.
- El-Hadad, M., Mustafa, M., Selim, S. M., El-Tayeb, T., Mahgoob, A., & Aziz, N. H. A. (2011). The nematocidal effect of some bacterial biofertilizers on *Meloidogyne incognita* in sandy soil. *Brazilian Journal of Microbiology*, 42(1), 105-113.

- El-Sheshtawy, H., Aiad, I., Osman, M., Abo-ELnasr, A., & Kobisy, A. (2015). Production of biosurfactant from *Bacillus licheniformis* for microbial enhanced oil recovery and inhibition the growth of sulfate reducing bacteria. *Egyptian Journal of Petroleum*, 24(2), 155-162.
- Elraies, K. A., & Tan, I. M. (2012). *The Application of a New Polymeric Surfactant for Chemical EOR*: INTECH Open Access Publisher.
- Fang, X., Wang, Q., Bai, B., Liu, C. X., Tang, Y., Shuler, P. J., & Goddard III, W. A. (2007). *Engineering rhamnolipid biosurfactants as agents for microbial enhanced oil recovery*. Paper presented at the International Symposium on Oilfield Chemistry.
- Filho, J. H., Carioca, O. B., Gonzales, R. B., de Lucena, L., & Tavares, C. A. (2012). *Biosurfactants: Production and Utilization in Oil Sludge Cleaning*. Paper presented at the Presented at the SPE EOR Conference at Oil and Gas West Asia held in Muscat, Oman 16 - 18 April 2012.
- Fisher, T. (2016). Phusion DNA Polymerases. <https://www.thermofisher.com/uk/en/home/brands/thermo-scientific/molecular-biology/thermo-scientific-molecular-biology-products/phusion.html>.
- Fossum, K., Herikstad, H., Binde, M., & Pettersen, K. (1985). Isolation of *Bacillus subtilis* in connection with bovine mastitis. *Nordisk veterinaermedicin*, 38(4), 233-236.
- Friberg, S., & Ahmad, S. (1971). Liquid crystals and the foaming capacity of an amine dissolved in water and p-xylene. *Journal of Colloid and Interface Science*, 35(1), 175.
- Frommer, W., Ager, B., Archer, L., Brunius, G., Collins, C., Donikian, R., . . . Küenzi, M. (1989). Safe biotechnology. *Applied Microbiology and Biotechnology*, 30(6), 541-552.
- Galanos, J., Perera, S., Smith, H., O'Neal, D., Sheorey, H., & Waters, M. J. (2003). Bacteremia due to three *Bacillus* species in a case of Munchausen's syndrome. *Journal of Clinical Microbiology*, 41(5), 2247-2248.
- Godec, M. L. (2011). Global technology roadmap for CCS in industry sectoral assessment CO2 enhanced oil recovery. *Arlington, Virginia*.
- Griffiths, R. I., Whiteley, A. S., O'Donnell, A. G., & Bailey, M. J. (2000). Rapid method for coextraction of DNA and RNA from natural environments for analysis of ribosomal DNA-and rRNA-based microbial community composition. *Applied and environmental microbiology*, 66(12), 5488-5491.
- Gulick, K. E., & McCain Jr, W. D. (1998). *Waterflooding heterogeneous reservoirs: An overview of industry experiences and practices*. Paper presented at the International Petroleum Conference and Exhibition of Mexico.
- Hammershaimb, E., Kuuskraa, V., & Stosur, G. (1983). *Recovery efficiency of enhanced oil recovery methods: a review of significant field tests*. Paper presented at the SPE Annual Technical Conference and Exhibition.

- Hamouda, A. A., & Karoussi, O. (2008). Effect of temperature, wettability and relative permeability on oil recovery from oil-wet chalk. *Energies*, 1(1), 19-34.
- Hansen, F. K. (1990). ramé-hart, inc.
- Hasiba, H., & Jessen, F. (1968). Film-forming compounds from crude oils, interfacial films and paraffin deposition. *Journal of Canadian Petroleum Technology*, 7(01), 1-12.
- Hirasaki, G. (1991). Wettability: fundamentals and surface forces. *SPE Formation Evaluation*, 6(02), 217-226.
- Hsieh, F.-C., Li, M.-C., Lin, T.-C., & Kao, S.-S. (2004). Rapid detection and characterization of surfactin-producing *Bacillus subtilis* and closely related species based on PCR. *Current microbiology*, 49(3), 186-191.
- Ihde, D. C., & Armstrong, D. (1973). Clinical spectrum of infection due to *Bacillus* species. *The American journal of medicine*, 55(6), 839-845.
- Ikoku, C. U. (1985). Economic analysis and investment decisions.
- Ivanković, T., & Hrenović, J. (2010). Surfactants in the environment. *Arhiv za higijenu rada i toksikologiju*, 61(1), 95-109.
- Jeong, H., Park, S.-Y., Chung, W.-H., Kim, S. H., Kim, N., Park, S.-H., & Kim, J. F. (2011). Draft genome sequence of the *Paenibacillus polymyxa* type strain (ATCC 842T), a plant growth-promoting bacterium. *Journal of Bacteriology*, 193(18), 5026-5027.
- Johnson, A. (1979). *Microbial oil release technique for enhanced oil recovery*. Paper presented at the Proceedings of the Conference on Microbiological Processes Useful in Enhanced Oil Recovery.
- Johnson, S., Salehi, M., Eisert, K., & Fox, S. (2009). *Using Biosurfactants Produced from Agriculture Process Waste Streams to Improve Oil Recovery in Fractured Carbonate Reservoirs*. Retrieved from <http://www.osti.gov/scitech/servlets/purl/945026/>
- Joshi, S., Bharucha, C., Jha, S., Yadav, S., Nerurkar, A., & Desai, A. J. (2008). Biosurfactant production using molasses and whey under thermophilic conditions. *Bioresource Technology*, 99(1), 195-199.
- Karimi, M., Mahmoodi, M., Niazi, A., Al-Wahaibi, Y., & Ayatollahi, S. (2012). Investigating wettability alteration during MEOR process, a micro/macro scale analysis. *Colloids Surf B Biointerfaces*, 95, 129-136. doi:10.1016/j.colsurfb.2012.02.035
- Kim, H.-S., Jeon, J.-W., Kim, B.-H., Ahn, C.-Y., Oh, H.-M., & Yoon, B.-D. (2006). Extracellular production of a glycolipid biosurfactant, mannosylerythritol lipid, by *Candida* sp. SY16 using fed-batch fermentation. *Applied Microbiology and Biotechnology*, 70(4), 391-396. doi:10.1007/s00253-005-0092-9
- Kim, K. K., Lee, K. C., Yu, H., Ryoo, S., Park, Y., & Lee, J.-S. (2010). *Paenibacillus sputi* sp. nov., isolated from the sputum of a patient with pulmonary disease. *International journal of systematic and evolutionary microbiology*, 60(10), 2371-2376.

- Kitamoto, D., Ikegami, T., Suzuki, G., Sasaki, A., Takeyama, Y.-i., Idemoto, Y., . . . Yanagishita, H. (2001). Microbial conversion of n-alkanes into glycolipid biosurfactants, mannosylerythritol lipids, by *Pseudozyma* (*Candida antarctica*). *Biotechnology Letters*, 23(20), 1709-1714. doi:10.1023/A:1012464717259
- Kowalewski, E., Rueslåtten, I., Steen, K. H., Bødtker, G., & Torsæter, O. (2006). Microbial improved oil recovery—bacterial induced wettability and interfacial tension effects on oil production. *Journal of Petroleum Science and Engineering*, 52(1-4), 275-286. doi:10.1016/j.petrol.2006.03.011
- Kuznetsov, S. (1950). Possibilities of production of methane in oil fields of Saratov and Buguruslan. *Mikrobiologiya*, 19(3), 193.
- Kuznetsov, S. I. (1963). *Introduction to geological microbiology*: McGraw-Hill.
- Lal, S., & Tabacchioni, S. (2009). Ecology and biotechnological potential of *Paenibacillus polymyxa*: a minireview. *Indian Journal of Microbiology*, 49(1), 2-10.
- Lazar, I., Petrisor, I., & Yen, T. (2007). Microbial enhanced oil recovery (MEOR). *Petroleum Science and Technology*, 25(11), 1353-1366.
- Lin, S.-Y., Chen, L.-J., Xyu, J.-W., & Wang, W.-J. (1995). An examination on the accuracy of interfacial tension measurement from pendant drop profiles. *Langmuir*, 11(10), 4159-4166.
- Liu, R., Dai, M., Wu, X., Li, M., & Liu, X. (2012). Suppression of the root-knot nematode [*Meloidogyne incognita* (Kofoid & White) Chitwood] on tomato by dual inoculation with arbuscular mycorrhizal fungi and plant growth-promoting rhizobacteria. *Mycorrhiza*, 22(4), 289-296.
- Logan, N. (1988). *Bacillus* species of medical and veterinary importance. *Journal of medical microbiology*, 25(3), 157-165.
- Louisajb. (2011). Structure of Surfactin. *Wikipedia* <https://en.wikipedia.org/wiki/File:Surfactin.png>.
- Lukondeh, T., Ashbolt, N. J., & Rogers, P. L. (2003). Evaluation of *Kluyveromyces marxianus* as a source of yeast autolysates. *Journal of Industrial Microbial Biotechnology*, 30, 52-56. doi:10.1007/s10295-002-0008-y
- Lyons, W. C., & Plisga, G. J. (2011). *Standard handbook of petroleum and natural gas engineering*: Gulf Professional Publishing.
- Magot, M. (2005). Indigenous microbial communities in oil fields. *Petroleum microbiology*. ASM Press, Washington, DC, 21-33.
- Mata-Sandoval, J. C., Karns, J., & Torrents, A. (2001). Effect of nutritional and environmental conditions on the production and composition of rhamnolipids by *P. aeruginosa* UG2.pdf. *Microbiology Research*, 155, 249-256.
- Max, S. P., Klaus, D. T., & Ronald, E. W. (1991). Plant design and economics for chemical engineers. *International edition*.

- McCaffery, F. G. (1972). Measurement of interfacial tensions and contact angles at high temperature and pressure. *Journal of Canadian Petroleum Technology*, 11(03).
- McInerney, M. J., Javaheri, M., & Nagle, D. P., Jr. (1990). Properties of the biosurfactant produced by *Bacillus licheniformis* strain JF-2. *J Ind Microbiol*, 5(2-3), 95-101.
- McInerney, M. J., Nagle, D. P., & Knapp, R. M. (2005). Microbially enhanced oil recovery: past, present, and future *Petroleum microbiology* (pp. 215-238): American Society of Microbiology.
- McLaney, E., & Atrill, P. (2015). *Accounting and Finance: An Introduction 8th edition*: Pearson Higher Ed.
- McPhee, C., Reed, J., & Zubizarreta, I. (2015). Core analysis : a best practice guide. Retrieved from <http://search.ebscohost.com/login.aspx?direct=true&scope=site&db=nlebk&db=nlabk&AN=1107651>
- Michaels, A., & Hauser, E. (1951). Interfacial Tension at Elevated Pressure and Temperature. II. Interfacial Properties of Hydrocarbon–Water Systems. *The Journal of Physical Chemistry*, 55(3), 408-421.
- Miller, R. G., & Sorrell, S. R. (2014). The future of oil supply: The Royal Society.
- Möbius, D., Miller, R., & Fainerman, V. B. (2001). *Surfactants: chemistry, interfacial properties, applications* (Vol. 13): Elsevier.
- Morrow, N. R. (1990). Wettability and its effect on oil recovery. *Journal of petroleum technology*, 42(12), 1,476-471,484.
- Muggeridge, A., Cockin, A., Webb, K., Frampton, H., Collins, I., Moulds, T., & Salino, P. (2014). Recovery rates, enhanced oil recovery and technological limits. *Phil. Trans. R. Soc. A*, 372(2006), 20120320.
- Muthusamy, K., Gopalakrishnan, S., Ravi, T., & Sivachidambaram. (2008). Biosurfactants Properties commercial production and application.pdf. *Current Science*, 94(6), 736.
- Myers, D. (1999). *Surfaces, interfaces, and colloids*: Wiley-Vch New York etc.
- Nakamura, L., Roberts, M. S., & Cohan, F. M. (1999). Relationship between the *Bacillus subtilis* clades associated with strains 168 and W23: a proposal for *B. subtilis* subsp. *subtilis* and *B. subtilis* subsp. *spizizenii*. *International journal of systematic bacteriology*, 49, 1211-1215.
- Nakano, M. M., Corbell, N., Besson, J., & Zuber, P. (1992). Isolation and characterization of *sfp*: a gene that functions in the production of the lipopeptide biosurfactant, surfactin, in *Bacillus subtilis*. *Molecular and General Genetics MGG*, 232(2), 313-321.
- Nasu, Y., Nosaka, Y., Otsuka, Y., Tsuruga, T., Nakajima, M., Watanabe, Y., & Jin, M. (2003). A case of *Paenibacillus polymyxa* bacteremia in a patient with cerebral infarction. *Kansenshogaku zasshi. The Journal of the Japanese Association for Infectious Diseases*, 77(10), 844-848.

- NCBI. (2016). Primer-Blast. *National Centre for Biotechnology Information*, <https://blast.ncbi.nlm.nih.gov/Blast.cgi>(25th May 2016).
- Nicholson, W. L., Munakata, N., Horneck, G., Melosh, H. J., & Setlow, P. (2000). Resistance of *Bacillus* endospores to extreme terrestrial and extraterrestrial environments. *Microbiology and Molecular Biology Reviews*, 64(3), 548-572.
- Nitschke, M., & Pastore, G. M. (2006). Production and properties of a surfactant obtained from *Bacillus subtilis* grown on cassava wastewater. *Bioresource Technology*, 97(2), 336-341. doi:<http://dx.doi.org/10.1016/j.biortech.2005.02.044>
- Noah, K., Bruhn, D., & Bala, G. (2005). Surfactin Production from Potato Process Effluent by *Bacillus subtilis* in a Chemostat. In B. Davison, B. Evans, M. Finkelstein, & J. McMillan (Eds.), *Twenty-Sixth Symposium on Biotechnology for Fuels and Chemicals* (pp. 465-473): Humana Press.
- OECD/IEA. (2008). *World Energy Outlook*.
- Okasha, T. M., & Alshiwaish, A. (2009). *Effect of brine salinity on interfacial tension in Arab-D carbonate reservoir, Saudi Arabia*. Paper presented at the SPE Middle East Oil and Gas Show and Conference.
- Olive, D. M., & Bean, P. (1999). Principles and applications of methods for DNA-based typing of microbial organisms. *Journal of Clinical Microbiology*, 37(6), 1661-1669.
- Omoregie, E., Ufodike, E., & Onwuliri, C. (1997). Effects of water soluble fractions of crude oil on carbohydrate reserves of *Oreochromis niloticus*(L.). *Journal of Aquatic Sciences*, 12, 1-7.
- Ouyang, J., Pei, Z., Lutwick, L., Dalal, S., Yang, L., Cassai, N., . . . Bluth, M. (2008). *Paenibacillus thiaminolyticus*: a new cause of human infection, inducing bacteremia in a patient on hemodialysis. *Annals of Clinical & Laboratory Science*, 38(4), 393-400.
- Pacwa-Płociniczak, M., Płaza, G. A., Piotrowska-Seget, Z., & Cameotra, S. S. (2011). Environmental applications of biosurfactants: recent advances. *International Journal of Molecular Sciences*, 12(1), 633-654.
- Pathak, K. V., Keharia, H., Gupta, K., Thakur, S. S., & Balaram, P. (2012). Lipopeptides from the banyan endophyte, *Bacillus subtilis* K1: mass spectrometric characterization of a library of fengycins. *Journal of the American Society for Mass Spectrometry*, 23(10), 1716-1728.
- Pekin, G., Vardar-Sukan, F., & Kosaric, N. (2005). Production of Sophorolipids from *Candida bombicola* ATCC 22214 Using Turkish Corn Oil and Honey. *Engineering in Life Sciences*, 5(4), 357-362. doi:10.1002/elsc.200520086
- Perez, A. R., Abanes-De Mello, A., & Pogliano, K. (2000). SpoIIB Localizes to Active Sites of Septal Biogenesis and Spatially Regulates Septal Thinning during Engulfment in *Bacillus subtilis*. *Journal of Bacteriology*, 182(4), 1096-1108.

- Perfumo, A., Rancich, I., & Banat, I. M. (2010). Possibilities and challenges for biosurfactants use in petroleum industry *Biosurfactants* (pp. 135-145): Springer.
- Perry, R. H., & Green, D. W. (1999). *Perry's chemical engineers' handbook*: McGraw-Hill Professional.
- Pichtel, J. (2016). Oil and Gas Production Wastewater: Soil Contamination and Pollution Prevention. *Applied and Environmental Soil Science*, 2016.
- Polson, E. J., Buckman, J. O., Bowen, D. G., Todd, A. C., Gow, M. M., & Cuthbert, S. J. (2010). An Environmental-Scanning-Electron-Microscope Investigation Into the Effect of Biofilm on the Wettability of Quartz. *15*(01), 223-227. doi:10.2118/114421-PA
- Priest, F. G. (2015). *Paenibacillus*. *Bergey's Manual of Systematics of Archaea and Bacteria*.
- Providenti, M. A., Begin, M., Hynes, S., Lamarche, C., Chitty, D., Hahn, J., . . . Smith, M. L. (2009). Identification and application of AFLP-derived genetic markers for quantitative PCR-based tracking of *Bacillus* and *Paenibacillus* spp. released in soil. *Canadian Journal of Microbiology*, 55(10), 1166-1175.
- Purwasena, I., Sugai, Y., & Sasaki, K. (2014). Estimation of the potential of an anaerobic thermophilic oil-degrading bacterium as a candidate for MEOR. *Journal of Petroleum Exploration and Production Technology*, 4(2), 189-200. doi:10.1007/s13202-013-0095-5
- Radke, C., Kavscek, A., & Wong, H. (1992). *A pore-level scenario for the development of mixed wettability in oil reservoirs*. Paper presented at the SPE Annual Technical Conference and Exhibition.
- Rahman, K. S. M., Rahman, T. J., McClean, S., Marchant, R., & Banat, I. M. (2002). Rhamnolipid Biosurfactant Production by Strains of *Pseudomonas aeruginosa* Using Low-Cost Raw Materials. *Biotechnology Progress*, 18(6), 1277-1281. doi:10.1021/bp020071x
- Rahman, P. K., & Gakpe, E. (2008). Production, characterisation and applications of biosurfactants-Review. *Biotechnology*.
- Raz, T., & Hillson, D. (2005). A comparative review of risk management standards. *Risk Management*, 7(4), 53-66.
- Raza, W., Yang, W., & Shen, Q. (2008). *Paenibacillus polymyxa*: antibiotics, hydrolytic enzymes and hazard assessment. *Journal of Plant Pathology*, 419-430.
- Rosenberg, E., & Ron, E. (1999). High-and low-molecular-mass microbial surfactants. *Applied Microbiology and Biotechnology*, 52(2), 154-162.
- Saharan, B., Sahu, R., & Sharma, D. (2012). A Review on Biosurfactants Fermentation Current Developments and Perspectives.pdf. *Genetic Engineering and Biotechnology*, 2011, 1-14.

- Salathiel, R. (1973). Oil recovery by surface film drainage in mixed-wettability rocks. *Journal of petroleum technology*, 25(10), 1,216-211,224.
- Salehi, M. (2009). Enhancing the Spontaneous Imbibition Process in Naturally Fractured Reservoirs through Wettability Alteration Using Surfactant: Mechanistic Study and Feasibility of Using Biosurfactants Produced from Agriculture Waste Streams.pdf. *PhD Dissertation, University of Kansas*, 22-100.
- Sandrea, I., & Sandrea, R. (2007). Recovery factors leave vast target for EOR technologies. *Oil & gas journal*, 105(41), 44-48.
- Santos, D. K. F., Rufino, R. D., Luna, J. M., Santos, V. A., & Sarubbo, L. A. (2016). Biosurfactants: multifunctional biomolecules of the 21st century. *International Journal of Molecular Sciences*, 17(3), 401.
- Santos, R., Loh, W., Bannwart, A., & Trevisan, O. (2014). An overview of heavy oil properties and its recovery and transportation methods. *Brazilian Journal of Chemical Engineering*, 31(3), 571-590.
- Sarafzadeh, P., Niazi, A., Oboodi, V., Ravanbakhsh, M., Hezave, A. Z., Ayatollahi, S. S., & Raeissi, S. (2014). Investigating the efficiency of MEOR processes using *Enterobacter cloacae* and *Bacillus stearothermophilus* SUCPM# 14 (biosurfactant-producing strains) in carbonated reservoirs. *Journal of Petroleum Science and Engineering*, 113, 46-53.
- Sarubbo, L., Marçal, M., Neves, M., Silva, M., Porto, L., & Campos-Takaki, G. (2001). Bioemulsifier production in batch culture using glucose as carbon source by *Candida lipolytica*. *Applied Biochemistry and Biotechnology*, 95(1), 59-67. doi:10.1385/ABAB:95:1:59
- Sen, R. (2008). Biotechnology in petroleum recovery: the microbial EOR. *Progress in Energy and Combustion Science*, 34(6), 714-724.
- Shabani Afrapoli, M., Nikooee, E., Alipour, S., & Torsater, O. (2011). *Experimental and Analytical Study of Microscopic Displacement Mechanisms of MIOR in Porous Media*. Paper presented at the SPE AMERICS E & P Health, Safety, Security and Environmental Conference, Houston, Texas, USA.
- Shepherd, R., Rockey, J., Sutherland, I. W., & Roller, S. (1995). Novel bioemulsifiers from microorganisms for use in foods. *Journal of Biotechnology*, 40(3), 207-217.
- Shibulal, B., Al-Bahry, S. N., Al-Wahaibi, Y. M., Elshafie, A. E., Al-Bemani, A. S., & Joshi, S. J. (2014). Microbial Enhanced Heavy Oil Recovery by the Aid of Inhabitant Spore-Forming Bacteria: An Insight Review. *The Scientific World Journal*, 2014.
- Silva, R. d. C. F., Almeida, D. G., Rufino, R. D., Luna, J. M., Santos, V. A., & Sarubbo, L. A. (2014). Applications of biosurfactants in the petroleum industry and the remediation of oil spills. *International Journal of Molecular Sciences*, 15(7), 12523-12542.

- Solaiman, D. Y., Ashby, R., Nuñez, A., & Foglia, T. (2004). Production of sophorolipids by *Candida bombicola* grown on soy molasses as substrate*,**. *Biotechnology Letters*, 26(15), 1241-1245. doi:10.1023/B:BILE.0000036605.80577.30
- Somasundaran, P., & Zhang, L. (2006). Adsorption of surfactants on minerals for wettability control in improved oil recovery processes. *Journal of Petroleum Science and Engineering*, 52(1-4), 198-212. doi:<http://dx.doi.org/10.1016/j.petrol.2006.03.022>
- Springham, D. G. (1984). Microbiological methods for the enhancement of oil recovery. *Biotechnology and genetic engineering reviews*, 1(1), 187-222.
- Strassner, J. (1968). Effect of pH on interfacial films and stability of crude oil-water emulsions. *Journal of petroleum technology*, 20(03), 303-312.
- Sun, X., Zhang, Y., Chen, G., & Gai, Z. (2017). Application of Nanoparticles in Enhanced Oil Recovery: A Critical Review of Recent Progress. *Energies*, 10(3), 345.
- Taylor, S. E. (2001). Surfactants. Fundamentals and Applications in the Petroleum Industry: Cambridge University Press; ISBN No.: 0 521 64067 9; Edited by L.L. Schramm, 2000, 621 pp. *Journal of Petroleum Science and Engineering*, 30(3-4), 258-259. doi:[http://dx.doi.org/10.1016/S0920-4105\(01\)00115-2](http://dx.doi.org/10.1016/S0920-4105(01)00115-2)
- Thanomsub, B., Watcharachaipong, T., Chotelersak, K., Arunrattiyakorn, P., Nitoda, T., & Kanzaki, H. (2004). Monoacylglycerols: glycolipid biosurfactants produced by a thermotolerant yeast, *Candida ishiwadae*. *Journal of Applied Microbiology*, 96(3), 588-592. doi:10.1111/j.1365-2672.2004.02202.x
- Timmusk, S. (2003). *Mechanism of action of the plant growth promoting bacterium Paenibacillus polymyxa*. Acta Universitatis Upsaliensis.
- Timmusk, S., Grantcharova, N., & Wagner, E. G. H. (2005). *Paenibacillus polymyxa* invades plant roots and forms biofilms. *Applied and environmental microbiology*, 71(11), 7292-7300.
- Timmusk, S., & Wagner, E. G. H. (1999). The plant-growth-promoting rhizobacterium *Paenibacillus polymyxa* induces changes in *Arabidopsis thaliana* gene expression: a possible connection between biotic and abiotic stress responses. *Molecular Plant-Microbe Interactions*, 12(11), 951-959.
- Trummler, K., Effenberger, F., & Syltatk, C. (2003). An integrated microbial/enzymatic process for production of rhamnolipids and L-(+)-rhamnose from rapeseed oil with *Pseudomonas* sp. DSM 2874. *European Journal of Lipid Science and Technology*, 105(10), 563-571. doi:10.1002/ejlt.200300816
- Updegraff, D., & Wren, G. B. (1954). The release of oil from petroleum-bearing materials by sulfate-reducing bacteria. *Applied microbiology*, 2(6), 309.
- USHHS. (1986). *Bacillus subtilis* U.S. Department of Health and Human Services, 1986, <https://www.usa.gov/federal-agencies/u-s-department-of-health-and-human-services>.

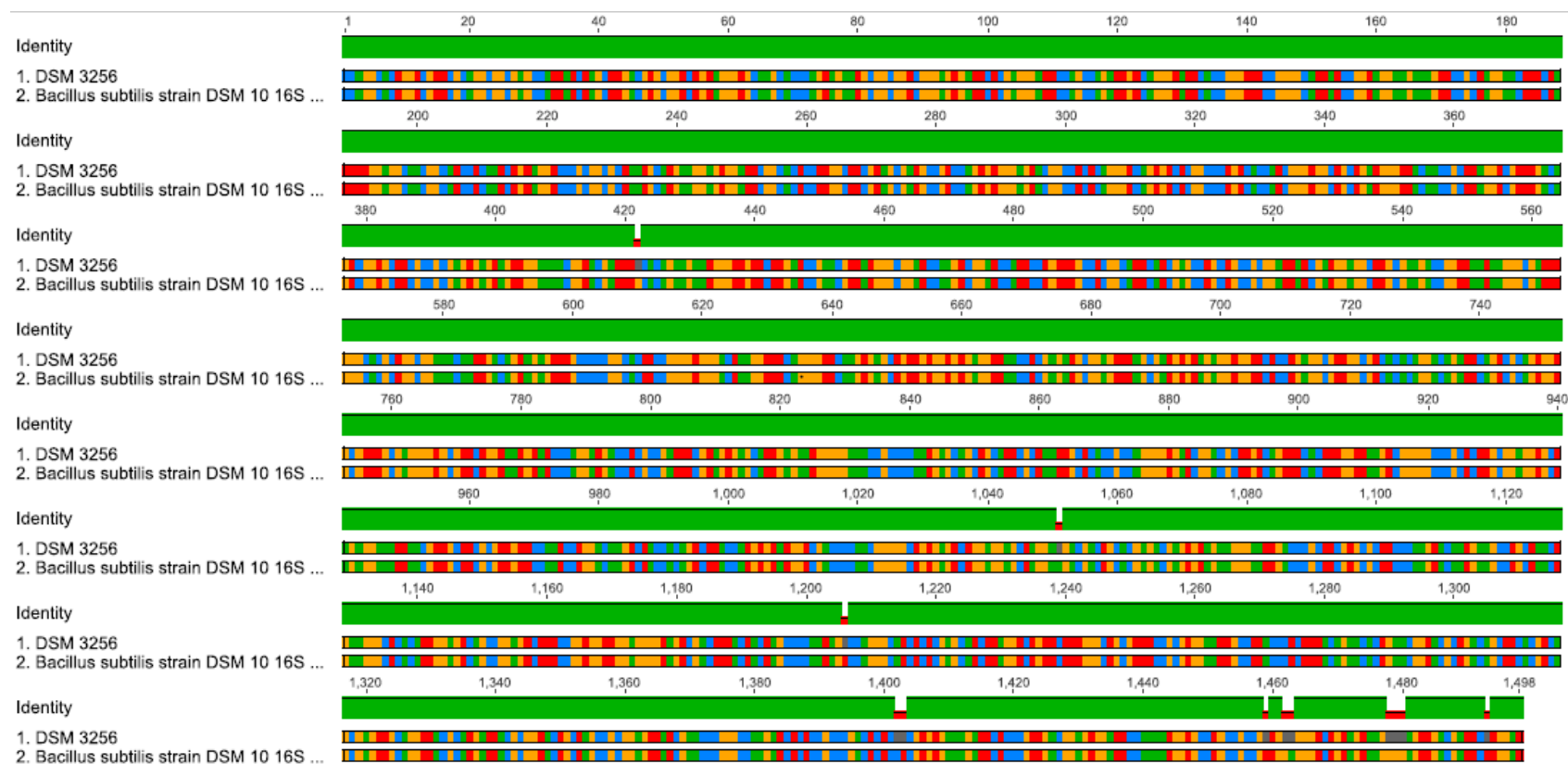
- Vance-Harrop, M. H., Gusmão, N. B. d., & Campos-Takaki, G. M. d. (2003). New bioemulsifiers produced by *Candida lipolytica* using D-glucose and babassu oil as carbon sources. *Brazilian Journal of Microbiology*, 34, 120-123.
- Vazquez-Duhalt, R., & Quintero-Ramirez, R. (2004). Biotechnological approach for development of microbial enhanced oil recovery technique. *Petroleum Biotechnology: Developments and Perspectives*, 151, 405 -445.
- Venhuis, S. H., & Mehrvar, M. (2004). Health effects, environmental impacts, and photochemical degradation of selected surfactants in water. *International Journal of photoenergy*, 6(3), 115-125.
- Wang, W., & Gupta, A. (1995). *Investigation of the effect of temperature and pressure on wettability using modified pendant drop method*. Paper presented at the SPE Annual Technical Conference and Exhibition.
- Willey, J. (2008). *Prescott, Harley, and Klein's Microbiology-7th international ed./Joanne M. Willey, Linda M. Sherwood, Christopher J. Woolverton*: New York [etc.]: McGraw-Hill Higher Education.
- Wills, M. (2000). *Ekologicheskaya Vahkta Sakhalina (Sakhalin Environment Watch Ph. D. Thesis M. Inst. Petroleum*.
- Wilson, K., & Walker, J. (2010). *Principles and techniques of biochemistry and molecular biology*: Cambridge university press.
- Woodward, R. P. (2013). Surface tension measurements using the drop shape method. *First Ten Angstroms*, <http://www.firsttenangstroms.com/pdfdocs/STPaper.pdf>. Accessed, 28.
- Wu, Y., Shuler, P. J., Blanco, M., Tang, Y., & Goddard, W. A. (2006). *A study of wetting behavior and surfactant EOR in carbonates with model compounds*. Paper presented at the SPE/DOE Symposium on Improved Oil Recovery.
- Yang, M.-W., Wei, H.-H., & Lin, S.-Y. (2007). A theoretical study on surfactant adsorption kinetics: Effect of bubble shape on dynamic surface tension. *Langmuir*, 23(25), 12606-12616.
- Yarbrough, H., & Coty, V. (1983). *Microbial enhanced oil recovery from the upper crustaceous nactoch formation*. Paper presented at the Proceedings of the International Conference on Microbial Enhancement of Oil Recovery.
- Ying, G.-G. (2006). Fate, behavior and effects of surfactants and their degradation products in the environment. *Environment international*, 32(3), 417-431.
- Zinjarde, S. S., & Pant, A. (2002). Emulsifier from a tropical marine yeast *Yarrowia lipolytica* NCIM 3589.pdf. *Journal of Basic Microbiology*, 42, 67-73.
- Zobell, C. E. (1946). Bacteriological process for treatment of fluid-bearing earth formations: Google Patents.
- ZoBell, C. E. (1947). Bacterial release of oil, from oil-bearing materials. *World oil*, 1, 35-41.

APPENDICES

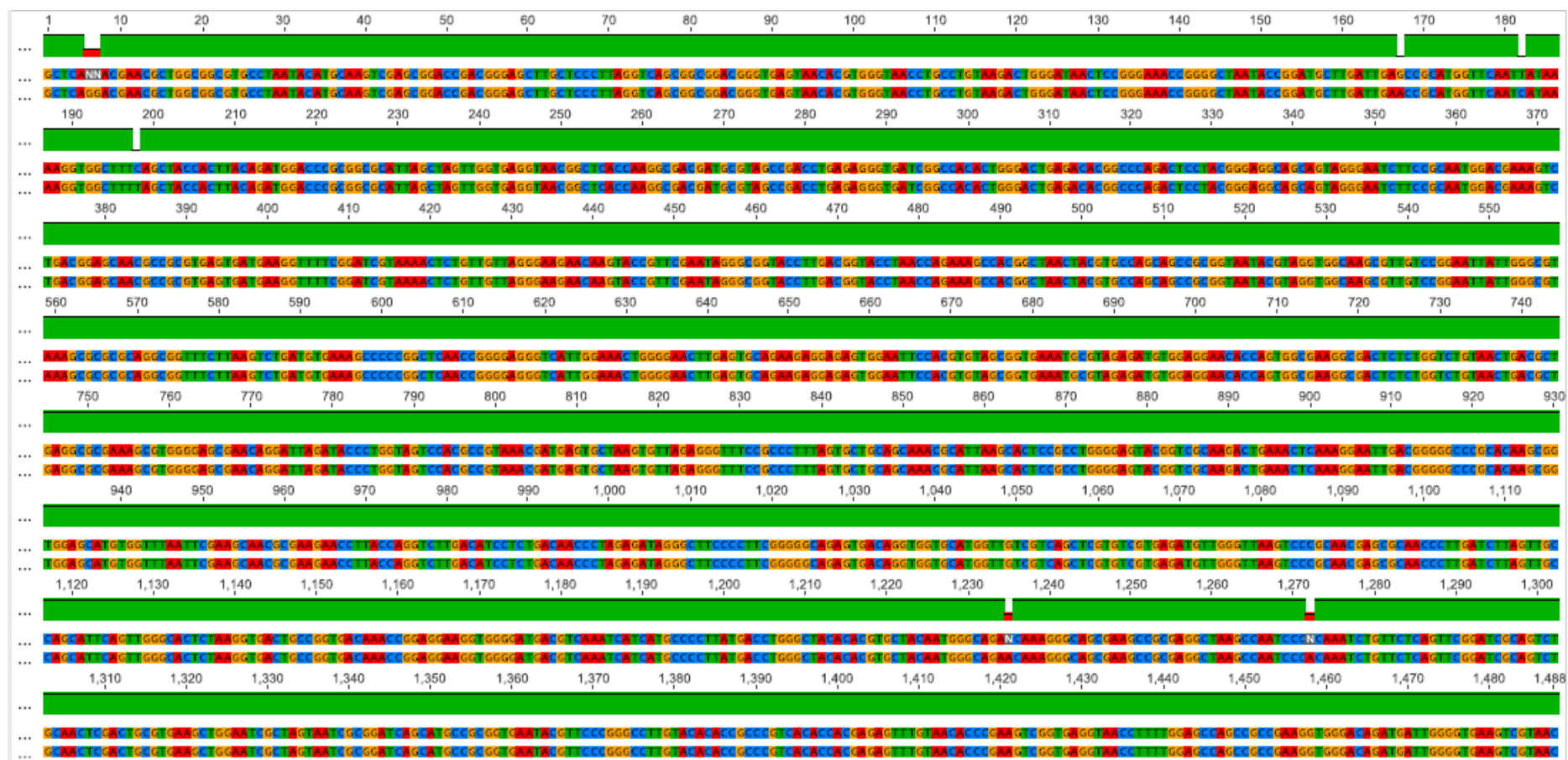
Appendix A Journal Publications and Conferences

1. **Ukwungwu, S.V.**, Abbas, A.J. and Nasr, G.G., 2016. Experimental investigation of the impact of biosurfactants on residual-oil recovery. 18th International Conference on Biological Ecosystems and Ecological Networks, Madrid, Spain, 24 - 25 March 2016.
2. **Ukwungwu, S.V.**, Abbas, A.J. and Nasr, G.G., 2016. Experimental investigation of the impact of biosurfactants on residual-oil recovery. *International Journal of Biological, Biomolecular, Agricultural, Food and Biotechnological Engineering*, 10(3), pp.130-133.
3. **Ukwungwu, S.V.**, Abbas, A.J. and Nasr, G.G., Allison, H., Goodman, S., 2017. Wettability Effects on Bandera Gray Sandstone using Biosurfactants. *Journal of Engineering Technology*. Volume 6, Issue 2, July, 2017, PP.605-617.

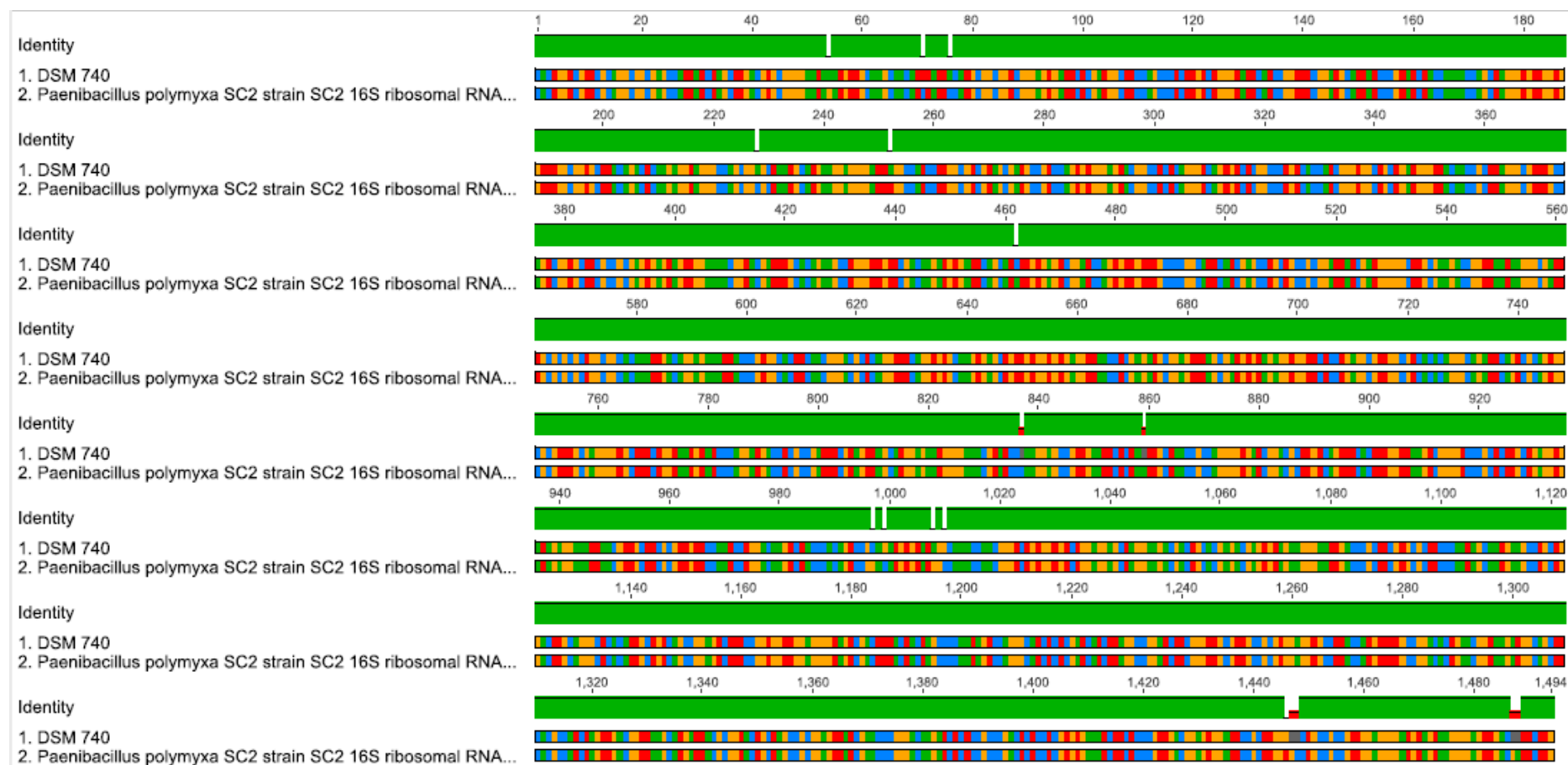
Appendix B 16S ribosomal RNA gene



B1: *Bacillus subtilis* (DSM 3256), complete sequence



B2: *Bacillus licheniformis* (DSM 1913), complete sequence



B3: *Paenibacillus polymyxa* (DSM 740), complete sequence

Appendix C: The DROPimage program

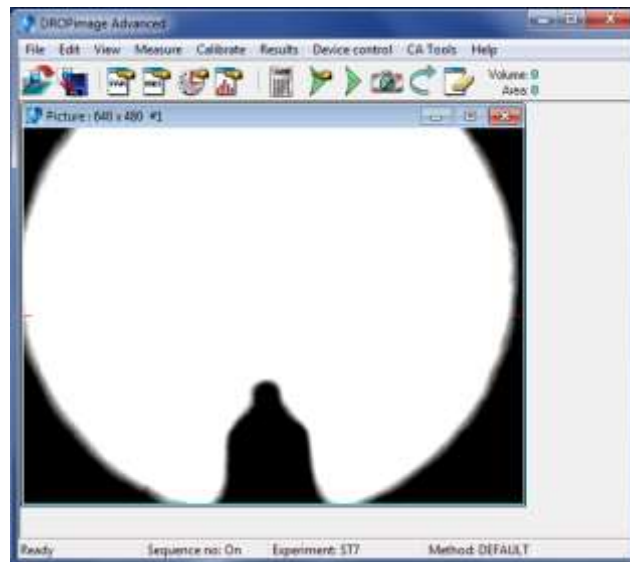
Using a pendant drop system, it is possible to register the evolution of a drop of oil into another as a function of time. Images of the drop are taken automatically at a certain frequency which depends on the time duration of the test. The images are digitized by a frame grabber resident in the computer and are analysed on line measuring, therefore, the interfacial tension “on line” during the experiment. The contours of the drops are analysed to infer interfacial tension from the profile of the drop using different programs. The whole process of digitization and analysis of the drop lasts less than 40 seconds. It consists of four steps:

- i. capture and digitization of the image of the pendant drop
- ii. extraction of the drop contour, determination of the radius of curvature at the apex necessary for the calculation of interfacial tension
- iii. smoothing of the extracted contour of the drop using polynomial regression
- iv. shape comparison between the theoretical and experimental drop, inferring the interfacial tension value.

1. Image display on-screen and real-time

The primary window contains the captured picture. This image is scalable and is utilised to set the limits and begin position for the edge detection algorithm. The detected edge is also plotted in this image as a visual sign for the right operation of the edge detection. A real-time (live) display can be overlaid the primary window, or be shown in a separate window.

After calibrating and setting up the instrument according to the instruction provided, the micro-syringe assembly is then filled with the test liquid, while the straight needle to the syringe is attached firmly. The dispensing valve on the micro-syringe is then turned on to remove air from the needle. The DROPimage Advanced software is then started. The micro-syringe is adjusted into the fixture so that the tip of the needle is visible in the centre top of the DROPimage live image as seen as shown below.



Visible tip of needle

Source: (Hansen, 1990)

A new experiment is begun using the experiment Wizard, by clicking on File > New Experiment Wizard or using the shortcut on the keyboard by hitting Ctrl-T. The dialog box will appear as shown below.



Setting up a new experiment

Source: (Hansen, 1990)

The first choice “Surface Tension – Pendant” or third choice “Contact Angle” is selected one at a time only when the individual experiment is to be conducted. In this case for example we

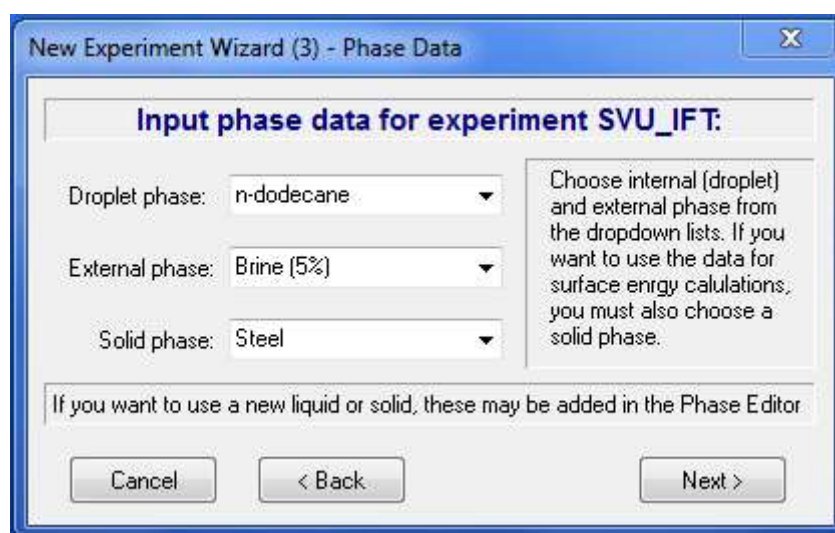
select the first choice “Surface Tension – Pendant. By clicking next, the following screen will appear where the experiment name is entered “SVU_IFT”, as seen in the figure below.



Naming the new experiment

Source: (Hansen, 1990)

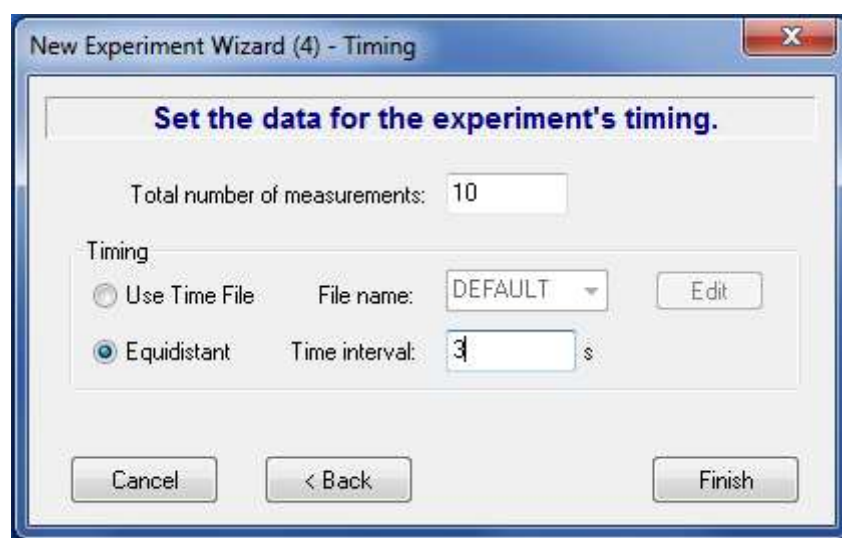
On the next screen the phase data is inputted shown below. For the droplet phase, ‘heavy oil’ was selected from the list. For the External phase, in this case formation water, Brine (5%) was selected. And then the solid phase is steel (the needle). Note here that the droplet phase used in this study was added using the Phase editor since it was not in the drop down list.



Inputting phase data for experiment “surface tension”

Source: (Hansen, 1990)

Now the goal of this experiment was to take the average of ten surface tension measurements over 30 seconds while the drop is at ambient and elevated temperature, humidity and pressure. After inputting the phase data, on the next screen “10” was entered for the number of measurements. For the timing, the equidistant option was selected to create a new time file and the “Time Interval was set to “3” which means that the measurements were taken three seconds apart, as show below.

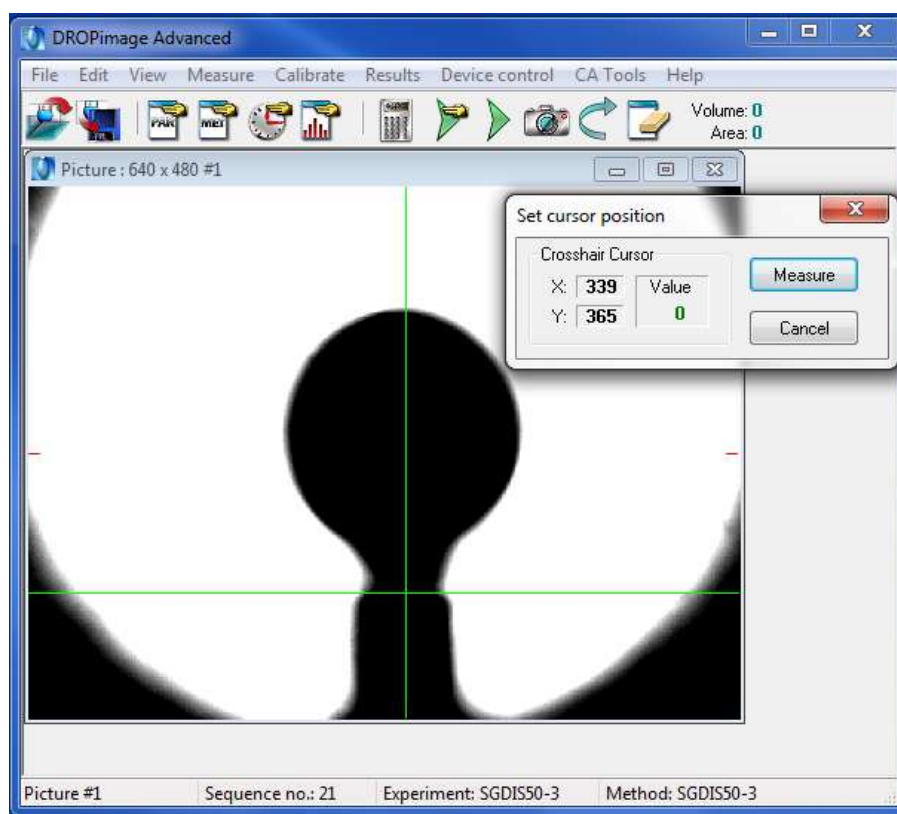


Setting data for the experiment’s timing

Source: (Hansen, 1990)

At this point, on clicking the finish button, the DROPimage will create a Parameter and Method file for the experiment. And Yes was clicked to run the experiment.

The valve below the cell is then opened to dispense the test liquid in order to produce a pendant drop (an oil film) as shown below. And as a rule of thumb, you want to use enough volume to produce a drop that is stable and not so large that it releases itself from the needle, as can be seen below.



Drop film showing the crosshair lines

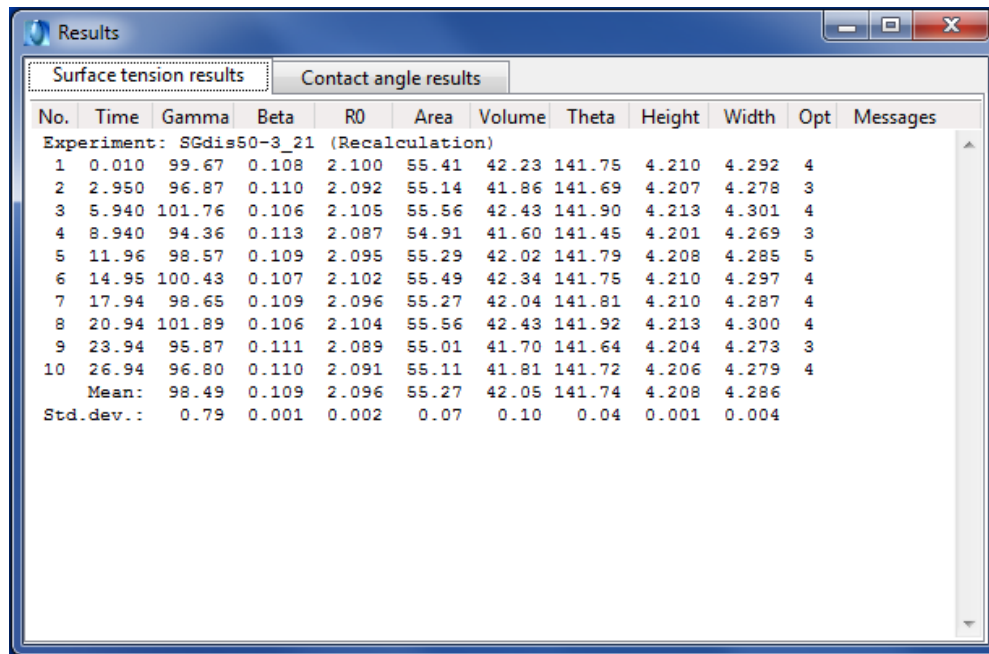
Source: (Hansen, 1990)

After creating the drop, it was important to make sure that the lighting is set properly. The background was set to be white while the needle and perimeter of the drop set to be black. The interface between the drop phase and external phase should be crisp. Otherwise the lens was refocused and a new picture taken. The crosshair lines were placed so that the horizontal line passes through the interface between the needle and the oil drop and the vertical line passes through the centre of the drop and needle as shown above. By clicking Measure, on the “Set cursor position” dialog box, the experiment began.

2. Results tabulation display

All experimental results were displayed in a tabular form in the program’s results shown below. This window contains two tabbed notebooks, one for surface tension measurements and one for separate (contrary to those included with surface tension results) contact angles measurements. These results might likewise be shown in a different report window that is specially designed for printing. The program contains a plotting function for visual display

similar to the table below. The drop image for each experiment also appears in the desktop after taking the IFT measurement but without the crosshair lines.



Results											
Surface tension results											
No.	Time	Gamma	Beta	RO	Area	Volume	Theta	Height	Width	Opt	Messages
Experiment: SGdis50-3_21 (Recalculation)											
1	0.010	99.67	0.108	2.100	55.41	42.23	141.75	4.210	4.292	4	
2	2.950	96.87	0.110	2.092	55.14	41.86	141.69	4.207	4.278	3	
3	5.940	101.76	0.106	2.105	55.56	42.43	141.90	4.213	4.301	4	
4	8.940	94.36	0.113	2.087	54.91	41.60	141.45	4.201	4.269	3	
5	11.96	98.57	0.109	2.095	55.29	42.02	141.79	4.208	4.285	5	
6	14.95	100.43	0.107	2.102	55.49	42.34	141.75	4.210	4.297	4	
7	17.94	98.65	0.109	2.096	55.27	42.04	141.81	4.210	4.287	4	
8	20.94	101.89	0.106	2.104	55.56	42.43	141.92	4.213	4.300	4	
9	23.94	95.87	0.111	2.089	55.01	41.70	141.64	4.204	4.273	3	
10	26.94	96.80	0.110	2.091	55.11	41.81	141.72	4.206	4.279	4	
Mean:		98.49	0.109	2.096	55.27	42.05	141.74	4.208	4.286		
Std.dev.:		0.79	0.001	0.002	0.07	0.10	0.04	0.001	0.004		

Surface tension results window

Source: (Hansen, 1990)

1. The result window provided the following information:
2. No.: run number, e.g 1, 2, 3....
3. Time: precise time in seconds of measurement relative to the start of the current run.
4. Gamma: surface tension in mN/m.
5. Beta: shape factor; as a rule, a number between 0.2 and 0.4 is good.
6. RO: the radius of curvature at the drop's apex in nm.
7. Area: the drop surface area in mm².
8. Volume: the drop volume in mm³.
9. Theta: the contact angle at the drop limit (horizontal) baseline.
10. Height: the total measured distance from baseline to the drop apex in mm.
11. Width: the dimension in mm at the maximum width.
12. Opt: the number of optimizations performed.
13. Messages: errors or other messages.

3. Method Driven Measurement

A method comprises of a collection of parameters that portrays how and when measurements are made and how results are saved and presented. All measurements of surface tension and contact angle depend on measurement **Methods** (aside from single contact angle measurements). A method's parameters are saved in a text file. Methods are created and edited in the **Method Editor**. All measurement of interfacial tensions must refer to a method, and quite a lot of measurements can utilise the same method as shown below.

There are basically two sorts of methods, depending on the first field, *Data source*. In the event that this is set to *Video*, data are taken from the edge grabber board for further treatment as per alternate parameters. On the off chance that *Data source* is *Disk file* then this is a **Recalculation** method that tells the program to read data from a disk file, which must have been produced by a method where the data source is *Video*.

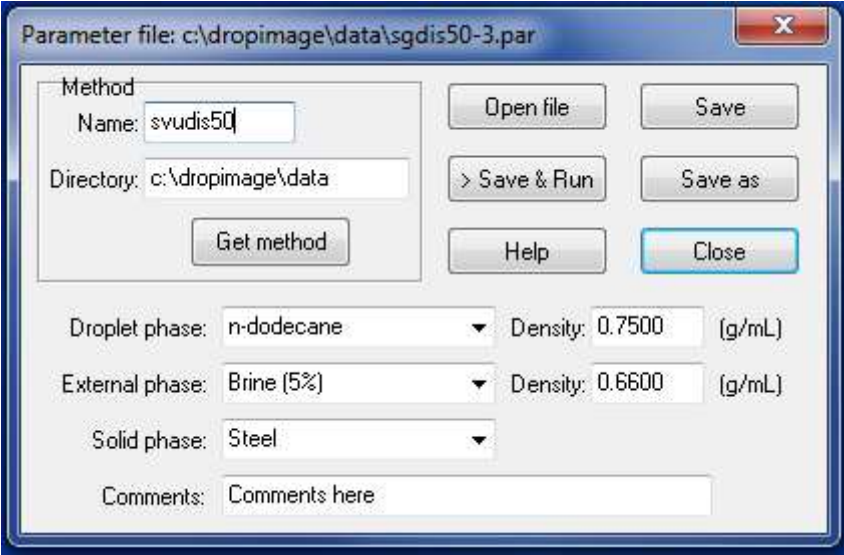


Method editor without the oscillation option.

Source: (Hansen, 1990)

4. Measurement Parameters

Keeping in mind, the end goal is to calculate surface tensions, the program must know the densities of the two phases (drop and continuous phase), and the image amplification. These data are saved in a **Parameter File** seen in the figure below. The parameters are created and edited in the **Parameter Editor**. This editor is connected to the **Phases data file** that contains the density data of numerous mainstream liquids and gases. This data file is retained in a different **Phase Editor**. Notwithstanding the input parameters in the Parameter editor, two parameters are consequently included from the calibration values. By means of the measurement parameters, surface tension can be measured by a simple basic methodology leading to single or multiple readings as indicated by the method in the parameter file.



The screenshot shows a 'Parameter Editor' window with the title bar 'Parameter file: c:\dropimage\data\sgdis50-3.par'. The window contains several input fields and buttons. The 'Method' section has a 'Name' field with 'svudis50' and a 'Directory' field with 'c:\dropimage\data'. There are buttons for 'Open file', 'Save', '> Save & Run', 'Save as', 'Get method', 'Help', and 'Close'. Below these, there are three dropdown menus for 'Droplet phase' (set to 'n-dodecane'), 'External phase' (set to 'Brine (5%)'), and 'Solid phase' (set to 'Steel'). Each dropdown menu has a corresponding 'Density' field with values '0.7500 (g/mL)', '0.6600 (g/mL)', and an empty field respectively. At the bottom, there is a 'Comments' field with the text 'Comments here'.

Parameter editor

Source: (Hansen, 1990)

Appendix D: Experimental IFT data for *BS-1* cells (*B. subtilis* cells)

T (°C)	Pressure (MPa)					
	0.15	3.10	5.10	10.44	12.51	13.89
26	36.25	39.85	38.78	38.01	37.75	36.80
32	29.45	24.46	24.94	23.95	23.86	23.55
42	18.23	17.77	17.83	18.16	18.11	17.52
60	15.87	15.72	15.44	15.42	15.22	15.18
75	15.34	14.51	14.47	14.41	14.21	13.29

Appendix E: IFT data with time and pressure for *BS-1* (*B. subtilis* cells)**E-1: At 32°C**

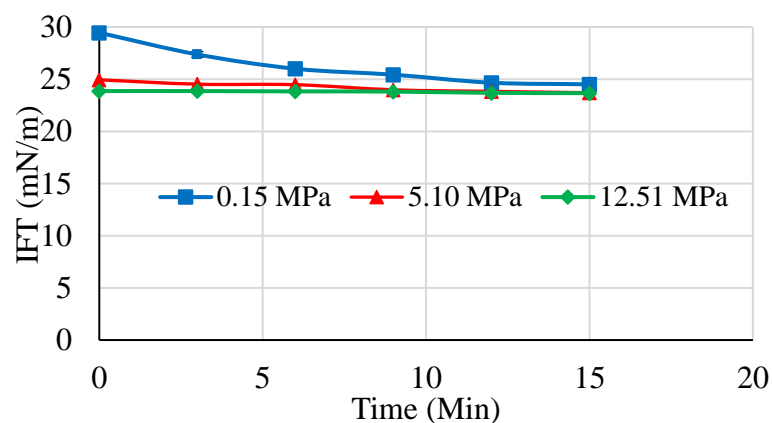
Time (Mins)	Pressure (MPa)		
	0.15	5.10	12.51
0	29.45	24.94	23.86
3	27.37	24.52	23.86
6	26.00	24.47	23.83
9	25.43	23.98	23.81
12	24.66	23.83	23.69
15	24.51	23.70	23.66

E-2: At 42°C

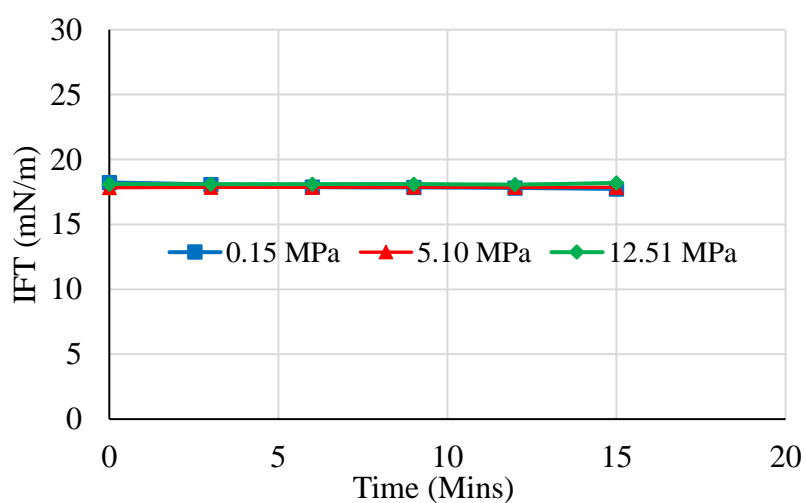
Time (Mins)	Pressure (MPa)		
	0.15	5.10	12.51
0	18.23	17.83	18.11
3	18.08	17.85	18.10
6	17.87	17.86	18.10
9	17.85	17.87	18.11
12	17.81	17.85	18.07
15	17.73	17.86	18.20

E-3: At 75°C

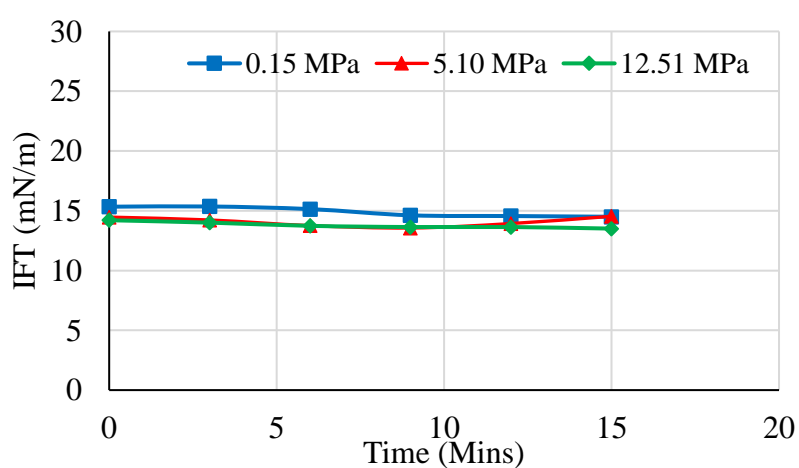
Time (Mins)	Pressure (MPa)		
	0.15	5.10	12.51
0	15.34	14.47	14.21
3	15.36	14.23	14.01
6	15.14	13.76	13.74
9	14.62	13.56	13.64
12	14.56	13.93	13.64
15	14.50	14.54	13.51



Appendix E-1: Effect of time on IFT for *BS-I* cells at 32°C



Appendix E-2: Effect of time on IFT for *BS-I* cells at 42°C



Appendix E-3: Effect of time on IFT for *BS-I* cells at 75°C

Appendix F: Experimental IFT data for *BS-1* cell-free

T (°C)	Pressure (MPa)					
	0.15	3.10	5.10	10.44	12.51	13.89
26	31.95	40.08	43.02	43.70	47.06	40.49
32	31.66	28.73	29.45	26.18	27.19	24.57
42	17.99	16.42	16.39	16.21	16.18	15.74
60	14.09	13.70	13.36	13.30	13.25	12.90
75	12.63	11.47	11.42	11.06	10.95	10.94

Appendix G: Variation of IFT data with time and pressure for *BS-1* (*B. subtilis* cell-free) supernatant**G-1: At 32°C**

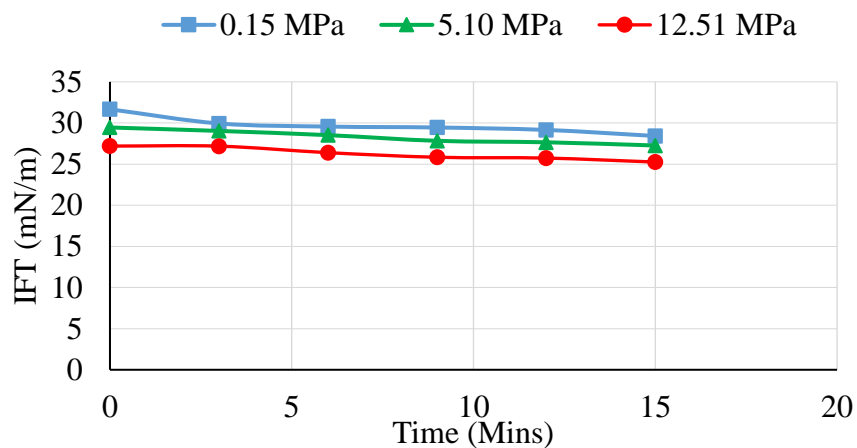
Time (Mins)	Pressure (MPa)		
	0.15	5.10	12.51
0	31.66	29.45	27.19
3	29.94	29.03	27.18
6	29.56	28.52	26.39
9	29.45	27.83	25.83
12	29.15	27.65	25.73
15	28.42	27.26	25.25

G-2: At 42°C

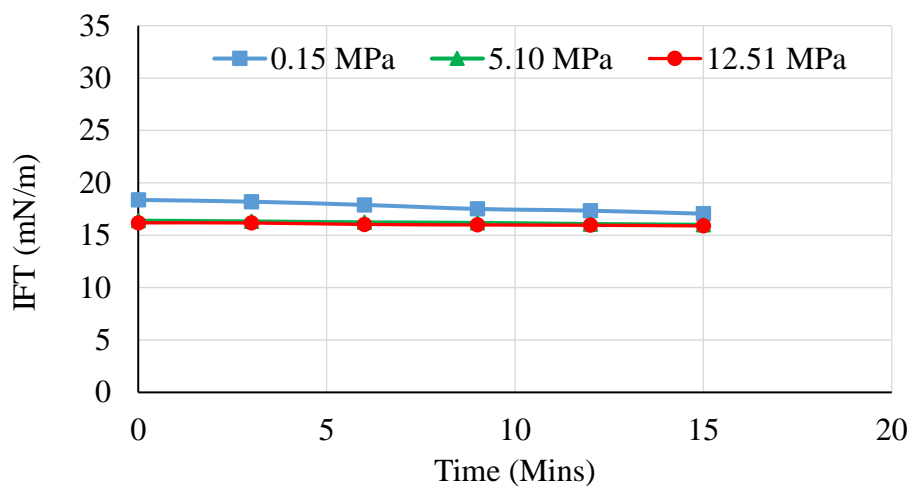
Time (Mins)	Pressure (MPa)		
	0.05	5.10	12.51
0	18.37	16.39	16.18
3	18.20	16.32	16.17
6	17.89	16.23	16.03
9	17.51	16.18	15.98
12	17.34	16.07	15.95
15	17.05	16.00	15.89

G-3: At 75°C

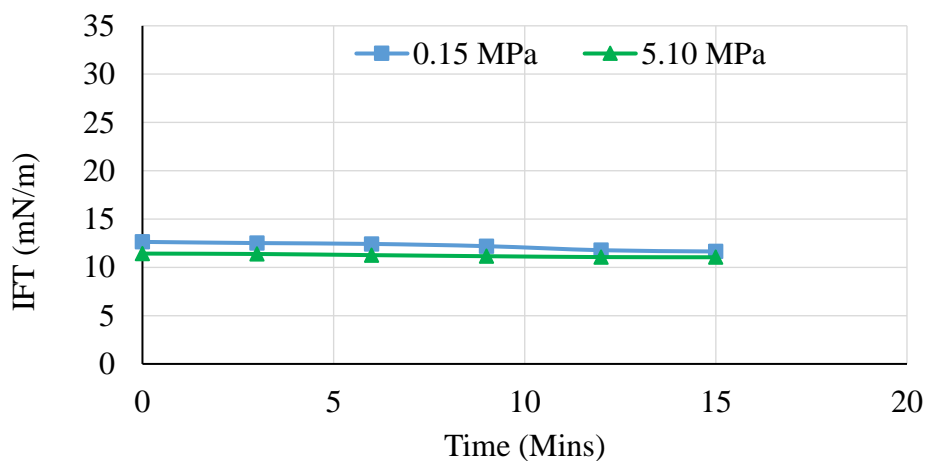
Time (Mins)	Pressure (MPa)		
	0.15	5.10	12.51
0	12.63	11.42	-
3	12.51	11.38	-
6	12.42	11.26	-
9	12.19	11.15	-
12	11.77	11.06	-
15	11.64	11.04	-



Appendix G-1: Effect of time on IFT for *BS-I* cell - free at 32°C



Appendix G-2: Effect of time on IFT for *BS-I* cell - free at 42°C



Appendix G-3: Effect of time on IFT for *BS-I* cell – free at 75°C

Appendix H: IFT with temperature at constant pressure for *BS-2* with cells

T (°C)	Pressure (MPa)					
	0.15	3.10	5.10	10.44	12.51	13.89
26	23.87	23.12	22.72	22.05	21.89	21.10
32	20.44	20.22	20.11	21.04	20.69	19.49
42	16.07	15.15	14.86	13.98	13.97	13.72
60	13.10	13.18	13.29	13.46	13.39	13.33
75	12.99	12.34	12.12	12.29	11.43	11.37

Appendix I: IFT with time for *BS-2* biosurfactant with cells**I-1: At 42°C**

Time (Mins)	Pressure (MPa)		
	0.15	5.10	12.51
0	16.07	14.86	13.97
3	15.26	14.86	13.98
6	15.25	14.8	13.95
9	15.19	14.68	13.9
12	15.18	14.63	13.83
15	15.11	14.55	13.79

I-2: At 75°C

Time (Mins)	Pressure (MPa)		
	0.15	5.10	12.51
0	12.99	12.12	11.43
3	12.99	11.89	11.53
6	12.96	11.53	11.5
9	12.97	11.32	11.69
12	12.44	11.05	11.62
15	12.25	10.84	11.52

Appendix J: IFT with pressure at constant temperatures for *BS-2* cell-free

T (°C)	Pressure (MPa)					
	0.15	3.10	5.10	10.44	12.51	13.89
26	21.14	19.81	19.06	18.36	16.96	14.97
32	17.99	15.44	14.80	14.19	13.43	12.72
42	13.76	10.65	10.60	9.52	9.21	9.16
60	8.30	7.91	7.10	6.81	6.35	5.80
75	6.69	6.41	6.24	5.17	4.75	4.49

Appendix K: IFT with time for *BS-2* cell-free supernatant

K-1: At 32°C

Time (Mins)	Pressure (MPa)		
	0.15	5.10	12.51
0	17.99	14.80	13.43
3	17.67	14.54	13.41
6	16.94	14.18	13.07
9	16.55	14.04	12.97
12	16.21	13.88	12.91
15	15.88	13.75	12.89

K-2: At 42°C

Time (Mins)	Pressure (MPa)		
	0.15	5.10	12.51
0	13.76	10.6	9.21
3	13.57	10.44	9.20
6	12.85	10.38	9.19
9	11.93	9.87	9.18
12	11.48	9.43	9.18
15	11.12	9.51	9.16

K-3: At 75°C

Time (Mins)	Pressure (MPa)		
	0.15	5.10	12.51
0	6.69	6.24	4.75
3	6.60	5.99	4.66
6	6.55	5.92	4.60
9	6.50	5.82	4.55
12	6.41	5.39	4.55
15	6.37	5.31	4.52

Appendix L: IFT with pressure at constant temperatures for *BS-3* cells

T (°C)	Pressure (MPa)					
	0.15	3.10	5.10	10.44	12.51	13.89
26	16.95	31.5	59.59	60.36	49.83	51.68
32	30.96	29.97	29.09	29.6	29.64	30.18
42	23.58	19.46	17.13	15.02	14.44	14.66
60	12.29	10.93	10.13	9.72	9.69	9.81
75	12.59	10.61	10.27	9.95	9.86	9.73

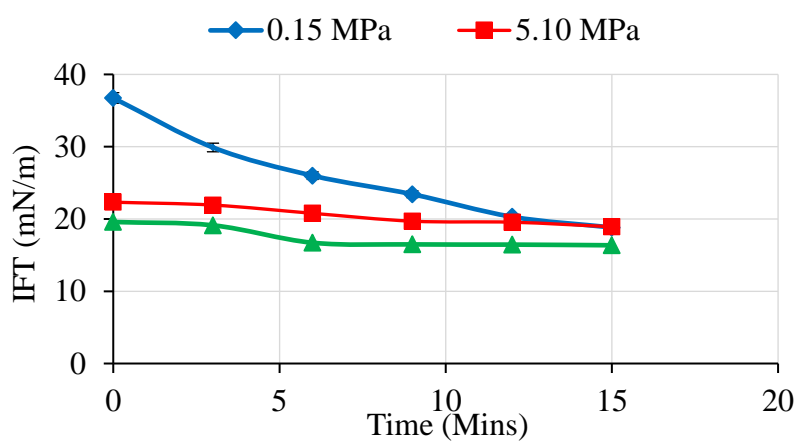
Appendix M: Experimental IFT data for *BS-3* cell-free

T (°C)	Pressure (MPa)					
	0.15	3.10	5.10	10.44	12.51	13.89
26	-	-	-	-	-	-
32	34.05	22.48	22.32	21.22	19.58	18.75
42	11.42	10.76	10.46	9.75	9.40	8.99
60	8.71	8.70	8.58	8.55	8.38	7.90
75	7.79	7.05	7.37	7.02	6.64	6.62

Appendix N: IFT data with time and pressure for *BS-3* cell-free supernatant

N-1: At 32°C

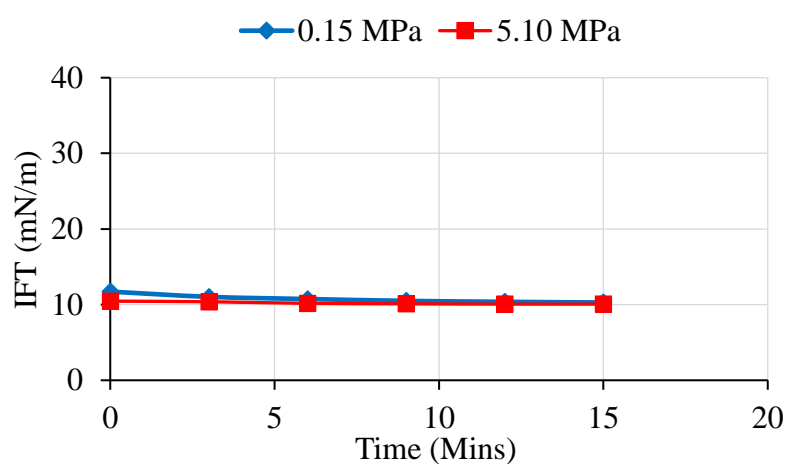
Time (Mins)	Pressure (MPa)		
	0.15	5.10	12.41
0	36.74	22.32	19.58
3	29.89	21.92	19.12
6	25.99	20.78	16.71
9	23.42	19.69	16.48
12	20.30	19.55	16.45
15	18.82	18.92	16.36



Appendix N-1: IFT data with time for *BS-3* cell-free at 32°C

N-2: At 42°C

Time (Mins)	Pressure (MPa)		
	0.15	5.10	12.51
0	11.72	10.46	-
3	11.03	10.38	-
6	10.74	10.17	-
9	10.50	10.11	-
12	10.37	10.07	-
15	10.28	10.07	-



Appendix N-2: IFT data with time for *BS-3* cell-free at 42°C

Appendix O: Comparison of IFT with temperature for BS1, *BS-2* & *BS-3* with cells

O-1: At 0.15 MPa

T (°C)	Biosurfactant		
	<i>BS-1</i>	<i>BS-2</i>	<i>BS-3</i>
26	36.25	23.87	16.95
32	29.45	20.44	30.96
42	18.23	16.07	23.58
60	15.87	13.10	12.29
75	15.34	12.99	12.59

O-2: At 3.10 MPa

T (°C)	Biosurfactant		
	<i>BS-1</i>	<i>BS-2</i>	<i>BS-3</i>
26	39.85	23.12	31.50
32	24.46	20.22	29.29
42	17.77	15.15	19.46
60	15.72	13.18	10.93
75	14.51	12.34	10.61

O-3: At 5.10 MPa

T(°C)	Biosurfactant		
	<i>BS-1</i>	<i>BS-2</i>	<i>BS-3</i>
26	38.78	22.72	59.69
32	24.94	20.11	29.09
42	17.83	14.86	17.13
60	15.44	13.29	10.13
75	14.47	12.12	10.27

O-4: At 10.44 MPa

T (°C)	Biosurfactant		
	<i>BS-1</i>	<i>BS-2</i>	<i>BS-3</i>
26	38.01	22.05	60.36
32	23.95	21.04	29.6
42	18.16	13.98	15.02
60	15.42	13.46	9.72
75	14.41	12.29	9.95

O-5: At 12.51 MPa

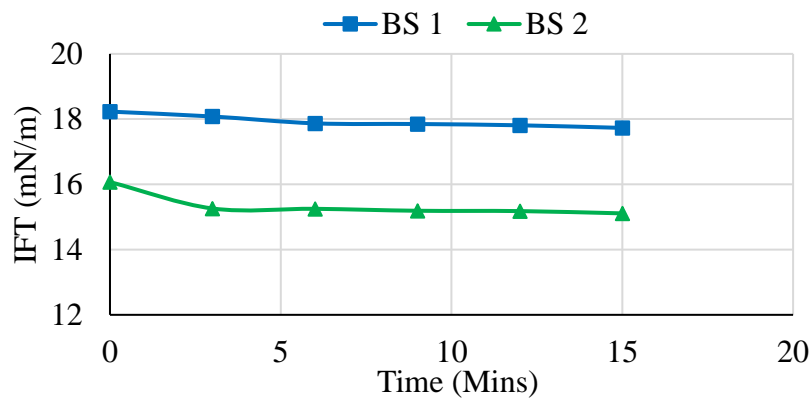
T (°C)	Biosurfactant		
	<i>BS-1</i>	<i>BS-2</i>	<i>BS-3</i>
26	37.75	21.89	49.83
32	23.86	20.69	29.64
42	18.11	13.97	14.44
60	15.22	13.39	9.69
75	14.21	11.43	9.86

O-6: At 13.89 MPa

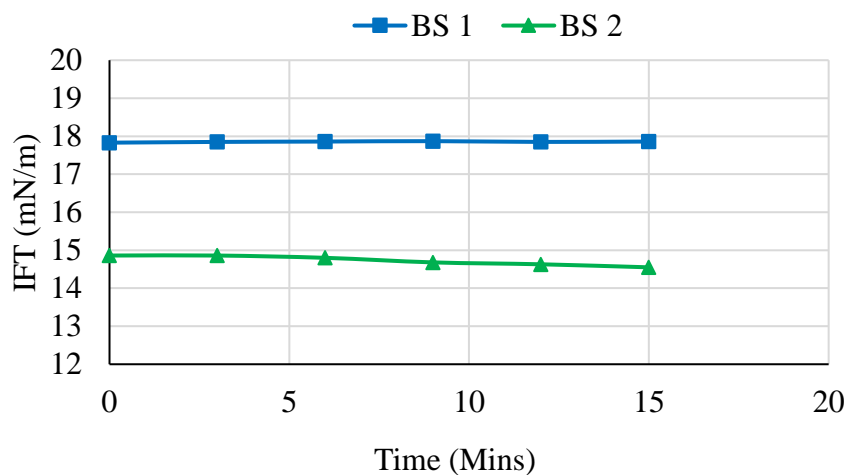
T (°C)	Biosurfactant		
	<i>BS-1</i>	<i>BS-2</i>	<i>BS-3</i>
26	36.8	21.1	51.68
32	23.55	19.49	30.18
42	17.52	13.72	14.66
60	15.18	13.33	9.81
75	13.29	11.37	9.73

Appendix P: Comparison of IFT with time for *BS-1* & *BS-2* biosurfactants with cells

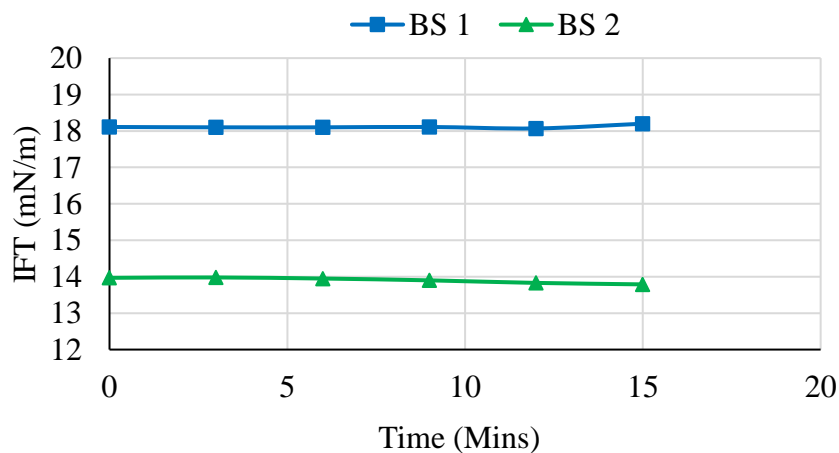
P-1: At constant temperature 42°C



(a) At constant pressure of 0.15 MPa

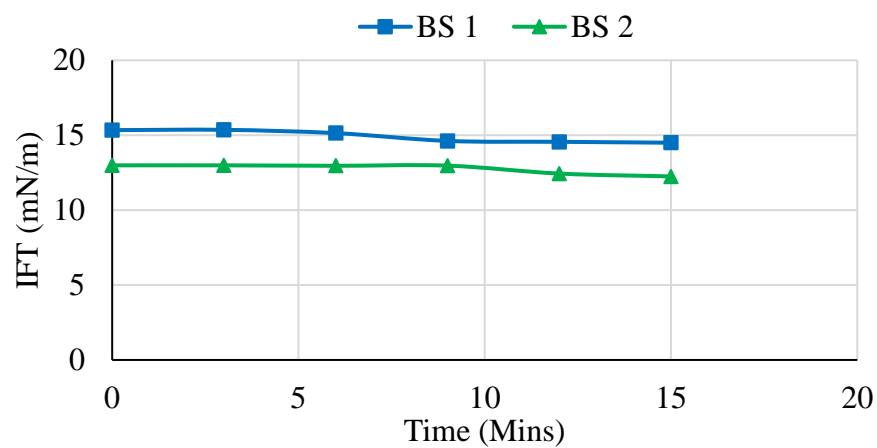


(b) At constant pressure of 5.10 MPa

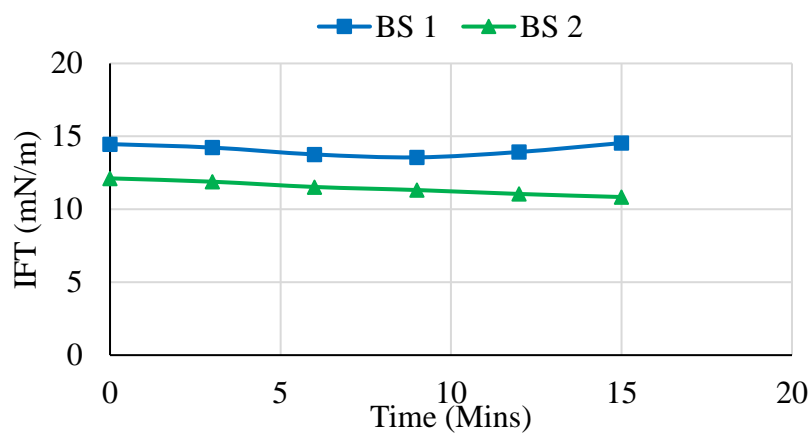


(c) At constant pressure of 12.15 MPa

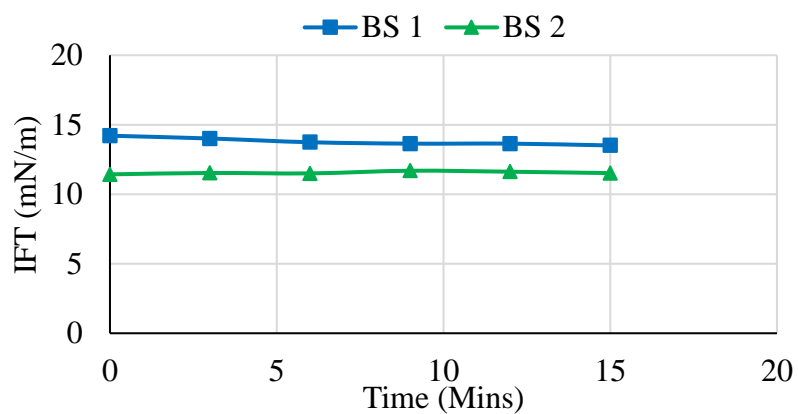
P-2: At constant temperature 75°C



(a) At constant pressure of 0.15 MPa



(b) At constant pressure of 5.10 MPa



(c) At constant pressure of 12.15 MPa

P-1A: Comparison of IFT with time for cell-free *BS-1* & *BS-2* biosurfactants at 42°C
At 0.15 MPa

Time (Mins)	Biosurfactant	
	<i>BS-1</i>	<i>BS-2</i>
0	18.23	16.07
3	18.08	15.26
6	17.87	15.25
9	17.85	15.19
12	17.81	15.18
15	17.73	15.11

At 5.10 MPa

Time (Mins)	Biosurfactant	
	<i>BS-1</i>	<i>BS-2</i>
0	17.83	14.86
3	17.85	14.86
6	17.86	14.80
9	17.87	14.68
12	17.85	14.63
15	17.86	14.55

At 12.51 MPa

Time (Mins)	Biosurfactant	
	<i>BS-1</i>	<i>BS-2</i>
0	18.11	13.97
3	18.10	13.98
6	18.10	13.95
9	18.11	13.90
12	18.07	13.83
15	18.20	13.79

P-2B: Comparison of IFT with time for cell-free *BS-1* & *BS-2* biosurfactants at 75°C

At 0.15 MPa

Time (Mins)	Biosurfactant	
	<i>BS-1</i>	<i>BS-2</i>
0	15.34	12.99
3	15.36	12.99
6	15.14	12.96
9	14.62	12.97
12	14.56	12.44
15	14.5	12.25

At 5.10 MPa

Time (Mins)	Biosurfactant	
	<i>BS-1</i>	<i>BS-2</i>
0	14.47	12.12
3	14.23	11.89
6	13.76	11.53
9	13.56	11.32
12	13.93	11.05
15	14.54	10.84

At 12.51 MPa

Time (Mins)	Biosurfactant	
	<i>BS-1</i>	<i>BS-2</i>
0	14.21	11.43
3	14.01	11.53
6	13.74	11.5
9	13.64	11.69
12	13.64	11.62
15	13.51	11.52

Appendix Q: Comparison of IFT with temperature for cell-free *BS-1*, *BS-2* & *BS-3*

Q-1: At constant pressure of 0.15 MPa

T (°C)	Biosurfactant		
	<i>BS-1</i>	<i>BS-2</i>	<i>BS-3</i>
26	31.95	21.14	-
32	31.66	17.99	34.05
42	17.99	13.76	11.42
60	14.09	8.3	8.71
75	12.63	6.69	7.79

Q-2: At constant pressure of 3.10 MPa

T (°C)	Biosurfactant		
	<i>BS-1</i>	<i>BS-2</i>	<i>BS-3</i>
26	40.08	19.81	-
32	28.73	15.44	22.48
42	16.42	10.65	10.76
60	13.7	7.91	8.7
75	11.47	6.41	7.05

Q-3: At constant pressure of 5.10 MPa

T (°C)	Biosurfactant		
	<i>BS-1</i>	<i>BS-2</i>	<i>BS-3</i>
26	43.02	19.06	-
32	29.45	14.8	22.32
42	16.39	10.6	10.46
60	13.36	7.1	8.58
75	11.42	6.24	7.37

Q-4: At constant pressure of 10.44 MPa

T (°C)	Biosurfactant		
	<i>BS-1</i>	<i>BS-2</i>	<i>BS-3</i>
26	43.7	18.36	-
32	26.18	14.19	21.22
42	16.21	9.52	9.75
60	13.3	6.81	8.55
75	11.06	5.17	7.02

Q-5: At constant pressure of 12.51 MPa

T (°C)	Biosurfactant		
	<i>BS-1</i>	<i>BS-2</i>	<i>BS-3</i>
26	47.06	16.96	-
32	27.19	13.43	19.58
42	16.18	9.21	9.4
60	13.25	6.35	8.38
75	10.95	4.75	6.64

Q-6: At constant pressure of 13.89 MPa

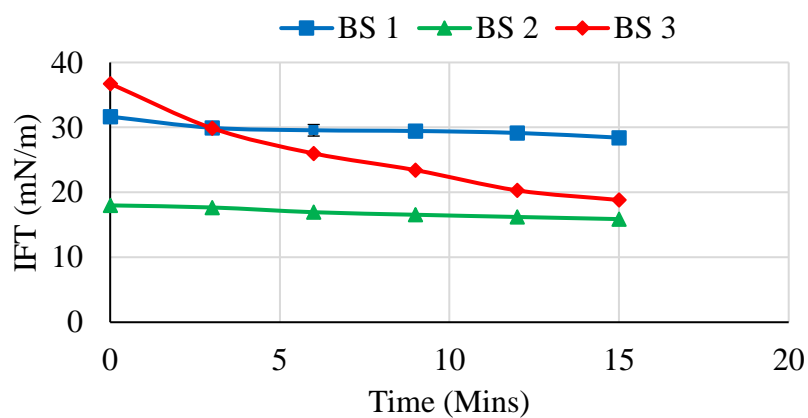
T (°C)	Biosurfactant		
	B1	B2	B3
26	40.49	14.97	-
32	24.57	12.72	18.75
42	15.74	9.16	8.99
60	12.9	5.8	7.9
75	10.94	4.49	6.62

Appendix R: Comparison of IFT with time for cell-free biosurfactants

R-1: At temperature of 32°C

At 0.15 MPa

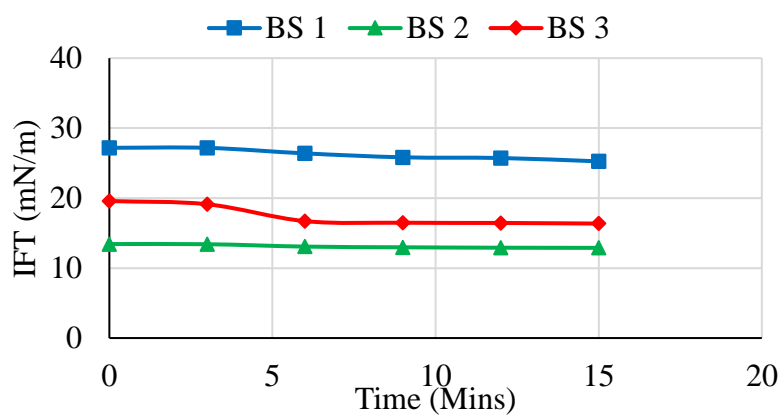
Biosurfactant			
Time (Mins)	<i>BS-1</i>	<i>BS-2</i>	<i>BS-3</i>
0	31.66	17.99	36.74
3	29.94	17.67	29.89
6	29.56	16.94	25.99
9	29.45	16.55	23.42
12	29.15	16.21	20.3
15	28.42	15.88	18.82



(a) At constant pressure of 0.15 MPa

At 5.10 MPa

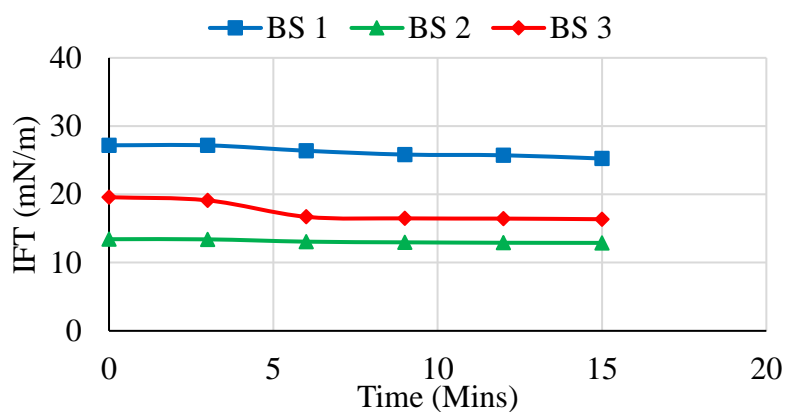
Time (Mins)	Biosurfactant		
	BS1	BS2	BS3
0	29.45	14.8	22.32
3	29.03	14.54	21.92
6	28.52	14.18	20.78
9	27.83	14.04	19.69
12	27.65	13.88	19.55
15	27.26	13.75	18.92



(b) At constant pressure of 5.10 MPa

At 12.15 MPa

Time (Mins)	Biosurfactant		
	<i>BS-1</i>	<i>BS-2</i>	<i>BS-3</i>
0	27.19	13.43	19.58
3	27.18	13.41	19.12
6	26.39	13.07	16.71
9	25.83	12.97	16.48
12	25.73	12.91	16.45
15	25.25	12.89	16.36

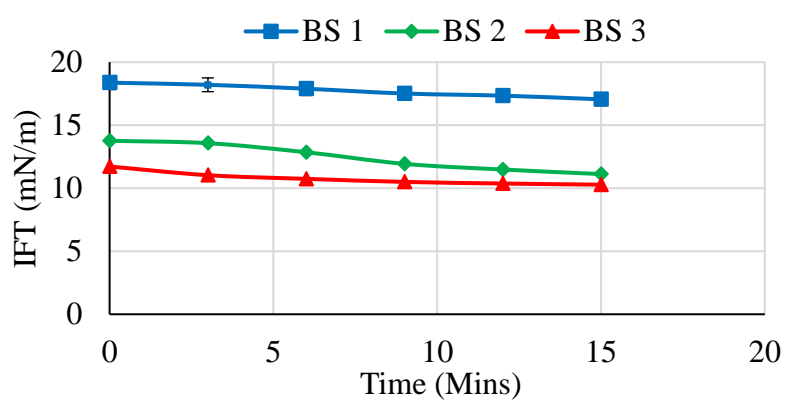


(c) At constant pressure of 12.15 MPa

R-2: At temperature of 42°C

At 0.15 MPa

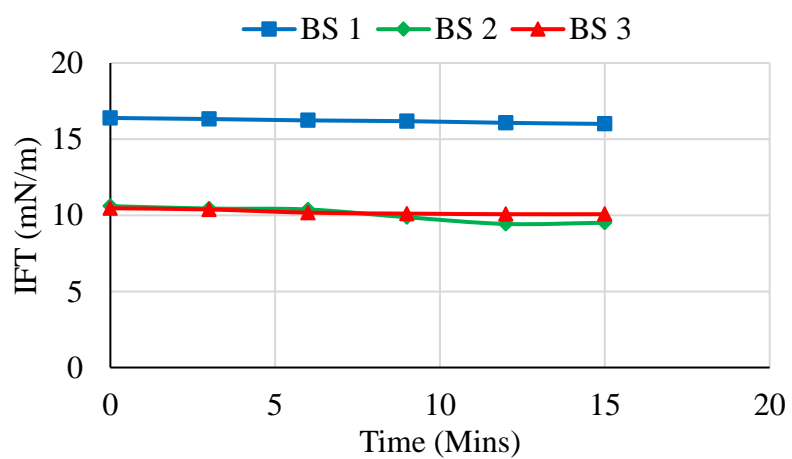
Time (Mins)	Biosurfactant		
	BS1	BS2	BS3
0	18.37	13.76	11.72
3	18.2	13.57	11.03
6	17.89	12.85	10.74
9	17.51	11.93	10.5
12	17.34	11.48	10.37
15	17.05	11.12	10.28



(a) At constant pressure of 0.15 MPa

At 5.10 MPa

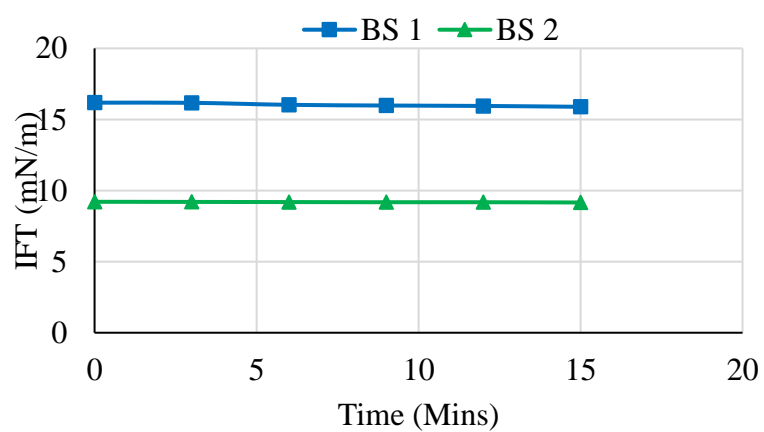
Time (Mins)	Biosurfactant		
	<i>BS-1</i>	<i>BS-2</i>	<i>BS-3</i>
0	16.39	10.6	10.46
3	16.32	10.44	10.38
6	16.23	10.38	10.17
9	16.18	9.87	10.11
12	16.07	9.43	10.07
15	16	9.51	10.07



(b) At constant pressure of 5.10 MPa

At 12.51 MPa

Time (Mins)	Biosurfactant	
	<i>BS-1</i>	<i>BS-2</i>
0	16.18	9.21
3	16.17	9.2
6	16.03	9.19
9	15.98	9.18
12	15.95	9.18
15	15.89	9.16

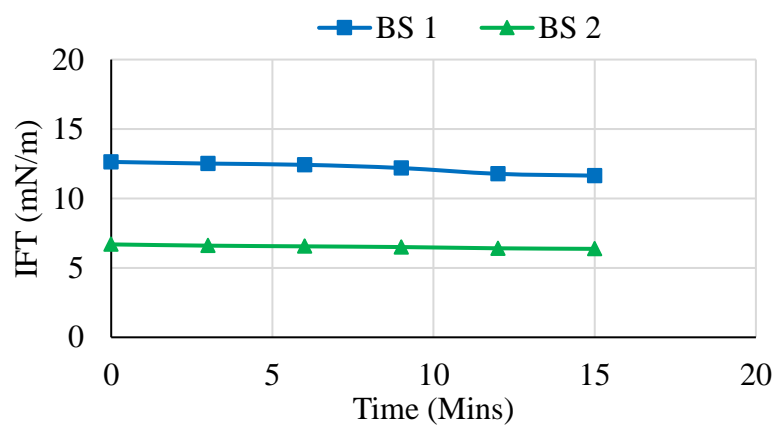


(c) At constant pressure of 12.15 MPa

R-3: At temperature of 75°C

At constant pressure of 0.15 MPa

Time (Mins)	Biosurfactant	
	<i>BS-1</i>	<i>BS-2</i>
0	12.63	6.69
3	12.51	6.60
6	12.42	6.55
9	12.19	6.50
12	11.77	6.41
15	11.64	6.37



At constant pressure of 5.10 MPa

Time (Mins)	Biosurfactant	
	<i>BS-1</i>	<i>BS-2</i>
0	11.42	6.24
3	11.38	5.99
6	11.26	5.92
9	11.15	5.82
12	11.06	5.39
15	11.04	5.31

